

UNIVERSITY OF PRETORIA
FACULTY OF VETERINARY SCIENCE
DEPARTMENT OF PARACLINICAL SCIENCES

**LIVER HISTOPATHOLOGY IN DOGS WITH NATURALLY
ACQUIRED *BABESIA ROSSI* INFECTION**

AUTHOR:
Heidi Horrell

DEGREE:
MSc

STUDENT NUMBER:
15100830

Contact details:

Email: heidi.horrell@gmail.com

SUPERVISOR: Prof. Andrew Leisewitz

CO-SUPERVISOR: Dr. Sarah J. Clift

Date submitted: September 2023

ACKNOWLEDGEMENTS

This has been a labour of love, and it has not come without its' difficulties. It has become something that I am deeply proud of and know that I gave my whole heart and soul to. I will also never underestimate the amount of effort that is needed to write a thesis ever again.

To my supervisors, Andy and Sarah, I would still be floundering around on my research proposal if it wasn't for you two. Thank you for too many hours of patience and invaluable input that you have both given me. You both went above and beyond in helping me to shape this thesis into what it is today. You have given me a much deeper understanding of research, and I did not think that I would have enjoyed it as much as I did. Thank you for pushing me up this hill during the many, many times that I thought I wanted to give up and slide down it. I am forever grateful, and could not have asked for better support and guidance.

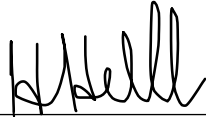
To my boyfriend, Ryan. I didn't know what I was signing up for when I first started this, but thank you for being the source of never-ending support that you are. You have carried this little family of ours by yourself for a long time now, and for that, I am incredibly grateful. I can't wait to be able to do the same for you. You think far too highly of me, but yet you keep me so grounded. I am so lucky to have you be a part of my life.

To my parents and brother, thank you for the financial and emotional support through this entire career choice of mine. It has been a long 8.5 years, so I think it's time to finally take a break. You have made me into everything I am, and your unconditional love has pushed me further than I ever thought was possible. I'm so excited to be able to stop telling you about how much I'm procrastinating and rather about all the exciting hobbies I'll have developed once this is finished!

To my co-workers, Nicholl and Jo, I am so lucky to have you in my life and to be able to learn so much from the both of you. You made my first working experience the best that I could have ever imagined, and such a supportive environment. Thank you for all the laughs, thank you for all the knowledge – just thank you.

DECLARATION

I, **Heidi Horrell**, hereby declare that the work on which this thesis is based is my own independent work and that neither the whole work nor part of it has been, is being, or shall be submitted for another degree at this or another university, institution for tertiary education or professional examination body.



Heidi Horrell

10 September 2023

Date

ETHICS STATEMENT

I, Heidi Horrell, have obtained the necessary research ethics approval (REC040-21) for the research described in this dissertation; I declare that I have observed the ethical standards required in terms of the University of Pretoria's code of ethics for researchers and the policy guidelines for responsible research.

CONTENTS

<i>ACKNOWLEDGEMENTS</i>	2
<i>DECLARATION</i>	3
<i>ETHICS STATEMENT</i>	4
<i>CONTENTS</i>	5
<i>LIST OF FIGURES</i>	7
<i>LIST OF TABLES</i>	12
<i>ABBREVIATION LIST</i>	13
<i>SUMMARY</i>	15
1. <i>INTRODUCTION</i>	16
2. <i>JUSTIFICATION</i>	18
2.1 <i>LITERATURE REVIEW</i>	18
2.1.1 Structure and function of the liver	18
2.1.1.1 Gross anatomy of the canine liver	18
2.1.1.2 Liver function	19
2.1.1.3 Histology of the canine liver	23
2.1.2 Liver pathology in haemoparasitic disease	27
2.1.2.1 Pathology of the liver in canine babesiosis	27
2.1.2.2 Pathology of the liver in <i>Plasmodium falciparum</i> malaria	28
2.1.4 Babesia in non-canids	29
2.1.4.1 Bovine babesiosis	29
2.1.4.2 Ovine babesiosis	29
2.1.4.3 Gerbil babesiosis	30
2.1.4.4 Murine babesiosis	30
2.1.4.5 Equine babesiosis	30
2.1.4.6 Feline babesiosis	30
2.1.4.7 Human babesiosis	31
2.1.5 Overview of canine babesiosis	31
2.1.5.1 Uncomplicated babesiosis	32
2.1.5.2 Complicated babesiosis	33
2.1.5.3 Diagnosis	35
2.1.6 Biochemical markers of liver function and hepatocyte injury	35
2.1.6.1 Biomarkers of liver function	35
2.1.6.2 Biomarkers of liver damage/hepatocyte injury	38
2.1.6.3 Biomarkers of cholestasis	38
2.1.7 Immunohistochemistry (IHC)	40
2.1.8 Prognosis	41
2.4 <i>AIM OF THE STUDY</i>	41
2.5 <i>HYPOTHESIS</i>	42
3. <i>METHODS AND MATERIALS</i>	42
3.1 <i>EXPERIMENTAL DESIGN</i>	42
3.1.1 Infected dogs: Sources	42
3.1.2 Control dogs: Sources	42
3.1.3 Infected dogs: Inclusion criteria	43
3.1.4 Infected dogs: Exclusion criteria	43
3.1.5 Control animals: Inclusion criteria	43
3.1.6 Control dogs: Exclusion criteria	43
3.1.7 Ante-mortem procedures on control dogs	44

3.1.8 Postmortems and sampling for histopathology	44
3.1.9 Histopathology and histochemistry	45
3.1.10 Immunohistochemistry	45
3.1.11 Evaluation of histopathology, histochemistry and IHC	47
3.2 DATA ANALYSIS AND STATISTICS.....	47
4. RESULTS.....	49
4.1 BLOOD RESULTS	49
4.1.1 Haematological values	49
4.1.2 Serum biochemistry values	50
4.2 HISTOPATHOLOGY.....	51
4.2.1 Control cases	51
4.2.2 Infected cases.....	53
4.3 HISTOCHEMICAL STAINS	67
4.3.1. Martius Scarlet Blue (MSB) stain.....	67
4.3.2. Gordon and Sweet’s silver (GSS) stain.....	70
4.3.3 Perls’ Prussian blue stain.....	72
4.3.4 Luxol Fast Blue (LFB) stain	75
4.4 IMMUNOHISTOCHEMISTRY	77
4.4.1 Control Cases.....	77
4.4.2 <i>B. rossi</i> -infected dogs	78
4.4.2.1 CD3	79
4.4.2.2 CD20	82
4.4.2.3 CD204	85
4.4.2.4 Iba-1	88
4.4.2.5 MAC387.....	91
4.4.2.6 MUM-1	94
4.4.3 Immunohistochemistry overview.....	97
5. DISCUSSION	100
5.1 HISTOPATHOLOGY.....	100
5.1.1 Sinusoids, spaces of Disse and lymphatics	100
5.1.2 Hepatocytes	102
5.1.3 Cholestasis.....	104
5.1.4 Extramedullary haematopoiesis (EMH).....	105
5.1.5 Kupffer cells.....	106
5.1.6 Haemosiderin	106
5.2 IMMUNOHISTOCHEMISTRY (IHC).....	107
5.2.1 Monocyte-macrophages	107
5.2.2 Lymphocytes and plasma cells	110
6. CONCLUSION	112
REFERENCES.....	113
APPENDICES	135
Appendix A: Full blood results	135
Appendix B: Histopathology score sheet.....	137
Appendix C: Histopathology detailed scoring scheme	140

LIST OF FIGURES

FIGURE 1: SCHEMATIC DIAGRAM SHOWING THE THREE MAJOR DIVISIONS OF THE CANINE LIVER AND THE INDIVIDUAL LOBES OF EACH DIVISION. THE BRANCHES OF THE PORTAL VEIN ARE ALSO DEPICTED. C. = CAUDATE LOBE, R.L. = RIGHT LATERAL LOBE, R.M. = RIGHT MIDDLE LOBE, RM = RIGHT MIDDLE LOBE, Q. = QUADRATE LOBE, L.M. = LEFT MIDDLE LOBE, L.L. = LEFT LATERAL LOBE, P = PAPILLARY PROCESS, G.B = GALL BLADDER. (PERMISSION FOR USE GRANTED BY COPYRIGHT CLEARANCE CENTER'S RIGHTS LINK [®] ON 30/03/2023). SOURCE: (SLEIGHT AND THOMFORD, 1970).....	18
FIGURE 2: SCHEMATIC DIAGRAM SHOWING BILIRUBIN METABOLISM WITHIN THE BLOOD VESSELS, MACROPHAGES, LIVER, INTESTINE AND KIDNEY. SENESCENT RED BLOOD CELLS ARE PHAGOCYTOSED BY MONONUCLEAR MACROPHAGES WITHIN THE CIRCULATION, RELEASING HAEMOGLOBIN. THE HAEMOGLOBIN IS THEN CATABOLIZED TO PRODUCE HEME, WHICH IS THEN REDUCED AND OXIDIZED TO BILIRUBIN. THE BILIRUBIN IS THEN BOUND TO ALBUMIN AND IS TRANSPORTED TO THE LIVER, WHERE IT IS SEPARATED AGAIN AND TAKEN UP BY THE HEPATOCYTES. IT IS TRANSPORTED TO THE SMOOTH ENDOPLASMIC RETICULUM WITHIN THE HEPATOCYTE AS A BILIRUBIN-LIGAND COMPLEX, AND IS THEN COMBINED WITH GLUCURONIC ACID TO FORM CONJUGATED BILIRUBIN. THIS CONJUGATED BILIRUBIN IS THEN RELEASED INTO THE INTESTINE WITH BILE, HYDROLYZED AND REDUCED TO CREATE UROBILINOGEN. THE MAJORITY OF UROBILINOGEN (ABOUT 90%) IS EXCRETED IN THE FAECES AS STERCIBILIN, WITH A SMALL AMOUNT BEING REABSORBED INTO THE CIRCULATION TO BE EXCRETED WITH THE BILE, THEREFORE FORMING THE ENTEROHEPATIC CIRCULATION. THE REMAINING AMOUNT (ABOUT 10%) IS EXCRETED THROUGH THE KIDNEYS IN THE URINE. (PERMISSION GRANTED FOR USE BY SPANDIDOS PUBLICATIONS 03/02/2023). SOURCE: (WANG ET AL., 2021)21	
FIGURE 3: SCHEMATIC DIAGRAM SHOWING THE HEPATIC LOBULE, ITS MICROSCOPIC ZONES AND METABOLIC FUNCTIONS. (PERMISSION GRANTED FOR USE BY ELSEVIER 03/02/2023). SOURCE: (MANTHORPE ET AL., 2020)	23
FIGURE 4: PHOTOMICROGRAPH OF THE LIVER SHOWING A HEPATIC LOBULE WITH SIX PORTAL TRACTS (PT) AT THE PERIPHERY AND A CENTRAL VEIN (CV) IN THE MIDDLE. BLOOD FLOWS FROM THE PT TO THE CV (RED ARROW), WHILE BILE FLOWS IN THE OPPOSITE DIRECTION (GREEN ARROW). THE ACINUS IS INDICATED BY THE THICKER CURVED LINES COMPRISING ZONES 1-3. HAEMATOXYLIN AND EOSIN (HE) STAINING. (PHOTO COURTESY OF DR JENNIFER FINDEIS-HOSEY, URM). SOURCE: (BELL, 2020)	24
FIGURE 5: PHOTOMICROGRAPH OF THE LIVER DEMONSTRATING NORMAL HEPATOCYTES (BLACK ARROWS) AS WELL AS A BINUCLEATED HEPATOCYTE (BLACK CIRCLE). HE STAINING. (PHOTO COURTESY OF KIMBERLEY J. EVASON, M.D., PH.D, PERMISSION GRANTED BY PATHOLOGYOUTLINES.COM ON 02/02/2023). SOURCE: (LEONARD N, 2021).....	24
FIGURE 6: PHOTOMICROGRAPH OF THE LIVER SHOWING THE CENTRAL VEIN (CV) AND THE SINUSOIDS THAT RADIATE OUTWARDS FROM IT (BLACK ARROWS). HE STAINING. SOURCE: (BELL, 2020).	25
FIGURE 7: SCHEMATIC DIAGRAM SHOWING THE RELATIONSHIP BETWEEN HEPATIC CORDS, SINUSOIDS, KUPFFER CELLS, THE SPACE OF DISSE AND THE STELLATE (ITO) CELLS. SINUSOIDS RUN BETWEEN THE HEPATIC PLATES WITH FENESTRATED CAPILLARIES THAT ALLOW FOR EASY EXCHANGE OF OXYGEN, BLOOD AND NUTRIENTS BETWEEN THE BLOOD VESSELS AND HEPATOCYTES. KUPFFER CELLS LINE THE LUMINAL SURFACE OF SINUSOIDAL ENDOTHELIAL CELLS. THE SPACE OF DISSE IS FOUND BETWEEN THE ENDOTHELIAL CELLS AND HEPATOCYTES AND IS ALSO THE LOCATION OF THE HEPATIC STELLATE CELLS. BILE CANALICULI RUN BETWEEN THE HEPATOCYTES. (PHOTO COURTESY OF DR AJ VAN WETTERE, SCHOOL OF VETERINARY MEDICINE, UTAH STATE UNIVERSITY AND DR JE ZACHARY, COLLEGE OF VETERINARY MEDICINE, UNIVERSITY OF ILLINOIS. PERMISSION GRANTED FOR USE BY ELSEVIER 03/02/2023). SOURCE: (BROWN, 2017).	26
FIGURE 8: PHOTOMICROGRAPH OF A NORMAL DOG LIVER (CONTROL NO. 2) SHOWING A PORTAL TRACT CONTAINING A BRANCH OF THE PORTAL VEIN, HEPATIC ARTERY, BILE DUCT (RED ARROW), ENDOTHELIAL CELLS LINING A LYMPHATIC DUCT (BLACK ARROWS) AND A SINUSOID CONTAINING RED BLOOD CELLS (YELLOW ARROW). PV = PORTAL VEIN, HA = HEPATIC ARTERY. HE STAINING AT 200X MAGNIFICATION.	26
FIGURE 9: PHOTOMICROGRAPH OF A NORMAL DOG LIVER (CONTROL NO. 2) SHOWING A PORTAL TRACT. PV = PORTAL VEIN, BD = BILE DUCT, HA = HEPATIC ARTERY, L = LYMPHATIC VESSEL. HAEMATOXYLIN AND EOSIN (HE) STAINING AT 200X MAGNIFICATION.	51
FIGURE 10: PHOTOMICROGRAPH OF A NORMAL DOG LIVER (CONTROL NO. 4) SHOWING THE PORTAL TRACT WITH NORMAL FLATTENED, ELONGATED ENDOTHELIAL CELLS (BLACK CIRCLES) LINING THE PORTAL VEIN. PV = PORTAL VEIN. HE STAINING AT 400X MAGNIFICATION.	52
FIGURE 11: PHOTOMICROGRAPH OF A NORMAL DOG LIVER (CONTROL NO. 2) SHOWING THE MIDZONAL AREA. HEPATOCYTE CORDS ARE VISUALISED (BLACK ARROWS) WITH SINUSOIDS CONTAINING ERYTHROCYTES, SURROUNDED BY THE SPACE OF DISSE (BLUE ARROWS). BINUCLEATED HEPATOCYTES ARE ALSO PRESENT (YELLOW CIRCLES) WITH MAGNIFIED PORTIONS (LARGER BLACK CIRCLES). HE STAINING AT 400X MAGNIFICATION.	52
FIGURE 12: PHOTOMICROGRAPH OF A NORMAL DOG LIVER (CONTROL NO. 2) SHOWING THE CENTRILOBULAR AREA. LYMPHATIC VESSELS CONTAINING HOMOGENOUS PALE EOSINOPHILIC MATERIAL ARE VISUALIZED (BLACK STARS), AND BINUCLEATION OF HEPATOCYTES INDICATING TURNOVER (GREEN CIRCLES) WITH MAGNIFIED VIEWS AT 400X MAGNIFICATION (LARGER BLACK CIRCLES). CV = CENTRAL VEIN, L = LYMPHATIC VESSEL. HE STAINING AT 200X MAGNIFICATION.	53

- FIGURE 13: A.** PHOTOMICROGRAPH OF A NORMAL DOG LIVER (CONTROL NO. 2) SHOWING CENTRIOBLULAR, MIDZONAL AND PORTAL TRACTS THAT ARE NORMAL AND DISTINCT. CV = CENTRAL VEIN, PV = PORTAL VEIN. HE STAINING AT 100X MAGNIFICATION. **B.** PHOTOMICROGRAPH OF AN INFECTED DOG LIVER (CASE NO. 20) WITH MODERATE CENTRIOBLULAR NECROSIS (DELINEATED BY THE DOTTED BLACK CIRCLE) ASSOCIATED WITH MARKEDLY DILATED, BLOODLESS SINUSOIDS. THE DISTINCTION BETWEEN CENTRIOBLULAR, MIDZONAL AND PERIportal AREAS IS NOT AS OBVIOUS IN IMAGE B AS IT IS IN IMAGE A (OR FIGURE 12). PT = PORTAL TRACT, CV = CENTRAL VEIN (SOLID BLACK CIRCLE). HE STAINING AT 100X MAGNIFICATION. 54
- FIGURE 14: A.** PHOTOMICROGRAPH OF A NORMAL DOG LIVER (CONTROL NO. 2) SHOWING A MILDLY CONGESTED CENTRAL VEIN. CV = CENTRAL VEIN. HE STAINING AT 200X MAGNIFICATION. **B.** PHOTOMICROGRAPH OF AN INFECTED DOG LIVER (CASE NO. 50) SHOWING SEVERE CENTRIOBLULAR (ALSO REFERRED TO AS PERIACINAR) CONGESTION. CV = CENTRAL VEIN. HE STAINING AT 200X MAGNIFICATION. 55
- FIGURE 15: A.** PHOTOMICROGRAPH OF AN INFECTED DOG LIVER (CASE NO. 50) SHOWING A PORTAL TRACT WITH SEVERE LEUCOSTASIS IN THE PORTAL VEIN (BLACK STAR). PV = PORTAL VEIN, BD = BILE DUCT, HA = HEPATIC ARTERY. HE STAINING AT 400X MAGNIFICATION. **B.** PHOTOMICROGRAPH OF AN INFECTED DOG LIVER (CASE NO. 117) SHOWING A PORTAL TRACT WITH BILE STASIS IN A BILE DUCT (BLACK CIRCLE), CANALICULAR CHOLESTASIS WITHIN THE LIMITING PLATE OF HEPATOCYTES (RED CIRCLE), A HEPATOCYTE CONTAINING A VESICULAR NUCLEUS (GREEN CIRCLE), MODERATE LEUCOSTASIS IN THE PORTAL VEIN (BLUE CIRCLE), SCATTERED NUCLEATED RED BLOOD CELLS INDICATING ERYTHROPOEISIS (YELLOW CIRCLES), AS WELL AS A DISTENDED LYMPHATIC VESSEL CONTAINING HOMOGENOUS PALE EOSINOPHILIC MATERIAL (BLACK STAR). PV = PORTAL VEIN, BD = BILE DUCT, L = LYMPHATIC VESSEL. HE STAINING AT 400X MAGNIFICATION. 57
- FIGURE 16:** PHOTOMICROGRAPH OF AN INFECTED DOG LIVER (CASE NO. 117) SHOWING A PORTAL TRACT WITH SEVERE CONGESTION (BLUE CIRCLE) AND MONONUCLEAR LEUCOSTASIS (BLACK STAR) WITHIN THE PORTAL VEIN, DISTENDED LYMPHATIC VESSELS CONTAINING HOMOGENOUS PALE EOSINOPHILIC MATERIAL (YELLOW STARS), BILE STASIS WITHIN THE BILE DUCT (BLACK CIRCLE), AND PROMINENT WIDENING (MODERATE TO SEVERE OEDEMA) OF THE SPACE OF DISSE (BLACK ARROWS) SURROUNDING THE CONGESTED, HYPERCELLULAR SINUSOIDS (BLACK ARROWS). PV = PORTAL VEIN, BD = BILE DUCT, L = LYMPHATIC VESSEL. HE STAINING AT 400X MAGNIFICATION. 58
- FIGURE 17: A.** PHOTOMICROGRAPH OF A NORMAL DOG LIVER (CONTROL NO. 4) DEMONSTRATING THE MIDZONAL AREA. HE STAINING AT 200X MAGNIFICATION. **B.** PHOTOMICROGRAPH OF AN INFECTED DOG LIVER (CASE NO. 61) SHOWING PROMINENT WIDENING (MODERATE TO SEVERE OEDEMA) OF THE SPACE OF DISSE (BLACK ARROWS) SURROUNDING THE CONGESTED, HYPERCELLULAR SINUSOIDS. HE STAINING AT 200X MAGNIFICATION. 60
- FIGURE 18: A.** PHOTOMICROGRAPH OF AN INFECTED DOG LIVER (CASE NO. 50) SHOWING A MIDZONAL AREA WITH MITOTIC FIGURES (YELLOW CIRCLE) INDICATING HEPATOCYTE TURNOVER, HYPERTROPHIC, HAEMOSIDERIN-LADEN KUPFFER CELLS (GREEN CIRCLES), AND CANALICULAR CHOLESTASIS (BLACK CIRCLES). HE STAINING AT 600X MAGNIFICATION. **B.** PHOTOMICROGRAPH OF AN INFECTED DOG LIVER (CASE NO. 117) SHOWING A MIDZONAL AREA WITH INCREASED NUMBERS OF BINUCLEATED HEPATOCYTES INDICATING INCREASED TURNOVER (YELLOW CIRCLES), HYPERTROPHIC, HAEMOSIDERIN-LADEN KUPFFER CELLS (BLACK CIRCLES), NUCLEATED RED BLOOD CELLS (RED CIRCLES), CANALICULAR CHOLESTASIS (GREEN CIRCLES) AND MILD TO MODERATE HYDROPIC CHANGE/VACUOLAR DEGENERATION IN HEPATOCYTES (BLACK ARROWS). HE STAINING AT 600X MAGNIFICATION. 61
- FIGURE 19: A.** PHOTOMICROGRAPH OF AN INFECTED DOG LIVER (CASE NO. 61) SHOWING HEPATOCYTES IN THE MIDZONAL AREA WITH LARGE VESICULAR/EUCHROMATIC NUCLEI (BLACK CIRCLES), MARKED WIDENING (MODERATE TO SEVERE OEDEMA) OF THE SPACE OF DISSE (BLACK ARROWS), AS WELL AS INCREASED NUMBERS OF NUCLEATED RED BLOOD CELLS (YELLOW CIRCLES). HE STAINING AT 600X MAGNIFICATION. **B.** PHOTOMICROGRAPH OF AN INFECTED DOG LIVER (CASE NO. 50) SHOWING HYPERTROPHIC, HAEMOSIDERIN-LADEN KUPFFER CELLS (BLACK CIRCLE), MITOTIC FIGURES INDICATING TURNOVER (RED CIRCLE), AND CANALICULAR CHOLESTASIS (YELLOW CIRCLES). HE STAINING AT 600X MAGNIFICATION. 62
- FIGURE 20: A.** PHOTOMICROGRAPH OF A NORMAL DOG LIVER (CONTROL NO. 4) DEMONSTRATING A CENTRIOBLULAR AREA. CV = CENTRAL VEIN. HE STAINING AT 200X MAGNIFICATION **B.** PHOTOMICROGRAPH OF AN INFECTED DOG LIVER (CASE NO. 20) SHOWING A CENTRIOBLULAR AREA WITH BILE PIGMENT IN HEPATOCYTES (BLUE CIRCLES) AND PROMINENT WIDENING (SEVERE OEDEMA) OF THE SPACE OF DISSE (BLACK STARS) AND ONLY A SMALL AMOUNT OF BLOOD WITHIN THE SINUSOIDS. CV = CENTRAL VEIN. HE STAINING AT 400X MAGNIFICATION. 64
- FIGURE 21: A.** PHOTOMICROGRAPH OF AN INFECTED DOG LIVER (CASE NO. 117) SHOWING A CENTRIOBLULAR AREA WITH SEVERE CONGESTION OF THE CENTRAL VEIN AND ADJACENT SINUSOIDS, AND MODERATELY DISTENDED LYMPHATIC VESSELS CONTAINING HOMOGENOUS PALE EOSINOPHILIC MATERIAL (BLACK STARS). CV = CENTRAL VEIN, L = LYMPHATIC VESSEL. HE STAINING AT 100X MAGNIFICATION. **B.** PHOTOMICROGRAPH OF AN INFECTED DOG LIVER (CASE NO. 59) SHOWING A MODERATELY CONGESTED CENTRAL VEIN AND SURROUNDING SINUSOIDS, AND MODERATE MONONUCLEAR LEUCOSTASIS ESPECIALLY PROMINENT IN THE CENTRAL VEIN (BLACK STAR). MILD LYMPHATIC DISTENSION (YELLOW STARS) AND MILD OEDEMA ARE ALSO PRESENT (BLUE STARS). CV = CENTRAL VEIN. L = LYMPHATIC DUCT. HE STAINING AT 200X MAGNIFICATION. 65
- FIGURE 22: A.** PHOTOMICROGRAPH OF AN INFECTED DOG LIVER (CASE NO. 20) DEMONSTRATING A CENTRIOBLULAR AREA WITH MODERATE NUMBERS OF PERIVASCULAR (AND A FEW VASCULAR INTRAMURAL) MONONUCLEAR LEUCOCYTES (BLACK STARS), BINUCLEATED HEPATOCYTES (BLUE CIRCLES), KUPFFER CELL-ASSOCIATED HAEMOSIDERIN-LIKE PIGMENT (BLACK CIRCLE), BILE

PIGMENT IN HEPATOCYTES (RED CIRCLES), AS WELL AS MARKED WIDENING (SEVERE OEDEMA) OF THE SPACE OF DISSE (BLACK ARROWS). CV = CENTRAL VEIN. HE STAINING AT 400X MAGNIFICATION. **B.** PHOTOMICROGRAPH OF AN INFECTED DOG LIVER (CASE NO. 59) DEMONSTRATING A CENTRIOBULAR AREA WITH MODERATE ENDOTHELIAL CELL HYPERTROPHY (BLACK CIRCLES). CV = CENTRAL VEIN. HE STAINING AT 400X MAGNIFICATION. 66

FIGURE 23: A. PHOTOMICROGRAPH OF A NORMAL DOG LIVER (CONTROL NO. 4) SHOWING A PORTAL TRACT WITH NO EVIDENCE OF FIBRIN. PV = PORTAL VEIN, BD = BILE DUCT. MSB STAINING AT 400X MAGNIFICATION. **B.** PHOTOMICROGRAPH OF AN INFECTED DOG LIVER (CASE NO. 117) SHOWING A PORTAL TRACT WITH NO EVIDENCE OF FIBRIN. RED BLOOD CELLS STAIN YELLOW, COLLAGEN STAINS BLUE, INTRACANALICULAR BILE STAINS DARK PINK. PV = PORTAL VEIN. MSB STAINING AT 400X MAGNIFICATION. 67

FIGURE 24: A. PHOTOMICROGRAPH OF A NORMAL DOG LIVER (CONTROL NO. 4) SHOWING A MIDZONAL AREA WITH NO SIGNS OF FIBRIN PRESENT. MSB STAINING AT 400X MAGNIFICATION. **B.** PHOTOMICROGRAPH OF AN INFECTED DOG LIVER (CASE NO. 50) SHOWING A MIDZONAL AREA WITH NO FIBRIN PRESENT. MSB STAINING AT 400X MAGNIFICATION. 68

FIGURE 25: A. PHOTOMICROGRAPH OF A NORMAL DOG LIVER (CONTROL NO. 4) SHOWING A CENTRIOBULAR AREA WITH NO SIGNS OF FIBRIN PRESENT. CV = CENTRAL VEIN. MSB STAINING AT 400X MAGNIFICATION. **B.** PHOTOMICROGRAPH OF AN INFECTED DOG LIVER (CASE NO. 117) SHOWING A CENTRIOBULAR AREA WITH NO EVIDENCE OF FIBRIN PRESENT. CV = CENTRAL VEIN. MSB STAINING AT 400X MAGNIFICATION. 69

FIGURE 26: A. PHOTOMICROGRAPH OF A NORMAL DOG LIVER (CONTROL NO. 4) SHOWING A PORTAL TRACT WITH GSS STAINING OF RETICULAR FIBRES. PV = PORTAL VEIN. GSS STAINING AT 200X MAGNIFICATION. **B.** PHOTOMICROGRAPH OF AN INFECTED DOG LIVER (CASE NO. 117) SHOWING A PORTAL TRACT WITH GSS STAINING OF RETICULAR FIBRES, SIMILAR TO THAT IN NORMAL LIVER. PV = PORTAL VEIN. GSS STAINING AT 200X MAGNIFICATION. 70

FIGURE 27: A. PHOTOMICROGRAPH OF A NORMAL DOG LIVER (CONTROL NO. 2) SHOWING A CENTRAL VEIN WITH GSS STAINING OF RETICULAR FIBRES. PV = PORTAL VEIN. GSS STAINING AT 200X MAGNIFICATION. **B.** PHOTOMICROGRAPH OF AN INFECTED DOG LIVER (CASE NO. 50) SHOWING A CENTRIOBULAR AREA WITH NORMAL GSS STAINING. CV = CENTRAL VEIN. GSS STAINING AT 200X MAGNIFICATION. 71

FIGURE 28: A. PHOTOMICROGRAPH OF A NORMAL DOG LIVER (CONTROL NO. 2) SHOWING A PORTAL TRACT. SPARSELY SCATTERED HAEMOSIDERIN PIGMENT WAS IDENTIFIED (BLACK CIRCLES). PV = PORTAL VEIN, BD = BILE DUCT, HA = HEPATIC ARTERY. PERLS' PRUSSIAN BLUE STAINING AT 200X MAGNIFICATION. **B.** PHOTOMICROGRAPH OF AN INFECTED DOG LIVER (CASE NO. 50) SHOWING A PORTAL TRACT WITH WIDESPREAD HAEMOSIDERIN PIGMENTATION, ESPECIALLY PROMINENT IN ASSOCIATION WITH THE SINUSOIDS (BLACK ARROWS). PV = PORTAL VEIN. PERLS' PRUSSIAN BLUE STAINING AT 200X MAGNIFICATION. 72

FIGURE 29: A. PHOTOMICROGRAPH OF A NORMAL DOG LIVER (CONTROL NO. 2) SHOWING A MIDZONAL AREA WITH SCANT SINUSOIDAL HAEMOSIDERIN PIGMENT (BLACK CIRCLES). PERLS' PRUSSIAN BLUE STAINING AT 200X MAGNIFICATION. **B.** PHOTOMICROGRAPH OF AN INFECTED DOG LIVER (CASE NO. 110) SHOWING A MIDZONAL AREA WITH WIDESPREAD SINUSOID-ASSOCIATED HAEMOSIDERIN PIGMENT (BLACK ARROWS). PERLS' PRUSSIAN BLUE STAINING AT 200X MAGNIFICATION. 73

FIGURE 30: A. PHOTOMICROGRAPH OF A NORMAL DOG LIVER (CONTROL NO. 4) SHOWING A CENTRIOBULAR AREA WITH NO OBVIOUS HAEMOSIDERIN PIGMENT. CV = CENTRAL VEIN. PERLS' PRUSSIAN BLUE STAINING AT 200X MAGNIFICATION. **B.** PHOTOMICROGRAPH OF AN INFECTED DOG LIVER (CASE NO. 20) SHOWING A CENTRIOBULAR AREA WITH HAEMOSIDERIN PIGMENT IN THE PERIVASCULAR INTERSTITIUM (BLACK CIRCLES), AND IN ASSOCIATION WITH THE SINUSOIDS (YELLOW CIRCLES). CV = CENTRAL VEIN, PERLS' PRUSSIAN BLUE STAINING AT 200X MAGNIFICATION. 74

FIGURE 31: PHOTOMICROGRAPH OF AN INFECTED DOG LIVER (CASE NO. 61) SHOWING A PORTAL TRACT WITH INTRAERYTHROCYTIC B. ROSSI PARASITES (RED CIRCLES) IN THE PORTAL VEIN (PV) WITH MAGNIFIED VIEWS (LARGER BLACK CIRCLE). LFB STAINING AT 600X MAGNIFICATION. 75

FIGURE 32: PHOTOMICROGRAPH OF AN INFECTED DOG LIVER (CASE NO. 20) SHOWING A MIDZONAL AREA WITH INTRAERYTHROCYTIC B. ROSSI PARASITES (RED CIRCLES) IN SINUSOIDS WITH MAGNIFIED VIEWS (LARGER BLACK CIRCLE). LFB STAINING AT 600X MAGNIFICATION. 76

FIGURE 33: PHOTOMICROGRAPH OF AN INFECTED DOG LIVER (CASE NO. 20) SHOWING A CENTRIOBULAR AREA WITH INTRAERYTHROCYTIC B. ROSSI PARASITES (RED CIRCLES) IN THE CENTRAL VEIN (CV) WITH MAGNIFIED VIEWS (LARGER BLACK CIRCLE). LFB STAINING AT 600X MAGNIFICATION. 76

FIGURE 34: A. PHOTOMICROGRAPH OF A NORMAL DOG LIVER (CONTROL NO. 4) SHOWING A PORTAL TRACT WITH CD3-POSITIVE T-LYMPHOCYTES IN THE PERIVASCULAR AND PERIDUCTAL CONNECTIVE TISSUE (YELLOW CIRCLES). PV = PORTAL VEIN, BD = BILE DUCT. IHC STAINING AT 400X MAGNIFICATION. **B.** PHOTOMICROGRAPH OF AN INFECTED DOG LIVER (CASE NO. 59) SHOWING A PORTAL VEIN WITH INTRALUMINAL AND PERIVASCULAR CD3-POSITIVE T-LYMPHOCYTES. THERE IS NON-SPECIFIC LABELING OF HEPATOCYTES (BLUE ARROWS). PV = PORTAL TRACT. IHC STAINING AT 400X MAGNIFICATION. 80

FIGURE 35: A. PHOTOMICROGRAPH OF A NORMAL DOG LIVER (CONTROL NO. 4) SHOWING A MIDZONAL AREA WITH CD3-POSITIVE T-LYMPHOCYTES OCCURRING PREDOMINANTLY INTRAVASCULARLY. IHC STAINING AT 400X MAGNIFICATION. **B.** PHOTOMICROGRAPH OF AN INFECTED DOG LIVER (CASE NO. 106) SHOWING A MIDZONAL AREA WITH A COMPARATIVELY INCREASED NUMBER OF CD3-POSITIVE T-LYMPHOCYTES, PREDOMINANTLY OCCURRING INTRAVASCULARLY. IHC STAINING AT 400X MAGNIFICATION. 80

- FIGURE 36: A.** PHOTOMICROGRAPH OF A NORMAL DOG LIVER (CONTROL NO. 4) SHOWING A CENTRIOBULAR AREA WITH NO OBVIOUS CD3-POSITIVE T-LYMPHOCYTES PRESENT. CV = CENTRAL VEIN. IHC STAINING AT 400X MAGNIFICATION. **B.** PHOTOMICROGRAPH OF AN INFECTED DOG LIVER (CASE NO. 88) SHOWING A CENTRIOBULAR AREA WITH A COMPARATIVELY INCREASED NUMBER OF CD3-POSITIVE T-LYMPHOCYTES PRESENT IN THE PERIVASCULAR INTERSTITIUM. THERE IS NON-SPECIFIC LABELING OF PLASMA (BLACK ARROWS). CV = CENTRAL VEIN. IHC STAINING AT 400X MAGNIFICATION. 81
- FIGURE 37: A.** PHOTOMICROGRAPH OF A NORMAL DOG LIVER (CONTROL NO. 11) SHOWING A PORTAL TRACT WITH RARE CD20-POSITIVE B-LYMPHOCYTES AND PLASMA CELLS (RED CIRCLE) IN THE PERIVASCULAR AND PERIDUCTAL INTERSTITIUM. THERE IS NON-SPECIFIC LABELING OF PLASMA (BLACK STAR). PV = PORTAL VEIN, HA = HEPATIC ARTERY, BD = BILE DUCT. IHC STAINING AT 400X MAGNIFICATION. **B.** PHOTOMICROGRAPH OF AN INFECTED DOG LIVER (CASE NO. 117) SHOWING A PORTAL TRACT WITH A COMPARATIVELY INCREASED NUMBER OF CD20-POSITIVE B-LYMPHOCYTES AND PLASMA CELLS PRESENT IN THE PERIVASCULAR AND PERIDUCTAL INTERSTITIUM. THERE IS SIMILAR NON-SPECIFIC LABELING OF PLASMA (BLACK STARS). PV = PORTAL VEIN. IHC STAINING AT 400X MAGNIFICATION. 83
- FIGURE 38: A.** PHOTOMICROGRAPH OF A NORMAL DOG LIVER (CONTROL NO. 2) SHOWING A MIDZONAL AREA WITH CD20-POSITIVE B-LYMPHOCYTES AND PLASMA CELLS PRESENT (RED CIRCLE) WITH MAGNIFIED VIEWS (BLACK CIRCLE). IHC STAINING AT 200X MAGNIFICATION. **B.** PHOTOMICROGRAPH OF AN INFECTED DOG LIVER (CASE NO. 110) SHOWING A MIDZONAL AREA WITH A COMPARATIVELY INCREASED NUMBER OF INTRAVASCULAR CD20-POSITIVE B CELLS (RED CIRCLES) AND SCATTERED PLASMA CELLS WITH MAGNIFIED VIEWS (BLACK CIRCLE). THERE IS NON-SPECIFIC LABELING OF PLASMA (BLACK STAR). IHC STAINING AT 200X MAGNIFICATION. 83
- FIGURE 39: A.** PHOTOMICROGRAPH OF A NORMAL DOG LIVER (CONTROL NO. 4) SHOWING A CENTRIOBULAR AREA WITH A FEW SCATTERED CD20-POSITIVE B-LYMPHOCYTES AND PLASMA CELLS PRESENT IN THE PERIVASCULAR INTERSTITIUM (RED CIRCLES). THERE IS NON-SPECIFIC LABELING OF PLASMA (BLACK STAR). CV = CENTRAL VEIN. IHC STAINING AT 400X MAGNIFICATION. **B.** PHOTOMICROGRAPH OF AN INFECTED DOG LIVER (CASE NO. 117) SHOWING A CENTRIOBULAR AREA WITH A COMPARATIVELY INCREASED NUMBER OF CD20-POSITIVE B-LYMPHOCYTES AND PLASMA CELLS PRESENT IN THE PERIVASCULAR INTERSTITIUM (RED CIRCLES). THERE IS QUITE EXTENSIVE NON-SPECIFIC LABELING OF PLASMA (BLACK STAR). CV = CENTRAL VEIN. IHC STAINING AT 400X MAGNIFICATION. 84
- FIGURE 40: A.** PHOTOMICROGRAPH OF A NORMAL DOG LIVER (CONTROL NO. 9) SHOWING A PORTAL TRACT WITH SINUSOID-ASSOCIATED CD204-POSITIVE MONOCYTE-MACROPHAGES (RED CIRCLES) IN SINUSOIDAL LUMENS (LIKELY CORRESPONDING WITH KUPFFER CELLS) AND A FEW POSITIVE CELLS IN THE INTERSTITIUM OF THE PORTAL TRACT. PV = PORTAL VEIN, HA = HEPATIC ARTERY, BD = BILE DUCT. IHC STAINING AT 400X MAGNIFICATION. **B.** PHOTOMICROGRAPH OF AN INFECTED DOG LIVER (CASE NO. 59) SHOWING A PORTAL TRACT WITH INCREASED NUMBERS OF SINUSOIDAL CD204-POSITIVE MONOCYTE-MACROPHAGES (BLUE CIRCLES) AND SCATTERED POSITIVE CELLS IN THE PERIVASCULAR INTERSTITIUM (RED CIRCLES). PV = PORTAL VEIN, BD = BILE DUCT. IHC STAINING AT 400X MAGNIFICATION. 86
- FIGURE 41: A.** PHOTOMICROGRAPH OF A NORMAL DOG LIVER (CONTROL NO. 9) SHOWING A MIDZONAL AREA WITH CD204-POSITIVE SINUSOID-ASSOCIATED MONOCYTE-MACROPHAGES (LIKELY CORRESPONDING WITH KUPFFER CELLS). IHC STAINING AT 400X MAGNIFICATION. **B.** PHOTOMICROGRAPH OF AN INFECTED DOG LIVER (CASE NO. 59) SHOWING A MIDZONAL AREA WITH A COMPARATIVELY INCREASED NUMBER OF CD204-POSITIVE SINUSOIDAL MONOCYTE-MACROPHAGES. IHC STAINING AT 400X MAGNIFICATION. 86
- FIGURE 42: A.** PHOTOMICROGRAPH OF A NORMAL DOG LIVER (CONTROL NO. 9) SHOWING A CENTRIOBULAR AREA WITH NO CD204-POSITIVE MONOCYTE-MACROPHAGES IN THE IMMEDIATE VICINITY OF THE CENTRAL VEIN (BLACK OUTLINE), BUT POSITIVELY STAINED MONOCYTE-MACROPHAGES ARE EVIDENT IN THE SINUSOIDS OF THE ADJACENT MIDZONAL AREA. CV = CENTRAL VEIN. IHC STAINING AT 400X MAGNIFICATION. **B.** PHOTOMICROGRAPH OF AN INFECTED DOG LIVER (CASE NO. 64) SHOWING A CENTRIOBULAR AREA (BLACK OUTLINE) WITH A COMPARATIVELY INCREASED NUMBER OF CD204-POSITIVE MONOCYTE-MACROPHAGES IN THE PERIVASCULAR INTERSTITIUM (BLACK CIRCLES) AND LUMENS OF ADJACENT SINUSOIDS. CV = CENTRAL VEIN. IHC STAINING AT 400X MAGNIFICATION. 87
- FIGURE 43: A.** PHOTOMICROGRAPH OF A NORMAL DOG LIVER (CONTROL NO. 4) SHOWING A PORTAL TRACT (BLACK CIRCLE) WITH IBA-1-POSITIVE MONOCYTE-MACROPHAGES AND DENDRITIC CELLS PREDOMINANTLY IN THE PERIVASCULAR INTERSTITIUM (BLUE CIRCLES). THERE ARE MANY MORE IBA-1-POSITIVE MACROPHAGES AND DENDRITIC CELLS IN THE ADJACENT MIDZONAL AREA. IHC STAINING AT 200X MAGNIFICATION. **B.** PHOTOMICROGRAPH OF AN INFECTED DOG LIVER (CASE NO. 59) SPECIMEN SHOWING A PORTAL TRACT (BLACK OUTLINE) WITH A COMPARATIVELY INCREASED NUMBER OF IBA-1-POSITIVE CELLS IN THE PORTAL VEIN (RED CIRCLE) AND IN THE PERIVASCULAR AND PERIDUCTAL INTERSTITIUM (BLUE CIRCLES). PV = PORTAL VEIN, BD = BILE DUCT. IHC STAINING AT 200X MAGNIFICATION. 89
- FIGURE 44: A.** PHOTOMICROGRAPH OF A NORMAL DOG LIVER (CONTROL NO. 2) SHOWING A MIDZONAL AREA WITH SCATTERED SINUSOID-ASSOCIATED IBA-1-POSITIVE MONOCYTE-MACROPHAGES AND DENDRITIC CELLS. IHC STAINING AT 200X MAGNIFICATION. **B.** PHOTOMICROGRAPH OF AN INFECTED DOG LIVER (CASE NO. 51) SHOWING A MIDZONAL AREA WITH A COMPARATIVELY INCREASED NUMBER OF SINUSOID-ASSOCIATED IBA-1-POSITIVE CELLS. IHC AT 200X MAGNIFICATION. 89
- FIGURE 45: A.** PHOTOMICROGRAPH OF A NORMAL DOG LIVER (CONTROL NO. 9) SHOWING A CENTRIOBULAR AREA (BLACK OUTLINE) WITH SCATTERED IBA-1-POSITIVE MONOCYTE-MACROPHAGES AND DENDRITIC CELLS MAINLY IN THE PERIVASCULAR

INTERSTITIUM (BLUE CIRCLES). CV = CENTRAL VEIN. IHC STAINING AT 200X MAGNIFICATION. **B.** PHOTOMICROGRAPH OF AN INFECTED DOG LIVER (CASE NO. 91) SHOWING A CENTRIOBULAR AREA (BLACK OUTLINE) WITH A COMPARATIVELY INCREASED NUMBER OF IBA-1-POSITIVE CELLS ADJACENT TO THE LIMITING PLATE (BLUE CIRCLES) AND WITHIN VASCULAR LUMENS (RED CIRCLES). CV = CENTRAL VEIN. IHC STAINING AT 200X MAGNIFICATION..... 90

FIGURE 46: A. PHOTOMICROGRAPH OF A NORMAL DOG LIVER (CONTROL NO. 4) SHOWING A PORTAL TRACT WITH MAC387-POSITIVE LEUCOCYTES PRESENT IN THE PERIVASCULAR INTERSTITIUM WITH MAGNIFIED VIEWS (BLACK CIRCLE). PV = PORTAL VEIN. IHC STAINING AT 200X MAGNIFICATION. **B.** PHOTOMICROGRAPH OF AN INFECTED DOG LIVER (CASE NO. 59) SHOWING A PORTAL TRACT WITH A COMPARATIVELY INCREASED NUMBER OF MAC387-POSITIVE LEUCOCYTES PREDOMINANTLY WITHIN VASCULAR LUMENS (BLUE CIRCLE), AND ALSO WITHIN THE PERIVASCULAR AND PERIDUCTULAR INTERSTITIUM (RED CIRCLES). PV = PORTAL VEIN, BD = BILE DUCT. IHC STAINING AT 200X MAGNIFICATION. 92

FIGURE 47: A. PHOTOMICROGRAPH OF A NORMAL DOG LIVER (CONTROL NO. 2) SHOWING A MIDZONAL AREA WITH MAC387-POSITIVE LEUCOCYTES PRESENT WITHIN SINUSOIDAL LUMENS (RED CIRCLES) WITH MAGNIFIED VIEWS (BLACK CIRCLES). IHC STAINING AT 200X MAGNIFICATION. **B.** PHOTOMICROGRAPH OF AN INFECTED DOG LIVER (CASE NO. 50) SHOWING A MIDZONAL AREA WITH AN INCREASED NUMBER OF MAC387-POSITIVE LEUCOCYTES, PARTICULARLY PROMINENT WITHIN SINUSOIDAL LUMENS (RED CIRCLE) WITH MAGNIFIED VIEWS (BLACK CIRCLE). IHC STAINING AT 200X MAGNIFICATION. 92

FIGURE 48: A. PHOTOMICROGRAPH OF A NORMAL DOG LIVER (CONTROL NO. 2) SHOWING A CENTRIOBULAR AREA (BLACK CIRCLE) WITH A SINGLE MAC387-POSITIVE LEUCOCYTE WITHIN THE LUMEN OF THE CENTRAL VEIN (BLUE CIRCLE). CV = CENTRAL VEIN. IHC STAINING AT 200X MAGNIFICATION. **B.** PHOTOMICROGRAPH OF AN INFECTED DOG LIVER (CASE NO. 117) SHOWING A CENTRIOBULAR AREA (BLACK CIRCLE) WITH A COMPARATIVELY INCREASED NUMBER OF MAC387-POSITIVE LEUCOCYTES, ESPECIALLY PROMINENT WITHIN THE LUMEN OF THE CENTRAL VEIN (BLUE CIRCLE); THERE ARE ALSO A FEW SCATTERED POSITIVE CELLS IN THE PERIVASCULAR CONNECTIVE TISSUE (RED CIRCLES). CV = CENTRAL VEIN. IHC STAINING AT 200X MAGNIFICATION. 93

FIGURE 49: A. PHOTOMICROGRAPH OF A NORMAL DOG LIVER (CONTROL NO. 9) SHOWING A PORTAL TRACT WITH MUM-1-POSITIVE PLASMA CELLS AND B-LYMPHOCYTES IN THE PERIVASCULAR AND PERIDUCTAL CONNECTIVE TISSUE (RED CIRCLES). THERE IS NON-SPECIFIC LABELING OF PLASMA (BLACK STAR). PV = PORTAL VEIN, BD = BILE DUCT, HA = HEPATIC ARTERY. IHC STAINING AT 400X MAGNIFICATION. **B.** PHOTOMICROGRAPH OF AN INFECTED DOG LIVER (CASE NO. 117) SHOWING A PORTAL TRACT WITH A COMPARATIVELY INCREASED NUMBER OF MUM-1-POSITIVE CELLS, PARTICULARLY OBVIOUS IN THE PERIDUCTAL AND PERIVASCULAR CONNECTIVE TISSUE. THERE IS EXTENSIVE NON-SPECIFIC LABELING OF HEPATOCYTES AND PLASMA (BLACK STARS). PV = PORTAL VEIN, BD = BILE DUCT. IHC STAINING AT 400X MAGNIFICATION. 95

FIGURE 50: A. PHOTOMICROGRAPH OF A NORMAL DOG LIVER (CONTROL NO. 2) SHOWING A MIDZONAL AREA WITH SCARCE MUM-1-POSITIVE PLASMA CELLS AND B-LYMPHOCYTES (YELLOW CIRCLES) WITH MAGNIFIED VIEWS (BLACK CIRCLES). THERE IS NON-SPECIFIC LABELING OF PLASMA IN SINUSOIDS (BLACK STARS). IHC STAINING AT 400X MAGNIFICATION. **B.** PHOTOMICROGRAPH OF AN INFECTED DOG LIVER (CASE NO. 110) SHOWING A MIDZONAL AREA WITH COMPARATIVELY INCREASED SINUSOID-ASSOCIATED MUM-1-POSITIVE CELLS (RED CIRCLES) WITH MAGNIFIED VIEWS (BLACK CIRCLES). THERE IS NON-SPECIFIC LABELING OF HEPATOCYTES AND PLASMA IN THE IMAGE (BLACK STARS). IHC AT 400X MAGNIFICATION. 95

FIGURE 51: A. PHOTOMICROGRAPH OF A NORMAL DOG LIVER (CONTROL NO. 2) SHOWING A CENTRIOBULAR AREA WITH SCARCE MUM-1-POSITIVE PLASMA CELLS AND B-LYMPHOCYTES IN THE PERIVASCULAR INTERSTITIUM (YELLOW CIRCLE). THERE IS NON-SPECIFIC LABELING OF HEPATOCYTES (BLACK STARS). CV = CENTRAL VEIN. IHC STAINING AT 400X MAGNIFICATION. **B.** PHOTOMICROGRAPH OF AN INFECTED DOG LIVER (CASE NO. 110) SHOWING A CENTRIOBULAR AREA WITH A COMPARATIVELY INCREASED NUMBER OF MUM-1-POSITIVE CELLS (MAINLY PLASMA CELLS) IN THE PERIVASCULAR INTERSTITIUM. THERE IS NON-SPECIFIC LABELING OF HEPATOCYTES AND PLASMA (BLACK STARS). CV = CENTRAL VEIN. IHC STAINING AT 400X MAGNIFICATION. 96

LIST OF TABLES

TABLE 1: LIST OF SELECTED LEUCOCYTE ANTIBODIES AND IMMUNOHISTOCHEMICAL METHODS USED ON LIVER SPECIMENS FROM HEALTHY CONTROL DOGS AND DOGS NATURALLY INFECTED WITH <i>BABESIA ROSSI</i> .	46
TABLE 2: A SUMMARY OF THE LIVER-SPECIFIC SERUM HAEMATOLOGY RESULTS FROM THE CONTROL AND <i>B. ROSSI</i> -INFECTED CASES. THE LAB-SPECIFIC REFERENCE RANGE, MEDIAN AND RANGE OF BOTH THE CONTROL (N=4) AND <i>B. ROSSI</i> -INFECTED CASES (N=10) IS LISTED BELOW WITH THE <i>P</i> -VALUE COMPARING THE CONTROL AND INFECTED CASES.	49
TABLE 3: A SUMMARY OF THE LIVER-SPECIFIC SERUM HAEMATOLOGY RESULTS FROM THE CONTROL AND <i>B. ROSSI</i> -INFECTED CASES. THE LAB-SPECIFIC REFERENCE RANGE, MEDIAN AND RANGE OF BOTH THE CONTROL (N=4) AND <i>B. ROSSI</i> -INFECTED CASES (N=10) IS LISTED BELOW WITH THE <i>P</i> -VALUE COMPARING THE CONTROL AND INFECTED CASES.	50
TABLE 4: QUANTIFICATION OF SELECTED IMMUNOHISTOCHEMICALLY LABELLED LEUCOCYTES IN THE CONTROL DOG LIVER SPECIMENS (N=4). THE MEDIAN NUMBER, STANDARD DEVIATION, AND MINIMUM AND MAXIMUM NUMBER OF LEUCOCYTES OF EACH PHENOTYPE PER HIGH POWER FIELD/HPF (400X MAGNIFICATION) ARE LISTED FOR EACH HEPATIC ZONE (CENTRILOBULAR, MIDZONAL OR PORTAL). ALL VALUES REPRESENT ABSOLUTE CELL COUNTS.	77
TABLE 5: QUANTIFICATION OF SELECTED IMMUNOHISTOCHEMICALLY LABELLED LEUCOCYTES IN THE CONTROL DOG LIVER SPECIMENS (N=4). THE MEDIAN NUMBER, STANDARD DEVIATION, AND MINIMUM AND MAXIMUM NUMBER OF POSITIVE CELLS ARE LISTED IN THE LIVER AS A WHOLE (NON-ZONAL). ALL VALUES REPRESENT ABSOLUTE CELL COUNTS.	78
TABLE 6: QUANTIFICATION OF CD3-IMMUNOREACTIVE T-LYMPHOCYTES IN THE <i>B. ROSSI</i> -INFECTED LIVERS (N=10) COMPARED TO THE CONTROLS (N=4). THE MEDIAN NUMBER OF POSITIVE CELLS (PER HPF/400X MAGNIFICATION) PER HEPATIC ZONE (PORTAL TRACT, MIDZONAL AND CENTRILOBULAR), AS WELL AS THE <i>P</i> -VALUES ARE LISTED. ALL VALUES REPRESENT ABSOLUTE CELL COUNTS.	79
TABLE 7: QUANTIFICATION OF CD20-IMMUNOREACTIVE B-LYMPHOCYTES AND PLASMA CELLS IN THE <i>B. ROSSI</i> -INFECTED LIVERS (N=10) COMPARED TO THE CONTROLS (N=4). THE MEDIAN NUMBER OF POSITIVE CELLS (PER HPF/400X MAGNIFICATION) PER HEPATIC ZONE (PORTAL TRACT, MIDZONAL AND CENTRILOBULAR), AS WELL AS THE <i>P</i> -VALUES ARE LISTED. ALL VALUES REPRESENT ABSOLUTE CELL COUNTS.	82
TABLE 8: QUANTIFICATION OF CD204-IMMUNOREACTIVE MACROPHAGES IN THE <i>B. ROSSI</i> -INFECTED LIVERS (N=10) COMPARED TO THE CONTROLS (N=4). THE MEDIAN NUMBER OF POSITIVE CELLS (PER HPF/400X MAGNIFICATION) PER HEPATIC ZONE (PORTAL TRACT, MIDZONAL AND CENTRILOBULAR), AS WELL AS THE <i>P</i> -VALUES ARE LISTED. ALL VALUES REPRESENT ABSOLUTE CELL COUNTS.	85
TABLE 9: QUANTIFICATION OF IBA-1-IMMUNOREACTIVE MONOCYTE-MACROPHAGES AND DENDRITIC CELLS IN THE <i>B. ROSSI</i> -INFECTED LIVERS (N=10) COMPARED TO THE CONTROLS (N=4). THE MEDIAN NUMBER OF POSITIVE CELLS (PER HPF/400X MAGNIFICATION) PER HEPATIC ZONE (PORTAL TRACT, MIDZONAL AND CENTRILOBULAR), AS WELL AS THE <i>P</i> -VALUES ARE LISTED. ALL VALUES REPRESENT ABSOLUTE CELL COUNTS.	88
TABLE 10: QUANTIFICATION OF MAC387-IMMUNOREACTIVE LEUCOCYTES (PREDOMINANTLY MONOCYTE-MACROPHAGES**) IN THE <i>B. ROSSI</i> -INFECTED LIVERS (N=10) COMPARED TO THE CONTROLS (N=4). THE MEDIAN NUMBER OF POSITIVE CELLS (PER HPF/400X MAGNIFICATION) PER HEPATIC ZONE (PORTAL TRACT, MIDZONAL AND CENTRILOBULAR), AS WELL AS THE <i>P</i> -VALUES ARE LISTED. ALL VALUES REPRESENT ABSOLUTE CELL COUNTS.	91
TABLE 11: QUANTIFICATION OF MUM-1-IMMUNOREACTIVE PLASMA CELLS AND MATURE B-LYMPHOCYTES IN THE <i>B. ROSSI</i> -INFECTED LIVERS (N=10) COMPARED TO THE CONTROLS (N=4). THE MEDIAN NUMBER OF POSITIVE CELLS (PER HPF/400X MAGNIFICATION) PER HEPATIC ZONE (PORTAL TRACT, MIDZONAL AND CENTRILOBULAR), AS WELL AS THE <i>P</i> -VALUES ARE LISTED. ALL VALUES REPRESENT ABSOLUTE CELL COUNTS.	94
TABLE 12: QUANTIFICATION OF IMMUNOPHENOTYPED LEUCOCYTES IN THE CONTROL (N=4) AND <i>B. ROSSI</i> -INFECTED (N=10) LIVER SAMPLES. THE MEDIAN NUMBER OF POSITIVE CELLS (PER HPF/400X MAGNIFICATION) PER HEPATIC ZONE (PORTAL TRACT, MIDZONAL AND CENTRILOBULAR), AS WELL AS THE STANDARD DEVIATION, MINIMUM AND MAXIMUM NUMBER OF POSITIVE CELLS, <i>P</i> -VALUE, AND MAGNITUDE OF INCREASE ARE LISTED. ALL VALUES REPRESENT ABSOLUTE CELL COUNTS.	97
TABLE 13: QUANTIFICATION OF IMMUNOPHENOTYPED LEUCOCYTES OF THE CONTROL (N=4) AND <i>B. ROSSI</i> -INFECTED (N=10) LIVER SAMPLES. THE MEDIAN NUMBER OF POSITIVE CELLS (PER HPF/400X MAGNIFICATION) IN THE LIVER AS A WHOLE (NON-ZONAL), AS WELL AS THE STANDARD DEVIATION, MINIMUM AND MAXIMUM NUMBER OF POSITIVE CELLS, <i>P</i> -VALUE, AND MAGNITUDE OF INCREASE ARE LISTED. ALL VALUES REPRESENT ABSOLUTE CELL COUNTS.	98

ABBREVIATION LIST

ALI = acute lung injury
ALT = alanine aminotransferase
ARC = absolute reticulocyte count
ARDS = acute respiratory distress syndrome
AST = aspartate aminotransferase
ATP = adenosine triphosphate
BSA = bovine serum albumin
BD = bile duct
CBC = complete blood count
CNS = central nervous system
CO = carbon monoxide
cPL = canine pancreatic lipase
CRP = C-reactive protein
CV = central vein
DAB = diaminobenzidine tetrachloride
DIC = disseminated intravascular coagulation
DNA = deoxyribonucleic acid
DPS = Department of Paraclinical Sciences
EDTA = ethylenediaminetetraacetic acid
EMH = extramedullary haematopoiesis
FDP's = fibrinogen degradation products
FVS = Faculty of Veterinary Sciences
HA = hepatic artery
Hct = haematocrit
HE = haematoxylin and eosin
HPF = high power field
IFN = interferon
IHC = immunohistochemistry
IL = interleukin
IMHA = immune-mediated haemolytic anaemia
L = lymphatic
LDH = lactate dehydrogenase
LGL = large granular lymphocyte
GGT = γ -Glutamyl-transpeptidase
GSS = Gordon and Sweets' silver
LFB = Luxol Fast Blue
M = molar
MODS = multiple organ dysfunction syndrome
MSB = Martius Scarlet Blue
MSR1 = macrophage scavenger receptor 1
NET = neutrophil extracellular trap
NK = natural killer
NO = nitric oxide
OVAH = Onderstepoort Veterinary Academic Hospital
PAMP = pathogen-associated molecular pattern
PBS = phosphate buffered saline
PCR = polymerase chain reaction
PEPCK = phosphoenolpyruvate carboxykinase
Perls' = Perls' Prussian Blue

PRR = pattern recognition receptor
PT = portal tract
PT = prothrombin time
PV = portal vein
RBC = red blood cell count
RLB = reverse line blot
ROS = reactive oxygen species
SAA = serum amyloid A
SAP = serum amyloid P
SIRS = systemic inflammatory response syndrome
SOP = standard operating procedure
SRA = scavenger receptor A
sSDMA = symmetric dimethylarginine
TGF- β = transforming growth factor- β
TLR = toll-like receptor
TNF- α = tumour necrosis factor α
TSP = total serum protein
UDP-glucuronyltransferase = Uridine 5'-diphospho-glucuronosyltransferase
UP = University of Pretoria
UPC = urine protein:creatinine
WBC = white blood cell count

SUMMARY

LIVER HISTOPATHOLOGY IN DOGS WITH NATURALLY ACQUIRED *BABESIA ROSSI* INFECTION

by

Heidi Horrell

Supervisor: Prof A L Leisewitz
Co-supervisor: Dr S J Clift
Department: Companion Animal Clinical Studies
Degree: MSc

Canine babesiosis, which, in sub-Saharan Africa, is caused by the tick-transmitted intraerythrocytic protozoan *Babesia rossi*, is one of the most common, clinically important tick-borne diseases of dogs in the region. The disease in dogs occurs in two forms, namely uncomplicated and complicated babesiosis. In the former, clinical signs are usually attributable to the effects of hemolysis. In complicated canine babesiosis, the disease is attributable to the host's immune response, with overwhelming systemic inflammation and multiple organ dysfunction being associated with high morbidity and mortality. The clinicopathological changes associated with complicated canine babesiosis are similar to those reported in fatal malaria and sepsis in humans. There are not many reports on the pathology of the liver in babesiosis and malaria. For the purpose of this study, liver samples were collected from 10 dogs with fatal babesiosis. Haematology, serum biochemistry and histologic data were compared with four healthy control dogs that were sourced from an animal shelter. The most significant elevations in haematology values were decreases in red cell count, haematocrit and platelet concentration, while the most significant increases in biochemistries were increases in ALT and urea. The most significant histologic lesions in the *Babesia*-infected dogs included dilation of the spaces of Disse due to oedema, cholestasis, hypertrophic Kupffer cells containing bile and haemosiderin pigments, central venous and sinusoidal congestion, multifocal centrilobular necrosis, inflammatory cell infiltrates consisting mostly of monocyte-macrophages (as determined by MAC387, Iba-1 and CD204), and evidence of significant extramedullary haematopoiesis. The hepatocytes showed numerous signs of cell injury such as presence of vesicular nuclei, hydropic vacuolation and anisokaryosis. Most of these changes can be ascribed to severe haemolysis and the associated hypoxia. Similar findings have been shown in the limited histomorphological studies on babesiosis, human malaria, and in patients with sepsis. These results are also complimentary of previous studies involving inflammatory cytokines and chemokines observed during the course of babesiosis, with the most significant increases being IL-6, IL-10, MCP-1, and TNF- α , all of which are monocyte-specific. These findings aid us in the understanding of the pathomechanisms behind the disease and enable us better treat the symptoms that present.

1. INTRODUCTION

Canine babesiosis is one of the most important tick-borne diseases in dogs caused by the intraerythrocytic protozoan *Babesia* belonging to the family Piroplasmida (Saari et al., 2018) and is transmitted by ixodid ticks. In South Africa, the two species that are most commonly dealt with are *Babesia rossi*, transmitted by *Haemaphysalis elliptica* and *H. leachi*, and *Babesia vogelli*, transmitted by *Rhipicephalus sanguineus* - *Babesia rossi* being the more virulent of the two and causing more severe clinical disease (Leisewitz et al., 2019b). The *Babesia* species invade the red blood cells of the dogs which results in a progressive anaemia and haemolysis (Schoeman, 2009). It can range in severity from subclinical to severe, depending on the age of the infected animal, immune status, splenectomy, and infection with concurrent diseases (Schoeman, 2009). The clinical signs that infected dogs present with are mostly due to the effects of the induced haemolysis. They vary depending on duration and progression, but are generally non-specific and range between: lethargy, anaemia, depression, pale mucous membranes, tachycardia, tachypnoea, anorexia, vomiting, splenomegaly, fever and weakness (Schoeman, 2009, Bilić et al., 2018). In more severe cases, jaundice, hypoalbuminaemia, hyperbilirubinaemia, haemoglobinuria or lymphadenomegaly may also be present (Weese and Evason, 2020, Bilić et al., 2018).

Babesia has been proven to be related morphologically, functionally and phylogenetically to the protozoal species *Plasmodium* - the cause of human malaria (Bilić et al., 2018). Because these two intra-erythrocytic protozoans have been proven to be so similar and have similar inflammatory processes, both diseases cause similar outcomes for those infected. Because of this fact, we are able to use the information gathered in studies about human *Plasmodium falciparum* in order to hypothesize what the histopathology of the liver in canine babesiosis will look like.

From a histopathological perspective in a murine model, there were varying degrees of diffuse non-suppurative, peri-portal and centrilobular hepatitis ranging in severity from mild to necrotic, with condensation of cell cytoplasm, karyolysis, pyknosis and karyorrhexis. With an increase in chronicity of the disease, the liver lesions extended outwards from the central lobules resulting in focal necrotic lesions (Hussein, 1977). Human-infected *Plasmodium falciparum* livers showed there was little change to the endothelial cells and hepatocytes, as well as a lack of fatty change or biliary duct proliferation (Viriyavejakul et al., 2014). Marked Kupffer cell hyperplasia containing haemazoin pigment, portal tract inflammation, steatosis and sinusoidal congestion that increased with the severity of the disease was present (Rupani and Amarapurkar, 2009). Those patients with hyperbilirubinaemia had increased amounts of haemazoin pigment deposition and hyperplastic Kupffer cells, increased numbers of inflammatory cells within the portal tract (mainly lymphocytes and plasma cells), and their sinusoidal areas were congested compared to the patients without (Viriyavejakul et al., 2014). Liver cell necrosis seems to be an inconsistent finding amongst studies, with some exhibiting as high as 41% (Rupani and Amarapurkar, 2009), while others have none (Viriyavejakul et al., 2014). The necrosis observed was not due to inflammation but was rather a coagulative necrosis with the cell membranes all preserved. Focal centrivascular necrosis present in one study done in Thai adults may have resulted from a lack of blood flow to the liver due to shock or due to parasitized erythrocytes sequestering in the micro-circulation leading to ischaemia of certain areas (Rupani and Amarapurkar, 2009). Kupffer cell and portal tract lymphocyte apoptosis was markedly increased in specimens with hyperbilirubinaemia compared to those without, while these specimens also showed increased numbers of apoptosis compared to the non-infected control group (Viriyavejakul et al., 2014).

The consensus in most of the studies seemed to be that the extent of the liver damage is positively correlated with the degree of intravascular haemolysis present (Dey et al., 2012).

Babesiosis can infect a wide range of vertebrate hosts, including humans, and therefore has significant importance worldwide (Bilić et al., 2018). The histopathology of the liver in canine babesiosis will have

to be examined to be able to accurately describe how *Babesia rossi* affects it, as there is currently no data available on the subject. This will aid in the understanding of the disease as a whole if we are able to visualize and try to understand the pathomechanisms behind it.

2. JUSTIFICATION

2.1 LITERATURE REVIEW

2.1.1 Structure and function of the liver

2.1.1.1 Gross anatomy of the canine liver

The liver is the largest internal organ in the body, contributing up to 2% of body weight and occupying the cranial abdomen caudal to the diaphragm (Brown, 2017). It is held in place by multiple ligaments, namely: the coronary and triangular ligaments attaching it to the diaphragm, the falciform ligament attaching it to the ventral abdomen, the round ligament (umbilical vein remnant) which is found within the falciform ligament, the gastrohepatic ligament attaching it to the stomach, and the hepatoduodenal ligament between the liver and the duodenum. The latter is the thickest ligament, containing nerves, lymphatic vessels, the common bile duct, the hepatic artery and the portal vein (Sleight and Thomford, 1970, Brown, 2017).

The liver has a smooth capsular surface, the parenchyma consisting of red-brown tissue that is divided into six lobes. These lobes are divided into three main components. The first component consists of the right-lateral and caudate lobes (the latter includes the papillary process). The central component comprises the right-central and quadrate lobes. Underneath these two lobes, is where the gall bladder sits in its fossa. The third component consists of the left-lateral and left-central lobes (Figure 1) (Sleight and Thomford, 1970).

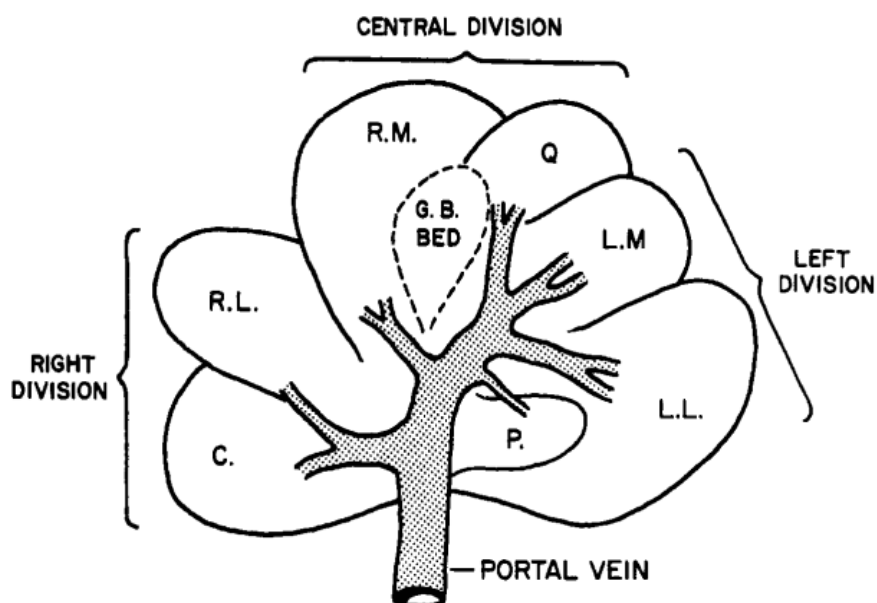


Figure 1: Schematic diagram showing the three major divisions of the canine liver and the individual lobes of each division. The branches of the portal vein are also depicted. C. = caudate lobe, R.L. = right lateral lobe, R.M. = right middle lobe, RM = right middle lobe, Q. = quadrate lobe, L.M. = left middle lobe, L.L. = left lateral lobe, P = papillary process, G.B = gall bladder. (Permission for use granted by Copyright Clearance Center's RightsLink® on 30/03/2023). Source: (Sleight and Thomford, 1970).

Portal veins:

The main portal vein runs within the hepatoduodenal ligament before splitting into branches to supply different parts of the liver. The right branch of the portal vein supplies blood to the right component of the liver, while the larger left branch divides again to supply the central and left components (Sleight

and Thomford, 1970). The portal vein supplies 70-80% of afferent blood flow to the liver after draining the intestinal tract (Brown, 2017).

Hepatic arteries:

The abdominal aorta gives rise to the celiac artery at the level of the first lumbar vertebrae, then branching to become the hepatic artery. It supplies the remaining 20-30% of the afferent blood flow to the liver (Brown, 2017). The arteries are also divided to supply the 3 components of the liver, the first branch supplying the right component (right lateral and caudate lobes), the second supplying the left component (left lateral, left central and the papillary process of the caudate lobe), while the third branch supplies the central component (right medial and quadrate lobes) (Sleight and Thomford, 1970).

Hepatic veins:

The hepatic veins drain blood from each component of the liver. The number, location and size of these veins differs among animals (Sleight and Thomford, 1970). The hepatic vein is very short and joins with the caudal vena cava soon after leaving the liver (Brown, 2017).

Bile ducts:

The gall bladder is connected to the extrahepatic bile ducts through a single cystic duct to join the common hepatic duct, which then forms the common bile duct (Sleight and Thomford, 1970). In dogs, the common bile duct runs from the end of the cystic duct to the duodenum and receives all the branches that drain the various components of the liver (McIntyre, 2008). The last part of the common bile duct then leads into the duodenum at the papilla of Vater along with the Sphincter of Oddi (McIntyre, 2008).

2.1.1.2 Liver function

Carbohydrates:

Metabolic zonation of the liver has been shown for many metabolic activities, such as the metabolism of carbohydrates, amino acids, lipids, ammonia and xenobiotic substances (Kietzmann, 2017). This allows for multiple opposing metabolic processes to occur simultaneously within the liver lobule. The liver plays a major role in maintaining blood glucose levels over short and long periods of time, as well as controlling carbohydrate metabolism.

To regulate the glucose concentration in the blood, the liver has three main mechanisms which constantly run in parallel to maintain a steady state, namely glycogenesis, glycogenolysis, and gluconeogenesis. Glycogenesis refers to the formation of glycogen (the storage form of glucose) from glucose molecules, whereas glycogenolysis is the process whereby glycogen is broken down into bio-available glucose (Postic et al., 2004). Gluconeogenesis is the process whereby non-carbohydrate substances (lactate, amino acids and glycerol) are converted into glucose (Zhang et al., 2019). These mechanisms are controlled by the hormones insulin, glucagon and glucocorticoids. Glycogenesis has been associated with the centrilobular hepatocytes, where higher concentrations of the enzymes responsible for the synthesis of glycogen (glucokinase and pyruvate kinase) have been isolated. Glycogenolysis and gluconeogenesis have been found to occur primarily in the periportal hepatocytes, where higher concentrations of the enzymes responsible for glucose output (glucose-6-phosphatase, fructose 1,6 bisphosphatase and phosphoenolpyruvate carboxykinase (PEPCK)) have been isolated (Jungermann, 1988). The metabolic zonation of these three processes is largely dependent on the oxygen gradient within the liver acinus, and an important physiological feature in maintaining blood adequate glucose levels (McIntyre, 2008, Jungermann, 1988).

Hepatic glycogen metabolism is co-ordinated by two main enzymes: glycogen synthase (pivotal in glycogenesis) and glycogen phosphorylase (pivotal in glycogenolysis) (McIntyre, 2008). High blood concentrations of insulin is the stimulus for release of glycogen synthase, while hyperglycaemia inhibits glycogen phosphorylase. Thus, glycogen synthesis is mediated by portal vein hyperglycaemia (McIntyre, 2008).

While fasting, the liver is responsible for ensuring that the central nervous system is supplied with enough glucose, as well as maintaining the fasting plasma glucose levels. It will process 25-33% of ingested carbohydrates (namely glucose and fructose) within the first five hours post-prandially, using 20-30% of this amount to restore hepatic glycogen (Brown, 2017, Postic et al., 2004). Once homeostatic glucose concentrations have been achieved, the amount in excess is oxidized to become fatty acids or converted to fat by the synthesis of lipids (McIntyre, 2008, Brown, 2017).

Proteins, clotting factors and urea metabolism:

The liver is responsible for the synthesis of the majority of plasma proteins such as albumin, multiple transport proteins, some of the clotting factors (II, V, VII-XIII), lipoproteins, fibrinolysis proteins, acute phase proteins and some components of the complement system (Brown, 2017). It plays a crucial role in the catabolism and anabolism of serum proteins, and although none of the changes within the serum protein levels are liver specific, low albumin and high gamma globulin levels are commonly used as indicators of liver function (Brown, 2017).

The liver also is a major source of both pro-coagulant proteins as well as the compounds responsible for fibrinolysis. Because products of the liver play a part in both the formation of blood clots as well as clot lysis, it controls coagulation homeostasis, therefore hepatic disease can present with a multitude of complex coagulopathies (Roberts and Cederbaum, 1972).

The majority of plasma procoagulant proteins (factors II, V, VII, IX, X, XI, XIII) are produced by the hepatic parenchymal cells (Prins et al., 2010). The liver is also the site of fibrinogen synthesis, the stimulus for production being an increase in fibrinogen degradation products (FDPs), rather than a decrease in the concentration of plasma fibrinogen (McIntyre, 2008). The liver is also responsible for clearing procoagulant proteins from the blood circulation in order to maintain fluidity of the blood within the vasculature (Prins et al., 2010). Hepatocytes are also the site of production of plasminogen, the inactive precursor of plasmin, a major fibrinolytic enzyme.

The liver is also the primary site of ammonia metabolism, which is formed from the breakdown of amino acids. Ammonia, which is highly toxic, is converted to urea through the urea cycle which occurs in the liver, and is then excreted in the urine (Brown, 2017). Ureagenesis is restricted to the periportal hepatocytes, and any excess ammonia will be reabsorbed by the centrilobular hepatocytes to prevent build-up (Kietzmann, 2017). Hepatic disease results in decreased ammonia metabolism, and the resultant hyperammonaemia may lead to neurological signs, known as hepatic encephalopathy (Ong et al., 2003).

Bile synthesis:

The main exocrine function of the liver is bile secretion and excretion (Brown, 2017). Bile is an aqueous solution that contains high concentrations of physiological waste such as excess cholesterol, bilirubin, heavy metals, xenobiotics, water, bile acids and other substances (Dawson, 2018). Bile also aids in the process of digestion, particularly of lipids, plays a role in neutralizing the acid pH of the gastric ingesta (Brown, 2017), as well as having an innate immune function (Dawson, 2018).

Bile acids are composed of cholesterol which is conjugated in the liver. They are secreted into the bile canaliculi from the hepatocytes, creating an osmotic concentration gradient between the two

structures, resulting in water following into the bile canaliculi. 95% of the bile acids are then recycled, being reabsorbed into the portal blood from the ileum, and re-secreted into the bile. This process is known as “enterohepatic circulation” (Brown, 2017). The remaining 5% of the bile acids that are not reabsorbed within the intestines are excreted in the faeces (Dawson, 2018).

Bilirubin metabolism:

Bilirubin is also a major component of bile, and is produced from the breakdown of haemoglobin subsequent to the degradation of senescent or abnormal erythrocytes (Brown, 2017). Erythrocytes are normally phagocytosed by macrophages within the spleen, bone marrow and liver resulting in the two main breakdown products: heme and globin. The globin is further degraded within macrophages, leaving the constituents to be filtered back into the amino acid pool to be recycled by the body. The iron component of heme is bound to iron-binding proteins and is also recycled by the body. The remaining portion is oxidized to form biliverdin and further reduced to bilirubin (Figure 2) (Brown, 2017).

There are three phases in bilirubin elimination from the body, namely uptake, conjugation, and excretion (Brown, 2017). Uptake involves the hepatocytes separating the bilirubin from the bilirubin-albumin complex to remove it from the circulation. Conjugation involves bilirubin being combined with glucuronic acid in the endoplasmic reticulum, making it water soluble and less toxic to the body. Excretion involves the active transport of bilirubin from the hepatocytes into the bile through the bile canaliculi. The last phase is the rate-limiting step in most species (Figure 2) (Brown, 2017).

Conjugated bilirubin is converted to urobilinogen within the gastrointestinal tract by resident bacteria. A small portion of urobilinogen is then reabsorbed into the portal blood, and transported back to the liver via enterohepatic circulation. The remaining larger portion of urobilinogen is re-secreted into the bile after absorption by the gastrointestinal tract. Small amounts of urobilinogen are normal in urine as it is filtered easily by the glomeruli in the kidneys, while the rest that is not absorbed from the intestine forms stercobilin which gives faeces its brown colour (Figure 2) (Brown, 2017).

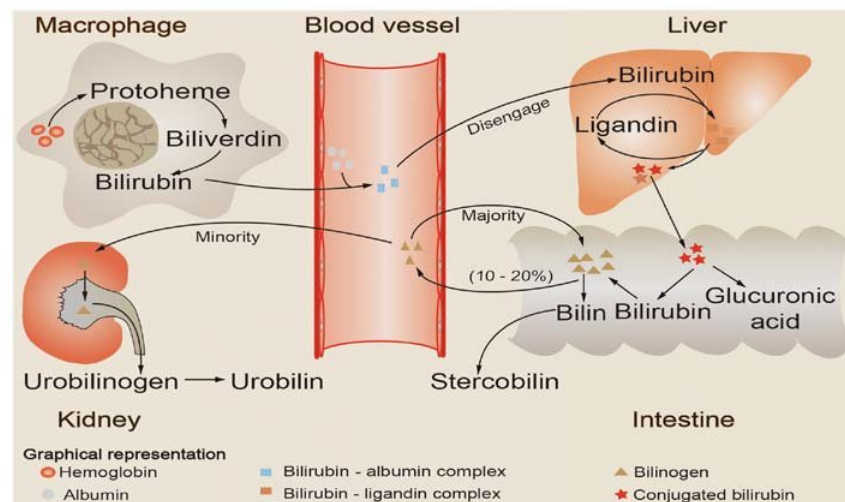


Figure 2: Schematic diagram showing bilirubin metabolism within the blood vessels, macrophages, liver, intestine and kidney. Senescent red blood cells are phagocytosed by mononuclear macrophages within the circulation, releasing haemoglobin. The haemoglobin is then catabolized to produce heme, which is then reduced and oxidized to bilirubin. The bilirubin is then bound to albumin and is transported to the liver, where it is separated again and taken up by the hepatocytes. It is transported to the smooth endoplasmic reticulum within the hepatocyte as a bilirubin-ligand complex, and is then combined with glucuronic acid to form conjugated bilirubin. This conjugated bilirubin is then released into the intestine with bile, hydrolyzed and reduced to create urobilinogen. The majority of urobilinogen (about 90%) is excreted in the faeces as stercobilin, with a small amount being reabsorbed into the circulation to be excreted with the bile, therefore forming the enterohepatic circulation. The remaining amount (about 10%) is excreted through the kidneys in the urine. (Permission granted for use by Spandidos Publications 03/02/2023). Source: (Wang et al., 2021)

Lipids:

The liver is involved in the production and degradation of plasma lipids, namely cholesterol, triglycerides, phospholipids and lipoproteins. It is important in fatty acid metabolism, as it can synthesize fatty acids during hyperglycaemia, and oxidize fatty acids in order to be used as an energy source during hypoglycaemia. Cholesterol is synthesized, secreted and broken down solely within the hepatocytes (McIntyre, 2008, Brown, 2017). Positive correlations between oxygen deprivation of the hepatocytes and fatty liver/steatosis have been discovered, while the enzymes responsible for lipid synthesis have been found in high concentrations within the centrilobular regions (Schleicher et al., 2015, Kietzmann, 2017).

Xenobiotic metabolism:

The term “xenobiotic” refers to any foreign substance not familiar to or not occurring within the normal metabolic pathways of a living organism (Evans, 2013). This includes drugs, insecticides and endogenous substances such as steroids which require conversion in order to be eliminated from the body. Within the hepatocytes, the smooth endoplasmic reticulum employs P450 enzymes to metabolize these substances for excretion from the body in the bile or urine (Brown, 2017).

Immune function:

The liver plays an important role in immunity - systemically, locally and through mucosal immunity. It is the first organ to encounter foreign antigens originating from the gastrointestinal tract, containing the highest number of cells (in most species) belonging to the innate immune system (approximately 10% of the total cells found in the liver). These cells include Kupffer cells, hepatic large granular lymphocytes (LGLs)/natural killer (NK) cells, and mononuclear phagocytes, and are present in higher numbers in comparison to cells of the adaptive immune system (T- and B-lymphocytes) (Brown, 2017). Systemically, the liver is responsible for the synthesis of acute phase proteins, the three most important in dogs being serum amyloid A (SAA), C-reactive protein (CRP), and serum amyloid P (SAP).

The Kupffer cells that line the sinusoids of the liver provide an important defence against infectious agents, endotoxins and foreign materials absorbed from the intestines in all domestic species. Pigs, goats and cattle have pulmonary intravascular macrophages within the alveolar capillaries that perform the same function, and are therefore less reliant on their hepatic Kupffer cells as a first line of defence in comparison to dogs (Brain et al., 1999).

Extramedullary haematopoiesis (EMH):

Extramedullary haematopoiesis (EMH) is defined as the production and development of blood cells outside of the bone marrow (Johns and Christopher, 2012). This generally occurs secondary to inflammatory conditions and a variety of myeloproliferative and lymphoproliferative disorders that reactivate the stem cells. Stem cell reactivation, and therefore EMH, can occur in any tissue, however the liver and spleen are the two organs in which it is most common. Other organs include the myocardium, lungs, kidneys, small intestine, skeletal muscle, adrenal glands, lymph nodes, peritoneum and adipose tissue. Activated macrophages could possibly play a role in reactivating stem cells, due to their wide distribution throughout the body and their ability to induce stromal proliferation (Johns and Christopher, 2012). Hepatic EMH most commonly occurs in the sinusoidal areas, but has also been found in perisinusoidal and portal areas. The exact mechanism to induce EMH has been narrowed down to five possible causes: bone marrow failure; bone marrow stimulation; chronic hypoxia stimulating erythropoiesis; tissue inflammation, injury or repair; and abnormal systemic or localized chemokine production (Johns and Christopher, 2012).

2.1.1.3 Histology of the canine liver

The liver is surrounded by a thin Glisson's capsule which consists of collagen fibres, fibroblasts, myofibroblasts, small blood vessels and lymphatics. The three main components of the hepatic parenchyma are the portal tracts, the centrilobular veins, and the lobular parenchyma, comprising 3%, 4% and 93% of the total hepatic parenchyma, respectively (McIntyre, 2008). The structural unit of the liver parenchyma is a hexagonal unit referred to as a lobule. It comprises a branch of the hepatic vein (referred to as the central vein) which is located in the middle of the lobule. At each of the six points of the hepatic lobule is a portal tract or portal triad, which contains branches of the hepatic artery and portal vein, bile ducts, lymphatics, nerves, and a few lymphocytes, surrounded by fibroblasts and loose connective tissue (Figures 3-4). 700000 lobules make up the liver parenchyma, each lobule measuring between 0.5-2.0mm in diameter (Brown, 2017). Lobules can be further subdivided into portal, midzonal and centrilobular zones. Running between the unicellular cords of hepatocytes that make up the hepatic parenchyma are vascular sinusoids that allow for the exchange of nutrients between the blood and hepatocytes through fenestrated endothelium (McIntyre, 2008).

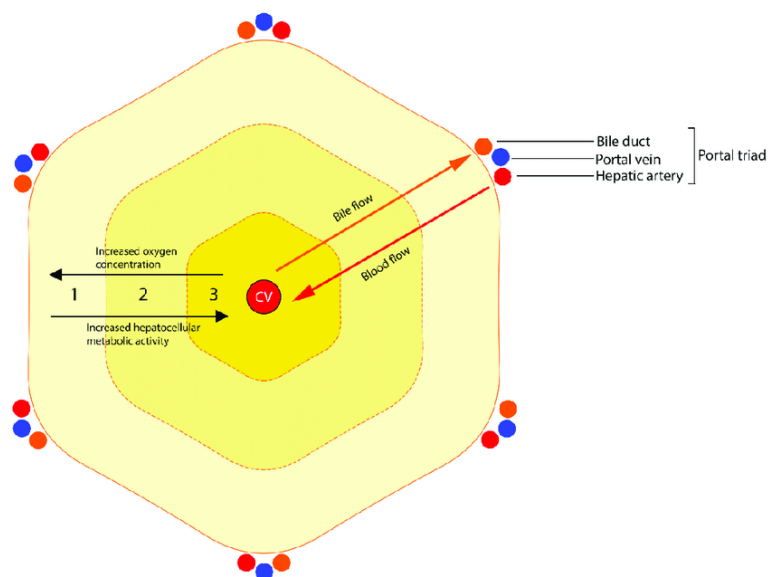


Figure 3: Schematic diagram showing the hepatic lobule, its microscopic zones and metabolic functions. (Permission granted for use by Elsevier 03/02/2023). Source: (Manthorpe et al., 2020)

Another way of viewing the liver is as a bile-secreting gland, which consists of acini as the subunit of the parenchyma instead of hepatic lobules (Brown, 2017). The acini are diamond-shaped with afferent branches of the portal vein and hepatic artery at the centre, and the "central vein" (branch of the hepatic vein) located at the periphery. Each central vein drains the blood from the multiple acini surrounding it. The acini can also be divided into three zones: zone 1 surrounding the afferent blood arriving from the hepatic artery and portal vein, zone 2 in the middle, and zone 3 surrounding the branch of the hepatic vein (Brown, 2017). Bile flows from the biliary canaliculi of the hepatocytes in zone 3 through zones 2 and 1, and then into the bile ducts in the portal tracts (Figures 3-4) (Brown, 2017).

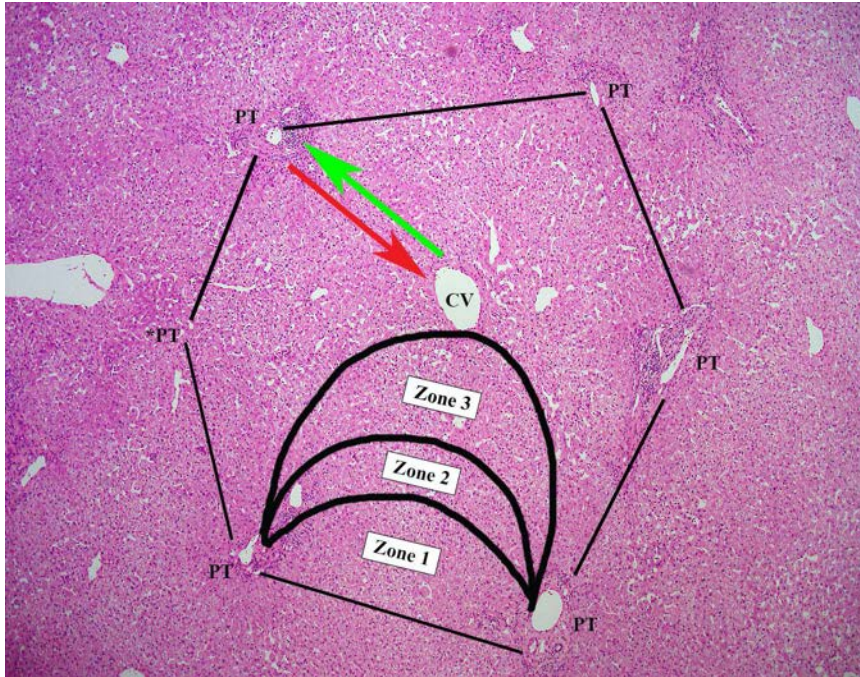


Figure 4: Photomicrograph of the liver showing a hepatic lobule with six portal tracts (PT) at the periphery and a central vein (CV) in the middle. Blood flows from the PT to the CV (red arrow), while bile flows in the opposite direction (green arrow). The acinus is indicated by the thicker curved lines comprising zones 1-3. Haematoxylin and eosin (HE) staining. (Photo courtesy of Dr Jennifer Findeis-Hosey, URM). Source: (Bell, 2020)

Hepatocytes:

Hepatocytes are polygonal in shape and contain pale eosinophilic cytoplasm with one or two round nuclei (Figure 5, Figure 8) (Bowen, 2020). Anastomosing cords or plates of hepatocytes radiate outwards from the central vein. Hepatocytes border either other hepatocytes (via their lateral face) or sinusoids (via their sinusoidal face) (WSAVA, 2006). A small portion of the lateral face is modified to form bile canaliculi, and the cell membrane of the sinusoidal face has microvilli that increase the absorptive surface area. A canalicular membrane forms the intercellular space, and the lateral membrane of the hepatocyte has specialized structures that connect hepatocytes to each other (McIntyre, 2008).

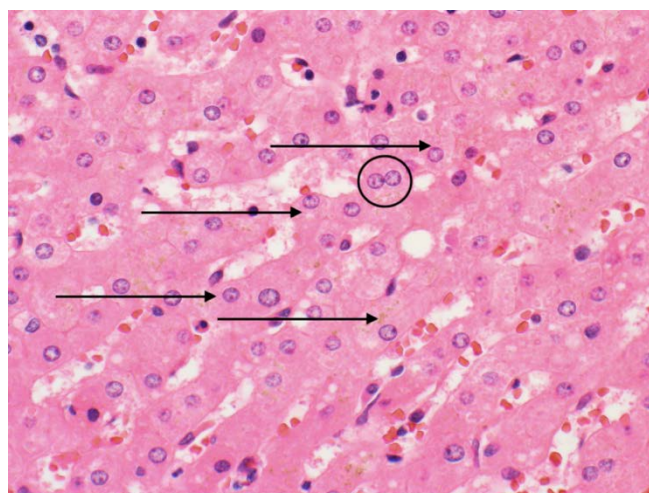


Figure 5: Photomicrograph of the liver demonstrating normal hepatocytes (black arrows) as well as a binucleated hepatocyte (black circle). HE staining. (Photo courtesy of Kimberley J. Evason, M.D., Ph.D, permission granted by PathologyOutlines.com on 02/02/2023). Source: (Leonard N, 2021).

Sinusoids:

Sinusoids are specialized capillaries that are lined by fenestrated endothelial cells, Kupffer cells (specialized macrophages), fat-storing cells and hepatic LGLs/NK cells. Sinusoidal endothelial cells are subtended by a discontinuous basal lamina and have open fenestrations which enables easy exchange between the blood and hepatocytes through the space of Disse. Blood from the portal vein and hepatic artery is mixed together within the sinusoids (Brown, 2017). The blood drains from the sinusoids into the central veins which lead into the hepatic veins. The sinusoids are generally of a narrower diameter, more tortuous and tightly packed together around zone 1, and they become increasingly parallel and straight as they reach zone 3 (Figures 6-8) (McIntyre, 2008).

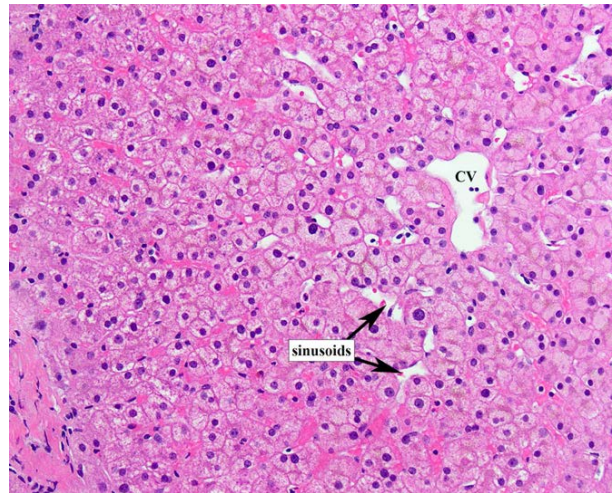


Figure 6: Photomicrograph of the liver showing the central vein (CV) and the sinusoids that radiate outwards from it (black arrows). HE staining. Source: (Bell, 2020).

Kupffer cells:

Kupffer cells are members of the monocyte-macrophage phagocytic system that line the sinusoidal endothelium. They contain multiple lysosomes that enable them to phagocytose a variety of substances including infectious agents, denatured or senescent erythrocytes, immune complexes, denatured albumin and bacteria (McIntyre, 2008, Brown, 2017). These macrophages are able to migrate along the sinusoids to areas of tissue damage, where they can function as antigen-presenting cells, and produce proinflammatory cytokines that stimulate the hepatocytes to produce acute phase proteins and activate the immune system (Brown, 2017).

Stellate cells:

These cells are found in the intercellular spaces between hepatocytes and in the space of Disse. They store Vitamin A in cytoplasmic vacuoles, regulate the tone of the microvasculature, and secrete collagen and extracellular matrix once activated, resulting in fibrosis. They also play a major role in regeneration of the liver, and in the hepatic immune response (Brown, 2017, McIntyre, 2008)

Space of Disse:

The space of Disse is a specialized space filled with blood plasma that is located between the hepatocytes and sinusoids. Hepatocytes bordering the space of Disse absorb plasma constituents through their microvilli and synthesized products (such as glucose, clotting factors etc.) can be secreted by hepatocytes into this space. The gaps in the sinusoidal endothelial cells are too small to allow erythrocytes to pass through, however, the modified fenestrated endothelial cells and discontinuous basal lamina facilitate the free movement of plasma (Figure 7) (Brown, 2017).

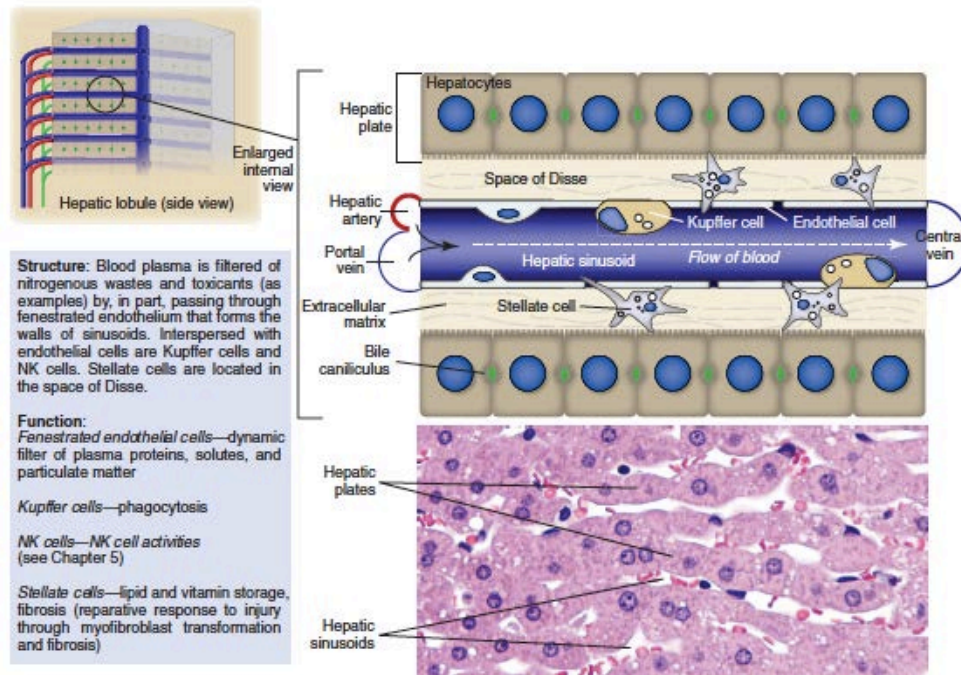


Figure 7: Schematic diagram showing the relationship between hepatic cords, sinusoids, Kupffer cells, the space of Disse and the stellate (Ito) cells. Sinusoids run between the hepatic plates with fenestrated capillaries that allow for easy exchange of oxygen, blood and nutrients between the blood vessels and hepatocytes. Kupffer cells line the luminal surface of sinusoidal endothelial cells. The space of Disse is found between the endothelial cells and hepatocytes and is also the location of the hepatic stellate cells. Bile canaliculi run between the hepatocytes. (Photo courtesy of Dr AJ Van Wettere, School of Veterinary Medicine, Utah State University and Dr JE Zachary, College of Veterinary Medicine, University of Illinois. Permission granted for use by Elsevier 03/02/2023). Source: (Brown, 2017).

Biliary system:

The intrahepatic biliary tree is involved in the formation of bile and its export into the duodenum. It begins with the canaliculi within the centrilobular (periacinar/zone 3) area of the hepatic lobule/acinus. Bile flows in the opposite direction to blood, which aids in the concentration of bile as it flows towards the bile ductules (lined by biliary epithelial cells) in the portal tracts (Figure 8) (Brown, 2017, McIntyre, 2008).

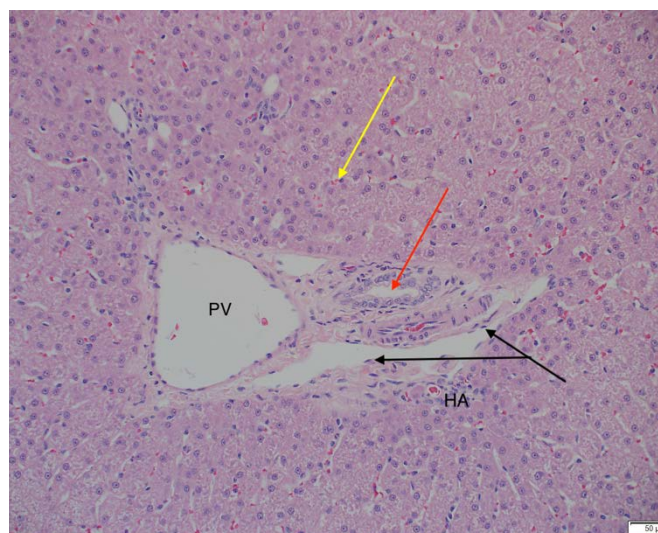


Figure 8: Photomicrograph of a normal dog liver (control no. 2) showing a portal tract containing a branch of the portal vein, hepatic artery, bile duct (red arrow), endothelial cells lining a lymphatic duct (black arrows) and a sinusoid containing red blood cells (yellow arrow). PV = portal vein, HA = hepatic artery. HE staining at 200x magnification.

2.1.2 Liver pathology in haemoparasitic disease

The liver is involved in the cleansing of portal blood and destruction of erythrocytes that are aged or infected by a variety of haemoparasites, and is therefore one of the pivotal organs to be affected by haemoparasitic diseases such as babesiosis, malaria, anaplasmosis etc. (Esmailnejad et al., 2018, Sardinha et al., 2010, Dkhil et al., 2010). Erythrophagocytosis occurs to a significant degree in the liver and spleen, both of parasitized and non-parasitized red blood cells (Maegraith et al., 1957).

Invasion of haemoparasites into red blood cells results in oxidative stress in the erythrocytes as well as the hepatocytes, caused by an increase in free radicals leading to cell membrane failure, protein dysfunction and deoxyribonucleic acid (DNA) damage (Homer et al., 2000, Dkhil et al., 2013). The oxidative stress exceeds the capacity of the antioxidant system, which is shown by decreased levels of glutathione and catalase, resulting in the liver being more sensitive to damaging factors (Hamid et al., 2014). Reactive oxygen species (ROS), which are produced during oxidative stress, are responsible for liver damage, and have been found with a variety of haemoparasites such as babesiosis, hepatoozoonosis and theileriosis (Dkhil et al., 2010). One mechanism for the liver's involvement in the systemic inflammatory response syndrome (SIRS) and multiple organ dysfunction syndrome (MODS) involves the dysregulation of hepatocytes by the toxic metabolites released by activated Kupffer cells during sepsis (Meng et al., 1992). Another proposed mechanism is that there is reduced phagocytic activity of the Kupffer cells, resulting in increased levels of endotoxins and inflammatory mediators within the systemic circulation, damaging the other organs, and predisposing patients to SIRS and MODS (Durila et al., 2012).

Reversible cell injury is characterized by cell swelling and cytoplasmic vacuolation (due to fatty change and/or hydropic degeneration). This is often a result of hypoxia with reduced adenosine triphosphatase (ATP) and subsequent reduced activity of the sodium-potassium ATPase pump leading to increased intracellular sodium, and therefore the inflow of water. Feathery cytoplasmic vacuolation due to glycogen accumulation is seen in cases of steroid hepatopathy. In the case of our infected samples, there was also cell death (irreversible), which will be referred to very specifically as centrilobular necrosis of hepatocytes which is usually hypoxia related. Hepatocytes have a high turnover rate, which makes them susceptible to injury as a result of metabolic disturbances, for example hypoxia due to chronic anaemia in haemoparasitic diseases (Brown, 2017). During hypoxic injuries, centrilobular hepatocellular changes such as cellular swelling due to steatosis and/or marked accumulation of glycogen within the hepatocytes are observed (Brown, 2017).

2.1.2.1 Pathology of the liver in canine babesiosis

In dogs infected with *Babesia gibsoni*, the livers were found to have diffuse mononuclear leucocyte-predominant centrilobular and periportal hepatitis, centrilobular hepatocellular atrophy, perivenular fibrosis, diffuse extramedullary haematopoiesis (EMH), and diffuse Kupffer cell hypertrophy (Wozniak et al., 1997). Some Kupffer cells contained haemosiderin pigment and phagocytosed erythrocytes. Intrasinusoidal fibrin deposits were present throughout the livers, with randomly oriented swollen, vacuolated hepatocytes resembling a steroid hepatopathy. There was thickening of the fibrous connective tissue around the central veins, with evidence of perivascular lymphocytes, plasma cells, macrophages, and neutrophils (Wozniak et al., 1997).

In dogs infected with *Babesia canis*, the livers were found to have diffuse, acute, mononuclear leucocyte-predominant serous hepatitis and cholestasis, with multifocal hepatocyte necrosis and fatty change in centrilobular hepatocytes (Mathe et al., 2006). The central veins and sinusoids showed dilatation and congestion, but no signs of thrombi. Hypertrophic Kupffer cells were present throughout, with large amounts of phagocytosed haemosiderin pigment, which was also evident in

the hepatocytes. Centrilobular hepatocellular necrosis was a consistent finding throughout samples, and in severe cases, the necrosis extended into the midzonal areas. The periportal hepatocytes were largely unchanged, however, fatty change of the periportal hepatocytes was present in cases of severe centrilobular necrosis (Gilles et al., 1953). As has been observed with haemoparasites such as *Babesia* and falciparum malaria, sequestration of parasitized erythrocytes within capillaries of the liver is also common finding, resulting in a decreased number of circulating erythrocytes (Maegraith et al., 1957, Hussein, 1977, Yeruham et al., 1998).

There is currently no published data on the hepatic pathology induced by *B. rossi* infection in the dog.

2.1.2.2 Pathology of the liver in *Plasmodium falciparum* malaria

The *Babesia* genus is morphologically and phylogenetically related to the *Plasmodium* genus, which includes species that cause human malaria (Bilić et al., 2018, Reyers et al., 1998). Both *Babesia* and *Plasmodium* spp. are transmitted to mammals via an arthropod vector and both are erythrocyte-invasive (Clark and Jacobson, 1998). The pathogenesis of babesiosis and malaria has been compared for decades. They also exhibit many similar clinical symptoms, most of which can be attributed to the host immune response to the infection rather than direct damage caused by the parasite itself (Krause et al., 2007, Maegraith et al., 1957). Due to similarities in the proposed pathomechanisms of canine babesiosis and human malaria, it is of interest to evaluate the effect of the human parasite *Plasmodium falciparum* on the liver (Krause et al., 2007).

Grossly, hepatomegaly is characteristic of falciparum malaria in humans (Rupani and Amarapurkar, 2009). Histopathological findings include swollen hepatocytes due to steatosis (Kochar et al., 2003b), multifocal hepatocyte necrosis, portal tract inflammation, sinusoidal congestion, haemozoin pigment deposition (Viriyavejakul et al., 2014, Whitten et al., 2011), and cholestasis (due to the monocyte-macrophage phagocytic system becoming overwhelmed and hepatocyte microvillus disturbance) (WHO, 2000, Viriyavejakul et al., 2014). Kupffer cell hyperplasia is also a common finding, often associated with erythrophagocytosis, and intracytoplasmic accumulation of pigments (lipofuscin and haemosiderin) (Krishnan and Karnad, 2003, Rupani and Amarapurkar, 2009, Kochar et al., 2003b). *Plasmodium falciparum* parasites have the unique ability to cytoadhere to the vascular endothelium of certain organs (lung, heart, brain, liver, and kidney), subcutaneous adipose tissue and placenta (Scherf et al., 2008). Focal to multifocal aggregates of macrophages forming granulomatous lesions or “malarial nodules” were also found (Chawla et al., 1989, Kochar et al., 2003b, Srichaikul, 1959). There is little change to the endothelial cells, as well as a lack of bile duct proliferation (Viriyavejakul et al., 2014). Patients with hyperbilirubinaemia had increased amounts of haemazoin pigment deposition and hyperplastic Kupffer cells, with increased numbers of lymphocytes and plasma cells within the portal tracts. (Viriyavejakul et al., 2014). Hepatocyte necrosis was also inconsistently observed across studies, with severities of necrosis varying from mild multifocal to severe centrilobular (Rupani and Amarapurkar, 2009, Viriyavejakul et al., 2014). Centrilobular necrosis in malaria is thought to be due to hypoxic damage resulting from shock, vasoconstriction, sequestration of parasitized erythrocytes in the micro-circulation leading to ischaemia of certain areas, or endotoxemia due to disruption of the gut barrier (Day et al., 2000, Rupani and Amarapurkar, 2009). Inflammatory infiltrates consist of lymphocytes, macrophages and plasma cells (Rupani and Amarapurkar, 2009, Goljan et al., 2000, Kochar et al., 2003b). Intraerythrocytic parasites were a rare finding on histopathology (Kochar et al., 2003b). The consensus in most of the studies was that the extent of liver damage is positively correlated with the degree of intravascular haemolysis (Dey et al., 2012) and disease severity (Rupani and Amarapurkar, 2009).

2.1.4 Babesia in non-canids

Babesiosis can infect a wide range of vertebrate hosts, including humans, and therefore has is of importance worldwide (Bilić et al., 2018).

2.1.4.1 Bovine babesiosis

Cattle are affected by *Babesia bovis*, *B. bigemina*, and *B. divergens* which are transmitted by *Rhipicephalus* spp., *Boophilus* spp. and *Ixodes ricinus*, respectively (Uilenberg, 1981, Sergent, 1945). Babesiosis in cattle is often referred to as “red water” due to the haemoglobinuria that is exhibited (due to intravascular haemolysis). Other clinical signs and clinicopathologic abnormalities include increased capillary permeability, oedema, coagulopathies, and hypotension (Wright et al., 1989, Ahmed, 2002). Most of these signs are the result of the host’s immune response to the parasite and not the doings of the parasite itself (Ahmed, 2002).

Cattle with Asiatic redwater (*B. bovis*) tend to exhibit a low level parasitaemia, but neurological signs and evidence of respiratory compromise (due to accumulation of parasitized erythrocytes in the microvasculature of the lungs and brain) are common (Bock et al., 2004). The outcome of cerebral babesiosis is mostly fatal (De Vos, 1994). Cattle infected with *B. bigemina* and *B. divergens* tend to show high levels of parasitaemia, associated with severe haemolytic anaemia (Zintl et al., 2003). Other clinical symptoms associated with both diseases include fever, inappetence, depression, weakness, and increased respiratory rates (De Vos, 1994).

Pathology:

In cattle that were experimentally infected with *B. bovis* and *B. bigemina*, post mortems revealed enlarged livers, distended gall bladders filled with bile, anaemia and icterus (Pupin et al., 2019, Esmailnejad et al., 2021). The livers demonstrated cholestasis, bile duct hyperplasia and varied from cell swelling with vacuolar change to coagulative necrosis of hepatocytes centrilobularly (Pupin et al., 2019, Everitt et al., 1986, Esmailnejad et al., 2021). Both the hepatocytes and Kupffer cells contained haemosiderin pigment, the latter also containing parasitized and non-parasitized erythrocytes in splenectomized and non-splenectomized cattle (Everitt et al., 1986). The centrilobular sinusoids were moderately congested with non-parasitized erythrocytes, and intra- and extravascular mononuclear leucocytes were noted (mainly lymphocytes, plasma cells and macrophages), with leucostasis being most prominent in the central veins and portal veins (Everitt et al., 1986). Fibrosis of the liver was seen in those animals with a higher degree of parasitemia (Esmailnejad et al., 2021).

2.1.4.2 Ovine babesiosis

Sheep are mainly infected by two *Babesia* spp., namely *B. motasi* and *B. ovis*, which are transmitted by *Rhipicephalus bursa* and *Haemaphysalis* spp., respectively (Schnittger et al., 2012, Uilenberg, 2006). Haemoglobinuria, pyrexia, anorexia, lethargy, and anaemia were found to be the most common clinical signs (Yeruham et al., 1998). Very little is known about the pathogenesis of *B. ovis*, but it is thought to be similar to *B. bovis* (Habela et al., 1991), with the exception of cerebral babesiosis, which does not occur in *B. ovis*-infected sheep (Wright et al., 1981).

Pathology:

In a group of sheep that were experimentally infected with *B. ovis* (Habela et al., 1991), the livers were macroscopically paler, slightly yellow, softer and purportedly appeared shrunken, with white striations compared to the control livers (Yeruham et al., 1998). Histologically, there were marked vascular changes including vasodilation and vascular stasis (Habela et al., 1991). Hepatocyte necrosis

with haemorrhage, along with cholangitis and pericholangitis was noted (Habela et al., 1991). Kupffer cells were haemosiderin-laden and occasionally exhibited apoptosis. Cholestasis was marked, which included bile pigment granules in hepatocytes (Habela et al., 1991).

2.1.4.3 Gerbil babesiosis

Gerbils (*Meriones ungliculatus*) were experimentally infected with sporozoites of *Babesia divergens*, which resulted in a similar clinical presentation as that described previously, including haemoglobinuria, fever, lethargy, and anaemia (Dkhil et al., 2010, Dkhil et al., 2013). At higher levels of parasitaemia the liver increased in size, became dark brown, oedematous, and friable. Parasitized erythrocytes and erythrophagocytic monocytes filled the sinusoids, there was evidence of Kupffer cell hyperplasia and erythrophagocytosis, with hepatocytic hydropic vacuolation. A marked inflammatory response was present, as evidenced by numerous lymphocytes, monocyte-macrophages and plasma cells in the perivascular interstitium (Dkhil et al., 2010, Dkhil et al., 2013). Despite the observation of high peroxisome concentrations in centrilobular perivascular hepatocytes, which is indicative of oxidative stress, apoptotic hepatocytes were rarely seen (Okła et al., 2014a).

2.1.4.4 Murine babesiosis

Rats experimentally infected with *B. microti* were used as a model system to study *B. microti* infection in humans (Okła et al., 2014a). Macroscopically, none of the livers were enlarged compared to the controls. However, Kupffer cell hyperplasia and extensive lymphocytic inflammation was present (Albertyńska et al., 2017). In another study, the authors noted that lymphocytes were aggregated around foci of injured hepatocytes (Kuzna-Grygiel and Kolodziejczyk, 2000). Adjacent to the injured hepatocytes were increased numbers of mitotic cells, with interspersed foci of fibrosis. Widespread hepatocyte hyperplasia was further evidence of regeneration and tissue repair (Okła et al., 2014a). The spaces of Disse were irregularly open, though completely compressed in areas, and no bile ductular changes were apparent. With time, there was no appreciable increase in lymphohistiocytic inflammation and evidence of hepatocyte regeneration was rarely observed in chronically infected cases (Kuzna-Grygiel and Kolodziejczyk, 2000).

Rats experimentally infected with *B. bigemina* had larger livers that were darker and more brittle than the controls (Esmailnejad et al., 2018). Histologically, cytoplasmic hydropic vacuolation of the hepatocytes was noted, while the sinusoids were severely congested with evidence of monocytic leucostasis, and lymphoplasmacytic inflammatory infiltrates throughout the parenchyma (Esmailnejad et al., 2018).

2.1.4.5 Equine babesiosis

This is caused by the protozoan parasite *B. caballi*, which is transmitted by *Dermacentor*, *Hyalomma* and *Rhipicephalus* tick species (Uilenberg, 2006). The disease is characterized by anaemia, icterus, lethargy, fever, hepato- and splenomegaly (De Waal, 1992). Macroscopically, the livers are described as swollen and pale with rounded edges (Allen et al., 1975). Histologically, there was centrilobular hepatocyte necrosis with cholestasis, Kupffer cell hyperplasia, distension of the spaces of Disse due to oedema, and intravascular thrombi were present (Mahoney et al., 1977, Roberts, 1962, De Waal, 1992, Allen et al., 1975).

2.1.4.6 Feline babesiosis

Clinically significant babesiosis is not common in cats, but *B. felis* is thought to be the most pathogenic species (Solano-Gallego and Baneth, 2011, Bosman et al., 2019). The tick vector is currently unknown

(Schnittger et al., 2012). In cats naturally and experimentally infected with *B. felis*, the livers were macroscopically enlarged, yellow-brown and mottled (Futter and Van Rijswijk, 1981). Histologically there was variable centrilobular necrosis, cholestasis, EMH, and haemosiderin pigment accumulation (Futter and Van Rijswijk, 1981).

2.1.4.7 Human babesiosis

It was initially thought that human babesiosis was only caused by *B. microti* and *B. divergens*, but in the last decade it has been discovered that a variety of *Babesia* spp. can cause clinical disease and even death (Schnittger et al., 2012). The disease is transmitted by *Ixodes* ticks, and, less commonly, through blood transfusions (Leiby, 2011, Oz and Westlund, 2012). Clinical signs range from asymptomatic to life-threatening, depending on the strength of the host's immune response (Zaidi and Singer, 2002), and whether or not they have a spleen (Krause et al., 2003). Haemolysis, acute respiratory distress syndrome (ARDS) and MODS are some of the complications that can arise, similar to falciparum malaria (Gray et al., 2010).

Similar to babesiosis in other mammalian species, clinical signs include fever, sweating, headaches and myalgia. In severe cases, icterus may develop due to the haemolytic anaemia, as well as hyperbilirubinuria (and even haemoglobinuria), vomiting and diarrhoea, with terminal disseminated intravascular coagulation and respiratory, cardiac, renal and/or hepatic failure (Zaidi and Singer, 2002, Schnittger et al., 2012).

To date, there is no published literature describing the histopathology of the liver of humans infected with *Babesia* spp.

2.1.5 Overview of canine babesiosis

Canine babesiosis is one of the most important tick-borne diseases in dogs. Parasite pathogenicity varies with the species (Bilić et al., 2018). For example, *Babesia canis*, transmitted by *Dermacentor reticulatus* ticks, occurs in southern and central Europe, and generally induces more severe clinical disease. *Babesia gibsoni* is transmitted by *Haemaphysalis bispinosa*, *Haemaphysalis longicornis*, and *Rhipicephalus sanguineus* ticks and, rarely, by means of blood transfusions (Weese and Evason, 2020), trans-placentally, and bite wounds (Saari et al., 2018). *Babesia gibsoni* has also been associated with a more chronic form of the disease that results in prolonged subclinical infection. In South Africa, the two most common species that infect dogs include *Babesia rossi*, transmitted by *Haemaphysalis elliptica* ticks, and *Babesia vogelli*, transmitted by *Rhipicephalus sanguineus* ticks. Of these two species, *B. rossi* is the more virulent of the two, causing more severe clinical disease (Leisewitz et al., 2019b, Penzhorn, 2011). *Babesia vogeli* is encountered far less frequently than *B. rossi*, and is considered to be of no clinical significance in South Africa (Rautenbach et al., 2018).

Aetiology:

It has long been hypothesized that the majority of clinical signs and mechanisms of disease can be attributed to the host's immune response, rather than the direct effects of the parasite (Jacobson, 2006). *Babesia* merozoites invade the red blood cells of vertebrates, which results in progressive haemolytic anaemia (Schoeman, 2009). The immunological response to infection may vary according to the age of the host, with younger dogs being more commonly affected and more-likely to develop immune-mediated haemolysis, while older dogs are inclined to develop overwhelming systemic inflammation (Reyers et al., 1998, Goddard et al., 2016). The incubation period ranges from 4-21 days (Schoeman, 2009, Bilić et al., 2018). Disease can vary in severity from subclinical (with few/no clinical signs) to severe, again depending on the age of the animal infected, immune status, previous history of splenectomy, and/or infection with concurrent diseases (Schoeman, 2009, Morters et al., 2020).

Mortality rates range from 1% in *B. vogelli* infections to 45% in *B. rossi* infections (Bilić et al., 2018). An asymptomatic carrier state in dogs has been convincingly demonstrated (Morters et al., 2020), which means that subclinical, chronically infected or even recovered dogs may also be a source of infection (Schoeman, 2009, Morters et al., 2020). *Babesia* sporozoites are released in tick saliva within 2-3 days of attachment to the vertebrate host (Weese and Evason, 2020), however need time to mature in order to become infective (Bilić et al., 2018, Shortt, 1973, Jalovecka et al., 2019). They invade mammalian red blood cells by means of a specialized apical complex that penetrates the erythrocyte membrane (Potgieter and Els, 1979). Sporozoites then differentiate into trophozoites that undergo merogony to become merozoites, which then rupture the red blood cells in order to infect other red blood cells, and so the cycle continues. Due to the disease being transmitted by ticks, its prevalence is largely seasonal, increasing with the number of ticks during warm, humid months of the year (Bilić et al., 2018, Shakespeare, 1995).

2.1.5.1 Uncomplicated babesiosis

Clinical signs are mostly due to the effects of the host immune response to infection, mediated through systemic inflammation, as well as haemolysis. They vary depending on duration of illness and disease progression, but are generally non-specific and include lethargy, weakness, fever, anaemia, tachycardia, tachypnoea, anorexia, vomiting, thrombocytopenia and splenomegaly (Kettner et al., 2003, Schoeman, 2009, Bilić et al., 2018, Köster et al., 2015, Abdullahi et al., 1990). In more severe cases, icterus, hypoalbuminaemia, haemoglobinuria and lymphadenomegaly may also be present (Weese and Evason, 2020, Bilić et al., 2018, Leisewitz et al., 2019b, Irwin and Hutchinson, 1991). Disease severity is variable, ranging from subclinical infections (with few or no clinical signs), through to severe (typically peracute) infections, with the latter having higher mortality rates (Kraje, 2001).

The haemolysis is thought to be caused by three basic mechanisms. The first of these refers to erythrolysis as a result of membrane damage by merozoites exiting red blood cells. The second mechanism is a function of erythrocyte removal by macrophages of the spleen, liver and bone marrow. The last mechanism involves immune activation with intra- and extravascular haemolysis occurring subsequent to the production of anti-erythrocyte antibodies and activation of the complement cascade (Jacobson and Clark, 1994, Maegraith et al., 1957). As the degree of anaemia has been shown to not be correlated with the degree of parasitaemia or haemolysis, other factors must be taken into consideration (Eichenberger et al., 2017). Examples include the sludging of erythrocytes in peripheral capillaries, oxidative damage to erythrocytes (Murase et al., 1996), or an inappropriate/inadequate regenerative response to the severe anaemia (Seejarim, 2020).

The high levels of conjugated bilirubin in the blood of dogs with babesiosis led some authors to hypothesize that hypoxia might cause severe hepatocyte swelling with subsequent compression of the bile canaliculi. The degree of icterus observed is directly correlated with the degree of functional damage to hepatocytes (correlated with liver function enzymes such as alanine aminotransferase (ALT), alkaline phosphatase (ALP) etc.), as well as cholestasis (Malherbe, 1965).

The tissue hypoxia observed in babesiosis can be caused by a multitude of factors. These include the sequestration of erythrocytes in the microvasculature (Jacobson, 2006, Jacobson and Lobetti, 1996), vascular endothelial injury leading to endothelial activation and increased vascular permeability (Jacobson, 2006, Martin, 2020), disseminated intravascular coagulation (Radicheva) (Goddard et al., 2013), damage to the erythrocytes themselves as well as decreases in haemoglobin concentrations (Torti et al., 2020), auto-agglutination (Reyers et al., 1998), severe anaemia resulting in excessive lactate build-up (Leisewitz and Berry, 1996), massive cytokine release (Goddard et al., 2016, Leisewitz et al., 2019a), an increase in concentration of endogenously produced carbon monoxide (Taylor et al.,

1991), hypotension (Schetters et al., 2009) and pulmonary oedema (Martin, 2020, Bilić et al., 2018, Dvir et al., 2004, Lobetti et al., 2002).

2.1.5.2 Complicated babesiosis

Complicated babesiosis refers to the state of disease that is not attributed to the effects of haemolysis (Jacobson, 2006), but rather to the host's immune response to infection (Welzl et al., 2001). This state can be explained by the mechanisms of multiple organ dysfunction syndrome (MODS). Primary MODS occurs due to direct trauma to an organ, which causes a localized inflammatory response, followed by organ dysfunction. Secondary MODS occurs due to an infection or insult to one organ, resulting in systemic inflammatory response (SIRS) and dysfunction in other organs (Bone et al., 1992). The effects of this include acute kidney injury (specifically glomerulonephritis) (Schoeman, 2009), coagulopathies including disseminated intravascular coagulation (DIC) (Esmon et al., 1999, de Laforcade et al., 2003), hepatopathies resulting in icterus (Welzl et al., 2001), immune-mediated haemolytic anaemia (IMHA), acute respiratory distress syndromes (ARDS) (Jacobson and Clark, 1994), myocarditis and myocardial ischaemia, cerebral haemorrhages, shock (Jacobson, 2006), relative haemoconcentration (Jacobson and Clark, 1994, Welzl et al., 2001), enteric haemorrhage (Collett, 2000), hypotension (Schetters et al., 2009, Jacobson, 2006), hypoglycaemia (Keller et al., 2004), rhabdomyolysis (Jacobson and Clark, 1994, Jacobson, 2006), pancreatitis (Masuda et al., 2019, Koster et al., 2015) and severe acid-base abnormalities (Leisewitz et al., 2001).

The greater the number of organs affected, the greater the risk of mortality (Welzl et al., 2001). The organs that are most to least commonly affected include the liver, kidneys, muscle, lungs and central nervous system (CNS) (Welzl et al., 2001, Jacobson, 2006).

Hepatosi:

Hepatopathies are commonly associated with complicated *B. rossi* infections (Jacobson, 2006). This may be at least partially attributed to hypoxia due to the anaemia, which leads to diffuse hepatocellular swelling (Reyers et al., 1998). Severely anaemic dogs were found to have the highest degree of bilirubinaemia and bilirubinuria with macroscopically obvious icterus (Reyers et al., 1998, Jacobson and Clark, 1994). This is likely due to a combination of pre-hepatic and hepatic icterus (Leisewitz et al., 2019b, Gilles et al., 1953). Dogs with icterus were also inclined to be hypoglycaemic, which was associated with a poorer prognosis (Keller et al., 2004).

Haemoconcentration:

The rare complication of "red biliary syndrome" or haemoconcentration refers to the finding of a high haematocrit despite extensive haemolysis, which is accompanied by haemoglobinaemia, and, often, haemoglobinuria (Jacobson and Clark, 1994). The pathomechanism is poorly understood, but may be due to vascular injury with shifting of protein-rich fluid from the intra- to the extravascular compartment, resulting in a relative haemoconcentration (Bilić et al., 2018). In the absence of obvious vasculitis, there may be increased vascular permeability, therefore affecting not only the liver but the rest of the body too, and contributing to the progression of MODS (Guo et al., 2017). The idea of relative haemoconcentration is supported by the fact that the plasma protein levels do not increase in severely ill patients (Reyers et al., 1998). Haemoconcentration is thought to increase the risk of developing acute kidney injury, cerebral complications and MODS, increasing the risk of mortality (Welzl et al., 2001).

Acute kidney injury:

Kidney injury occurs in all dogs with babesiosis, but functional deficits were only found in dogs with severe complicated babesiosis (Defauw et al., 2020, Defauw et al., 2017). In cases of uncomplicated

babesiosis, the kidneys are minimally damaged, as evidenced by mild proteinuria and a slightly abnormal urine sediment (Lobetti and Jacobson, 2001). That said, both glomerular and tubular dysfunction do occur (Defauw et al., 2012). Clinical symptoms of anuria or oliguria with high creatinine levels despite fluid therapy generally indicates more extensive kidney damage (Jacobson and Clark, 1994). The finding of nephrosis at post mortem is consistent with hypoxic damage due to haemolysis (Matijatko et al., 2007), and is unlikely to be due to the effects of haemoglobinuria (Lobetti et al., 1996). The other possible cause could be the accumulation of inflammatory cytokines such as tumour necrosis factor- α (TNF- α) and interleukin-1 (IL-1) associated with sepsis that cause damage to the kidneys (Jacobson and Lobetti, 1996). Renal azotaemia is underdiagnosed in *B. rossi* infections, and has been shown to be negatively correlated with survival (Defauw et al., 2018). Damage done to the kidneys by inflammatory mediators leads to reduced renal perfusion and a decreased glomerular filtration rate (Zygner and Wedrychowicz, 2009). In dogs with complicated babesiosis, increases in glomerular injury biomarkers, urine protein:creatinine (UPC) ratio and symmetric dimethylarginine (sSDMA) were also observed (Defauw et al., 2020).

Rhabdomyolysis:

The pathomechanism behind the rhabdomyolysis observed in babesiosis cases is not yet clear, but several causes have been hypothesized. These include microvascular sequestration of parasitized erythrocytes leading to hypoxic damage, fever, sepsis, inflammatory cytokines (TNF- α and IL-1), and seizures can also contribute to muscle damage (Jacobson and Lobetti, 1996). It is a less frequent complication, along with cardiac dysfunction and pancreatitis (Bilić et al., 2018), but is usually also accompanied by acute renal failure (Jacobson and Lobetti, 1996). Notably, elevated levels of creatine kinase have been demonstrated in a significant number of cases, indicating that muscle damage is a common occurrence in *B. rossi* (Welzl et al., 2001).

Acute pancreatitis/pancreatic necrosis:

The pancreas is very sensitive to ischaemia and perfusion injuries, and most likely occurs due to the hypoxia induced by the intra- and extravascular haemolytic anaemia, leading to increased anaerobic activity of the tissues, production of harmful oxidising substances, and ultimately MODS (Welzl et al., 2001, Koster et al., 2015). Hypotensive shock, IMHA and haemoconcentration, and the effects of nitric oxide leading to vasoconstriction and ischaemic injury, as well as inflammatory cytokines such as TNF- α are other possible causes (Mohr et al., 2000). There were high correlations patients that had already been diagnosed with icterus, and those that developed pancreatitis (Mohr et al., 2000). Pancreatitis was found to be a common but poorly documented complication of babesiosis, but elevations in canine pancreatic lipase (cPL) were not associated with increased mortality (Koster et al., 2015).

Acute lung injury-acute respiratory distress syndrome:

Acute lung injury (ALI) and ARDS are classified on the basis of arterial hypoxaemia caused by lung pathology (damage to the endothelial and alveolar cell linings leading to cellular and fluid exudation and can lead to extensive interstitial fibrosis), resulting in decreased efficiency of gaseous exchange (Wilkins et al., 2007, Carvallo and Stevenson, 2022). Animals that develop this condition in babesiosis usually succumb to the disease within 24 hours of presentation. The ARDS is most likely due to increased alveolar capillary permeability as a result of SIRS, involving endothelial damage by reactive oxygen species and inflammatory cytokines (Jacobson and Clark, 1994). Histologically, there is increased pulmonary capillary leakage, as evidenced by protein-rich oedema (without increased pulmonary capillary pressure) and diffuse lymphohistiocytic-predominant inflammation in alveolar septa (Martin, 2020).

Cerebral babesiosis:

This rare complication of canine babesiosis is diagnosed on the basis of neurological symptoms for which no other cause can be identified, and is associated with a high mortality rate (Jacobson and

Clark, 1994, Leisewitz et al., 2019b, Welzl et al., 2001). Clinical signs that have been reported include incoordination, hindquarter paresis, muscle tremors, nystagmus, anisocoria, seizures, coma, paddling and opisothonus (Jacobson and Clark, 1994, Leisewitz et al., 2019b, Pardini, 2010). Macroscopic changes seen at post mortem include bilateral haemorrhages and malacia affecting the cerebral cortex, cerebellum and occipital lobes. Pathomechanisms are likely associated with vascular endothelial injury (as evidenced histologically by perivascular ring haemorrhages and vasogenic oedema), and possibly sludging of parasitized erythrocytes within the capillaries (Jacobson, 2006, Pardini, 2010). Parasitized erythrocytes that are sequestered in the microvasculature may induce the release of inflammatory cytokines and other mediators of tissue damage, as well as tissue hypoxia, leading to the neurological symptoms observed (Schetters and Eling, 1999). Hypoglycaemia (present in about 20% of complicated cases) is an important differential diagnosis for cerebral babesiosis (Jacobson, 2006).

2.1.5.3 Diagnosis

Babesia parasites can be visualized within the red blood cells on a Diff-quick stained, thin capillary blood smear, usually collected from the ear margin. *Babesia rossi* and *Babesia vogelli* piroplasms are classified as 'large' based on their morphological appearance within the erythrocytes in comparison to the other 'smaller' species (Schoeman, 2009). *Babesia rossi* is typically pear-shaped, paired, and 2.5-5µm in longest dimension, although more than two organisms have been identified within some erythrocytes (Bilić et al., 2018). *Babesia gibsoni* and the other small babesias are seen as singular 1-2.5µm bodies within red blood cells (Schoeman, 2009, Bilić et al., 2018). Parasitized red blood cells tend to concentrate at the periphery of blood smears (feathered edge and lateral margins), so inspecting these areas is often integral to the diagnosis of infection (Böhm et al., 2006). The level of parasitaemia seen in blood smears has been correlated with the severity of clinical signs (Böhm et al., 2006, Leisewitz et al., 2019a). If parasitaemia is low and is not visualized on a blood smear, polymerase chain reaction (PCR) is available to detect DNA specific to each *Babesia* spp. (Troskie et al., 2019).

2.1.6 Biochemical markers of liver function and hepatocyte injury

Hepatic biomarker assays that are used to assess liver function can be broadly divided into three categories: 1) Tests to establish the liver's ability to metabolize drugs and transport organic anions (serum bilirubin, urine bilirubin, urobilinogen); 2) Tests to detect hepatic injury (aminotransferases, ALP, γ -glutamyl-transpeptidase (GGT)); 3) Tests to establish the liver's biosynthetic ability (serum proteins, albumin, prothrombin time (PT), cholinesterase (BChE), urea, clotting factors) (Thapa and Walia, 2007, Giannini et al., 2005). Two major processes are responsible for variations in certain serum enzymes produced by the liver. The first process refers to the leakage of enzymes from hepatocytes (e.g. ALT, aspartate aminotransferase (AST)) due to increased permeability from cell membrane injury. The second process refers to the overproduction of enzymes due to cholestasis or induction from a stimulus (as is the case with ALP, GGT, bilirubin) (Robert J. Washabau, 2013). Liver enzyme tests are very sensitive, but not very specific (Kozat and Sepehrizadeh, 2017), and there is no single test available that can measure all aspects of liver function (Hoekstra et al., 2013).

2.1.6.1 Biomarkers of liver function

Bilirubin:

Bilirubin is a breakdown product of heme (Johnston, 1999). Measures of bilirubin give an indication of the uptake, conjugation and excretory functions of the liver (Hoekstra et al., 2013). An increase in serum bilirubin (hyperbilirubinaemia) occurs due to prehepatic, hepatic or post-hepatic causes. In prehepatic icterus, there is an increase in unconjugated bilirubin, due to increased haemolysis, as well

as decreased hepatic bilirubin clearance. The latter occurs if the hepatocytes undergo hypoxic damage due to the haemolytic anaemia, which results in hepatocyte dysfunction, and a decreased ability to conjugate the excess bilirubin (Kozat and Sepehrizadeh, 2017, Rothuizen et al., 1992). Therefore, strictly speaking, haemolysis (and therefore *B. rossi*) causes both prehepatic and hepatic icterus (Giannini et al., 2005, Kozat and Sepehrizadeh, 2017, Rothuizen and Van Den Ingh, 1988, Malherbe, 1965). Hyperbilirubinaemia is a common finding in dogs diagnosed with *B. rossi*, and a high concentration of bilirubin ($> 14.7 \mu\text{mol/L}$) is strongly correlated with mortality (Leisewitz et al., 2019b, Shabani et al., 2020). Similarly, increased amounts of unconjugated and conjugated bilirubin with elevated liver enzymes have been found in humans infected with *P. falciparum* (Jha et al., 2014, Limaye et al., 2012, Anand and Puri, 2005). Human patients with sepsis also exhibit hyperbilirubinaemia, which has been found to be a negative prognostic indicator (Patel et al., 2015, Yamano et al., 2016). Traces of conjugated bilirubin in the urine are a very sensitive indicator of increased serum bilirubin levels, as the renal threshold for bilirubin is very low (Thapa and Walia, 2007, Johnston, 1999). Hepatic causes of increased serum bilirubin usually involve hepatocyte damage, which prohibits the conjugation of bilirubin. In a healthy animal, unconjugated bilirubin is conjugated with glucuronic acid within the hepatocytes before being released into the bile (Johnston, 1999). Post-hepatic causes typically refer to obstructive or functional cholestasis resulting in an increase in conjugated bilirubin in the systemic circulation (Rothuizen et al., 1992, Gómez Selgas et al., 2014, Brown, 2017). Excretion of conjugated bilirubin into the bile is the step that is most affected in liver disease. An increase in serum bilirubin concentration is usually only detected once the liver has lost at least half of its excretory capacity (Johnston, 1999).

Bile acids:

Bile acids are cholesterol metabolites that are produced in the liver (Li et al., 2017a). They are a good measure of liver function, and are measured either as a single fasting sample, or pre-prandial (after starvation for 12 hours) and post-prandial (taken 2 hours after a meal) bile acid measures are compared (Kozat and Sepehrizadeh, 2017, Berry and Reichen, 1983). Evaluation of the post-prandial bile acid level has proven to be a very sensitive and specific screening test to detect hepatobiliary dysfunction, and is a good prognostic indicator in hepatobiliary disease (Barnes et al., 1975, Bauer et al., 2013, Thomas, 2017). Serum bile acids increase due to cholestasis, porto-systemic shunts, hepatic dysfunction, or any other disturbance to the enterohepatic circulation, and therefore are not disease-specific (Kozat and Sepehrizadeh, 2017). In dogs, post-prandial or fasting serum bile acids greater than $25 \mu\text{mol/L}$ indicate hepatocyte injury or portosystemic vascular anomalies (Center et al., 1985). A variation in bile acid levels can indicate that the liver is ineffective at uptake of the bile acid anions, inefficient in the conjugation of the anions, or inefficient in the excretion of the anions (Cornelius, 1980).

Elevated levels of serum bile acids have been found in dogs diagnosed with *B. rossi* (Welzl et al., 2001, Tuttle et al., 2003), as well as in human falciparum malaria (Gupta et al., 2017) and sepsis patients (Jenniskens et al., 2016). Bile acid accumulation has been shown to exacerbate the existing inflammation in these patients as they are toxic to the hepatocytes in large quantities (Thomas, 2017, Chiang and Ferrell, 2018). Bile acids can lead to hepatocyte damage/injury via several mechanisms. They may cause oxidative damage or stimulate hepatocytes to produce pro-inflammatory cytokines (IL-1, IL-10) and chemokines which recruit neutrophils and lymphocytes to the liver (Allen et al., 2011). Since the kidneys are involved in the elimination of bile acids and bilirubin through the urine (Mohapatra et al., 2016) and because these metabolites (in excess) have been found to be nephrotoxic, this could possibly contribute further to the MODS observed in these patients (Betjes and Bajema, 2006).

Albumin:

Albumin, which is synthesized by the liver, is the most abundant plasma protein in the body (Nicholson et al., 2000), and can be used to assess the synthetic function of the liver (Hoekstra et al., 2013). It is also a negative acute phase protein (Yamashita et al., 1994), meaning that it tends to decrease in inflammatory conditions (specifically in the presence of IL-1, IL-6 and TNF α), malnourishment and severe disease (Herrmann et al., 1992, Nicholson et al., 2000).

Mild hypoalbuminemia is a consistent finding in a variety of canine babesiosis studies (Reddy et al., 2016, Ullal et al., 2018, Areekul et al., 1980), together with hypoalbuminemia-induced alkalosis (Leisewitz et al., 2001). Rather than being due to a failure of albumin synthesis, inflammation resulting in the production of negative acute phase proteins, haemodilution or increased permeability of the endothelium (similar to what is seen in sepsis) could be reasons for the hypoalbuminaemia (Cray et al., 2009, Leisewitz et al., 2001). The half-life of albumin in the dog is approximately 10 days, and serum albumin levels have been found to decrease within 5 days of an acute inflammatory event (Yamashita et al., 1994), therefore ruling out synthesis failure as possible cause. Prolonged hypoalbuminemia has been noted up to 5 weeks after the initial *Babesia* infection (Vercammen et al., 1997), although globulin levels were unchanged for the most part (Leisewitz et al., 2019b). Hypoalbuminaemia is also a common finding in human malaria patients (Charoenpan et al., 1990, Arnold et al., 2013) and has been found to be significantly associated with acute renal failure and MODS (Vannaphan et al., 2010). It is a feature of end stage liver failure an indicator of mortality in humans and animals with sepsis (Arnau-Barrés et al., 2019, Gatta et al., 2012, Furukawa et al., 2019, Tamion, 2010, Futter and Van Rijswijk, 1981).

Prothrombin time (PT):

Prothrombin time measures the time it takes for prothrombin to be converted to thrombin, which involves factors II (prothrombin), V, VII, IX, X and fibrinogen that are all synthesized by the liver, and are dependent on Vitamin K availability (Limdi and Hyde, 2003, Daniel and Marshall, 1999). Prolonged PT is seen in many coagulation deficiencies including DIC, and coagulation abnormalities only occur after loss of at least 80% of liver function. It is therefore not a very specific or sensitive test of function (Johnston, 1999, Thapa and Walia, 2007). Elevations in PT are associated with Vitamin K deficiency, and occur commonly in patients with chronic cholestasis (Limdi and Hyde, 2003, Johnston, 1999). It may be used as a prognostic indicator in acute and chronic liver failure, with an increased PT predicting a poor outcome (Johnston, 1999, Friedman et al., 2003). It has a relatively short half-life (one day) and can therefore be used to monitor the progression of hepatic injury fairly accurately (Dufour et al., 2000). It should be used in conjunction with other more specific and sensitive liver function tests such as albumin, AST and ALT (Botta et al., 2003).

A prolonged PT has been shown in dogs diagnosed with *B. rossi*, but was more common in severe infections (Goddard et al., 2013, de Gopegui et al., 2007, Daste et al., 2013, Rafaj et al., 2009). Low levels of plasma prothrombin have been observed in dogs with babesiosis that presented with MODS, however, this has been thought to be caused by the overwhelming inflammatory response that is present in babesiosis rather than a lack of production by the liver (Ahmed, 2002, Clark and Jacobson, 1998, Hemmer et al., 2000, Welzl et al., 2001, Goddard et al., 2013, Kuleš et al., 2016).

Although the PT is typically within normal limits in human falciparum malaria patients, prolonged times have been shown to be positively correlated with increasing *Plasmodium* parasitaemia levels, usually in conjunction with very high serum bilirubin (Singh et al., 2010, Devarbhavi et al., 2005, Mathews et al., 2019, Abro et al., 2009, Jayashankar et al., 2016). In cases of mild sepsis, the PT has been found to be within normal limits, but prolonged times were found in patients with severe sepsis and septic shock (Mavrommatis et al., 2000, Plessier et al., 2003). Thus, PT can be used as a prognostic indicator in patients with sepsis (Kinasevitz et al., 2005). Prolonged times are associated with a

depletion of coagulation factors in severe sepsis patients, and may be an early indicator of DIC (Taylor Jr et al., 2001, Kinasewitz et al., 2005).

2.1.6.2 Biomarkers of liver damage/hepatocyte injury

Aminotransferases:

The aminotransferases include aspartate aminotransferase (AST) and alanine aminotransferase (ALT), which are direct indicators of hepatocellular injury (Limdi and Hyde, 2003, Center, 2007). Both play a pivotal role in gluconeogenesis, in the production of pyruvate and oxaloacetate. Aspartate aminotransferase is a cytosolic and mitochondrial enzyme with a half-life of less than one day (Webster and Cooper, 2014). It is present in the liver, cardiac and skeletal muscle, kidneys, brain, pancreas, lungs, leucocytes, and in red blood cells (Limdi and Hyde, 2003, Lala et al., 2022). This enzyme is less sensitive and specific for liver injury compared to ALT (Pratt and Kaplan, 2000), but has been found to increase in chronic liver disease (Nalpas et al., 1986).

Alanine aminotransferase is a cytosolic enzyme with a half-life of 2.5 days (Webster and Cooper, 2014) that is found in highest concentrations in the liver, making it a more specific indicator (than AST) of liver injury (Pratt and Kaplan, 2000). Alanine aminotransferase is found in highest concentrations in the periportal areas of the liver (zone 1), whereas AST is more concentrated in the centrilobular areas (zone 3), which facilitates localization of hepatocyte damage (Rej, 1989). However, since both enzymes occur in the cytoplasm, even small changes in cell membrane permeability can result in their release into the circulation. This limits their usefulness in determining the extent as well as the reversibility of the liver damage (Center, 2007). Aminotransferases are catabolized within the liver, so an increase could also indicate decreased liver function in disease (Kamimoto et al., 1985, Horiuchi et al., 1985). Since these enzymes are produced within hepatocytes, a decrease in serum levels could either mean resolution of the injury or that the liver is failing, therefore they cannot be used for prognostic purposes (Giannini et al., 2005).

In dogs diagnosed with *babesiosis*, elevated serum levels of ALT and AST were found, bearing in mind that increases could also be due to the concurrent haemolysis and/or kidney injury (Ubah et al., 2019, Furlanello et al., 2005, Zygnier et al., 2007, Shah et al., 2011, Bilwal et al., 2018, Mathe et al., 2006, Leisewitz et al., 2019b, Shabani et al., 2020). Both ALT and AST are useful initial indicators of sepsis (Durila et al., 2012), and increases have also been observed in human *falciparum* malaria patients (Chughlay et al., 2020, Kochar et al., 2003a).

2.1.6.3 Biomarkers of cholestasis

Alkaline phosphatase (ALP):

This enzyme is found in many cell membranes throughout the body, including canalicular membranes, the apical surface of bile duct and intestinal mucosal epithelial cells (Milne, 1985, Harris, 1990), the cell membranes of osteoblasts that are primarily involved in mineralization of bone (Harris, 1990), in seminal plasma (Turner and McDonnell, 2003), neuronal membranes and synaptic clefts in the cerebral cortex of primates (Fonta et al., 2004), as well as in granulocytes, with the exception of mature neutrophils in dogs and cats (Raskin and Valenciano, 2000). In dogs specifically, two isoenzymes of ALP are found. The first is a tissue non-specific isoenzyme (liver, kidney, placenta, semen, corticosteroid induced), and the second is an intestinal isoenzyme (Hank et al., 1993, Kutzler et al., 2003, Saini et al., 1978, Saini and Saini, 1978). In a healthy adult dog, the majority of the serum ALP is from the liver, with small amounts from the bone and via corticosteroid stimulation (Saini and Saini, 1978). In the diseased liver, ALP production is increased due to tissue injury, particularly in cholestatic diseases. Accumulated bile salts stimulate the release of ALP from the hepatocyte cell surfaces (Schlaeger et al., 1982). It is a very sensitive (80%) but poorly specific (51%) indicator of

hepatic disease (Center et al., 1992, Center, 2007), and should therefore be interpreted in conjunction with GGT (Limdi and Hyde, 2003). The half-life of hepatic ALP is approximately 70 hours (Dufour et al., 2000).

Modest elevations in ALP are common in canine babesiosis (Furlanello et al., 2005, Zygnier et al., 2007, Zygnier et al., 2011, Konto et al., 2014, Shabani et al., 2020), although, in a more recent study pertaining to 320 dogs diagnosed with *B. rossi*, changes in ALP and ALT were largely insignificant (Leisewitz et al., 2019b). An increased ALP level has been observed in patients diagnosed with *P. falciparum*, thought to be caused by haemolysis as well as hepatic injury. In addition, a positive correlation between serum ALP levels and the degree of parasitaemia was found (Oyewole et al., 2010, Onyesom and Onyemakonor, 2011, Ignatius et al., 2008, Al-Salahy et al., 2016). Increased ALP levels are also observed in patients with sepsis (Koskinas et al., 2008, Muftuoglu et al., 2006). Zygnier et al. (2011) found that serum ALP and ALT concentrations are not correlated with the degree of anaemia, which suggests that the parasite or the host response to the parasite causes a degree of liver damage (Zygnier et al., 2011).

γ-Glutamyl-transpeptidase (GGT):

This enzyme is a membrane-bound glycoprotein, and is found in high concentrations in hepatocytes and biliary epithelial cells, as well as the epithelial cells of the renal tubules, intestine, pancreas and prostate (Thapa and Walia, 2007, Giannini et al., 2005). Elevated GGT levels are a sensitive (87%) but poorly specific (50%) marker of cholestasis or bile duct obstruction in liver disease, as well as drug induction. However, it takes several days for the GGT level to rise in the blood after an insult has occurred (Johnston, 1999, Giannini et al., 2005, Webster and Cooper, 2014). When serum GGT is evaluated in conjunction with ALP, this helps to establish the source of ALP as being from the liver rather than bone. Serum GGT increases much more than ALP in obstructive liver disease (Lala et al., 2022), and can be used as an early indicator of hepatocyte injury or cholestasis (McIntyre and Rosalki, 1992)

Increases in GGT have been found in conjunction with increases in ALP in dogs diagnosed with babesiosis, leading to the conclusion that a liver specific insult occurs (Ubah et al., 2019, Zygnier et al., 2011, Thankachan et al., 2020, Crnogaj et al., 2010, Shabani et al., 2020). The GGT and ALP levels were found to be markedly increased in dogs with complicated babesiosis compared to those with the uncomplicated form (Crnogaj et al., 2010). An increased level of GGT that has been positively correlated with piroplasm parasitaemia has also been demonstrated in human malaria patients (Ehiem et al., 2021, Abro et al., 2009). Cholestasis is also described in patients with sepsis, that often have concurrently elevated GGT levels. In sepsis, inflammation can cause an elevation or a decrease in serum GGT (Oswari et al., 2013). Low values of GGT in patients that have sepsis-induced cholestasis indicate that the bile flow obstruction is at the level of the canalicular membrane of the hepatocytes, while high values indicate that the blockage is at the ductular level (Oswari et al., 2013). GGT is a good prognostic indicator for severe sepsis with low values being indicative of a poorer prognosis (Wang et al., 2006, Wang et al., 2008).

Lactate dehydrogenase (LDH):

This is a cytosolic enzyme that is concentrated in the following organs in descending order: Skeletal muscle, heart, kidney, intestine, liver, lung and pancreas (Crawford et al., 2006). It is also released during haemolysis, together with haemoglobin (Hoekstra et al., 2013). Lactate dehydrogenase acts at the last step of glycolysis under anaerobic conditions, and can be used as an indicator of hypoxia-associated tissue injury (Lu et al., 2018, Duman et al., 2016). It is a less specific marker of liver injury than AST and ALT (Gitlin and Serio, 1992). LDH is particularly elevated in animals with severe hepatic necrosis due to ischaemia (Seeto et al., 2000, Gitlin and Serio, 1992, Johnston, 1999), in conditions of oxidative stress and inflammation (Center, 2007, Jovanović et al., 2010), as well as shock liver (due to

ischaemia), hepatic lymphoma, and haemolysis associated with liver disease (Whitfield, 2001, Lala et al., 2022, Lu et al., 2018).

Higher levels of LDH (together with elevated ALT) have been described in canine babesiosis, thought to be the result of haemolysis with liver damage due to hypoxia (Schoeman, 2009, Reyers et al., 1998, Yamasaki et al., 2003, Dubova and Duboviy, 2018). Higher levels of LDH have been associated with poorer outcome (Reyers et al., 1998). Elevated levels of LDH together with liver necrosis has been described in humans with *P. falciparum* malaria (Singh et al., 2010). Patients with sepsis have elevated levels of LDH, which is negatively correlated with oxygenation status, but positively correlated with mortality (Lu et al., 2018, Duman et al., 2016, Zein et al., 2004).

Glucose:

Hyperglycaemia was found in 25% of *B. rossi*-infected dogs (Leisewitz et al., 2019b), and is directly correlated with disease severity (Plummer and Deane, 2016, Schoeman et al., 2007, Keller et al., 2004), it is not a good prognostic indicator in babesiosis (Keller et al., 2004). Hyperglycaemia in babesiosis is probably caused by an increase in counterregulatory hormones and inflammatory cytokines (e.g. cortisol, catecholamines, IL-6, TNF- α and glucagon), which stimulate excessive hepatic gluconeogenesis and promote peripheral insulin resistance (Marik and Raghavan, 2004, McCowen et al., 2001, Siegel et al., 1979)

Hypoglycaemia is a complication seen in cases of severe canine babesiosis and occurs in approximately 20% of total cases (Keller et al., 2004, Leisewitz et al., 2019b, Rees and Schoeman, 2008). A combination of icterus and high piroplasm parasitaemia have been shown to be significant risk factors for the development of hypoglycaemia (Keller et al., 2004, Leisewitz et al., 2019b, Rees and Schoeman, 2008, Jacobson and Lobetti, 2005, Böhm et al., 2006). It is more commonly observed in younger dogs with lower body weights (Rees and Schoeman, 2008), and may be due to a lack of stored glycogen and reduced ability to withstand the physiological stress placed on these animals in disease (Rees and Schoeman, 2008). Another potential cause could be increased glucose utilization in patients with severe disease (Binh et al., 1997). Hypoglycaemia is also a common finding in cases of severe human falciparum malaria, which has been hypothesized to be due to increased glucose consumption by the parasite itself (Roth Jr, 1990), together with a decrease in gluconeogenesis by the liver. This, however, is less likely as there is increased peripheral glucose consumption rather than decreased production in malaria (Davis et al., 1993). A decrease in gluconeogenesis normally only occurs in malaria patients with liver failure, which does not occur in *B. rossi* infections (Binh et al., 1997). Hypoglycaemia may also be caused by an increase in anaerobic glycolysis due to erythrocyte sequestration in the microvasculature (Rees and Schoeman, 2008) leading to a decrease in hepatic function (White et al., 2003, Jacobson and Lobetti, 2005). It also possible that the hypoglycaemia is exacerbated by fasting during infection-induced anorexia (Zijlmans et al., 2008, Madrid et al., 2015).

For the most part, in canine babesiosis, insulin levels were found to be low and appropriate for the degree of hypoglycaemia observed (Rees and Schoeman, 2008). In sepsis in humans, the increase in glucose consumption is mediated by inflammatory cytokines produced by macrophages in the spleen, liver and lungs (Mizock, 1995).

2.1.7 Immunohistochemistry (IHC)

Chromogenic immunohistochemistry (IHC) is a very useful tool for visualizing and therefore localizing antigens within tissues by exploiting antibody specificity (Duraiyan et al., 2012). This labelling technique uses specific antibodies and detection systems to identify a variety of target antigens in tissues (e.g. infectious agents, or molecular markers of specific cell types, or cellular processes such as

apoptosis, proliferation, etc.). Pertaining to research, the information obtained is used to inform the pathogenesis of the disease or condition in question (Ramos-Vara and Miller, 2014).

In studies of canine babesiosis and human malaria, hepatic inflammatory cell infiltrates comprised plasma cells, lymphocytes, macrophages and neutrophils (Viriyavejakul et al., 2014, Rupani and Amarapurkar, 2009, Goljan et al., 2000, Kochar et al., 2003b, Wozniak et al., 1997). Fibrin deposition within the sinusoids has also been mentioned in dogs infected *B. gibsoni* and *B. canis*, as well as haemosiderin pigmentation in the Kupffer cells (Wozniak et al., 1997, Mathe et al., 2006). Immunohistochemistry has been used to phenotype the leucocytes in a variety of organs from dogs with fatal *B. rossi* infections, including the spleen, lung, bone marrow and brain. So far, monocyte-macrophages have been identified as the major component of the host inflammatory response in these tissues (Henning et al., 2020, Martin, 2020, Bumby, 2022).

2.1.8 Prognosis

In complicated *B. rossi* cases, increased risk of mortality was associated with a wide variety of clinicopathological findings. These included: progression to MODS or SIRS (Welzl et al., 2001, Matijatko et al., 2012, Matijatko et al., 2009), haemoconcentration (Leisewitz et al., 2019b), severe anaemia, collapse at presentation, high piroplasm parasitaemia, hyperlactataemia, hypoglycaemia, leucopaenias, triglyceridaemia, thrombocytopaenia, increased phosphate concentrations, low total serum proteins (Nel et al., 2004, Keller et al., 2004, Eichenberger et al., 2016), severe mixed acid-base disturbances (Leisewitz et al., 2001), low vitamin D binding protein concentrations (Kuleš et al., 2014), high band neutrophil and lymphocyte counts (Kučer et al., 2008), coagulopathies and DIC (Goddard et al., 2013, Köster et al., 2009), presence of neurological signs, elevated urea, elevated creatinine, hyperbilirubinaemia, hypercortisolaemia, high levels of IL-6, and low total thyroid hormone concentration (Schoeman et al., 2007, Leisewitz et al., 2019b, Reyers et al., 1998, Schoeman, 2009). Increased mortality rates were also seen in dogs with higher systemic inflammatory cytokine levels, reinforcing the idea that the degree of inflammation is pivotal to the outcome of the disease (Goddard et al., 2016). In canine babesiosis, the severity of the clinical signs is also directly correlated with the level of piroplasm parasitaemia and host immune status (Homer et al., 2000, Böhm et al., 2006).

Complicated human malaria is also characterized by the presence of neurological signs, hypoglycaemia, high parasitaemia, high haematocrit, peripheral leucocytosis, high urea and creatinine, and hyperlactatemia. Human patients that present to hospital with severe malaria also exhibit at least a 3-fold increase in AST and ALT levels (WHO, 2000, Day et al., 2000). Liver involvement in malaria, also known as malarial hepatitis, has also been associated with a poor prognosis (Das et al., 2007).

2.4 AIM OF THE STUDY

As discussed above in the review of the literature, the current study aimed to investigate the microscopic and immunohistochemical changes within the liver of *Babesia rossi*-infected dogs. The histopathology was described in detail, and the proportion of immune cells (specifically mononuclear phagocytes and lymphoid cells) within the liver of dogs with *B. rossi* infection were compared to the livers of healthy dogs. Due to the similarities between malaria and babesiosis, the results from this study were compared with human and murine malaria study results as well as natural and experimental *Babesia* infections in a wide range of species.

2.5 HYPOTHESIS

Null Hypothesis (H0): There is no significant difference in liver histopathology between *Babesia rossi*-infected dogs and healthy dogs.

Alternative Hypothesis (H1): There is a significant difference in liver histopathology between *Babesia rossi*-infected dogs and healthy dogs that is characterised by inflammation dominated by the macrophage/monocyte phenotype.

3. METHODS AND MATERIALS

3.1 EXPERIMENTAL DESIGN

This was a semi quantitative, retrospective, case controlled descriptive study. Liver specimens from 10 dogs naturally infected with *Babesia rossi* that died or were euthanized were collected from a previously archived tissue bank. These were then compared histologically as well as immunohistochemically to the livers of 4 healthy dogs collected prospectively that were euthanized for welfare reasons.

Ethical approval for this project was granted by the University of Pretoria Animal Ethics committee (RECO40-21)

3.1.1 Infected dogs: Sources

Babesia rossi-infected dogs were sampled previously by the project supervisor (V034-14) (Leisewitz et al., 2019b). Infected dogs were sourced from the Onderstepoort Veterinary Academic Hospital (OVAH), Faculty of Veterinary Science (FVS), University of Pretoria (UP), from patients that were naturally infected by *B. rossi*, and brought in by their owners for veterinary care. *Babesia rossi* infection was diagnosed on a peripheral capillary stained blood smear, with later confirmation of infection by polymerase chain reaction (PCR) and reverse-line blot (RLB) hybridization assays on ethylenediaminetetraacetic acid (EDTA) blood samples (Matjila et al., 2008). Serum and EDTA blood samples were collected from these dogs prior to the administration of any treatment. These dogs were either treated and died, died before any treatment could be given, or were euthanized due to a poor prognosis. These dogs included one female and nine males, a range of ages (mean = 52.8 months, median = 50 months), a range of weights (mean = 28.9kg, median = 34kg), and a variety of different breeds (Boerboel, German Shepherd, Great Dane, Cocker Spaniel, Boxer, Rottweiler, Pitbull terrier and Africanis) were included. A poor prognosis was assigned on the basis of established criteria (Leisewitz et al., 2019b). Tissue samples collected at postmortem were formalin-fixed and paraffin-embedded before being archived. From the 20 samples that had complete serum biochemistry data and paraffin-embedded liver specimens, only 10 were selected for the study. Case selection was based on a combination of the following criteria: The degree of autolysis of the liver specimens (evaluated in haematoxylin and eosin (HE)-stained sections; only mildly autolyzed specimens were selected for the study), the amount of liver tissue available for histopathology and immunohistochemical labeling, and the severity of selected biomarkers of liver damage and dysfunction. Biochemical markers that were evaluated included alkaline phosphatase (ALP), alanine transferase (ALT), bilirubin, urea, and fasting bile acid concentrations.

3.1.2 Control dogs: Sources

The control dogs were considered healthy based on their habitus, physiological parameters (such as temperature, heart rate, mucous membrane colour etc.), and normal haematology and biochemistry data. Haemoparasites were ruled out by PCR-RLB from EDTA-preserved blood samples (Leisewitz et al., 2019b). These included three females and one male, a range of ages (mean = 18.3 months, median = 15.5 months), weights (mean = 13.6kg, median = 12.5kg), and breeds (Pitbull terrier, Africanis and Boerboel). These dogs were sourced from a welfare organization. They were euthanized by the standard method of pentobarbitone overdose administered intravenously (Underwood and Anthony, 2020). Liver specimens were collected from 10 dogs, but only four cases were considered suitable for the study, based on the strict application of inclusion and exclusion criteria (see 1.1.5 below).

3.1.3 Infected dogs: Inclusion criteria

- Client-owned dogs, naturally infected with *B. rossi* that presented for veterinary care.
- Dogs that were diagnosed with *B. rossi* on a Diff-Quik-stained peripheral capillary blood smear, confirmed retrospectively by PCR-RLB assay from EDTA-preserved blood.
- Dogs that died due to the infection or were euthanized due to a poor prognosis.
- Dogs of any age, sex, breed, and body weight.
- Dogs from which samples could be collected within 90 minutes after death.
- Dogs that received treatment for babesiosis as well as those that did not.
- Dogs that had owner consent for a full haematology profile (complete blood count (CBC)), serum biochemistry and a complete postmortem examination.

3.1.4 Infected dogs: Exclusion criteria

- Dogs that were PCR-positive for haemoparasites other than *B. rossi*, including *B. vogeli* and *Theileria* spp., and/or rickettsial bacteria, such as *Ehrlichia canis*, and *Anaplasma* spp.
- Dogs that received anti-inflammatory medication within the 4 weeks prior to presentation.
- Dogs for which a full haematology profile, serum biochemistry and complete postmortem data were not available.
- Dogs with co-morbidities detected during the postmortem examination, or after thorough histopathological evaluation.
- Dogs with a postmortem interval longer than 90 minutes.

3.1.5 Control animals: Inclusion criteria

- Attempts were made to approximate a match of the control group with the infected dog group pertaining to gender, age, and sterilization status.
- Dogs that were clinically healthy and showed no evidence of co-morbidities on evaluation of a complete blood count, serum biochemistry (including pre- and post-prandial bile acid determination), gross pathology, histopathology and PCR-RLB assays on EDTA-preserved blood.

3.1.6 Control dogs: Exclusion criteria

- Dogs that appeared sick on clinical examination.
- Dogs with any haematological or serum biochemistry abnormalities.
- Dogs that were PCR-positive for any haemoprotozoa including *B. rossi* and/or rickettsial bacteria including *Ehrlichia* and/or *Anaplasma* spp.

3.1.7 Ante-mortem procedures on control dogs

Prior to euthanasia, the control dogs were handled as follows:

- A clinical examination was done (physical evaluation, temperature, and peripheral blood smear).
- Food was withheld for 12 hours before 5ml of blood was drawn by venipuncture of either the jugular or cephalic vein using a 22G 1" needle and 5ml syringe. 2.5ml of blood was preserved in EDTA and used for the complete blood count and PCR RLB assay. The remaining 2.5ml of blood was stored in a serum tube and used for a biochemistry profile (including pre-prandial bile acid determination). Remaining blood, clots, plasma, and serum are archived in the Clinical Pathology laboratory in the minus 80 degrees Celsius freezer.
- Two hours after feeding, another 2ml of blood was drawn by venipuncture of either the jugular or cephalic vein and stored in serum tubes in order to measure the post-prandial bile acid concentration.
- Immediately after blood sampling, the dogs were euthanized humanely by standard overdose of Pentobarbitone administered intravenously (Underwood and Anthony, 2020).
- Haematology and serum biochemistry tests were run within five hours of sampling.

Complete blood count

The automated ADVIA 2000 haematology analyzer was used (Siemens), and the following parameters were assessed:

- Red blood cell count (RBC) measured in $10^{12}/L$.
- Hematocrit (Hct) expressed as a L/L.
- Thrombocyte count measured in $10^9/L$.
- White blood cell count (WBC) measured in $10^9/L$.
- Automated differential white blood cell count, including the percentage of neutrophils, band cells, monocytes, lymphocytes, eosinophils and basophils, and absolute neutrophil, monocyte, lymphocyte, eosinophil and basophil counts measured in $10^9/L$.
- Manual differential white cell counts and assessment of erythrocyte morphology was performed by a trained veterinary laboratory technologist.

Serum biochemistry profile

A minor medical profile was performed, measuring albumin, total serum protein (TSP), ALT, ALP, urea, creatinine, sodium, potassium, and chloride. Fasting and 2 hour post prandial bile acid levels were also determined. These data were generated on an automated analyzer (Cobas Integra 400 plus).

PCR-RLB assay

The PCR-RLB assay was performed on 500uL of EDTA anticoagulated blood that was stored at $-80^{\circ}C$ for approximately 3 days. DNA extraction was performed according to standard protocols (Purelink genomic DNA mini kit; Invitrogen) and the RLB hybridization assay was used to screen the DNA samples for *Babesia*, *Theileria*, *Anaplasma* and *Ehrlichia* spp., as previously described (Matjila et al., 2008).

3.1.8 Postmortems and sampling for histopathology

Postmortems and sampling of the liver for histopathology was performed previously by the project supervisor (Leisewitz et al., 2019b).

Liver samples were collected from the control dogs within an hour of euthanasia. For every dog, a $1cm^3$ sample was obtained from each liver lobe. Samples were fixed in 10% neutral buffered formalin for no longer than 5 days, then trimmed and embedded in paraffin.

3.1.9 Histopathology and histochemistry

The formalin-fixed, paraffin-embedded liver specimens were routinely sectioned at 4-5 μ m, stained with H&E according to standard operating procedures (SOPs) in the histopathology laboratory Department of Paraclinical Sciences (DPS), FVS, UP and examined with an Olympus CX21 light microscope. The least autolyzed, best-preserved, and most normal looking liver specimen was selected for additional histochemistry and immunohistochemistry (IHC) per control dog. For the *Babesia*-infected dogs, the lesions were consistent between all liver lobes, and so the least autolyzed, best-preserved liver specimen with the least artifacts was selected for additional histochemistry and IHC. Histochemical stains included the Gordon and Sweet's silver (GSS) staining method for reticular fibres, Perl's Prussian blue stain for ferric iron (haemosiderin), the Martius Scarlet Blue stain for fibrin, and the Luxol fast blue stain, traditionally used to stain myelin, but used in this study to help highlight the intraerythrocytic *Babesia* parasites in tissue sections (Lewis et al., 2022).

The histochemical stains were stained according to internal SOPs adapted from the method used by Bancroft (Bancroft and Gamble, 2008).

3.1.10 Immunohistochemistry

Routine chromogen-based indirect immunoperoxidase staining was performed by hand, according to optimized protocols in the IHC laboratory, DPS, FVS, UP (Henning et al., 2020). The sought-after cellular antigens included CD3 (for T-lymphocytes), CD20 (B-lymphocytes), CD204 (macrophages), Iba-1 (macrophages and dendritic cells), MAC387 (granulocytes, monocytes, and macrophages), and MUM-1/IRF-4 (mature B-lymphocytes and plasma cells). Table 1 is a summary of the primary antibodies (including host and clone), target cells, heat-induced antigen retrieval methods, primary antibody dilutions and incubation times.

Tissue sections from the control and *Babesia*-infected dogs were mounted on positively charged Superfrost glass slides and heated at 40°C overnight. Thereafter, slides were routinely dewaxed in xylene and rehydrated through graded ethanol, followed by rinsing in distilled water. In order to quench endogenous peroxidase activity, the slides were incubated with 3% hydrogen peroxide in methanol for 15 minutes at room temperature. Heat-induced epitope retrieval was performed in a microwave oven at 96°C, either in citrate buffer (pH=6) for 14 minutes or EDTA buffer (pH=9) for 21 minutes (Table 1). Slides were allowed to cool on the bench, followed by rinsing in distilled water, then in 0.1 molar (M) phosphate buffered saline (PBS; pH=7.6), containing 0.1% bovine serum albumin (BSA). Slides were then incubated with the primary antibodies at room temperature, as indicated in Table 1. After rinsing in distilled water, followed by PBS-BSA buffer, the slides were treated with a polymer-based detection method (BioGenex Super Sensitive Polymer-HRP IHC detection system, BioGenex, Fremont, USA), according to manufacturer's instructions. After rinsing in distilled water, followed by PBS-BSA buffer, immunoreactivity was visualized using a diaminobenzidine tetrachloride (DAB) substrate. Slides were then counterstained with Mayer's haematoxylin for 20 seconds, rinsed under tap water for 10 minutes, routinely dehydrated in ascending graded ethanols, cleared in xylene, mounted with entellan (Thermo Scientific) and coverslipped (Henning et al., 2020). Reactive dog lymph node and spleen samples were used as positive tissue controls and buffer was used instead of the primary antibody for negative reagent control purposes (to assess the specificity of each reaction). Positive staining was brown. CD3-specific immunoreactivity was cytoplasmic and membranous, CD20-specific staining was membranous, CD204 and Iba-1 immunoreactivity was both cytoplasmic and membranous, and MAC387 positivity was both nuclear and cytoplasmic, while MUM-1/IRF-4 immunoreactivity was predominantly nuclear.

Table 1: List of selected leucocyte antibodies and immunohistochemical methods used on liver specimens from healthy control dogs and dogs naturally infected with *Babesia rossi*.

Antibody	Target/s	Host/Clone	Manufacturer (catalogue no.)	Antigen retrieval (pH)	Dilution (incubation time)
CD3	T lymphocytes ¹ .	Rabbit polyclonal	Dako (A0452)	Citrate (pH6)	1:600 (1 hour)
CD20	Mature B lymphocytes ² and normal dog plasma cells ³ .	Rabbit polyclonal	Thermo Fisher Scientific (PA5-16701)	EDTA (pH9)	1:800 (2 hours)
CD204	Macrophages and dendritic cells ⁴ .	Mouse monoclonal (SRA-E5)	Abnova (MAB1710)	EDTA (pH9)	1:400 (1 hour)
Iba-1	Monocytes, macrophages, and dendritic cells ⁵ .	Rabbit polyclonal	Abcam (Ab178846)	Citrate (pH6)	1:1600 (2 hours)
Myeloid/histiocyte antigen	Monocyte-macrophages of bone marrow origin and circulating mature myeloid cells ⁶ .	Mouse monoclonal (MAC387)	Dako (M0747)	EDTA (pH9)	1:400 (1 hour)
MUM-1/IRF4	Small subset of germinal centre B-lymphocytes and plasma cells ⁷ .	Mouse monoclonal (MUM-1)	Dako (M7259)	EDTA (pH9)	1:50 (1 hour)
Histochemical Stain	Expression/function				
Luxol Fast Blue (LFB)	Highlights intraerythrocytic <i>B.rossi</i> parasites ⁸ .				

1. (Ferrer et al., 1993).

2. (Jubala et al., 2005).

3. (Personal observation - S.J Clift 2015, Henning et al., 2020).

4. (Kato et al., 2013b).

5. (Nakagawa et al., 2017)

6. (Villiers et al., 2006a).

7. (Herbeck et al., 2011).

8. (Personal observation – M Lewis 2021).

3.1.11 Evaluation of histopathology, histochemistry and IHC

All tissue sections were examined by the primary investigator (with the assistance of the supervisors), using an Olympus CX21 light microscope. The field number (Egginton and Gaffney) on the ocular of the microscope was 22 mm. Most of the time, the 40x objective was used for identification, description and scoring of criteria (see below) in *Babesia*-infected and control dog livers.

3.2 DATA ANALYSIS AND STATISTICS

The study was mainly descriptive, and histopathological, histochemical and immunohistochemical scoring was used to generate semi-quantitative data. Using carefully designed score sheets (Appendix B), with a detailed scoring scheme (Appendix C), developed with the supervisors, the livers from the *Babesia*-infected dogs were compared carefully with the normal control dog livers, and changes were identified, described, and scored/quantified, where possible (in the liver specimens as a whole, and in the centrilobular, midzonal and periportal zones of the hepatic lobule).

The following histological criteria were described and scored in the control and *Babesia*-infected liver specimens (Appendix B, Appendix C):

- 3.2.1 Absence/presence of a clear distinction between hepatic zones using the 20x objective
- 3.2.2 Absence/presence/severity of congestion using the 20x objective
- 3.2.3 Absence/presence of haemorrhage using the 20x objective
- 3.2.4 Absence/presence/severity of oedema using the 40x objective
- 3.2.5 Absence/presence/severity of hepatocyte necrosis using the 40x objective
- 3.2.6 Number of intravascular, vascular intramural (within the vascular wall) and perivascular/interstitial leucocytes (eosinophils, lymphocytes, neutrophils, plasma cells and monocyte-macrophages), later confirmed with IHC using the 40x objective
- 3.2.7 Absence/presence/severity of hepatocellular cytoplasmic vacuolation (lipid and/or hydropic change) using the 40x objective
- 3.2.8 Absence/presence of cholestasis using the 40x objective
- 3.2.9 Absence/presence of bile duct proliferation using the 40x objective
- 3.2.10 Absence/presence/severity of hepatitis using the 40x objective
- 3.2.11 Absence/presence/number of hypertrophic Kupffer cells (cells at least twice the size of normal Kupffer cells compared to the controls) using the 40x objective
- 3.2.12 Absence/presence of phagocytosed erythrocytes present using the 40x objective
- 3.2.13 Absence/presence/severity of intracytoplasmic pigment granules (haemosiderin, lipofuscin and bile) in hepatocytes, Kupffer cells, bile ducts, etc. using the 40x objective
- 3.2.14 Absence/presence/severity of extramedullary haematopoiesis present (presence of myeloid precursors, megakaryocytes and metarubricytes/normoblasts) using the 40x objective
- 3.2.15 Absence/presence/severity of endothelial cell hypertrophy, necrosis and/or loss using the 40x objective
- 3.2.16 Absence/presence of intra- and/or extravascular polymerized fibrin deposition using the 40x objective
- 3.2.17 Presence/absence/number of intraerythrocytic *B. rossi* parasites (number of parasites counted in three fields per zone per liver specimen) using the 60x objective

Criteria that were absent were assigned a score of 0, whereas those that were recorded as present were assigned a score of 1. Criteria that were assigned a severity score were scored out of 3: 0 being

absent, 1 being mild, 2 being moderate, 3 being severe. These groupings were established after repeated careful examination of the control samples and a normal number was defined, therefore each criterion had its own specific definition as defined in Appendix C. This resulted in the total achievable score being 126, and each liver sample was then ranked for severity based on the score achieved. The location of each criterion was specifically noted during the histological examination. Perl's Prussian blue stain was counted by identifying cell- and not obviously cell-associated positive staining clusters of pigment. Luxol fast blue stain was measured by counting the number of intra-erythrocytic parasites that were present. Each liver specimen was scored on two separate occasions with one week intervals by the primary investigator, without access to previous scoring data, in an attempt to reduce intra-observer bias, thereby improving accuracy/repeatability.

For the purpose of scoring the IHC, positively stained cells were counted manually on photomicrographs (20x objective; 200x magnification) of liver sections from the control and infected dogs taken with a Olympus DP72 camera. The positive cells for each immunophenotype were counted in three separate high-power fields (HPFs) in each of the 3 zones. A median for each of the three counts in each zone was calculated such that each zone had a median cell count reported. Also reported was the highest and lowest median count for all three zones together for the particular cell phenotype. This allowed the range of the median count (highest median to the lowest median for all 3 zones together for each cell type) to be recorded. The areas selected for counting were free from artefactual spaces or cracks and tissue folds, and showed clearly recognisable anatomical structures (e.g. central veins, bile ducts, etc.). The same procedure was followed with the control samples to establish an average and standard deviation, allowing a normal range to be created for the non-diseased livers. The location of the different leucocytes (intravascular, vascular intramural and/or perivascular/interstitial) was also recorded for each zone. Detailed histological descriptions were used in instances where scoring was not considered appropriate (e.g. the GSS staining of reticular fibres was not quantified, but the pattern of staining was compared between the control and infected samples).

Where numerical data was generated, statistical analysis was performed. Due to the small sample size, non-parametric tests were used to compare medians (Mann Whitney U) between groups. Statistical analysis was performed by using a statistical software package (SPSS, version 24, IBM). The significance was set at $P < 0.05$.

4. RESULTS

4.1 BLOOD RESULTS

4.1.1 Haematological values

The results of the relevant haematological values from the complete blood count are summarized in Table 2 below.

Table 2: A summary of the liver-specific serum haematology results from the control and *B. rossi*-infected cases. The lab-specific reference range, median and range of both the control (n=4) and *B. rossi*-infected cases (n=10) is listed below with the *P*-value comparing the control and infected cases.

Haematological parameter	Lab-specific reference range	Median value of the control cases (Standard deviation)	Range (minimum – maximum)	Median value of the <i>B. rossi</i> -infected cases (Standard deviation)	Range (minimum – maximum)	<i>P</i> -value* comparing the control vs. infected cases
Red cell count (RCC) ($\times 10^{12}/L$)	5.5 – 8.5	6.9 (0.8)	(5.7 - 7.5)	2.1 (1.6)	(1 - 5)	0.002
Haematocrit (Hct) (L/L)	0.4 – 0.6	0.4 (0.0)	(0.4 - 0.5)	0.2 (0.1)	(0.1 - 0.4)	0.002
Platelet concentration ($\times 10^9/L$)	200 – 500	359 (82.3)	(289 – 477)	40.5 (33.2)	(11 – 102)	0.002
White cell count (WCC) ($\times 10^9/L$)	6 - 15	7.1 (1.8)	(5.2 – 9.0)	13.4 (29.2)	(3.4 - 105.6)	0.076
Neutrophils (mature) ($\times 10^9/L$)	3 – 11.5	4.7 (1.8)	(2.2 - 6.1)	9.1 (19.1)	(0.9 - 67.3)	0.054
Neutrophils (band) ($\times 10^9/L$)	0 – 0.5	0 (0.1)	(0)	1.3 (6.5)	(1 - 21.8)	0.182
Lymphocytes ($\times 10^9/L$)	1 – 4.8	1.8 (0.4)	(1.6 - 2.3)	1.4 (1.5)	(0.4 - 5)	0.839
Monocytes ($\times 10^9/L$)	0.2 – 1.4	0.4 (0.1)	(0.4 - 0.5)	0.8 (4.0)	(0 - 13.5)	0.106

*Significant *P*-values (*P*-value <0.05) are in bold.

4.1.2 Serum biochemistry values

The results of the liver-specific serum biochemistry values are summarized in Table 3 below.

Table 3: A summary of the liver-specific serum haematology results from the control and *B. rossi*-infected cases. The lab-specific reference range, median and range of both the control (n=4) and *B. rossi*-infected cases (n=10) is listed below with the *P*-value comparing the control and infected cases.

Biochemistry parameter	Lab-specific reference range	Median value of the control cases (Standard deviation)	Range (minimum – maximum)	Median value of the <i>B. rossi</i> -infected cases (Standard deviation)	Range (minimum – maximum)	<i>P</i> -value* comparing the control vs. infected cases
ALP (U/L)	20 – 165	80.5 (44.1)	(27 - 126)	119 (411.6)	(80 - 1428)	0.142
ALT (U/L)	9 - 73	21.4 (7.2)	(10.3 - 25.7)	86.5 (321.1)	(34 - 930)	0.002
Bile acids (µmol/L)	0 – 8	3 (1.5)	(<1 - 4)	8.5 (215.1)	(2 - 690)	0.109
Urea (mmol/L)	2.3 – 8.9	3.1 (0.7)	(2.6 - 4.3)	20.7 (33.0)	(18.7 - 104.3)	0.048
Albumin (g/L)	28 – 41	33.3 (8.0)	(19.2 - 37)	19.6 (4.7)	(14.9 - 28.5)	0.054
Total serum protein (TSP) (g/L)	56 - 73	51.3 (5.9)	(47.3 - 60.2)	53.7 (11.5)	(38.2 - 71.7)	0.839
Bilirubin (µmol/L)	1 – 6.8	Not measured	Not measured	83.3 (137.6)	(7.2 - 465.4)	Not performed
Glucose (mmol/L)	3.3 – 5.5	Not measured	Not measured	3.6 (4.6)	(0.4 – 15.3)	Not performed.

*Significant *P*-values (*P*-value <0.05) are in bold.

** Bilirubin values of the *B. rossi*-infected cases were severely elevated compared to the normal lab-specific reference range.

*** Glucose values of the *B. rossi*-infected cases fell mostly within the lab-specific reference range.

4.2 HISTOPATHOLOGY

4.2.1 Control cases

Liver specimens from the control dogs were formalin-fixed within 15 minutes after euthanasia, hence there was minimal autolysis present in the samples. There was mild centrilobular congestion in all the liver specimens (to be expected after euthanasia with pentobarbitone). In all cases, the distinction between hepatic zones was clear (Figures 9-12).

Portal tracts

The portal tracts in the control liver samples appeared normal based on evaluation of selected criteria (Figure 9, Appendix C). Only one of the control samples had small quantities of haemosiderin pigment present within normal-sized Kupffer cells (Figure 28). Endothelial cells lining the portal veins and hepatic arteries were intact and typically flattened and elongated with diameters less than the diameter of a red blood cell (RBC) (Figure 10). Lymphatic vessels were occasionally slightly distended in the control livers, and a small amount of homogenous pale eosinophilic material was present in some of them (lymph) (Figure 9). A few intravascular normoblasts indicating extramedullary haematopoiesis (EMH) was present in two of the four samples, and the perisinusoidal space of Disse was not obvious (Figure 9). Inflammatory cells were sparse in the perivascular interstitium of the portal tracts, consisting of a few macrophages, neutrophils, plasma cells, and lymphocytes.

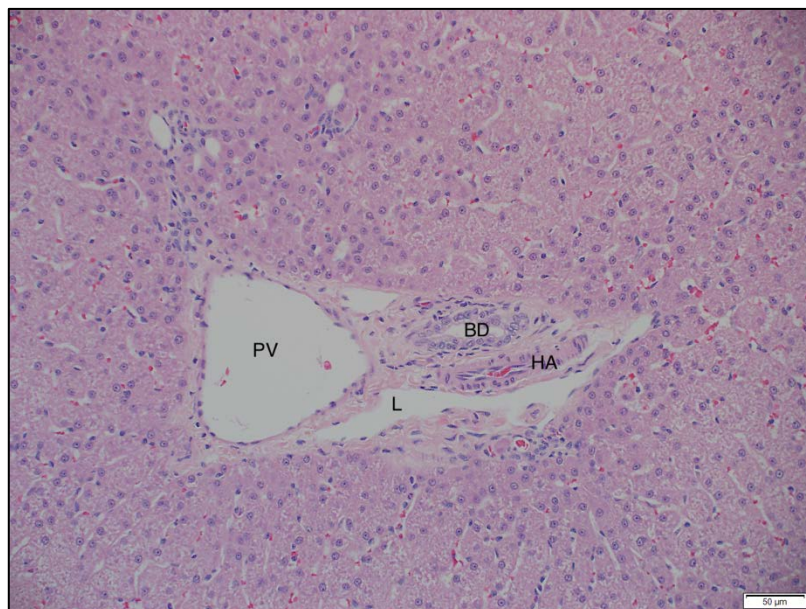


Figure 9: Photomicrograph of a normal dog liver (control no. 2) showing a portal tract. PV = portal vein, BD = bile duct, HA = hepatic artery, L = lymphatic vessel. Haematoxylin and eosin (HE) staining at 200x magnification.

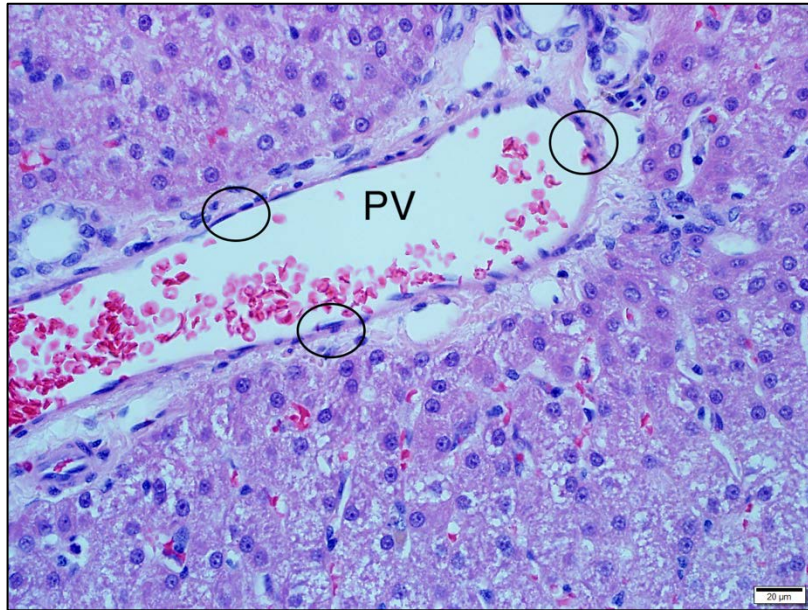


Figure 10: Photomicrograph of a normal dog liver (control no. 4) showing the portal tract with normal flattened, elongated endothelial cells (black circles) lining the portal vein. PV = portal vein. HE staining at 400x magnification.

Midzonal area

Midzonal hepatocytes showed no evidence of necrosis, fatty or hydropic change (Figure 11). Two of the four samples exhibited mitoses and binucleated hepatocytes (Figure 11). In one liver sample, a few Kupffer cells contained haemosiderin pigment (Figure 29). A few nucleated erythrocytes were present within the sinusoids in 3/4 of the samples. The space of Disse was not obviously distended in any of the specimens (Figure 11).

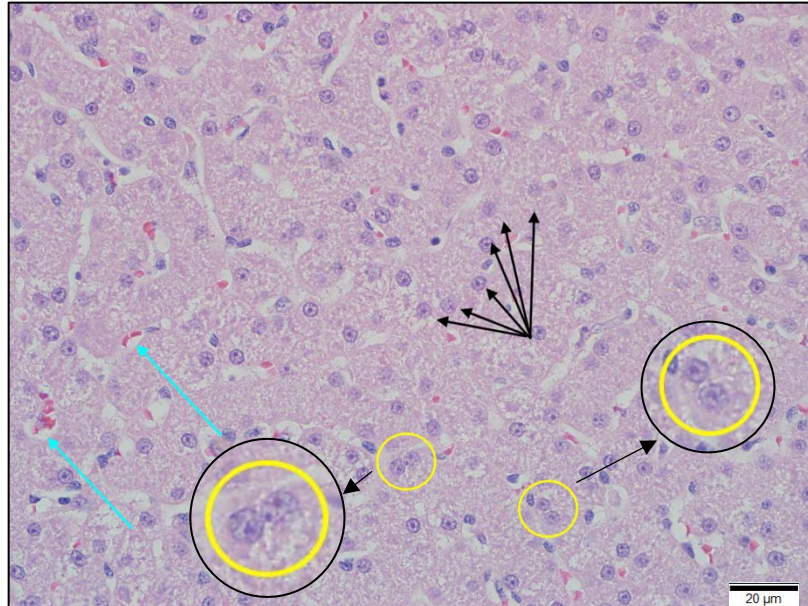


Figure 11: Photomicrograph of a normal dog liver (control no. 2) showing the midzonal area. Hepatocyte cords are visualised (black arrows) with sinusoids containing erythrocytes, surrounded by the space of Disse (blue arrows). Binucleated hepatocytes are also present (yellow circles) with magnified portions (larger black circles). HE staining at 400x magnification.

Centrilobular area

There were occasional mitotic figures and binucleated hepatocytes (Figure 12). Only one liver sample had small amounts of haemosiderin pigment granules in a few centrilobular hepatocytes and sinusoid-associated Kupffer cells (Figure 30). Central veins were lined by normal endothelium, with only one sample exhibiting a mild perivascular mononuclear leucocytic infiltrate comprising a few macrophages, plasma cells and lymphocytes. Another liver sample exhibited a greater number of small, mature lymphocytes compared within the perivascular interstitium compared to the other three samples. Lymphatic vessels were occasionally slightly distended, and in two samples, vessels contained homogenous pale eosinophilic material (lymph) (Figure 12). Only a few nucleated erythrocytes were present within the sinusoids in all samples.

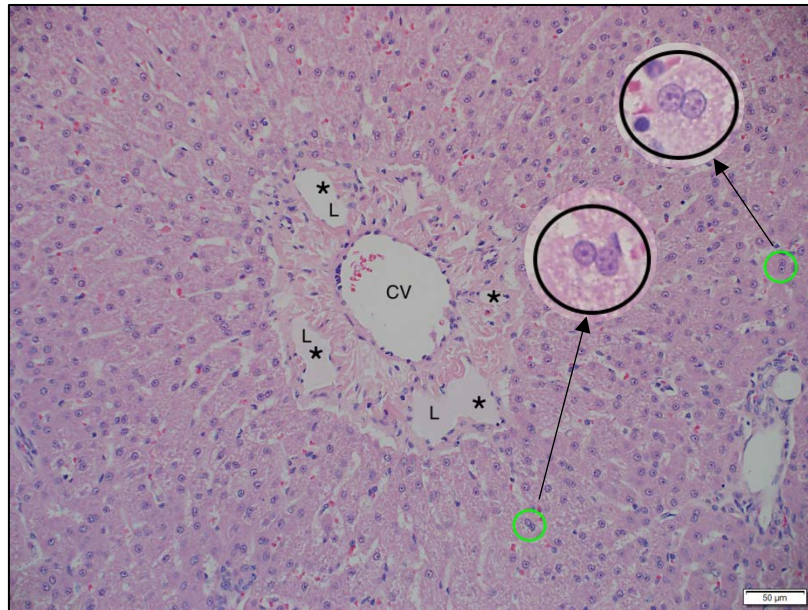


Figure 12: Photomicrograph of a normal dog liver (control no. 2) showing the centrilobular area. Lymphatic vessels containing homogenous pale eosinophilic material are visualized (black stars), and binucleation of hepatocytes indicating turnover (green circles) with magnified views at 400x magnification (larger black circles). CV = central vein, L = lymphatic vessel. HE staining at 200x magnification.

4.2.2 Infected cases

All the liver samples showed multifocal coalescing through to diffuse lesions that affected all zones. It was possible to distinguish between the different zones in most cases, but evidence of moderate centrilobular necrosis did sometimes make the distinction more difficult (Figure 13). Eight of 10 cases exhibited severe diffuse congestion, while the other two cases showed mild diffuse congestion, similar to the controls (Figure 14). No haemorrhages were identified in any of the cases.

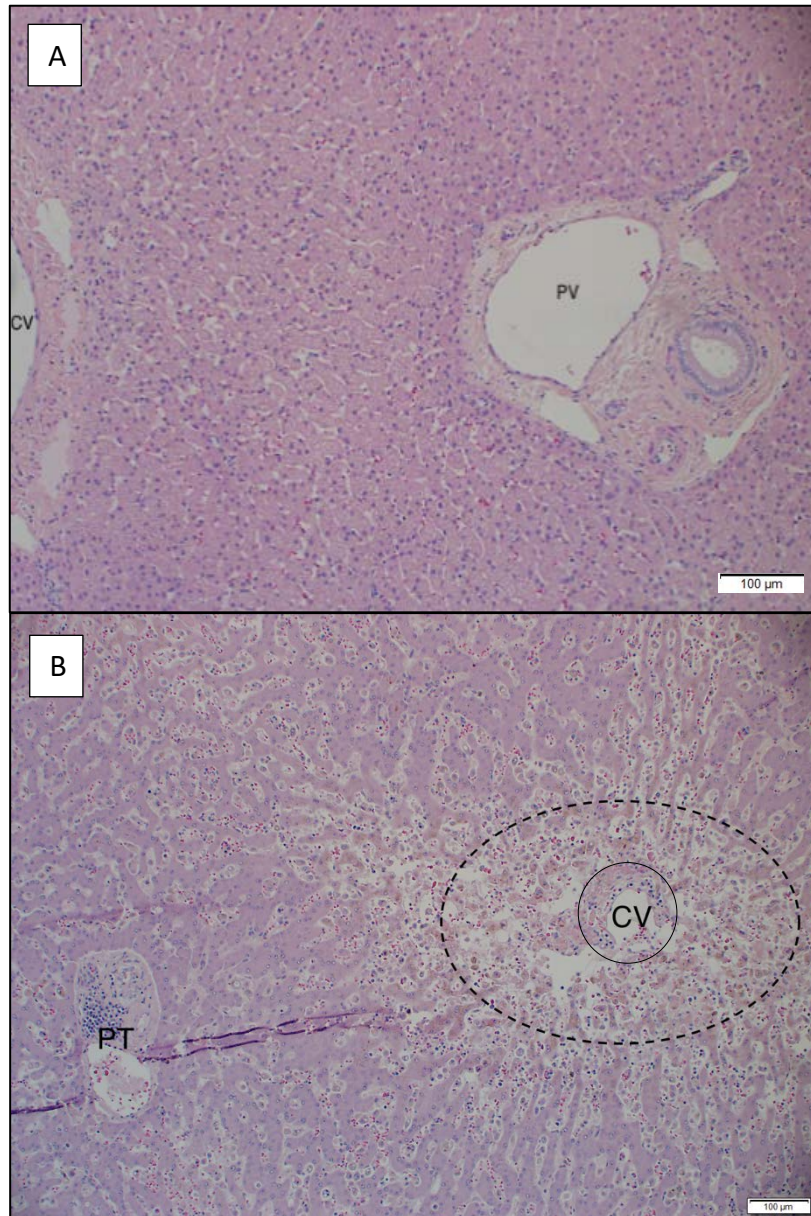


Figure 13: **A.** Photomicrograph of a normal dog liver (control no. 2) showing centrilobular, midzonal and portal tracts that are normal and distinct. CV = central vein, PV = portal vein. HE staining at 100x magnification. **B.** Photomicrograph of an infected dog liver (case no. 20) with moderate centrilobular necrosis (delineated by the dotted black circle) associated with markedly dilated, bloodless sinusoids. The distinction between centrilobular, midzonal and periportal areas is not as obvious in image B as it is in image A (or Figure 12). PT = portal tract, CV = central vein (solid black circle). HE staining at 100x magnification.

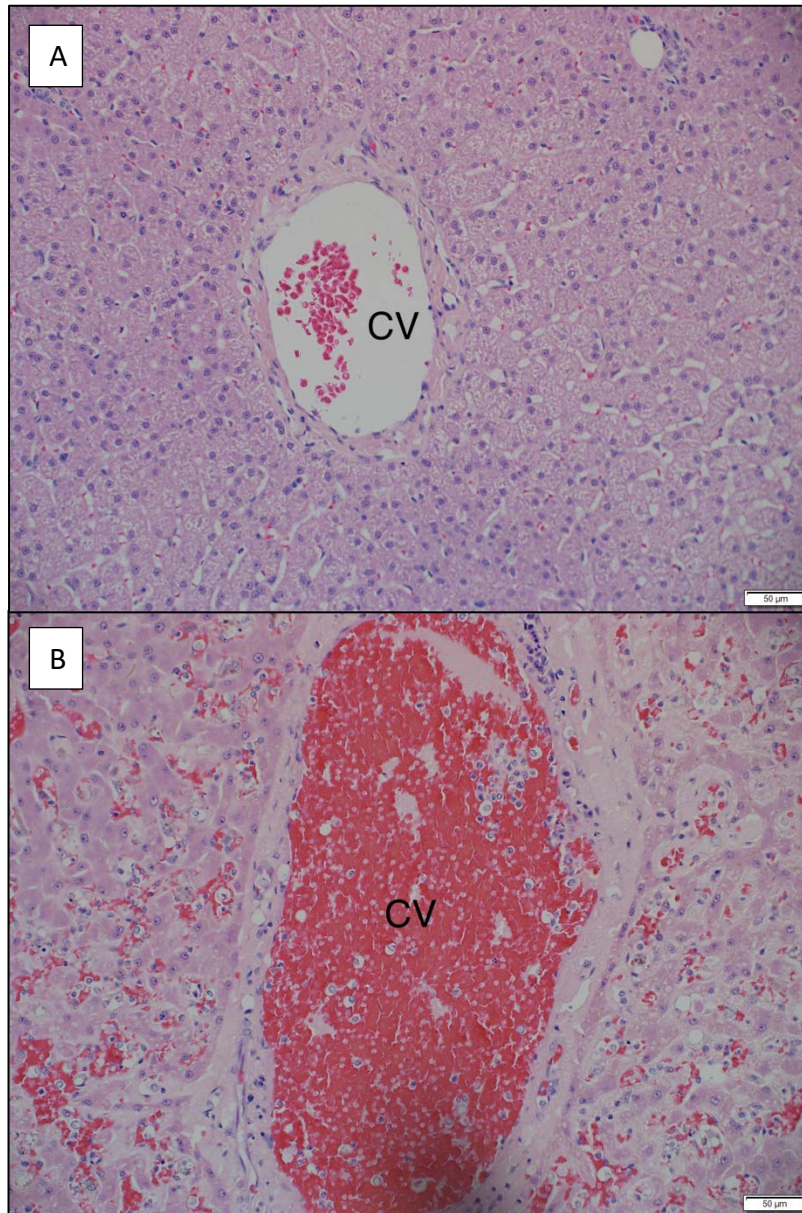


Figure 14: **A.** Photomicrograph of a normal dog liver (control no. 2) showing a mildly congested central vein. CV = central vein. HE staining at 200x magnification. **B.** Photomicrograph of an infected dog liver (case no. 50) showing severe centrilobular (also referred to as periacinar) congestion. CV = central vein. HE staining at 200x magnification.

Portal tract

In eight of the 10 infected cases, there was obvious bile ductular cholestasis with no evidence of bile duct proliferation (Figures 15-16). In the same cases, small amounts of bile pigment were identified in the intercellular bile canaliculi in the periportal areas as well as within periportal hepatocytes, but no bile was evident in the vicinity of the canal of Hering at the interface between hepatocytes and cholangiocytes in the region of the limiting plate of hepatocytes (Figure 15). None of the samples showed evidence of necrosis within the limiting plate of hepatocytes. Two of 10 samples showed severe hydropic vacuolation of periportal hepatocytes, while seven samples exhibited mild hydropic vacuolation, and one sample showed none. Seven of the 10 samples demonstrated prominent vesicular/euchromatic nuclei in multiple scattered hepatocytes at 400x magnification (Figure 15), while the other three showed none. Anisokaryosis of the limiting plate of hepatocytes was not observed. Mild hepatocyte turnover, as indicated by the presence of mitoses and binucleation, similar to the controls, was observed in eight of 10 samples with the remaining two samples exhibiting none (Figure 16). There were small amounts of haemosiderin pigment within the hepatocytes in eight of 10 samples while the remaining two samples had none (Figure 28). There was mild leucostasis in portal veins in 7/10 cases, with moderate and severe leucostasis evident within the portal veins in each of the remaining samples (Figures 15-16). Mild endothelial cell hypertrophy of the portal veins was present in 6/10 samples, with moderate endothelial cell hypertrophy in one sample and none in the remaining three cases. The hepatic arteries showed mild endothelial cell hypertrophy in 2/10 of the samples, and no endothelial cell hypertrophy present in the other 8/10 samples. Noticeably dilated lymphatics were seen in 9/10 of the samples, and in seven of these samples the distended lymphatics contained a homogeneous pale eosinophilic material (Figures 15-16). Extramedullary haematopoiesis, indicated by the presence of nucleated red blood cells, was prominent in 3/10 cases, while the other seven cases showed only mild EMH (similar to the controls), however megakaryocytes or obvious granulocytic precursors were not seen (Figures 16-17). There was severe distension of the space of Disse in all samples, with evidence of very pale eosinophilic feathery material within this space (oedema) (Figure 16). Intra- and perivascular monocyte-macrophages predominated in the periportal areas, with 6/10 samples containing many monocyte-macrophages, with the remaining four samples showing numerous monocyte-macrophages. Two of the 10 samples exhibited many neutrophils, three of the samples showed only a few neutrophils, and the remaining five samples exhibited none. Lymphocytes were present in all samples, with three samples containing many lymphocytes, the rest having only a few present. Plasma cells were present in all samples, with two of the samples containing many plasma cells, and the rest containing only a few. Eosinophils were not visualized in any of the samples.

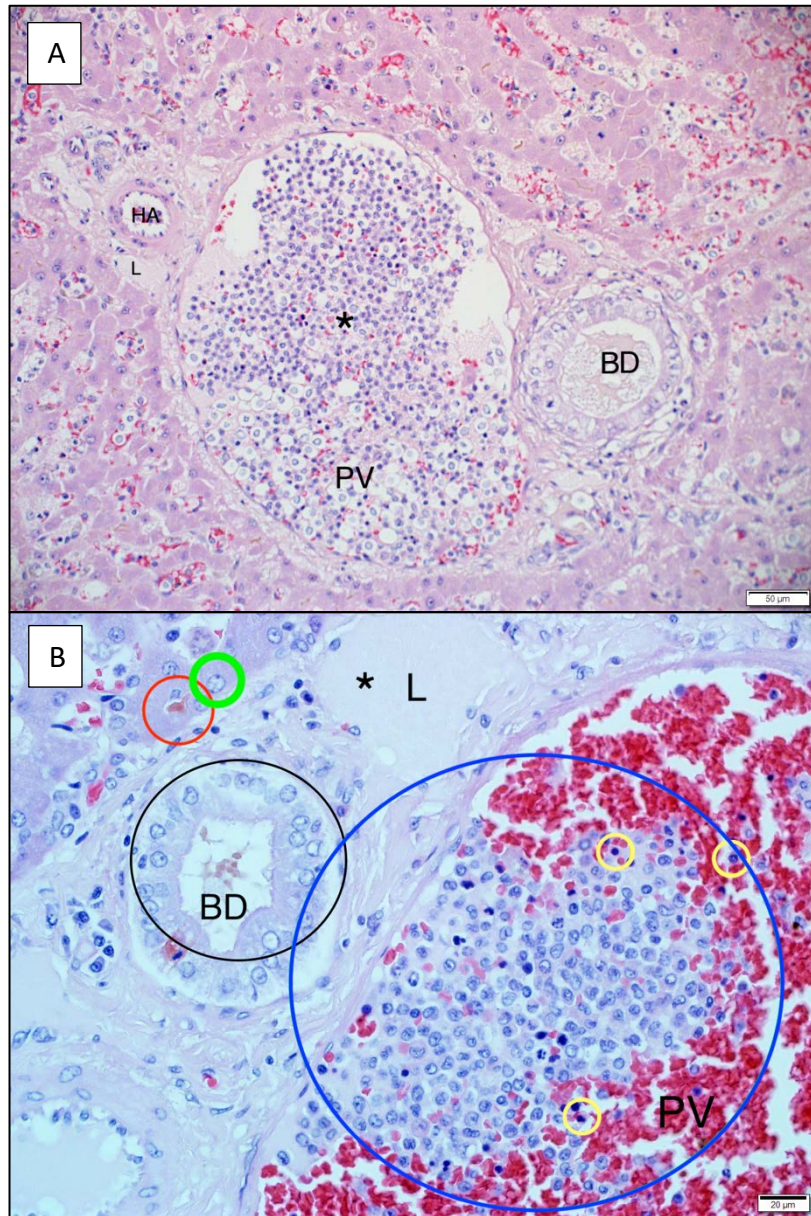


Figure 15: **A.** Photomicrograph of an infected dog liver (case no. 50) showing a portal tract with severe leucostasis in the portal vein (black star). PV = portal vein, BD = bile duct, HA = hepatic artery. HE staining at 400x magnification. **B.** Photomicrograph of an infected dog liver (case no. 117) showing a portal tract with bile stasis in a bile duct (black circle), canalicular cholestasis within the limiting plate of hepatocytes (red circle), a hepatocyte containing a vesicular nucleus (green circle), moderate leucostasis in the portal vein (blue circle), scattered nucleated red blood cells indicating erythropoiesis (yellow circles), as well as a distended lymphatic vessel containing homogenous pale eosinophilic material (black star). PV = portal vein, BD = bile duct, L = lymphatic vessel. HE staining at 400x magnification.

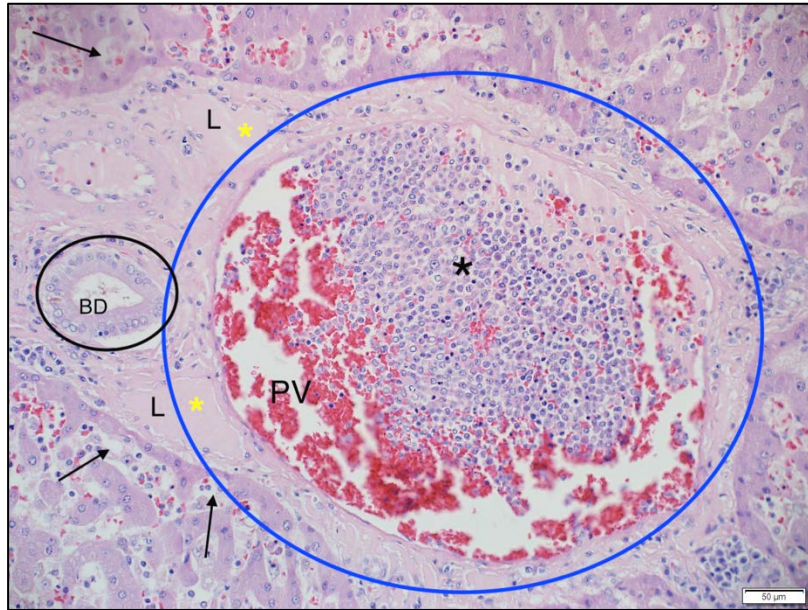


Figure 16: Photomicrograph of an infected dog liver (case no. 117) showing a portal tract with severe congestion (blue circle) and mononuclear leucostasis (black star) within the portal vein, distended lymphatic vessels containing homogenous pale eosinophilic material (yellow stars), bile stasis within the bile duct (black circle), and prominent widening (moderate to severe oedema) of the Space of Disse (black arrows) surrounding the congested, hypercellular sinusoids (black arrows). PV = portal vein, BD = bile duct, L = lymphatic vessel. HE staining at 400x magnification.

Midzonal area

Hepatocytes in the midzonal areas in five of the 10 samples demonstrated mild multifocal necrosis, while the remainder of the samples exhibited necrosis of single cells or small aggregates of hepatocytes (3-5 cells). Severe hydropic vacuolation of hepatocytes was seen in three of 10 samples, moderate hydropic vacuolation was present in one of the 10 samples, while the remaining six samples exhibited mild vacuolation; no lipid vacuolation was seen (Figure 18). Mild hepatocyte turnover (mitoses and binucleation), similar to the controls, was visualized in 7/10 samples, with moderate turnover identified in the remaining specimens (Figures 18-19). Mild anisokaryosis of hepatocytes was seen in 3/10 samples which was not noticeable in the rest of the samples, while large vesicular/euchromatic nuclei were identified in all but one of the samples (Figure 18). Haemosiderin pigment granules were present in 8/10 samples within the hepatocytes (Figure 29), while bile pigment was present in five of the 10 samples in the hepatocytes and bile canaliculi (Figures 17-18). Many hypertrophic Kupffer cells were present in 6/10 samples with the remaining four samples showing hypertrophy of only a few. The hypertrophic Kupffer cells contained phagocytosed haemosiderin pigment in only a few cells in four of the 10 samples, while the remaining six had many Kupffer cells containing haemosiderin pigment (Figure 29). Phagocytosed bile pigment was present in a few cells in six of the 10 samples, with the remaining four samples having many Kupffer cells containing bile pigment. Obvious lipofuscin pigment was rarely identified. Extramedullary haematopoiesis, indicated by the presence of nucleated red blood cells, was a prominent finding in 3/10 samples, while the other seven samples had mild EMH, however megakaryocytes or obvious granulocytic precursors were not seen (Figures 18-19). Severe widening of the space of Disse (oedema) was obvious in all samples (Figure 17, Figure 19).

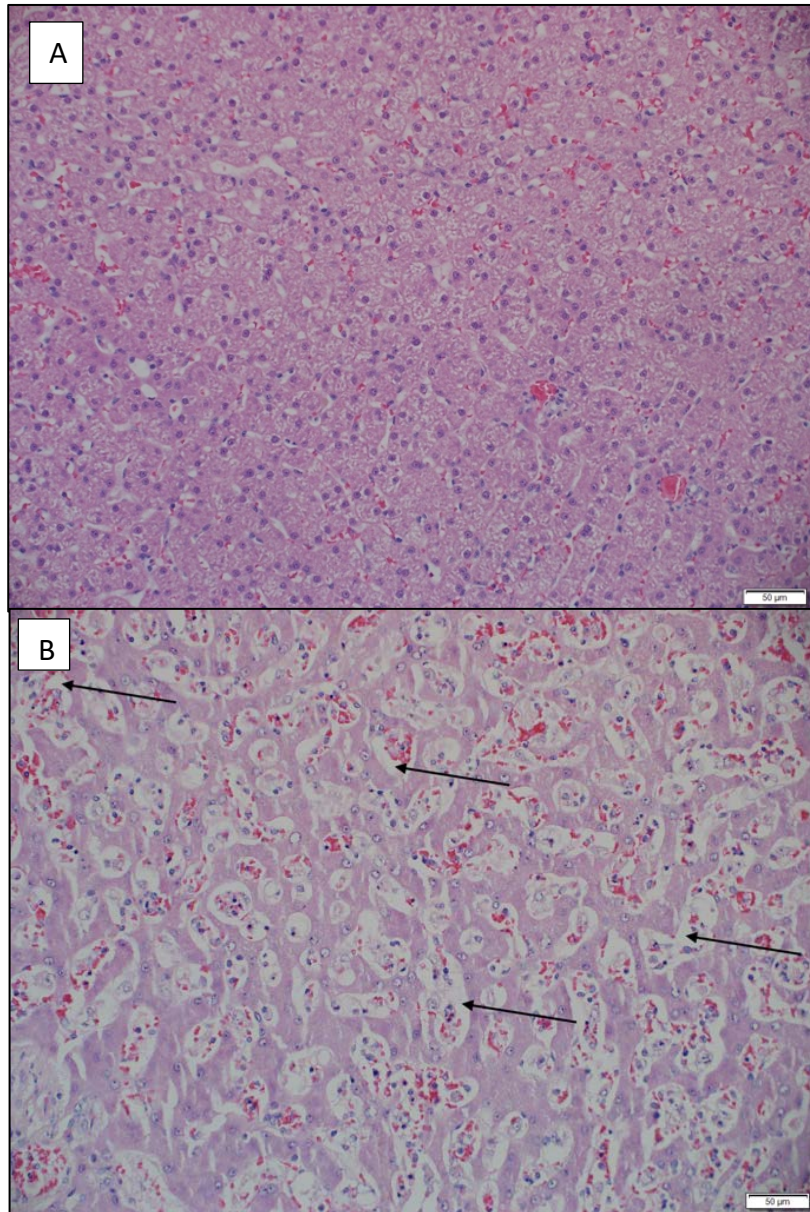


Figure 17: A. Photomicrograph of a normal dog liver (control no. 4) demonstrating the midzonal area. HE staining at 200x magnification. B. Photomicrograph of an infected dog liver (case no. 61) showing prominent widening (moderate to severe oedema) of the space of Disse (black arrows) surrounding the congested, hypercellular sinusoids. HE staining at 200x magnification.

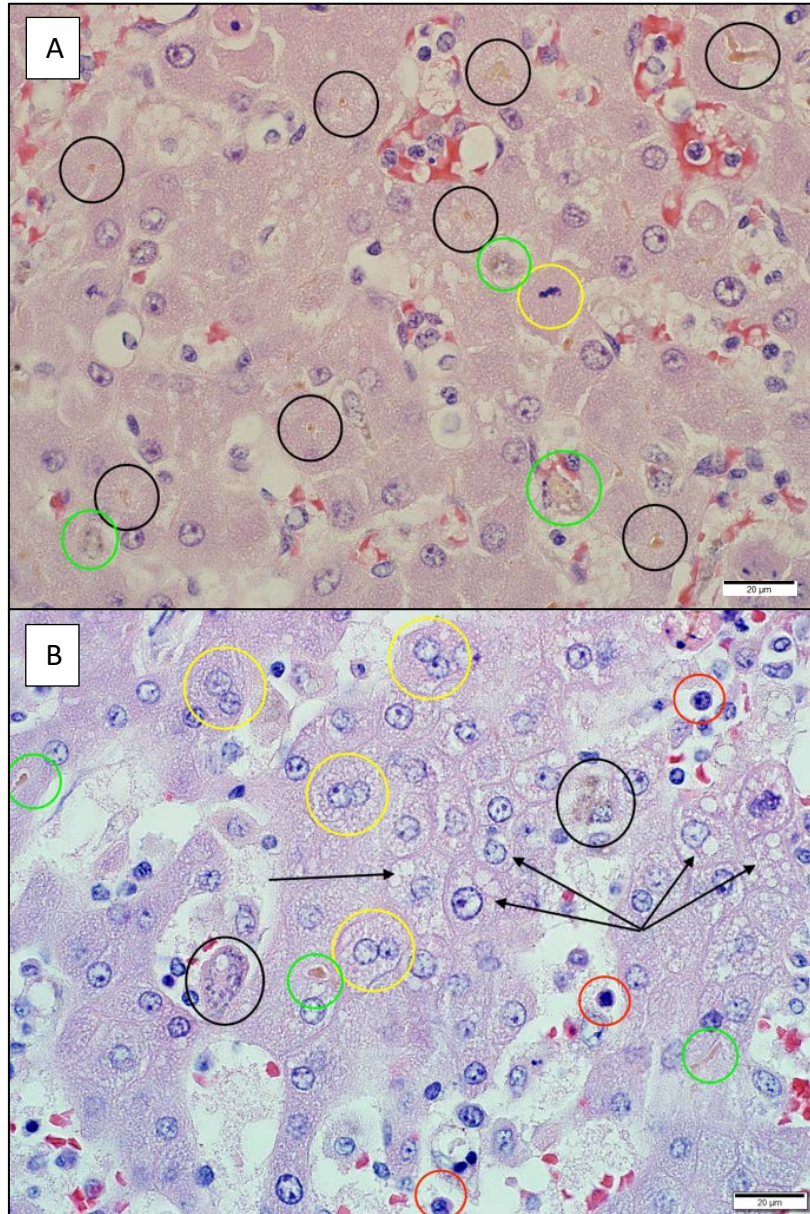


Figure 18: **A.** Photomicrograph of an infected dog liver (case no. 50) showing a midzonal area with mitotic figures (yellow circle) indicating hepatocyte turnover, hypertrophic, haemosiderin-laden Kupffer cells (green circles), and canalicular cholestasis (black circles). HE staining at 600x magnification. **B.** Photomicrograph of an infected dog liver (case no. 117) showing a midzonal area with increased numbers of binucleated hepatocytes indicating increased turnover (yellow circles), hypertrophic, haemosiderin-laden Kupffer cells (black circles), nucleated red blood cells (red circles), canalicular cholestasis (green circles) and mild to moderate hydropic change/vacuolar degeneration in hepatocytes (black arrows). HE staining at 600x magnification.

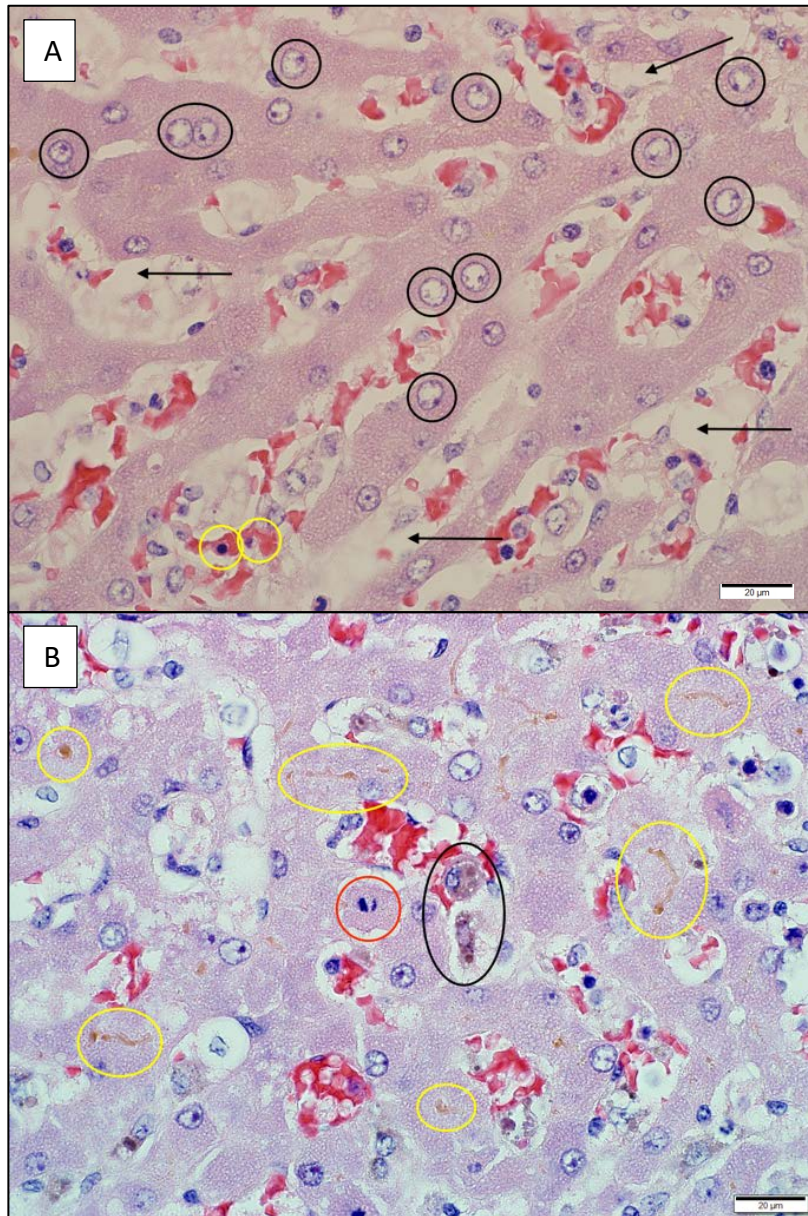


Figure 19: **A.** Photomicrograph of an infected dog liver (case no. 61) showing hepatocytes in the midzonal area with large vesicular/euchromatic nuclei (black circles), marked widening (moderate to severe oedema) of the space of Disse (black arrows), as well as increased numbers of nucleated red blood cells (yellow circles). HE staining at 600x magnification. **B.** Photomicrograph of an infected dog liver (case no. 50) showing hypertrophic, haemosiderin-laden Kupffer cells (black circle), mitotic figures indicating turnover (red circle), and canalicular cholestasis (yellow circles). HE staining at 600x magnification.

Centrilobular area

In 8/10 of the infected samples the centrilobular hepatocytes showed mild multifocal necrosis, while the remaining 2/10 showed none. Severe hydropic change was present in 8/10 samples, with the remaining two samples showing mild hydropic change. Fatty change was scarce, except for one of the samples in which there was severe macrovesicular fatty change. Hepatocytes commonly possessed enlarged vesicular nuclei in all samples. Hepatocyte anisokaryosis was also noted in 8/10 samples, and there was moderate hepatocyte turnover (mitoses and binucleate hepatocytes) in 1/10 samples (Figure 22), while the remaining samples only exhibited mild turnover (similar to the controls). Perivascular inflammatory cell infiltrates were seen in all the samples (Figure 20, Figure 22), and in 5/10 samples the majority of endothelial cells lining the central veins were moderately hypertrophic (Figure 22), while mild endothelial cell hypertrophy was seen in two samples, and no hypertrophy seen in three. Canalicular bile stasis was evident, haemosiderin, and non-Perls-positive yellow-brown finely granular pigment (bile or lipofuscin) was present within the hepatocytes in all samples (Figure 20, Figure 22, Figure 30). Severely hypertrophic haemosiderin- and bile-containing Kupffer cells were present in all the cases (Figure 30). The lymphatic vessels of the centrilobular areas were all severely distended and contained a homogenous pale eosinophilic material (Figure 21). Moderate numbers of nucleated erythrocytes were identified 5/10 samples, four samples contained only a few nucleated erythrocytes, and one sample contained none. There was marked widening of the spaces of Disse (severe oedema) in all the infected cases (Figure 20, Figure 22). Sinusoid-associated monocyte-macrophages were the most common inflammatory cells, with 5/10 samples showing many monocyte-macrophages in the perivascular interstitium; the other half of the cases exhibited only a few scattered cells in the interstitium. Neutrophils were also identified with 8/10 samples exhibiting only a few, while two samples had many present. Few (less than 20 cells per 400x magnification/HPF) lymphocytes and plasma cells were seen in 8/10 samples, while the other two samples had many.

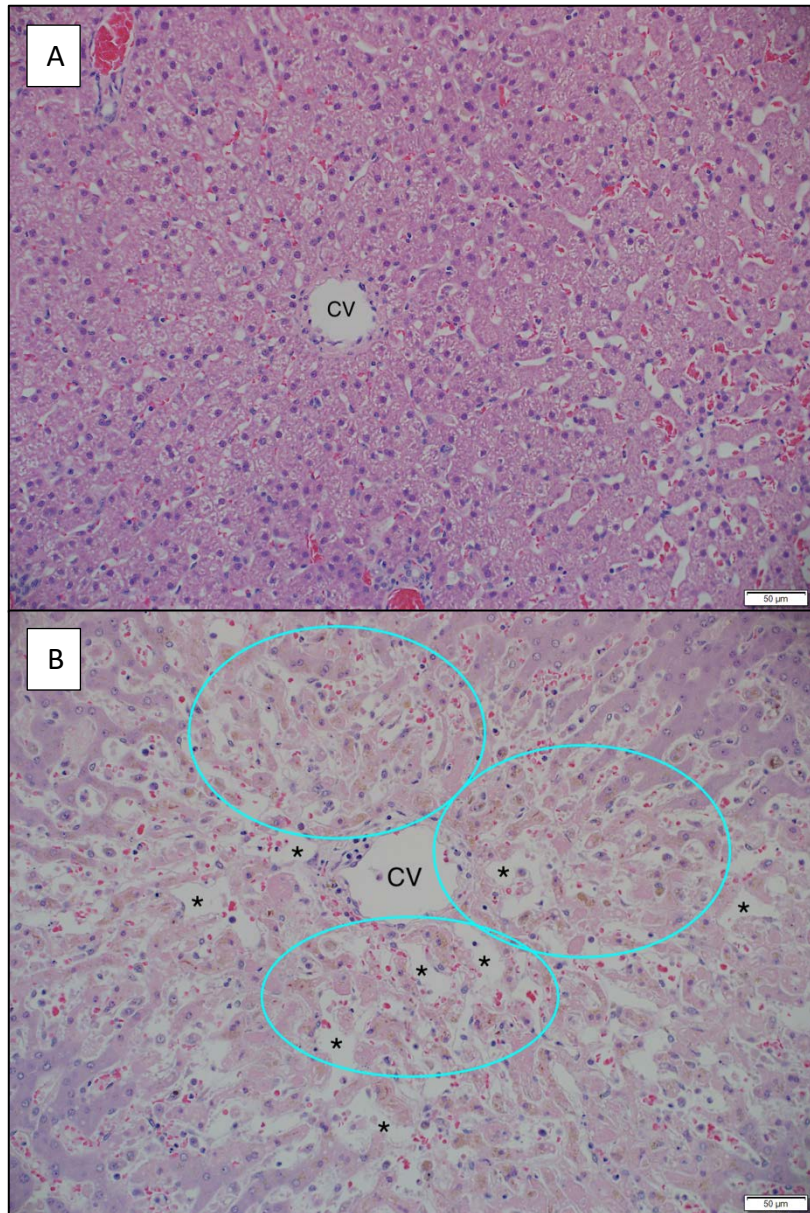


Figure 20: A. Photomicrograph of a normal dog liver (control no. 4) demonstrating a centrilobular area. CV = central vein. HE staining at 200x magnification B. Photomicrograph of an infected dog liver (case no. 20) showing a centrilobular area with bile pigment in hepatocytes (blue circles) and prominent widening (severe oedema) of the space of Disse (black stars) and only a small amount of blood within the sinusoids. CV = central vein. HE staining at 400x magnification.

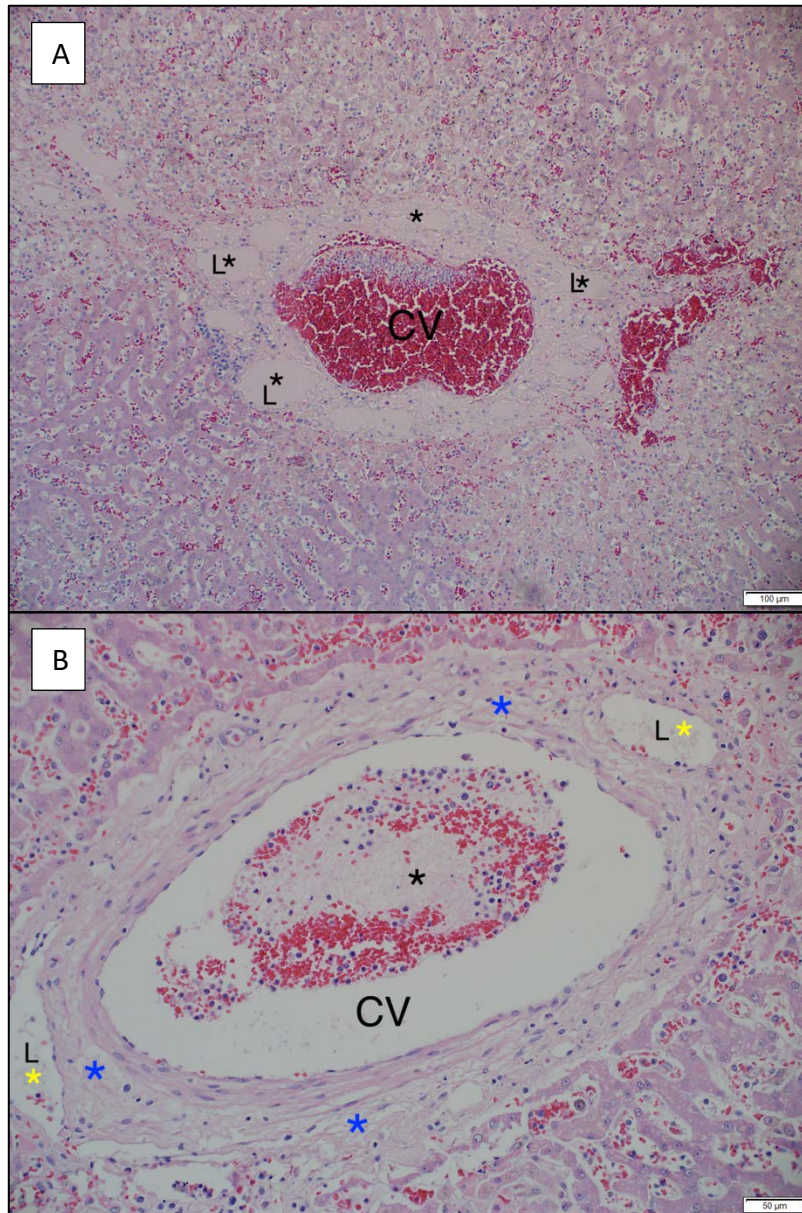


Figure 21: **A.** Photomicrograph of an infected dog liver (case no. 117) showing a centrilobular area with severe congestion of the central vein and adjacent sinusoids, and moderately distended lymphatic vessels containing homogenous pale eosinophilic material (black stars). CV = central vein, L = lymphatic vessel. HE staining at 100x magnification. **B.** Photomicrograph of an infected dog liver (case no. 59) showing a moderately congested central vein and surrounding sinusoids, and moderate mononuclear leucostasis especially prominent in the central vein (black star). Mild lymphatic distension (yellow stars) and mild oedema are also present (blue stars). CV = central vein. L = lymphatic duct. HE staining at 200x magnification.

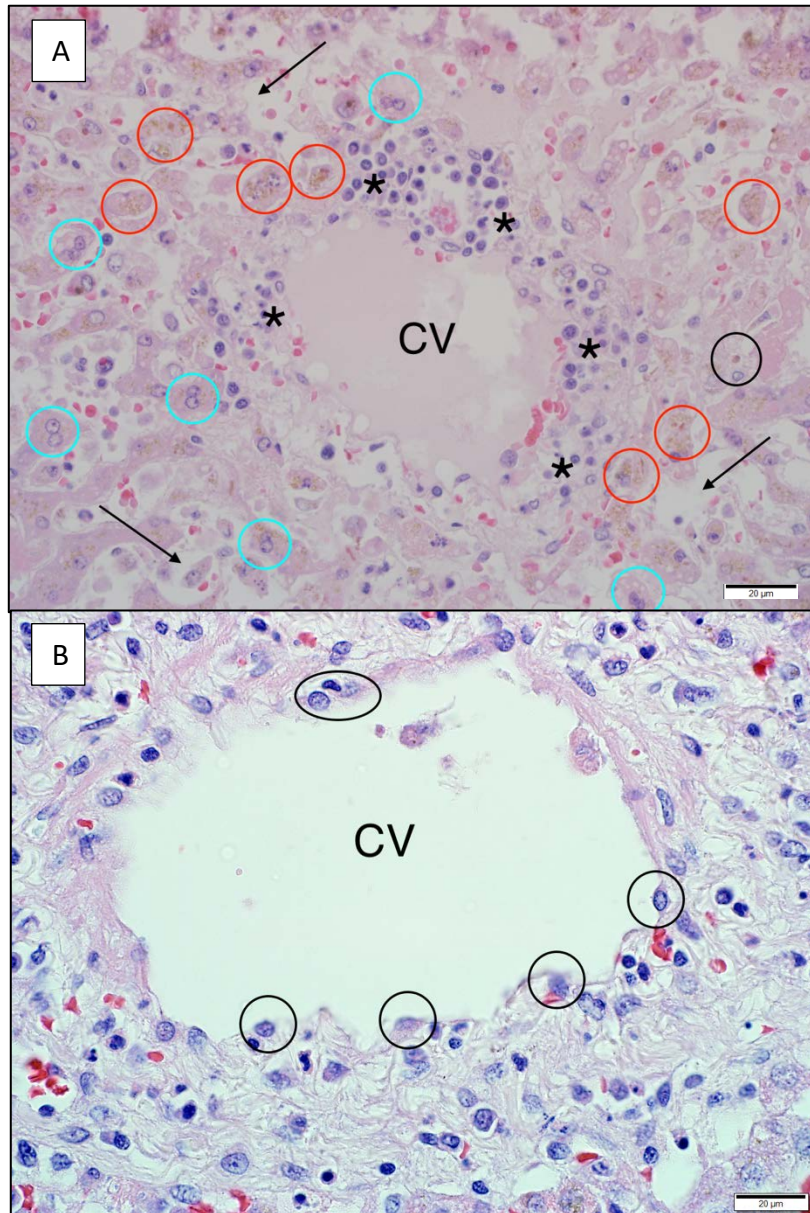


Figure 22: A. Photomicrograph of an infected dog liver (case no. 20) demonstrating a centrilobular area with moderate numbers of perivascular (and a few vascular intramural) mononuclear leucocytes (black stars), binucleated hepatocytes (blue circles), Kupffer cell-associated haemosiderin-like pigment (black circle), bile pigment in hepatocytes (red circles), as well as marked widening (severe oedema) of the space of Disse (black arrows). CV = central vein. HE staining at 400x magnification. B. Photomicrograph of an infected dog liver (case no. 59) demonstrating a centrilobular area with moderate endothelial cell hypertrophy (black circles). CV = central vein. HE staining at 400x magnification.

4.3 HISTOCHEMICAL STAINS

Selected histochemical stains were applied to the control liver samples to enhance the visualisation of intra- and/or extravascular polymerized fibrin, reticular fibres, haemosiderin pigment and intraerythrocytic *Babesia* parasites.

4.3.1. Martius Scarlet Blue (MSB) stain

The MSB staining technique was used to better visualise intra- and/or extravascular polymerised fibrin (which stains bright pink with this technique) in the different hepatic zones. No fibrin was identified in the control samples in the HE sections, or with the MSB technique. In general, fibrin was not convincingly identified in the liver specimens from this cohort of *B. rossi*-infected dogs (Figures 23-25).

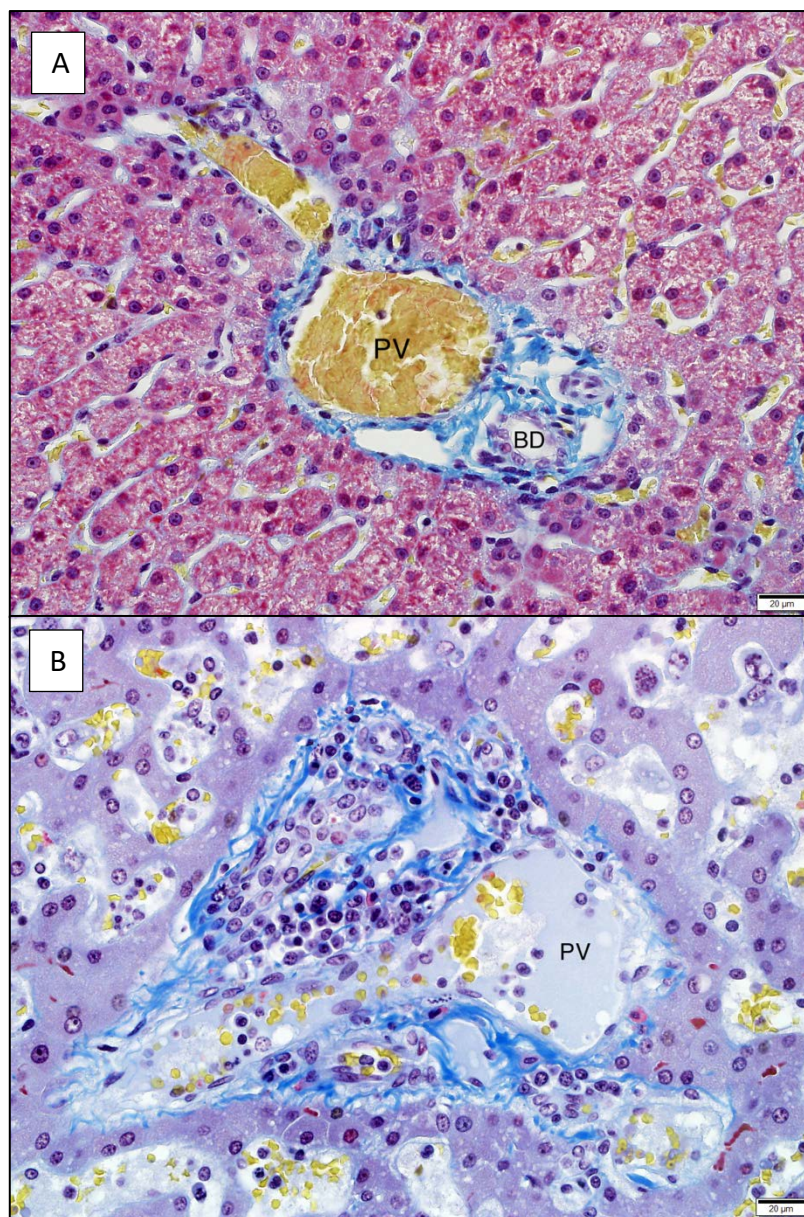


Figure 23: **A.** Photomicrograph of a normal dog liver (control no. 4) showing a portal tract with no evidence of fibrin. PV = portal vein, BD = bile duct. MSB staining at 400x magnification. **B.** Photomicrograph of an infected dog liver (case no. 117) showing a portal tract with no evidence of fibrin. Red blood cells stain yellow, collagen stains blue, intracanalicular bile stains dark pink. PV = portal vein. MSB staining at 400x magnification.

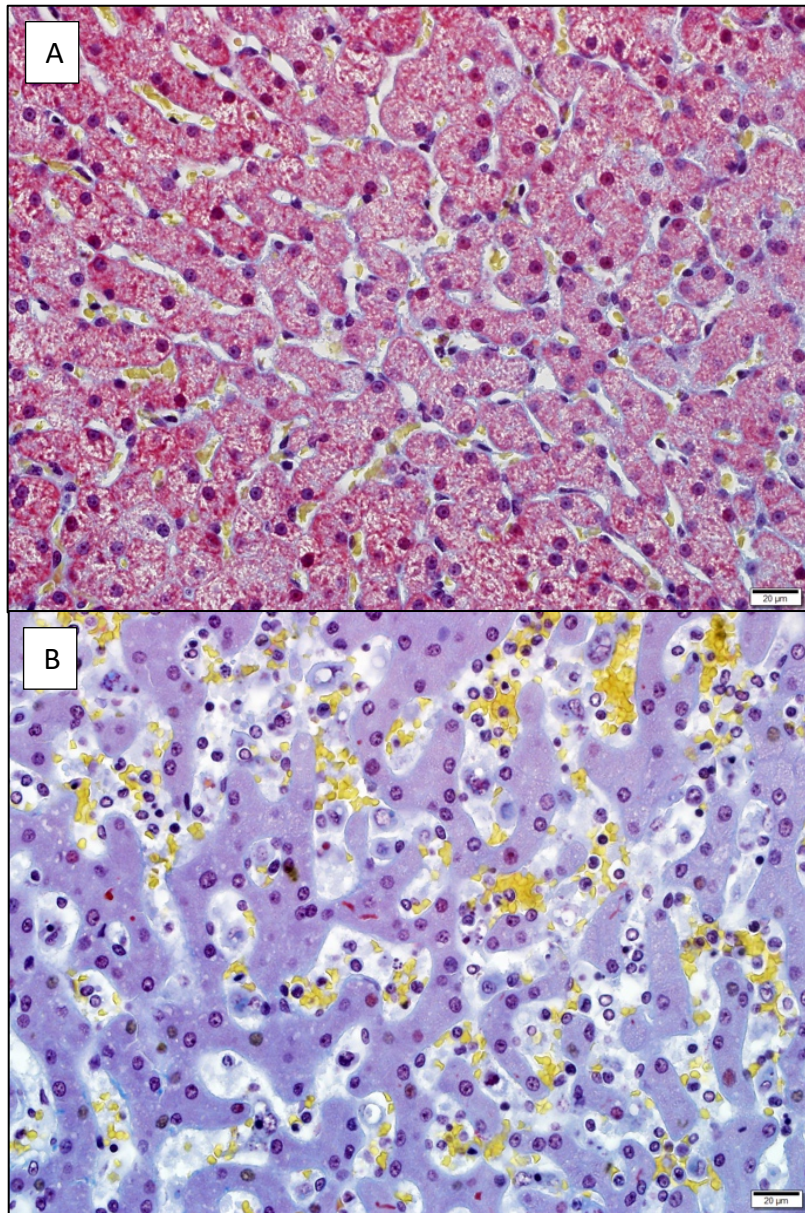


Figure 24: **A.** Photomicrograph of a normal dog liver (control no. 4) showing a midzonal area with no signs of fibrin present. MSB staining at 400x magnification. **B.** Photomicrograph of an infected dog liver (case no. 50) showing a midzonal area with no fibrin present. MSB staining at 400x magnification.

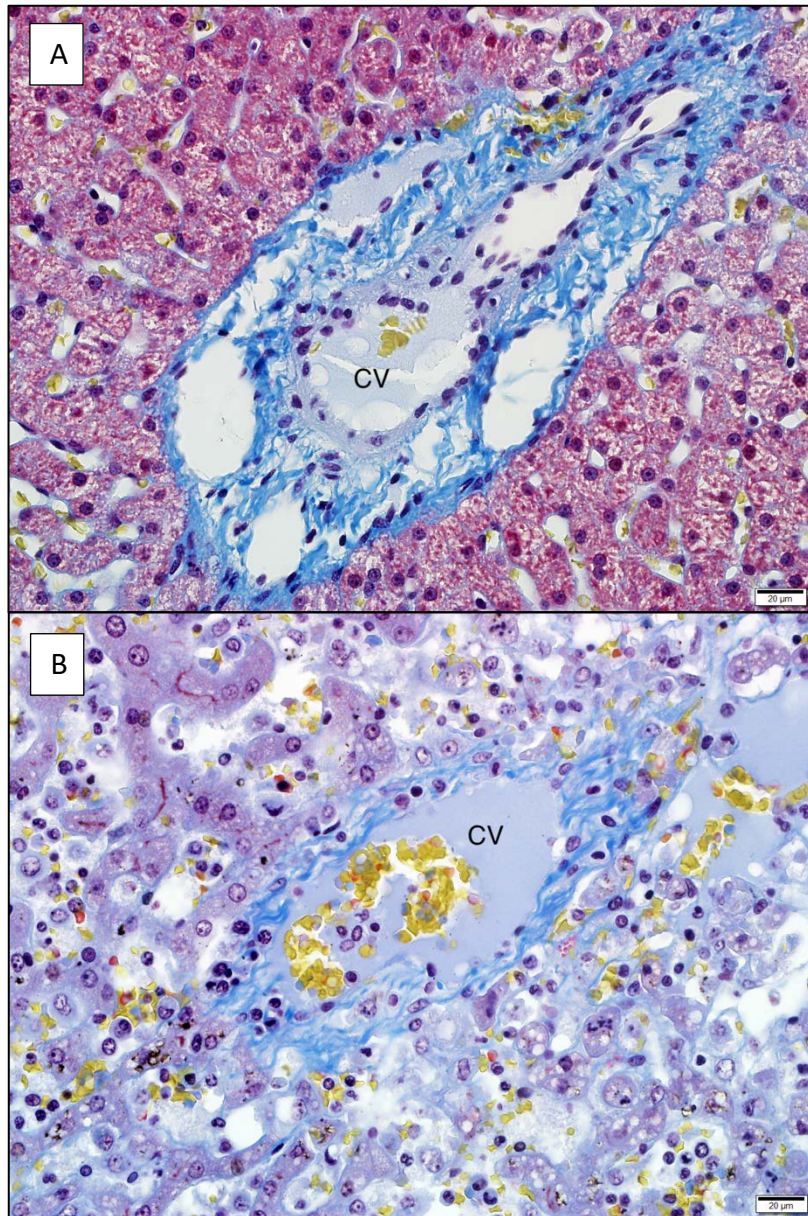


Figure 25: A. Photomicrograph of a normal dog liver (control no. 4) showing a centrilobular area with no signs of fibrin present. CV =central vein. MSB staining at 400x magnification. B. Photomicrograph of an infected dog liver (case no. 117) showing a centrilobular area with no evidence of fibrin present. CV = central vein. MSB staining at 400x magnification.

4.3.2. Gordon and Sweet's silver (GSS) stain

This staining method was used to visualise reticular fibres (which stain black with this method). There was no difference between the controls and infected cases, implying no structural change in the fibrous protein component of the extracellular matrix in the infected cases (Figure 26).

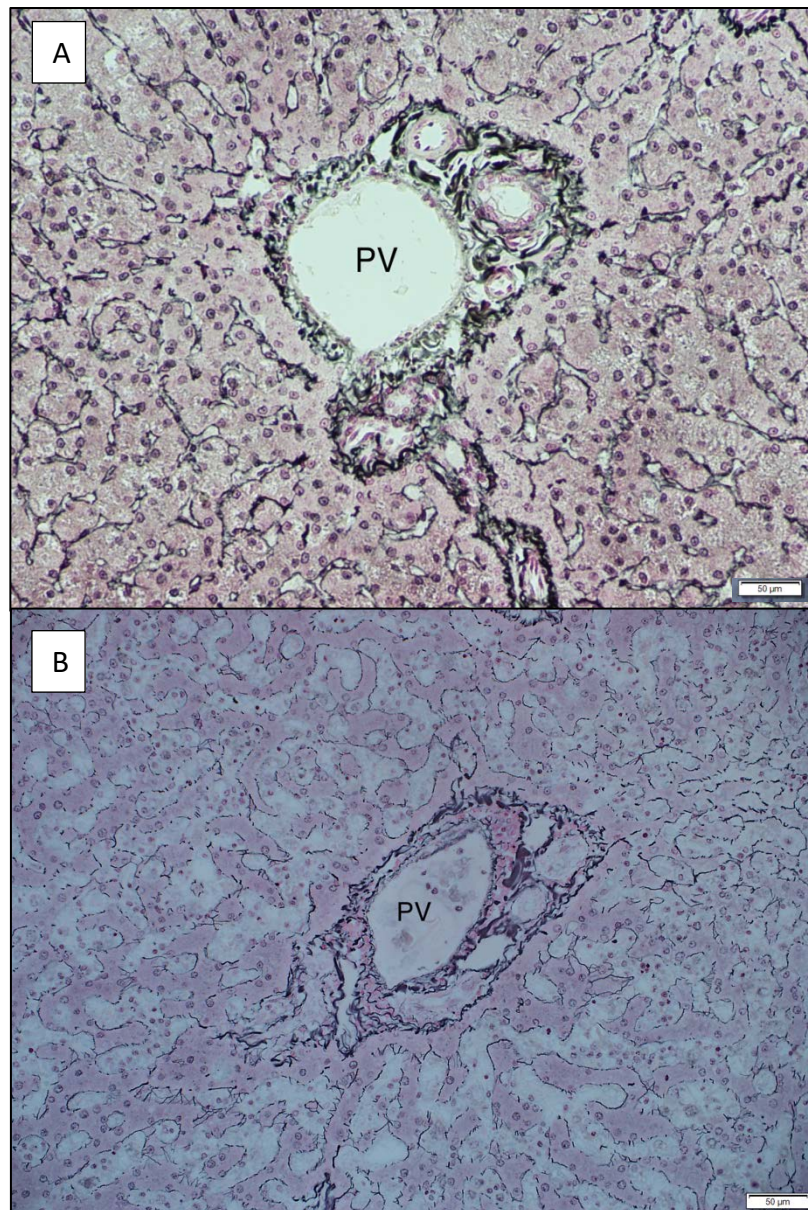


Figure 26: **A.** Photomicrograph of a normal dog liver (control no. 4) showing a portal tract with GSS staining of reticular fibres. PV = portal vein. GSS staining at 200x magnification. **B.** Photomicrograph of an infected dog liver (case no. 117) showing a portal tract with GSS staining of reticular fibres, similar to that in normal liver. PV = portal vein. GSS staining at 200x magnification.

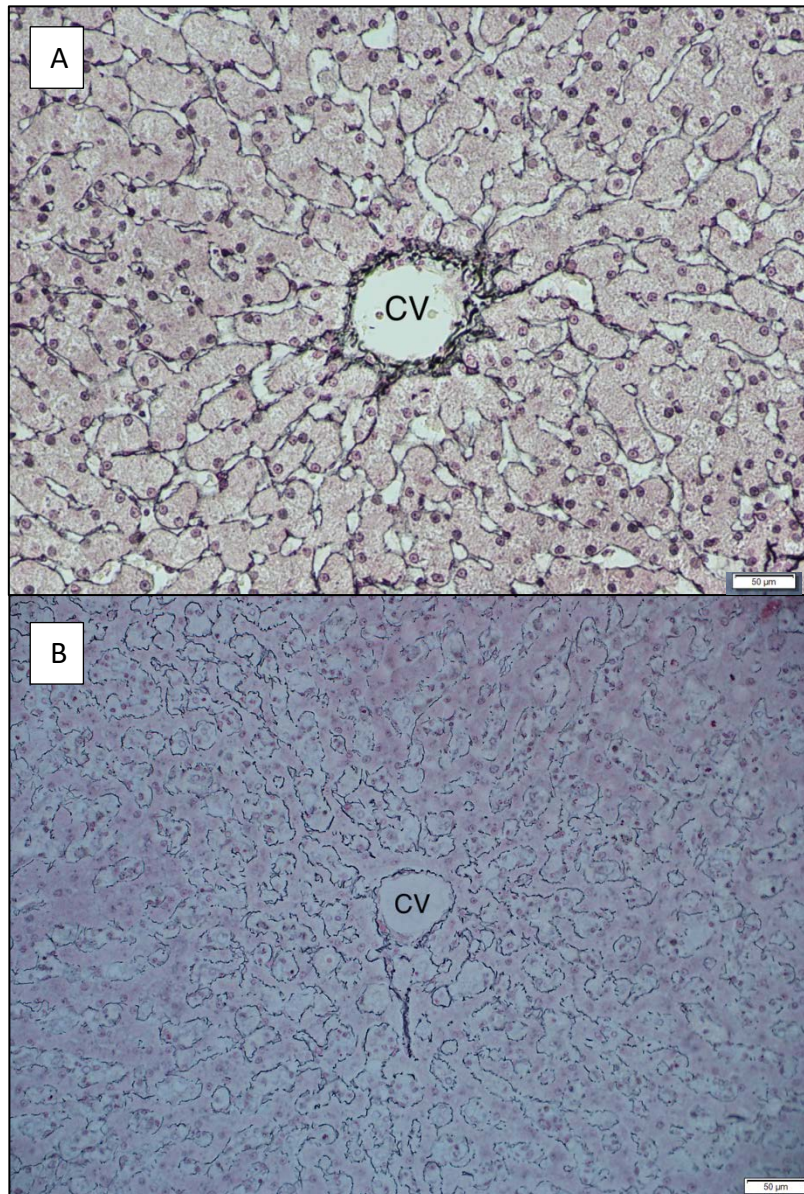


Figure 27: A. Photomicrograph of a normal dog liver (control no. 2) showing a central vein with GSS staining of reticular fibres. PV = portal vein. GSS staining at 200x magnification. B. Photomicrograph of an infected dog liver (case no. 50) showing a centrilobular area with normal GSS staining. CV = central vein. GSS staining at 200x magnification.

4.3.3 Perls' Prussian blue stain

This histochemical stain was used to enhance visualization of the intracellular haemosiderin iron-storage complex (which stains bright blue with this technique). Sparsely scattered haemosiderin-positive cell- and not obviously cell-associated clusters were observed in all the hepatic zones in the control dog samples. A median number of 0.5 with standard deviation of 2.6 haemosiderin-positive clusters were observed per liver sample. Conversely, in the infected dog liver specimens, there was ample cell-associated haemosiderin pigment (within the cytoplasm of mononuclear leucocytes within blood vessels), as well as some that was not obviously cell-associated, and in the perivascular interstitium in all zones (Figures 28-30). A median number of 53 with a standard deviation of 35.2 haemosiderin-positive clusters was observed per liver sample, making this a 106-fold increase compared to the controls. The *P*-value comparing the control to the infected cases was <0.001.

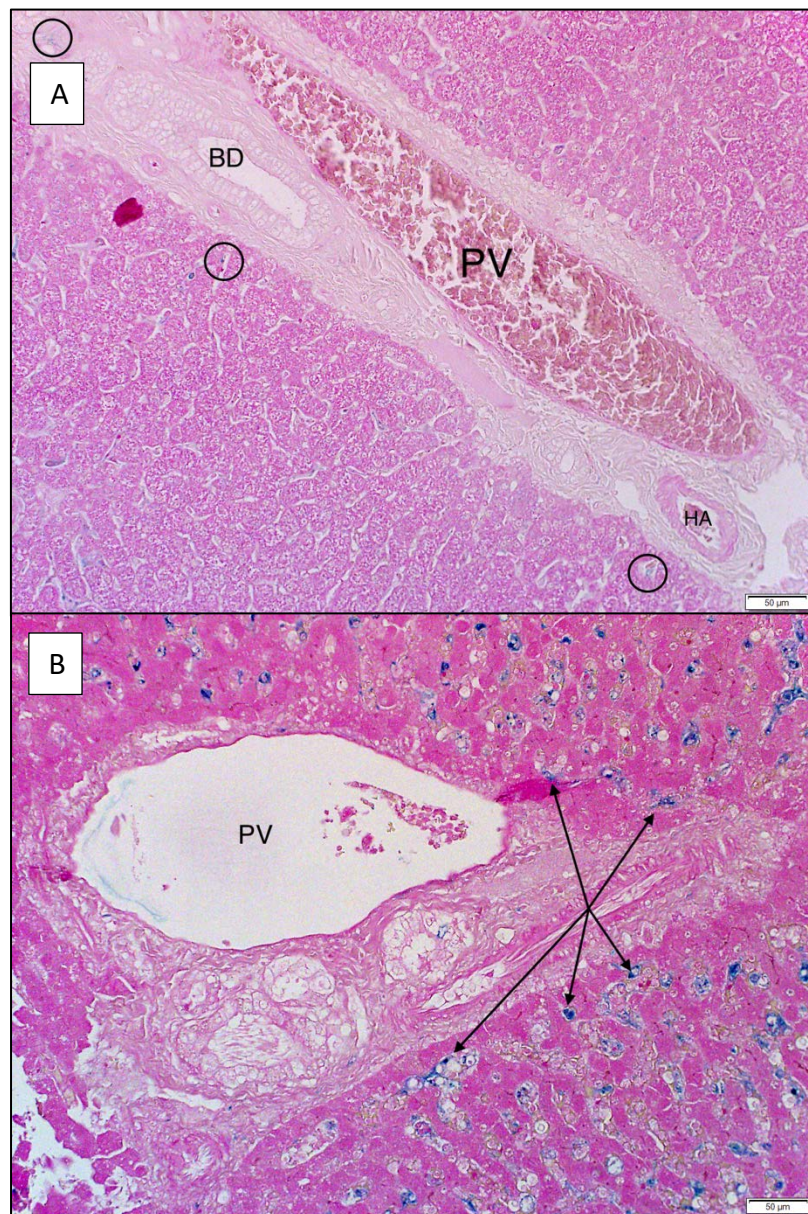


Figure 28: **A.** Photomicrograph of a normal dog liver (control no. 2) showing a portal tract. Sparsely scattered haemosiderin pigment was identified (black circles). PV = portal vein, BD = bile duct, HA = hepatic artery. Perls' Prussian blue staining at 200x magnification. **B.** Photomicrograph of an infected dog liver (case no. 50) showing a portal tract with widespread haemosiderin pigmentation, especially prominent in association with the sinusoids (black arrows). PV = portal vein. Perls' Prussian blue staining at 200x magnification.

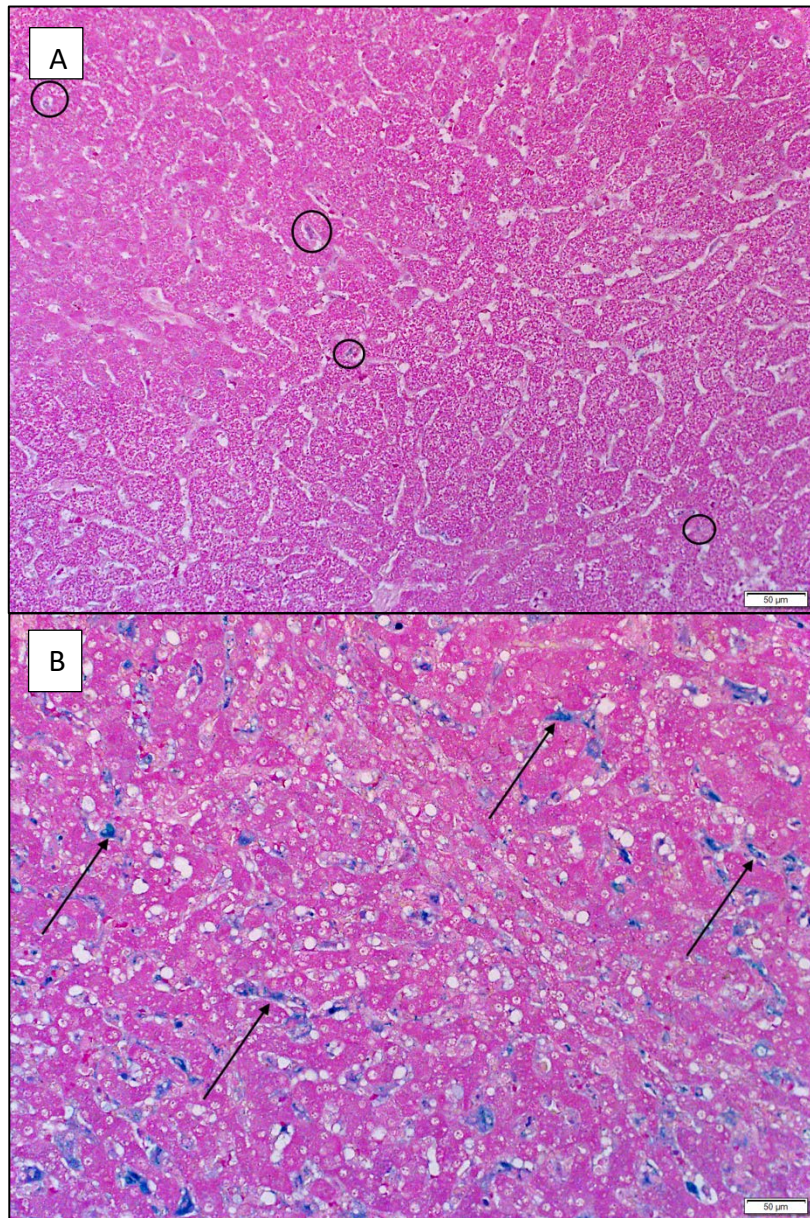


Figure 29: **A.** Photomicrograph of a normal dog liver (control no. 2) showing a midzonal area with scant sinusoidal haemosiderin pigment (black circles). Perls' Prussian blue staining at 200x magnification. **B.** Photomicrograph of an infected dog liver (case no. 110) showing a midzonal area with widespread sinusoid-associated haemosiderin pigment (black arrows). Perls' Prussian blue staining at 200x magnification.

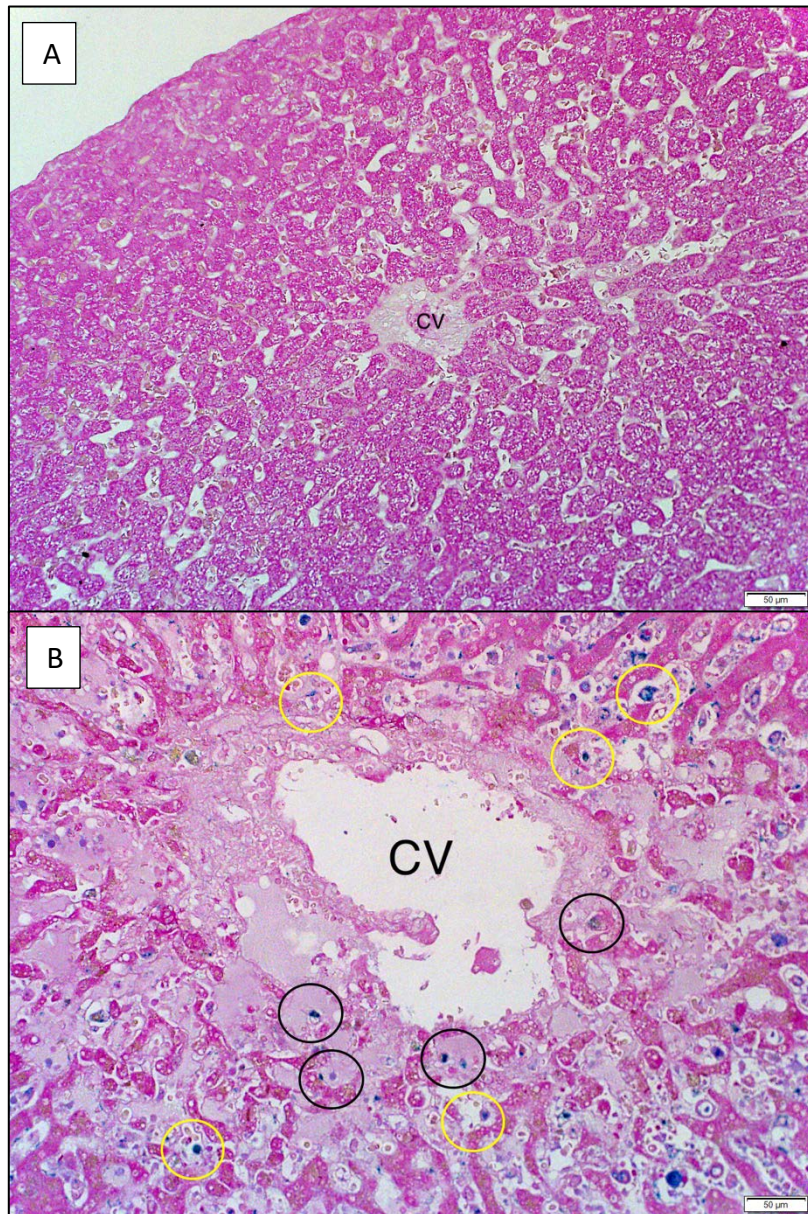


Figure 30: A. Photomicrograph of a normal dog liver (control no. 4) showing a centrilobular area with no obvious haemosiderin pigment. CV = central vein. Perl's Prussian blue staining at 200x magnification. B. Photomicrograph of an infected dog liver (case no. 20) showing a centrilobular area with haemosiderin pigment in the perivascular interstitium (black circles), and in association with the sinusoids (yellow circles). CV = central vein, Perl's Prussian blue staining at 200x magnification.

4.3.4 Luxol Fast Blue (LFB) stain

This stain is typically used to visualise myelin in histologic sections (which stains a blue colour with this staining technique). However, for the purpose of this study, the LFB stain was used to help visualise intraerythrocytic *Babesia* piroplasms (which also stain blue). No *Babesia* parasites were detected in HE- or LFB-stained liver sections from the control dogs. In contrast, piroplasms were detected in the infected dog liver specimens. Only a few (less than 10 parasites visualized per field at 400x magnification) piroplasms were observed in the portal tracts in 7/10 samples, while many (more than 10 parasites counted per field at 400x magnification) were present in the portal areas of the remaining 3 samples. Few parasites were visualized in 6/10 of the samples within the midzonal areas, many parasites were seen in 3/10 samples, and 1/10 of the samples had no parasites in the midzonal area. Few parasites were present in 7/10 samples in the centrilobular areas, while the remaining 3/10 samples had many intraerythrocytic parasites in the centrilobular areas. Overall, on average, similar numbers of parasites were seen in the different hepatic zones (Figures 31-33). A median number of 8.5 with a standard deviation of 15.4 *B. rossi* piroplasms were observed per liver sample. The *P*-value comparing the control to the infected cases was <0.001.

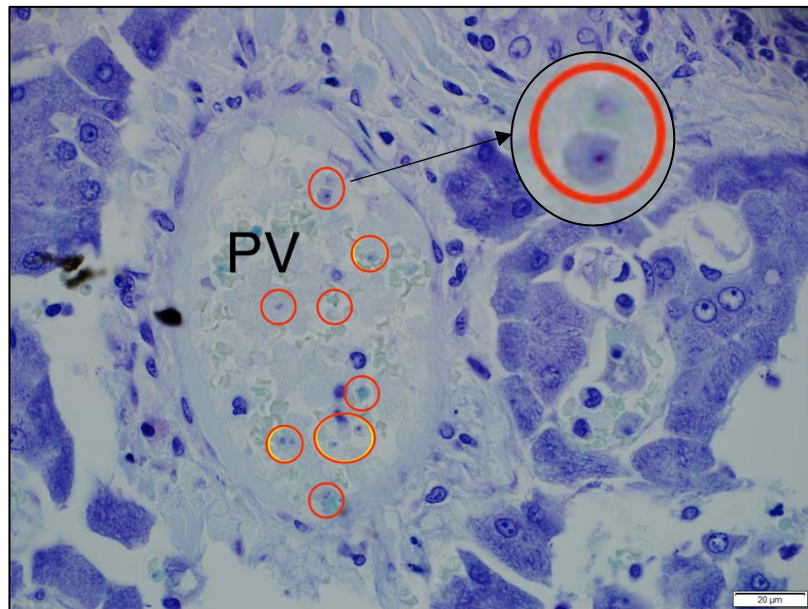


Figure 31: Photomicrograph of an infected dog liver (case no. 61) showing a portal tract with intraerythrocytic *B. rossi* parasites (red circles) in the portal vein (PV) with magnified views (larger black circle). LFB staining at 600x magnification.

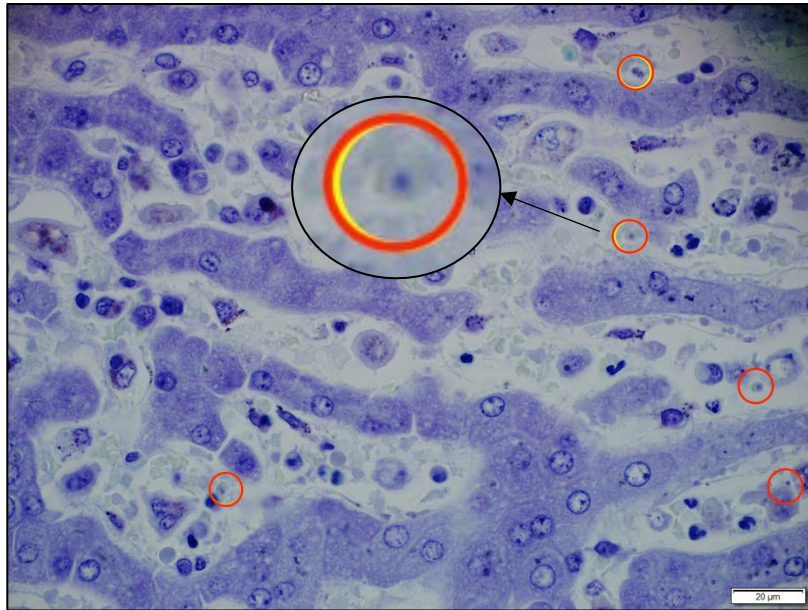


Figure 32: Photomicrograph of an infected dog liver (case no. 20) showing a midzonal area with intraerythrocytic *B. rossi* parasites (red circles) in sinusoids with magnified views (larger black circle). LFB staining at 600x magnification.

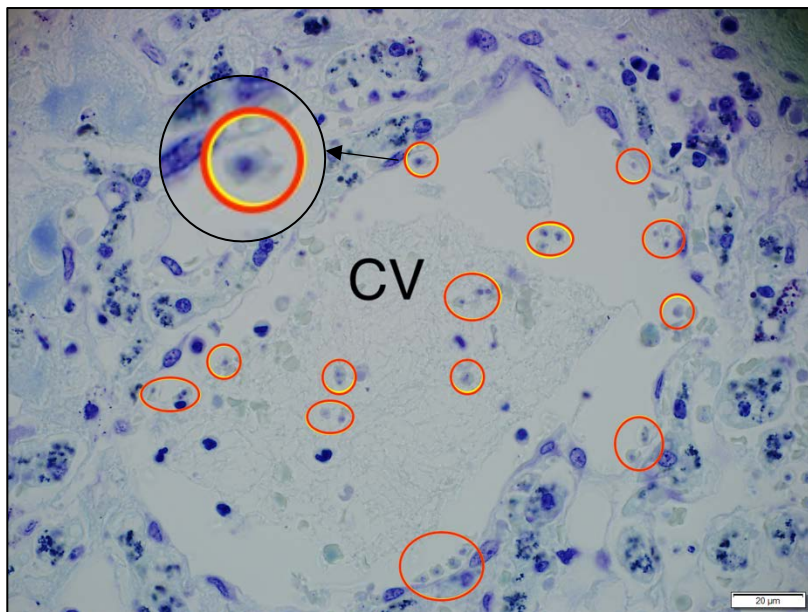


Figure 33: Photomicrograph of an infected dog liver (case no. 20) showing a centrilobular area with intraerythrocytic *B. rossi* parasites (red circles) in the central vein (CV) with magnified views (larger black circle). LFB staining at 600x magnification.

4.4 IMMUNOHISTOCHEMISTRY

4.4.1 Control Cases

Immunohistochemistry for selected leucocyte markers (T-lymphocytes, B-lymphocytes, plasma cells, monocyte-macrophages, and neutrophils) was performed on the control samples. The results are summarized for the different hepatic zones (Table 4) and per marker (non-zonal) (Table 5) below.

Table 4: Quantification of selected immunohistochemically labelled leucocytes in the control dog liver specimens (n=4). The median number, standard deviation, and minimum and maximum number of leucocytes of each phenotype per high power field/HPF (400x magnification) are listed for each hepatic zone (centrilobular, midzonal or portal). All values represent absolute cell counts.

Marker	Hepatic zone	Median number of positive cells (Standard Deviation)	Minimum	Maximum
CD3	Portal tract	6 (5.3)	0	16
	Midzonal	16.5 (5.7)	11	30
	Centrilobular	3 (10.8)	0	34
CD20	Portal tract	1.5 (1.2)	0	4
	Midzonal	4 (2.4)	1	9
	Centrilobular	1 (4.2)	0	11
CD204	Portal tract	7.5 (4.5)	3	15
	Midzonal	71 (14.9)	44	100
	Centrilobular	5 (3.0)	0	10
Iba-1	Portal tract	9 (2.5)	7	16
	Midzonal	107.5 (5.2)	102	117
	Centrilobular	5.5 (3.3)	1	13
MAC387	Portal tract	1 (2.0)	0	7
	Midzonal	22 (9.5)	6	31
	Centrilobular	1 (4.1)	0	13
MUM-1	Portal tract	2 (1.3)	0	4
	Midzonal	3 (2.8)	1	10
	Centrilobular	1 (3.0)	0	9

Based on the control group, the following normal ranges were established using the mean of the four cases plus one standard deviation per hepatic zone.

Table 5: Quantification of selected immunohistochemically labelled leucocytes in the control dog liver specimens (n=4). The median number, standard deviation, and minimum and maximum number of positive cells are listed in the liver as a whole (non-zonal). All values represent absolute cell counts.

Marker	Median number of positive cells (Standard Deviation)	Minimum	Maximum
CD3	27.5 (16.3)	18	68
CD20	5.5 (6.3)	2	19
CD204	85.0 (17.5)	48	110
Iba-1	123 (8.7)	111	139
MAC387	27.0 (12.4)	7	45
MUM-1	6.5 (5.6)	3	18

4.4.2 *B. rossi*-infected dogs

Immunohistochemistry for selected leucocyte markers (T-lymphocytes, B-lymphocytes, plasma cells, macrophages, monocytes, and neutrophils) were performed on the *B. rossi*-infected liver samples. The results of each marker are summarized for the different hepatic zones below (Tables 6 – 11).

4.4.2.1 CD3

Table 6: Quantification of CD3-immunoreactive T-lymphocytes in the *B. rossi*-infected livers (n=10) compared to the controls (n=4). The median number of positive cells (per HPF/400x magnification) per hepatic zone (portal tract, midzonal and centrilobular), as well as the *P*-values are listed. All values represent absolute cell counts.

<i>B. rossi</i>-infected cases			Control cases		<i>P</i>-value* comparing the control infected cases vs.
Infected dogs (Case no.)	Hepatic zone	Median number of positive cells/HPF	Median number of positive cells/HPF	Median number of positive cells/HPF	
Case 20	Portal tract	2.5	6.0	0.042	
	Midzonal	12.3	16.5	<0.001	
	Centrilobular	7.0	3.0	0.205	
Case 50	Portal tract	8.3	6.0	0.042	
	Midzonal	14.7	16.5	<0.001	
	Centrilobular	8.3	3.0	0.205	
Case 54	Portal tract	23.7	6.0	0.042	
	Midzonal	111.7	16.5	<0.001	
	Centrilobular	5.7	3.0	0.205	
Case 59	Portal tract	10.0	6.0	0.042	
	Midzonal	23.0	16.5	<0.001	
	Centrilobular	13.3	3.0	0.205	
Case 61	Portal tract	21.3	6.0	0.042	
	Midzonal	55.7	16.5	<0.001	
	Centrilobular	4.0	3.0	0.205	
Case 88	Portal tract	12.0	6.0	0.042	
	Midzonal	36.3	16.5	<0.001	
	Centrilobular	6.7	3.0	0.205	
Case 91	Portal tract	9.3	6.0	0.042	
	Midzonal	29.3	16.5	<0.001	
	Centrilobular	7.0	3.0	0.205	
Case 106	Portal tract	14.5	6.0	0.042	
	Midzonal	61.3	16.5	<0.001	
	Centrilobular	10.7	3.0	0.205	
Case 110	Portal tract	9.0	6.0	0.042	
	Midzonal	65.3	16.5	<0.001	
	Centrilobular	9.0	3.0	0.205	
Case 117	Portal tract	12.3	6.0	0.042	
	Midzonal	54.3	16.5	<0.001	
	Centrilobular	1.7	3.0	0.205	
Total medians	Portal tract	9	6.0	0.042	
	Midzonal	47	16.5	<0.001	
	Centrilobular	5	3.0	0.205	

Abbreviations: HPF = high power field (400x magnification).

*Significant *P*-values (*P*-value <0.05) are in bold.

The highest median number of CD3-positive T-lymphocytes found was 111.7, while the lowest median number was 1.7 CD3-positive cells per HPF. A median number of 9 CD3-positive T-lymphocytes per HPF was observed in the portal tracts, making this a 1.5-fold increase in the number of CD3-positive cells compared to the median of the controls for this zone. This value falls within the normal range as established by the control samples (Table 12). A median number of 47 CD3-positive T-lymphocytes per HPF was determined for the midzonal regions of the infected livers, making this a 2.8-fold increase compared to the median of the control samples (Table 12). This value falls above the normal range established by the control samples (Table 9). A median number of 5 CD3-positive T-lymphocytes was determined per HPF in the centrilobular regions, making this a 1.7-fold increase compared to the medians of the control samples for this zone. However, this value falls within the normal range established by the control samples (Table 12). The CD3-positive T-lymphocytes were predominantly located within the perivascular and periductal connective tissue in the control samples but were occasionally identified within vascular lumens. In the infected samples, they were found to a far greater extent within vascular lumens, but also occurred in the interstitium (Figures 34-36).

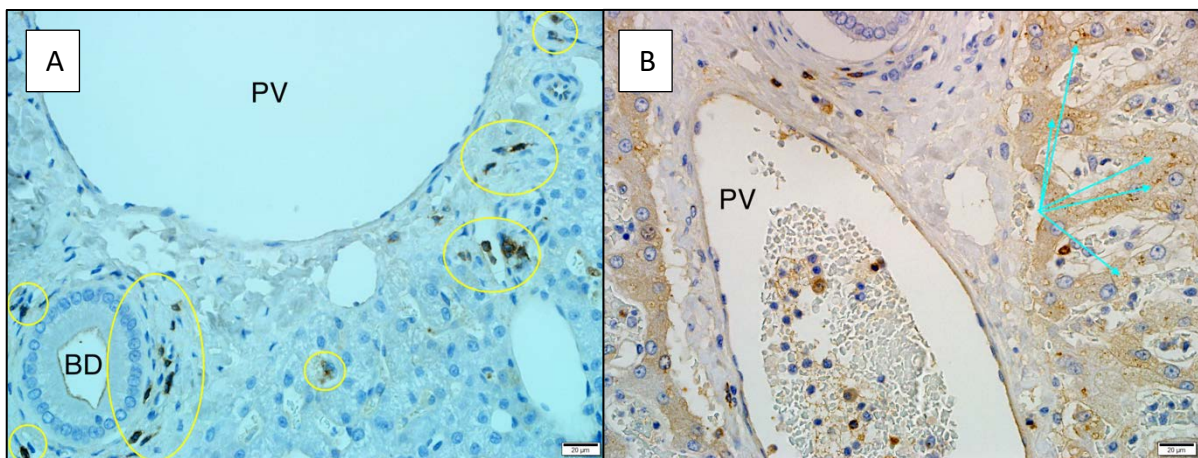


Figure 34: A. Photomicrograph of a normal dog liver (control no. 4) showing a portal tract with CD3-positive T-lymphocytes in the perivascular and periductal connective tissue (yellow circles). PV = portal vein, BD = bile duct. IHC staining at 400x magnification. B. Photomicrograph of an infected dog liver (case no. 59) showing a portal vein with intraluminal and perivascular CD3-positive T-lymphocytes. There is non-specific labeling of hepatocytes (blue arrows). PV = portal tract. IHC staining at 400x magnification.

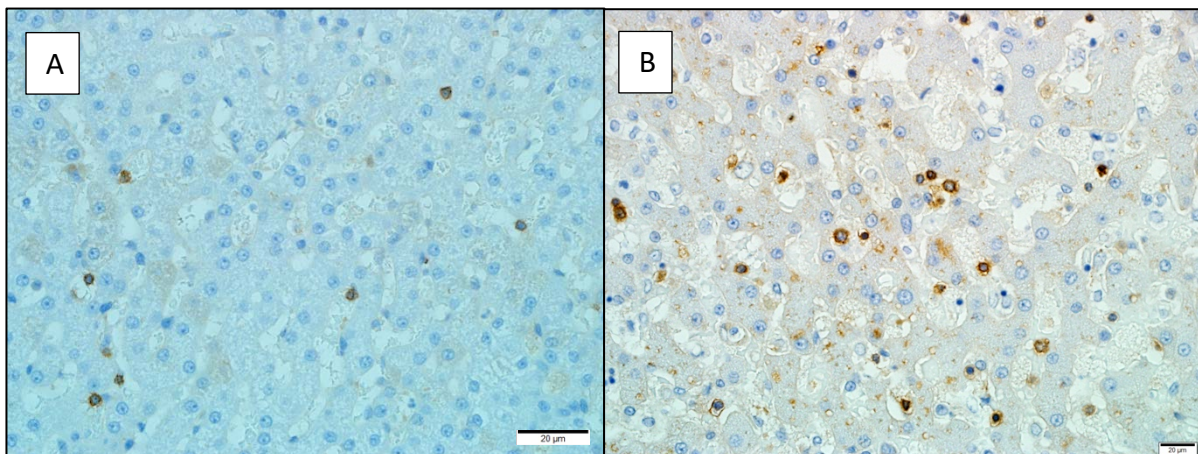


Figure 35: A. Photomicrograph of a normal dog liver (control no. 4) showing a midzonal area with CD3-positive T-lymphocytes occurring predominantly intravascularly. IHC staining at 400x magnification. B. Photomicrograph of an infected dog liver (case no. 106) showing a midzonal area with a comparatively increased number of CD3-positive T-lymphocytes, predominantly occurring intravascularly. IHC staining at 400x magnification.

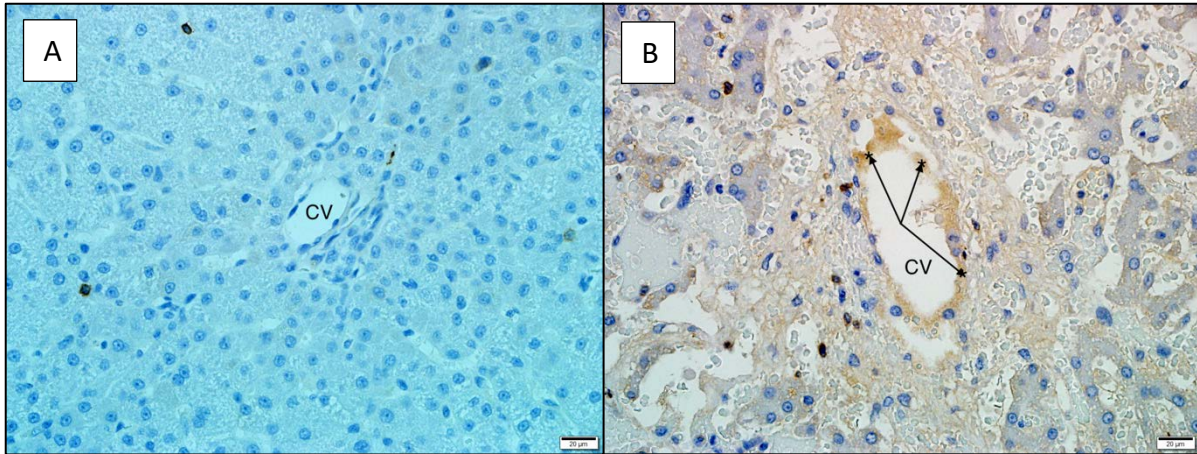


Figure 36: A. Photomicrograph of a normal dog liver (control no. 4) showing a centrilobular area with no obvious CD3-positive T-lymphocytes present. CV = central vein. IHC staining at 400x magnification. B. Photomicrograph of an infected dog liver (case no. 88) showing a centrilobular area with a comparatively increased number of CD3-positive T-lymphocytes present in the perivascular interstitium. There is non-specific labeling of plasma (black arrows). CV = central vein. IHC staining at 400x magnification.

4.4.2.2 CD20

Table 7: Quantification of CD20-immunoreactive B-lymphocytes and plasma cells in the *B. rossi*-infected livers (n=10) compared to the controls (n=4). The median number of positive cells (per HPF/400x magnification) per hepatic zone (portal tract, midzonal and centrilobular), as well as the *P*-values are listed. All values represent absolute cell counts.

<i>B. rossi</i>-infected cases			Control cases	<i>P</i>-value* comparing the control vs. infected cases
Infected dogs (Case no.)	Hepatic zone	Median number of positive cells/HPF	Median number of positive cells/HPF	
Case 20	Portal tract	9.3	1.5	<0.001
	Midzonal	5.7	4.0	0.001
	Centrilobular	35.3	1.0	<0.001
Case 50	Portal tract	3.7	1.5	<0.001
	Midzonal	3.0	4.0	0.001
	Centrilobular	6.0	1.0	<0.001
Case 54	Portal tract	8.3	1.5	<0.001
	Midzonal	14.3	4.0	0.001
	Centrilobular	12.0	1.0	<0.001
Case 59	Portal tract	2.3	1.5	<0.001
	Midzonal	3.0	4.0	0.001
	Centrilobular	16.0	1.0	<0.001
Case 61	Portal tract	2.0	1.5	<0.001
	Midzonal	9.3	4.0	0.001
	Centrilobular	8.3	1.0	<0.001
Case 88	Portal tract	3.3	1.5	<0.001
	Midzonal	9.3	4.0	0.001
	Centrilobular	3.7	1.0	<0.001
Case 91	Portal tract	4.7	1.5	<0.001
	Midzonal	9.3	4.0	0.001
	Centrilobular	14.0	1.0	<0.001
Case 106	Portal tract	4.7	1.5	<0.001
	Midzonal	10.3	4.0	0.001
	Centrilobular	6.7	1.0	<0.001
Case 110	Portal tract	24.0	1.5	<0.001
	Midzonal	18.3	4.0	0.001
	Centrilobular	44.3	1.0	<0.001
Case 117	Portal tract	41.0	1.5	<0.001
	Midzonal	8.0	4.0	0.001
	Centrilobular	11.7	1.0	<0.001
Total medians	Portal tract	5.0	1.5	<0.001
	Midzonal	9.0	4.0	0.001
	Centrilobular	9.5	1.0	<0.001

Abbreviations: HPF = high power field (400x magnification).

*Significant *P*-values (*P*-value <0.05) are in bold.

The highest median number of CD20-positive B-lymphocytes and plasma cells found was 44.3, while the lowest median number was 2 CD20-positive cells per HPF. A median number of 5 CD20-positive B-lymphocytes and plasma cells per HPF was observed in the portal tracts, making this a 3.3-fold increase in CD20-positive cells compared to the median of the control samples for this zone. This value falls above the normal range established by the control samples (Table 12). A median number of 9 CD20-positive B-lymphocytes and plasma cells was found per HPF in the midzonal regions of the infected livers, making this a 2.3-fold increase compared to the median of the controls. However, this value was still within the normal range, as established by the control samples (Table 12). A median number of 9.5 CD20-positive B-lymphocytes and plasma cells was found per HPF in the centrilobular regions, making this a 9.5-fold increase compared to the medians of the control samples for this zone. This value falls within the normal range as established by the control samples (Table 9). The CD20-positive B-lymphocytes and plasma cells were found mostly within the perivascular and periductal connective tissue in the infected and control liver samples, with occasional intravascular B-lymphocytes identified in some infected cases (Figures 37-39).

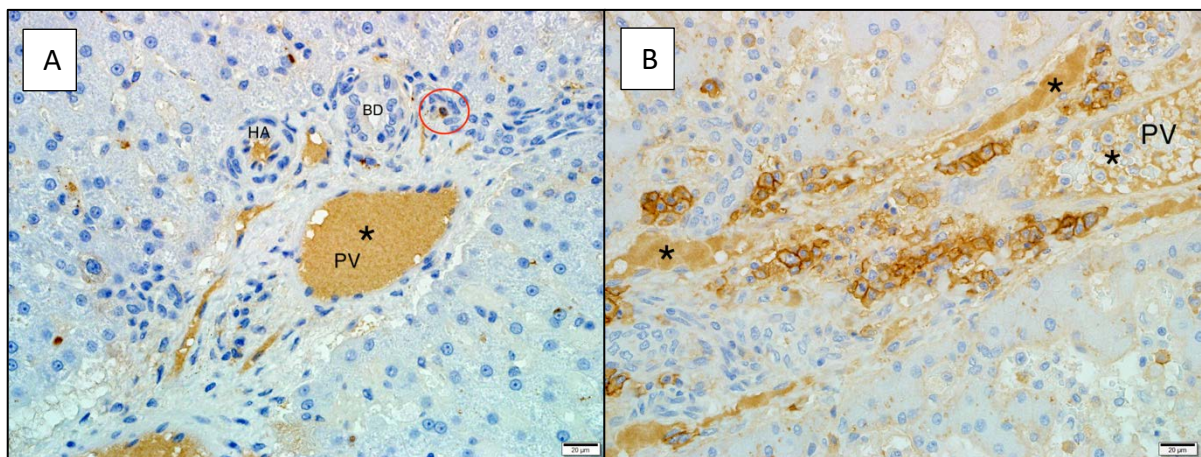


Figure 37: A. Photomicrograph of a normal dog liver (control no. 11) showing a portal tract with rare CD20-positive B-lymphocytes and plasma cells (red circle) in the perivascular and periductal interstitium. There is non-specific labeling of plasma (black star). PV = portal vein, HA = hepatic artery, BD = bile duct. IHC staining at 400x magnification. B. Photomicrograph of an infected dog liver (case no. 117) showing a portal tract with a comparatively increased number of CD20-positive B-lymphocytes and plasma cells present in the perivascular and periductal interstitium. There is similar non-specific labeling of plasma (black stars). PV = portal vein. IHC staining at 400x magnification.

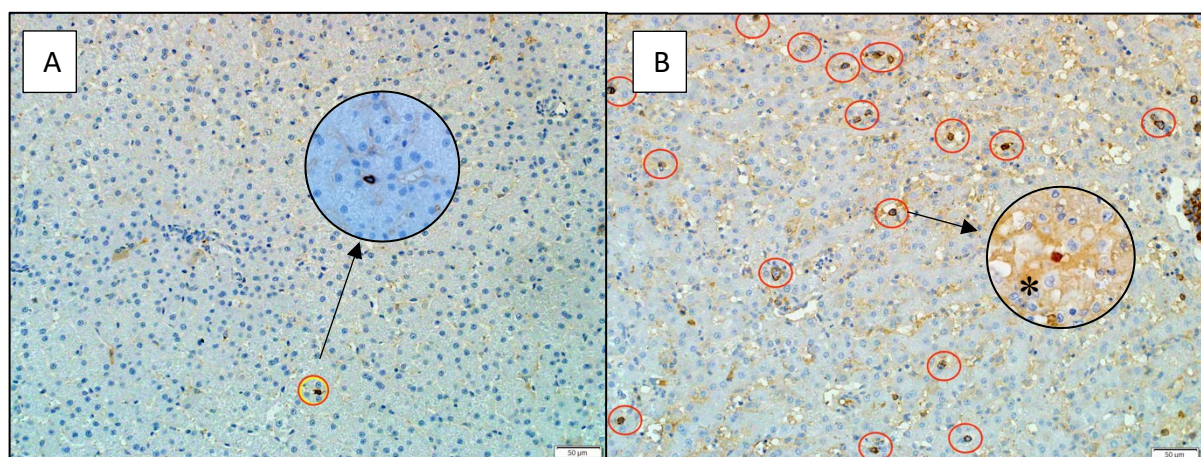


Figure 38: A. Photomicrograph of a normal dog liver (control no. 2) showing a midzonal area with CD20-positive B-lymphocytes and plasma cells present (red circle) with magnified views (black circle). IHC staining at 200x magnification. B. Photomicrograph of an infected dog liver (case no. 110) showing a midzonal area with a comparatively increased number of intravascular CD20-positive B cells (red circles) and scattered plasma cells with magnified views (black circle). There is non-specific labeling of plasma (black star). IHC staining at 200x magnification.

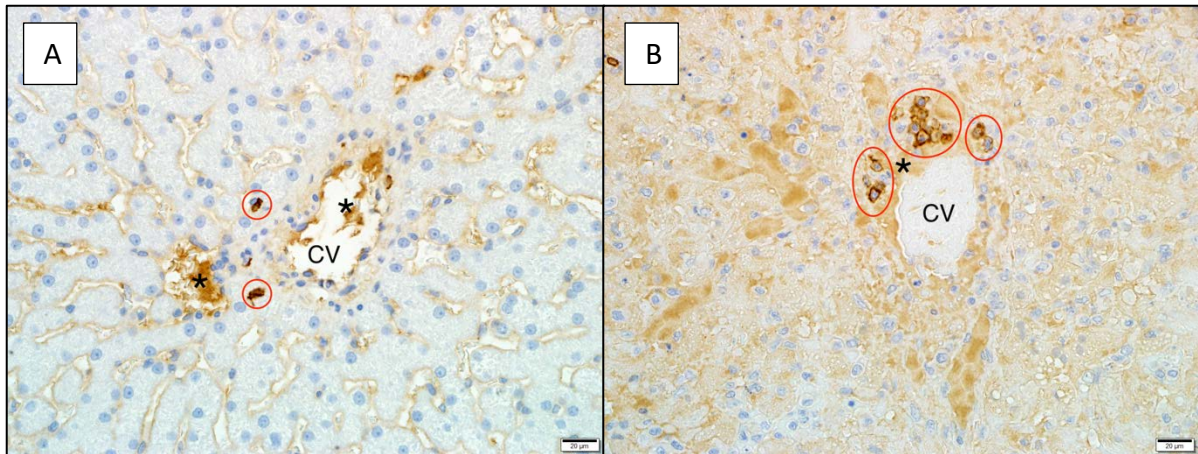


Figure 39: **A.** Photomicrograph of a normal dog liver (control no. 4) showing a centrilobular area with a few scattered CD20-positive B-lymphocytes and plasma cells present in the perivascular interstitium (red circles). There is non-specific labeling of plasma (black star). CV = central vein. IHC staining at 400x magnification. **B.** Photomicrograph of an infected dog liver (case no. 117) showing a centrilobular area with a comparatively increased number of CD20-positive B-lymphocytes and plasma cells present in the perivascular interstitium (red circles). There is quite extensive non-specific labeling of plasma (black star). CV = central vein. IHC staining at 400x magnification.

4.4.2.3 CD204

Table 8: Quantification of CD204-immunoreactive macrophages in the *B. rossi*-infected livers (n=10) compared to the controls (n=4). The median number of positive cells (per HPF/400x magnification) per hepatic zone (portal tract, midzonal and centrilobular), as well as the *P*-values are listed. All values represent absolute cell counts.

<i>B. rossi</i>-infected cases			Control cases	
Infected dogs (Case no.)	Hepatic zone	Median number of positive cells/HPF	Median number of positive cells/HPF	<i>P</i>-value* comparing the control vs. infected cases
Case 20	Portal tract	8.0	7.5	0.158
	Midzonal	88.0	71.0	<0.001
	Centrilobular	13.0	5.0	<0.001
Case 50	Portal tract	4.0	7.5	0.158
	Midzonal	77.3	71.0	<0.001
	Centrilobular	3.3	5.0	<0.001
Case 54	Portal tract	4.3	7.5	0.158
	Midzonal	131.0	71.0	<0.001
	Centrilobular	10.3	5.0	<0.001
Case 59	Portal tract	15.0	7.5	0.158
	Midzonal	128.7	71.0	<0.001
	Centrilobular	16.0	5.0	<0.001
Case 61	Portal tract	25.5	7.5	0.158
	Midzonal	128.3	71.0	<0.001
	Centrilobular	49.0	5.0	<0.001
Case 88	Portal tract	14.3	7.5	0.158
	Midzonal	126.0	71.0	<0.001
	Centrilobular	15.7	5.0	<0.001
Case 91	Portal tract	11.0	7.5	0.158
	Midzonal	140.3	71.0	<0.001
	Centrilobular	16.3	5.0	<0.001
Case 106	Portal tract	10.0	7.5	0.158
	Midzonal	130.3	71.0	<0.001
	Centrilobular	7.7	5.0	<0.001
Case 110	Portal tract	11.7	7.5	0.158
	Midzonal	132.7	71.0	<0.001
	Centrilobular	12.7	5.0	<0.001
Case 117	Portal tract	11.3	7.5	0.158
	Midzonal	177.0	71.0	<0.001
	Centrilobular	23.0	5.0	<0.001
Total medians	Portal tract	10	7.5	0.158
	Midzonal	132.5	71.0	<0.001
	Centrilobular	14	5.0	<0.001

Abbreviations: HPF = high power field (400x magnification).

*Significant *P*-values (*P*-value <0.05) are in bold.

The highest median number of CD204-reactive macrophages found was 177, while the lowest median number was 3.3 CD204-positive cells per HPF. A median number of 10 CD204-reactive macrophages per HPF was observed in the portal tracts, making this a 1.3-fold increase in CD204-positive cells compared to the median of the control samples for this zone. This value falls within the normal range as established by the control samples (Table 12). A median number of 132.5 CD204-positive macrophages was identified per HPF in the midzonal regions of the infected livers, making this a 1.9-fold increase compared to the median of the controls. This value falls above the normal range established by the control samples (Table 12). A median number of 14 CD204-positive macrophages was identified per HPF in the centrilobular regions, making this a 2.8-fold increase compared to the medians of the control samples. This value falls above the normal range established by the control samples (Table 12). In the control cases, the CD204-positive macrophages were typically sinusoid-associated and also occurred within the perivascular and periductal interstitium. In the infected cases, the sinusoidal monocyte-macrophages (likely corresponding with Kupffer cells) were markedly increased in number, while fewer positive cells were identified in the interstitium (Figures 40-42).

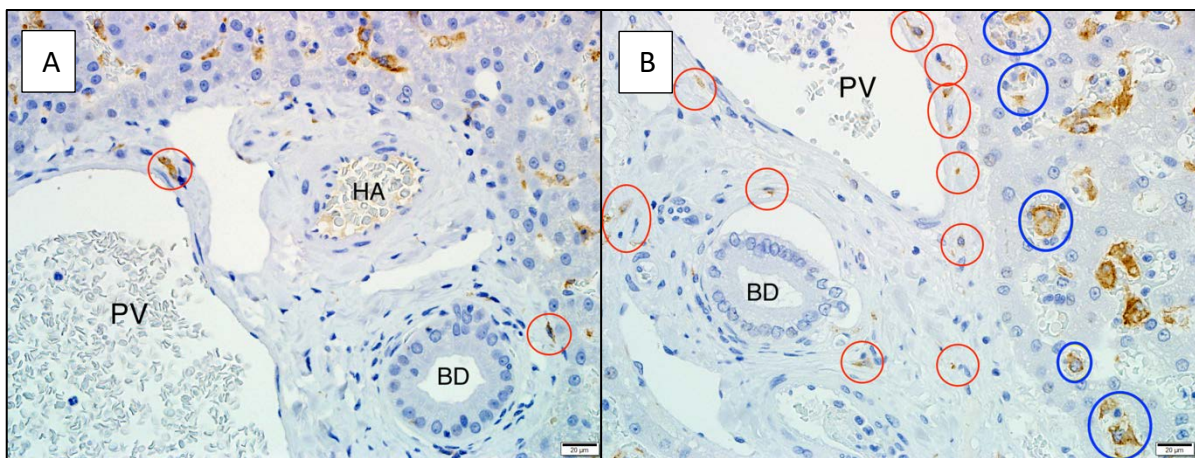


Figure 40: A. Photomicrograph of a normal dog liver (control no. 9) showing a portal tract with sinusoid-associated CD204-positive monocyte-macrophages (red circles) in sinusoidal lumens (likely corresponding with Kupffer cells) and a few positive cells in the interstitium of the portal tract. PV = portal vein, HA = hepatic artery, BD = bile duct. IHC staining at 400x magnification. B. Photomicrograph of an infected dog liver (case no. 59) showing a portal tract with increased numbers of sinusoidal CD204-positive monocyte-macrophages (blue circles) and scattered positive cells in the perivascular interstitium (red circles). PV = portal vein, BD = bile duct. IHC staining at 400x magnification.

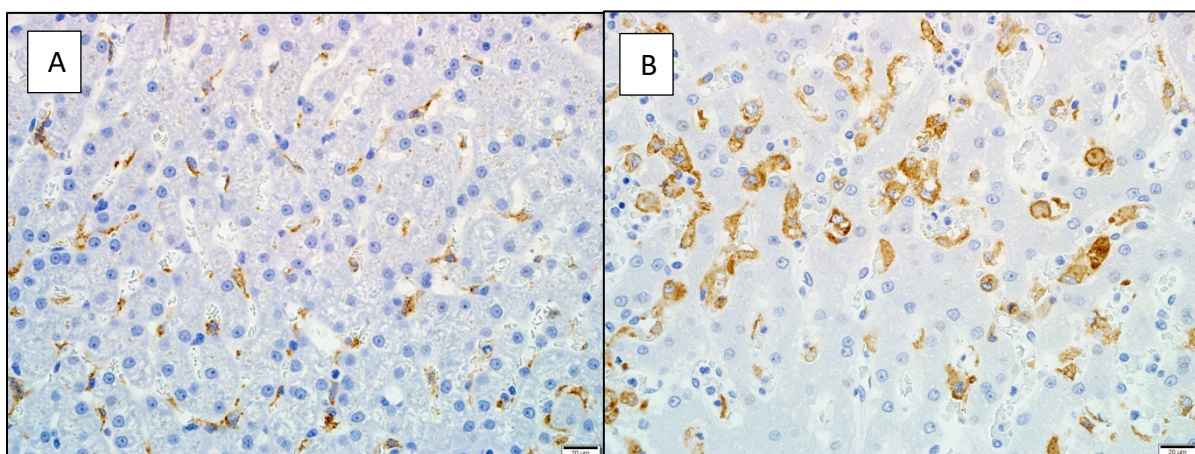


Figure 41: A. Photomicrograph of a normal dog liver (control no. 9) showing a midzonal area with CD204-positive sinusoid-associated monocyte-macrophages (likely corresponding with Kupffer cells). IHC staining at 400x magnification. B. Photomicrograph of an infected dog liver (case no. 59) showing a midzonal area with a comparatively increased number of CD204-positive sinusoidal monocyte-macrophages. IHC staining at 400x magnification.

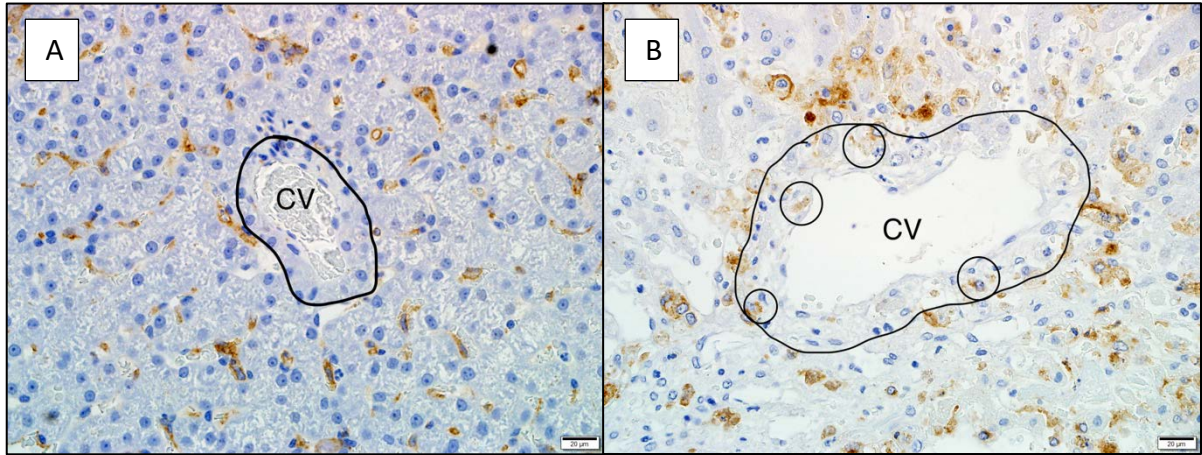


Figure 42: **A.** Photomicrograph of a normal dog liver (control no. 9) showing a centrilobular area with no CD204-positive monocyte-macrophages in the immediate vicinity of the central vein (black outline), but positively stained monocyte-macrophages are evident in the sinusoids of the adjacent midzonal area. CV = central vein. IHC staining at 400x magnification. **B.** Photomicrograph of an infected dog liver (case no. 64) showing a centrilobular area (black outline) with a comparatively increased number of CD204-positive monocyte-macrophages in the perivascular interstitium (black circles) and lumens of adjacent sinusoids. CV = central vein. IHC staining at 400x magnification.

4.4.2.4 Iba-1

Table 9: Quantification of Iba-1-immunoreactive monocyte-macrophages and dendritic cells in the *B. rossi*-infected livers (n=10) compared to the controls (n=4). The median number of positive cells (per HPF/400x magnification) per hepatic zone (portal tract, midzonal and centrilobular), as well as the *P*-values are listed. All values represent absolute cell counts.

<i>B. rossi</i>-infected cases			Control cases	
Infected dogs (Case no.)	Hepatic zone	Median number of positive cells/HPF	Median number of positive cells/HPF	<i>P</i>-value* comparing the control vs. infected cases
Case 20	Portal tract	7.5	9.0	0.251
	Midzonal	137.0	107.5	<0.001
	Centrilobular	7.3	5.5	<0.001
Case 50	Portal tract	6.3	9.0	0.251
	Midzonal	132.7	107.5	<0.001
	Centrilobular	8.5	5.5	<0.001
Case 54	Portal tract	9.7	9.0	0.251
	Midzonal	180.3	107.5	<0.001
	Centrilobular	5.0	5.5	<0.001
Case 59	Portal tract	14.0	9.0	0.251
	Midzonal	139.3	107.5	<0.001
	Centrilobular	24.7	5.5	<0.001
Case 61	Portal tract	13.0	9.0	0.251
	Midzonal	154.0	107.5	<0.001
	Centrilobular	49.0	5.5	<0.001
Case 88	Portal tract	13.3	9.0	0.251
	Midzonal	169.3	107.5	<0.001
	Centrilobular	13.3	5.5	<0.001
Case 91	Portal tract	10.3	9.0	0.251
	Midzonal	157.3	107.5	<0.001
	Centrilobular	21.5	5.5	<0.001
Case 106	Portal tract	14.0	9.0	0.251
	Midzonal	139.3	107.5	<0.001
	Centrilobular	10.0	5.5	<0.001
Case 110	Portal tract	4.0	9.0	0.251
	Midzonal	119.0	107.5	<0.001
	Centrilobular	14.3	5.5	<0.001
Case 117	Portal tract	11.7	9.0	0.251
	Midzonal	151.0	107.5	<0.001
	Centrilobular	26.3	5.5	<0.001
Total medians	Portal tract	11.5	9.0	0.251
	Midzonal	145.0	107.5	<0.001
	Centrilobular	11.5	5.5	<0.001

Abbreviations: HPF = high power field (400x magnification).

*Significant *P*-values (*P*-value <0.05) are in bold.

The highest median number of Iba-1-reactive monocyte-macrophages and dendritic cells found was 180.3, while the lowest median number was 4 Iba-1-positive cells per HPF. A median number of 11.5 Iba-1-positive cells per HPF was observed in the portal tracts, making this a 1.3-fold increase in Iba-1-positive cells compared to the median of the control samples for this zone. However, this value fell within the normal range as established by the control samples (Table 12). A median number of 145 Iba-1-positive cells was observed per HPF in the midzonal regions of the infected livers, making this a 1.3-fold increase compared to the median of the controls. This value falls above the normal range established by the control samples (Table 12). A median number of 11.5 Iba-1-positive cells was observed per HPF in the centrilobular regions, making this a 2.1-fold increase compared to the medians of the control samples for this zone. This value fell within the normal range as established by the control samples (Table 12). In the control samples, the Iba-1-positive cells were sinusoid-associated and also found in the perivascular and periductal interstitium. This was similar in the infected samples, but there were many larger Iba-1-positive sinusoid-associated monocyte-macrophages (likely corresponding with Kupffer cells) and dendritic cells per HPF compared to the controls (Figures 43-45).

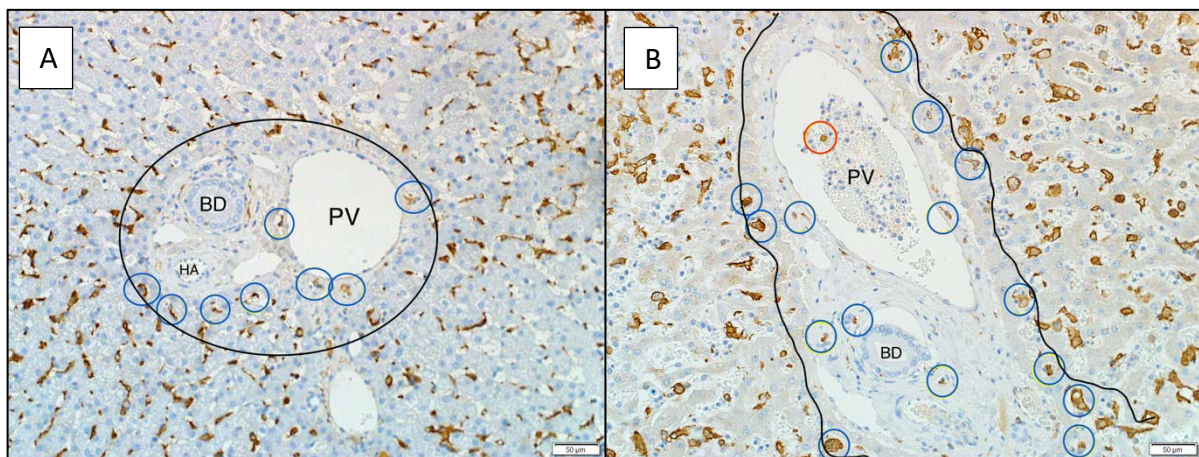


Figure 43: **A.** Photomicrograph of a normal dog liver (control no. 4) showing a portal tract (black circle) with Iba-1-positive monocyte-macrophages and dendritic cells predominantly in the perivascular interstitium (blue circles). There are many more Iba-1-positive macrophages and dendritic cells in the adjacent midzonal area. IHC staining at 200x magnification. **B.** Photomicrograph of an infected dog liver (case no. 59) specimen showing a portal tract (black outline) with a comparatively increased number of Iba-1-positive cells in the portal vein (red circle) and in the perivascular and periductal interstitium (blue circles). PV = portal vein, BD = bile duct. IHC staining at 200x magnification.

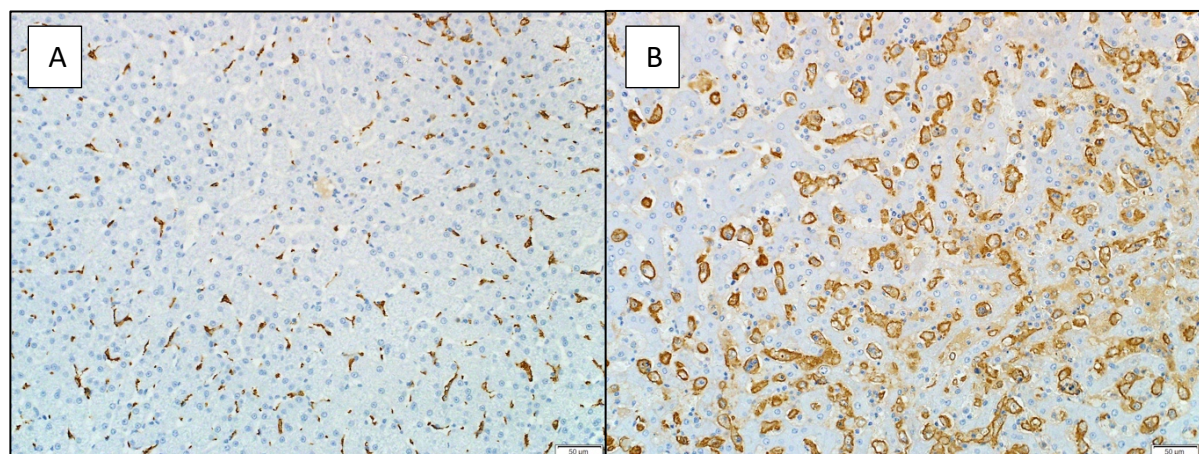


Figure 44: **A.** Photomicrograph of a normal dog liver (control no. 2) showing a midzonal area with scattered sinusoid-associated Iba-1-positive monocyte-macrophages and dendritic cells. IHC staining at 200x magnification. **B.** Photomicrograph of an infected dog liver (case no. 51) showing a midzonal area with a comparatively increased number of sinusoid-associated Iba-1-positive cells. IHC at 200x magnification.

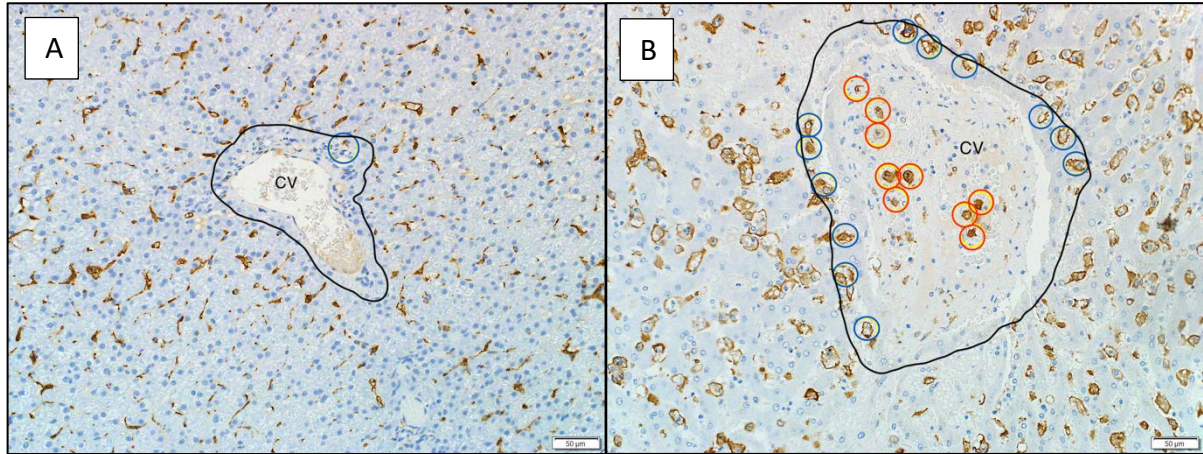


Figure 45: **A.** Photomicrograph of a normal dog liver (control no. 9) showing a centrilobular area (black outline) with scattered Iba-1-positive monocyte-macrophages and dendritic cells mainly in the perivascular interstitium (blue circles). CV = central vein. IHC staining at 200x magnification. **B.** Photomicrograph of an infected dog liver (case no. 91) showing a centrilobular area (black outline) with a comparatively increased number of Iba-1-positive cells adjacent to the limiting plate (blue circles) and within vascular lumens (red circles). CV = central vein. IHC staining at 200x magnification.

4.4.2.5 MAC387

Table 10: Quantification of MAC387-immunoreactive leucocytes (predominantly monocyte-macrophages**) in the *B. rossi*-infected livers (n=10) compared to the controls (n=4). The median number of positive cells (per HPF/400x magnification) per hepatic zone (portal tract, midzonal and centrilobular), as well as the *P*-values are listed. All values represent absolute cell counts.

<i>B. rossi</i>-infected cases			Control cases	<i>P</i>-value* comparing the control vs. infected cases
Infected dogs (Case no.)	Hepatic zone	Median number of positive cells/HPF	Median number of positive cells/HPF	
Case 20	Portal tract	4.7	1.0	<0.001
	Midzonal	87.7	22.0	<0.001
	Centrilobular	10.3	1.0	<0.001
Case 50	Portal tract	91.7	1.0	<0.001
	Midzonal	268.7	22.0	<0.001
	Centrilobular	66.0	1.0	<0.001
Case 54	Portal tract	35.0	1.0	<0.001
	Midzonal	205.3	22.0	<0.001
	Centrilobular	14.3	1.0	<0.001
Case 59	Portal tract	65.0	1.0	<0.001
	Midzonal	275.7	22.0	<0.001
	Centrilobular	118.3	1.0	<0.001
Case 61	Portal tract	36.7	1.0	<0.001
	Midzonal	282.7	22.0	<0.001
	Centrilobular	50.3	1.0	<0.001
Case 88	Portal tract	12.3	1.0	<0.001
	Midzonal	152.7	22.0	<0.001
	Centrilobular	13.3	1.0	<0.001
Case 91	Portal tract	26.7	1.0	<0.001
	Midzonal	253.3	22.0	<0.001
	Centrilobular	9.7	1.0	<0.001
Case 106	Portal tract	34.7	1.0	<0.001
	Midzonal	114	22.0	<0.001
	Centrilobular	15.7	1.0	<0.001
Case 110	Portal tract	11.7	1.0	<0.001
	Midzonal	101.3	22.0	<0.001
	Centrilobular	16.0	1.0	<0.001
Case 117	Portal tract	116.3	1.0	<0.001
	Midzonal	193.0	22.0	<0.001
	Centrilobular	38.7	1.0	<0.001
Total medians	Portal tract	26.5	1.0	<0.001
	Midzonal	189.0	22.0	<0.001
	Centrilobular	17.0	1.0	<0.001

Abbreviations: HPF = high power field (400x magnification).

*Significant *P*-values (*P*-value <0.05) are in bold.

** Generally, apart from 2/10 cases, few neutrophils were observed in the HE sections, so the MAC387 immunoreactivity refers largely to mononuclear phagocytes (monocyte-macrophages).

The highest median number of MAC387-positive leucocytes (monocytes, macrophages, and rare neutrophils) found was 268.7, while the lowest median number was 4.7 MAC387-positive cells per HPF. A median number of 26.5 MAC387-positive leucocytes per HPF was observed in the portal tracts, making this a 26.5-fold increase in MAC387-positive cells compared to the median of the control samples in this zone. This value falls above the normal range established by the control samples (Table 12). A median number of 189 MAC387-positive leucocytes was found per HPF in the midzonal regions of the infected livers, making this an 8.6-fold increase compared to the median of the controls. This value falls above the normal range established by the control samples (Table 12). A median number of 17 MAC387-positive leucocytes was found per HPF in the centrilobular regions, making this a 17-fold increase compared to the medians of the control samples. This falls above the normal range established by the control samples in this zone (Table 12). In the control specimens, the MAC387-positive leucocytes were predominantly located in the perivascular interstitium, with scattered sinusoid-associated and obvious intravascular leucocytes also occasionally visible. In the infected samples, MAC387-positive cells were found predominantly within vascular lumens, and to a lesser extent, also in the perivascular interstitium (Figures 46-48).

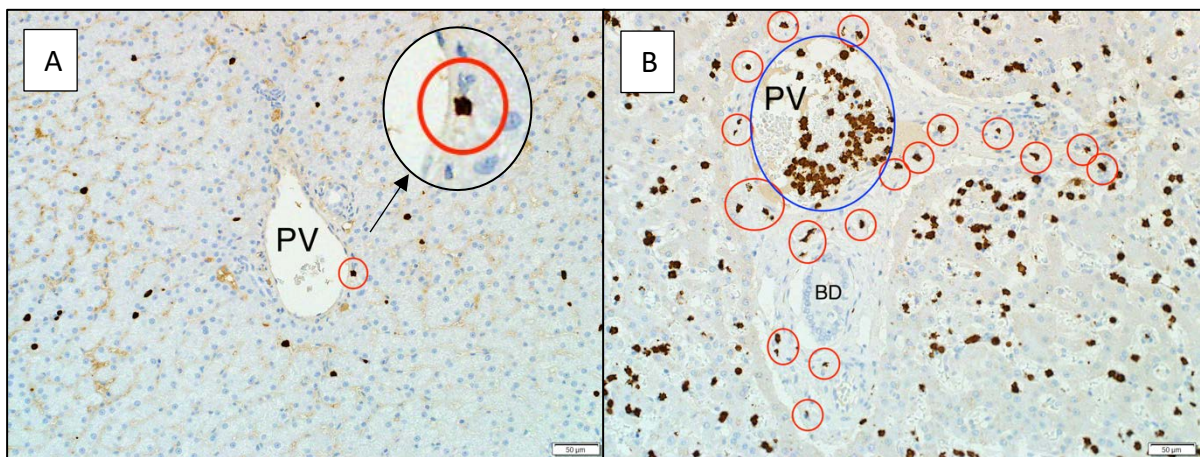


Figure 46: **A.** Photomicrograph of a normal dog liver (control no. 4) showing a portal tract with MAC387-positive leucocytes present in the perivascular interstitium with magnified views (black circle). PV = portal vein. IHC staining at 200x magnification. **B.** Photomicrograph of an infected dog liver (case no. 59) showing a portal tract with a comparatively increased number of MAC387-positive leucocytes predominantly within vascular lumens (blue circle), and also within the perivascular and periductal interstitium (red circles). PV = portal vein, BD = bile duct. IHC staining at 200x magnification.

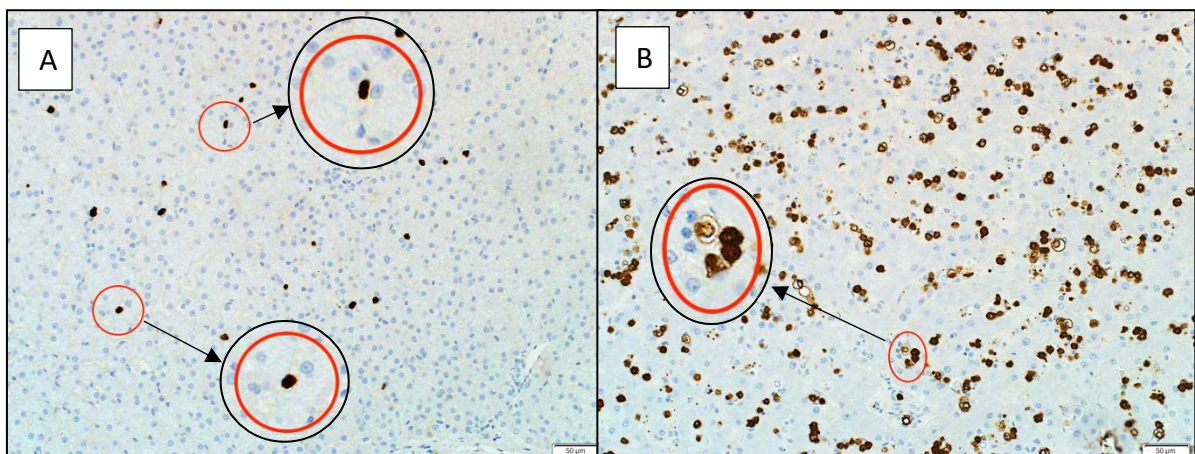


Figure 47: **A.** Photomicrograph of a normal dog liver (control no. 2) showing a midzonal area with MAC387-positive leucocytes present within sinusoidal lumens (red circles) with magnified views (black circles). IHC staining at 200x magnification. **B.** Photomicrograph of an infected dog liver (case no. 50) showing a midzonal area with an increased number of MAC387-positive leucocytes, particularly prominent within sinusoidal lumens (red circle) with magnified views (black circle). IHC staining at 200x magnification.

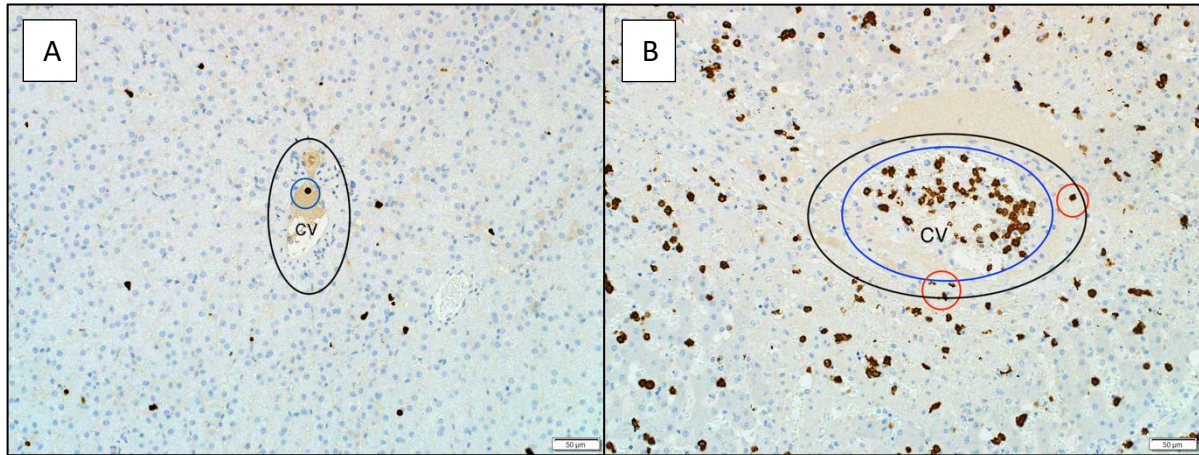


Figure 48: **A.** Photomicrograph of a normal dog liver (control no. 2) showing a centrilobular area (black circle) with a single MAC387-positive leucocyte within the lumen of the central vein (blue circle). CV = central vein. IHC staining at 200x magnification. **B.** Photomicrograph of an infected dog liver (case no. 117) showing a centrilobular area (black circle) with a comparatively increased number of MAC387-positive leucocytes, especially prominent within the lumen of the central vein (blue circle); there are also a few scattered positive cells in the perivascular connective tissue (red circles). CV = central vein. IHC staining at 200x magnification.

4.4.2.6 MUM-1

Table 11: Quantification of MUM-1-immunoreactive plasma cells and mature B-lymphocytes in the *B. rossi*-infected livers (n=10) compared to the controls (n=4). The median number of positive cells (per HPF/400x magnification) per hepatic zone (portal tract, midzonal and centrilobular), as well as the *P*-values are listed. All values represent absolute cell counts.

<i>B. rossi</i>-infected cases			Control cases	<i>P</i>-value* comparing the control vs. infected cases
Infected dogs (Case no.)	Hepatic zone	Median number of positive cells/HPF	Median number of positive cells/HPF	
Case 20	Portal tract	5.0	2	0.138
	Midzonal	4.7	3	0.554
	Centrilobular	28.7	1	0.003
Case 50	Portal tract	5.7	2	0.138
	Midzonal	3.3	3	0.554
	Centrilobular	8.3	1	0.003
Case 54	Portal tract	0.3	2	0.138
	Midzonal	5.7	3	0.554
	Centrilobular	1.7	1	0.003
Case 59	Portal tract	1.7	2	0.138
	Midzonal	3.0	3	0.554
	Centrilobular	6.0	1	0.003
Case 61	Portal tract	3.0	2	0.138
	Midzonal	5.0	3	0.554
	Centrilobular	6.0	1	0.003
Case 88	Portal tract	1.0	2	0.138
	Midzonal	2.0	3	0.554
	Centrilobular	2.3	1	0.003
Case 91	Portal tract	3.3	2	0.138
	Midzonal	3.0	3	0.554
	Centrilobular	2.0	1	0.003
Case 106	Portal tract	5.3	2	0.138
	Midzonal	4.7	3	0.554
	Centrilobular	7.3	1	0.003
Case 110	Portal tract	16.7	2	0.138
	Midzonal	14.7	3	0.554
	Centrilobular	86.3	1	0.003
Case 117	Portal tract	58.3	2	0.138
	Midzonal	3.7	3	0.554
	Centrilobular	1.7	1	0.003
Total medians	Portal tract	2.5	2	0.138
	Midzonal	4.0	3	0.554
	Centrilobular	3.5	1	0.003

Abbreviations: HPF = high power field (400x magnification).

*Significant *P*-values (*P*-value <0.05) are in bold.

The highest median number of MUM-1-positive plasma cells and mature B-lymphocytes found was 86.3, while the lowest median number was 0.3 MUM-1-positive cells per HPF. A median number of 2.5 MUM-1-positive cells per HPF was observed in the portal tracts, making this a 1.3-fold increase in MUM-1-positive cells compared to the median of the control samples in this zone. This value fell within the normal range as established by the control samples (Table 12). A median number of 4 MUM-1-positive plasma cells and B-lymphocytes was found per HPF in the midzonal regions of the infected livers, making this a 1.3-fold increase compared to the median of the controls, but this also fell within the normal range as established by the control samples (Table 12). A median number of 3.5 MUM-1-positive cells was found per HPF in the centrilobular regions, making this a 3.5-fold increase compared to the medians of the control samples in this zone, however this value also fell within the normal range as established by the control samples (Table 12). In the control samples, MUM-1-positive cells were confined to the perivascular interstitium, while in the infected samples, increased MUM-1-positive cells were observed in the perivascular and periductal interstitium (often corresponding with plasma cells), and in vascular lumens (corresponding with cells that had a more typical lymphocyte morphology) (Figures 49-51).

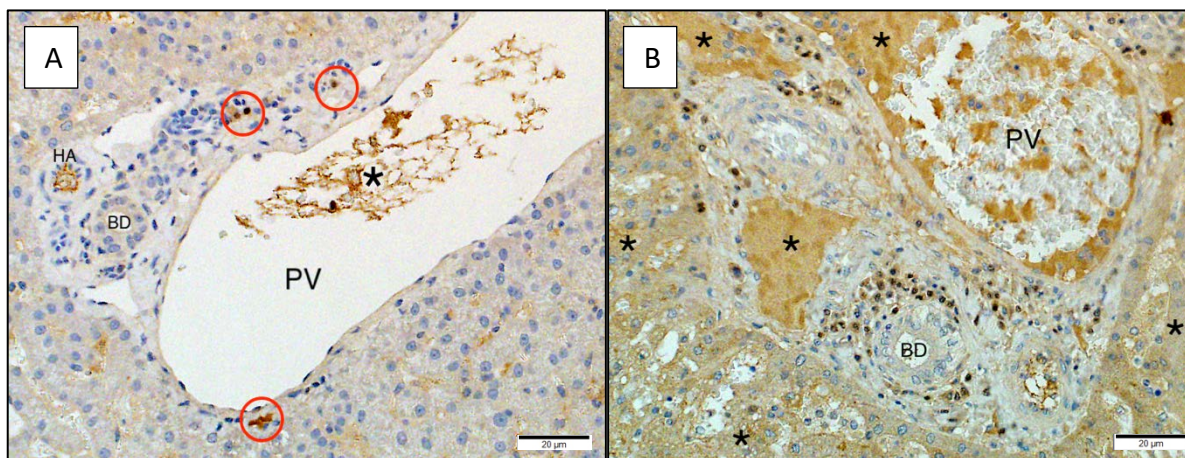


Figure 49: **A.** Photomicrograph of a normal dog liver (control no. 9) showing a portal tract with MUM-1-positive plasma cells and B-lymphocytes in the perivascular and periductal connective tissue (red circles). There is non-specific labeling of plasma (black star). PV = portal vein, BD = bile duct, HA = hepatic artery. IHC staining at 400x magnification. **B.** Photomicrograph of an infected dog liver (case no. 117) showing a portal tract with a comparatively increased number of MUM-1-positive cells, particularly obvious in the periductal and perivascular connective tissue. There is extensive non-specific labeling of hepatocytes and plasma (black stars). PV = portal vein, BD = bile duct. IHC staining at 400x magnification.

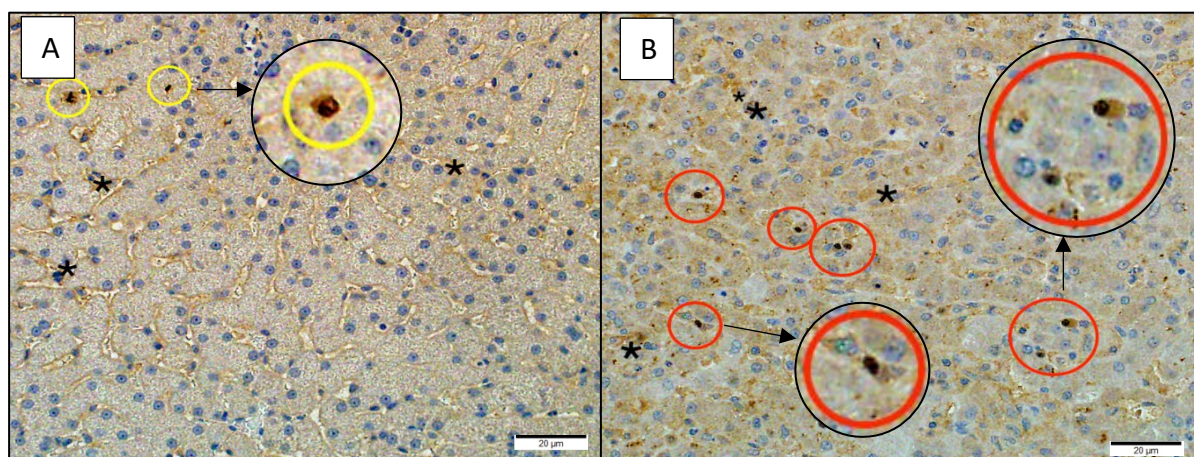


Figure 50: **A.** Photomicrograph of a normal dog liver (control no. 2) showing a midzonal area with scarce MUM-1-positive plasma cells and B-lymphocytes (yellow circles) with magnified views (black circles). There is non-specific labeling of plasma in sinusoids (black stars). IHC staining at 400x magnification. **B.** Photomicrograph of an infected dog liver (case no. 110) showing a midzonal area with comparatively increased sinusoid-associated MUM-1-positive cells (red circles) with magnified views (black circles). There is non-specific labeling of hepatocytes and plasma in the image (black stars). IHC at 400x magnification.

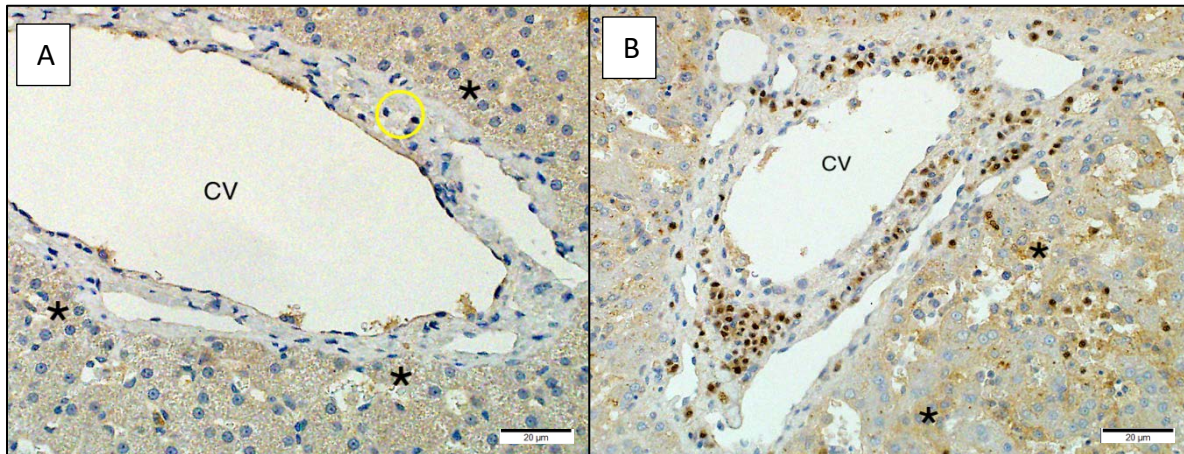


Figure 51: **A.** Photomicrograph of a normal dog liver (control no. 2) showing a centrilobular area with scarce MUM-1-positive plasma cells and B-lymphocytes in the perivascular interstitium (yellow circle). There is non-specific labeling of hepatocytes (black stars). CV = central vein. IHC staining at 400x magnification. **B.** Photomicrograph of an infected dog liver (case no. 110) showing a centrilobular area with a comparatively increased number of MUM-1-positive cells (mainly plasma cells) in the perivascular interstitium. There is non-specific labeling of hepatocytes and plasma (black stars). CV = central vein. IHC staining at 400x magnification.

4.4.3 Immunohistochemistry overview

The median numbers of leucocytes of different phenotypes in *Babesia rossi*-infected samples compared to the controls, per high power field (400x magnification), per hepatic zone, are summarized in Table 12.

Table 12: Quantification of immunophenotyped leucocytes in the control (n=4) and *B. rossi*-infected (n=10) liver samples. The median number of positive cells (per HPF/400x magnification) per hepatic zone (portal tract, midzonal and centrilobular), as well as the standard deviation, minimum and maximum number of positive cells, *P*-value, and magnitude of increase are listed. All values represent absolute cell counts.

Marker	Hepatic zone	<i>B. rossi</i> -infected cases		Control cases		<i>P</i> -value* vs. infected cases	Increase in magnitude in <i>B. rossi</i> - infected dogs
		Median number of positive cells/HPF (Standard deviation)	Range (minimum – maximum)	Median number of positive cells/HPF (Standard deviation)	Range (minimum – maximum)		
CD3	Portal tract	9.0 (7.8)	(2 – 36)	6 (5.3)	(0 – 16)	0.042	1.5-fold increase
	Midzonal	47.0 (31.5)	(7 – 137)	16.5 (5.7)	(11 – 30)	<0.001	2.8-fold increase
	Centrilobular	5.0 (4.8)	(2 – 19)	3 (10.8)	(0 – 34)	0.205	1.7-fold increase
CD20	Portal tract	5.0 (16.2)	(1 – 75)	1.5 (1.2)	(0 – 4)	<0.001	3.3-fold increase
	Midzonal	9.0 (5.3)	(1 – 26)	4 (2.4)	(1 – 9)	0.001	2.3-fold increase
	Centrilobular	9.5 (12.2)	(2 – 49)	1 (4.2)	(0 – 11)	<0.001	9.5-fold increase
CD204	Portal tract	10.0 (7.0)	(2 – 34)	7.5 (4.5)	(3 – 15)	0.158	1.3-fold increase
	Midzonal	132.5 (26.8)	(36 – 195)	71 (14.9)	(44 – 100)	<0.001	1.9-fold increase
	Centrilobular	14.0 (11.1)	(2 – 62)	5 (3.0)	(0 – 10)	<0.001	2.8-fold increase
Iba-1	Portal tract	11.5 (4.2)	(4 – 19)	9 (2.5)	(7 – 16)	0.251	1.3-fold increase
	Midzonal	145.0 (21.5)	(107 – 191)	107.5 (5.2)	(102 – 117)	<0.001	1.3-fold increase
	Centrilobular	11.5 (9.5)	(2 – 111)	5.5 (3.3)	(1 – 13)	<0.001	2.1-fold increase
MAC387	Portal tract	26.5 (59.8)	(2 – 300)	1 (2.0)	(0 – 7)	<0.001	26.5-fold increase
	Midzonal	189.0 (70.6)	(64 – 402)	22 (9.5)	(6 – 31)	<0.001	8.6-fold increase
	Centrilobular	17.0 (47.1)	(3 – 191)	1 (4.1)	(0 – 13)	<0.001	17-fold increase
MUM-1	Portal tract	2.5 (19.9)	(0 – 71)	2 (1.3)	(0 – 4)	0.138	1.3-fold increase
	Midzonal	4.0 (3.3)	(1 – 18)	3 (2.8)	(1 – 10)	0.554	1.3-fold increase
	Centrilobular	3.5 (25.2)	(1 – 114)	1 (3.0)	(0 – 9)	0.003	3.5-fold increase

Abbreviations: HPF = high power field (400x magnification).

*Significant *P*-values (*P*-value <0.05) are in bold.

CD3 – T-lymphocytes

CD20 – B-lymphocytes and plasma cells

CD204 – monocyte-macrophages

Iba-1 – macrophages and dendritic cells

MAC387 – bone marrow-derived leucocytes (monocytes, macrophages, and rare neutrophils)

MUM-1 – plasma cells (and mature B-lymphocytes)

The numbers of CD3-positive T-lymphocytes, CD20- and MUM1-positive B-lymphocytes and plasma cells, and Iba-1-, CD204-, and MAC387-positive monocyte-macrophages were increased in the liver samples of the infected dogs compared to the controls. The number of MAC387-positive leucocytes (predominantly monocyte-macrophages) was most obviously increased across all hepatic zones (portal tracts – 26.5-fold increase, midzonal – 8.6-fold increase, centrilobular – 17-fold increase). There was a similar increase in CD204- and Iba-1-positive monocyte-macrophages (and dendritic cells) in the midzonal area (CD204 – 1.9-fold increase, Iba-1 – 1.3-fold increase) and centrilobular zones (CD204 – 2.8-fold increase, Iba-1 – 2.1-fold increase). The number of CD3-positive T-lymphocytes was increased in both the portal tracts and midzonal areas, with 1.5-fold and 2.8-fold increases respectively. The number of CD20-positive B-lymphocytes and plasma cells was also noticeably increased in all zones, with a 1.3-fold increase in the portal tracts, a 1.9-fold increase in the midzonal areas and a 2.8-fold increase in the centrilobular zones. The number of MUM-1-positive plasma cells (and mature B-lymphocytes) was only increased in the centrilobular zone which had a 3.5-fold increase. There were only a few instances where the median number of immune-positive cells was greater than the normal range established for the control samples per hepatic zone. These included: CD3-positive T lymphocytes (midzonal), CD20-positive B-lymphocytes and plasma cells (portal tracts), CD204-positive monocyte-macrophages (midzonal and centrilobular), Iba-1-positive monocyte-macrophages (midzonal), and MAC387-positive leucocytes (portal tracts, midzonal and centrilobular).

Table 13 below summarizes the median number of leucocytes of different phenotype in the liver specimens as a whole (non-zonal) for *Babesia rossi*-infected dogs compared to control dogs.

Table 13: Quantification of immunophenotyped leucocytes of the control (n=4) and *B. rossi*-infected (n=10) liver samples. The median number of positive cells (per HPF/400x magnification) in the liver as a whole (non-zonal), as well as the standard deviation, minimum and maximum number of positive cells, *P*-value, and magnitude of increase are listed. All values represent absolute cell counts.

	<i>B. rossi</i>-infected cases	Control cases		
	Median number of positive cells/HPF (Standard deviation)	Median number of positive cells/HPF (Standard deviation)	<i>P</i>-value* of control vs. infected cases	Increase in magnitude in <i>B. rossi</i>-infected dogs
CD3	66.0 (35.2)	27.5 (16.3)	<0.001	2.4-fold increase
CD20	25.0 (22.9)	5.5 (6.3)	<0.001	4.5-fold increase
CD204	158.0 (36.1)	85.0 (17.5)	<0.001	1.9-fold increase
Iba-1	174.0 (26.3)	123 (8.7)	<0.001	1.4-fold increase
MAC387	260.5 (123.8)	27.0 (12.4)	<0.001	9.-fold increase

MUM-1	13.0 (32.4)	6.5 (5.6)	0.005	2-fold increase
-------	-------------	-----------	--------------	-----------------

Abbreviations: HPF = high power field (400x magnification).

*Significant *P*-values (*P*-value <0.05) are in bold.

When looking at each of the selected leucocyte markers for the liver samples overall (regardless of the zone), all the results were significant with a *P*-value of <0.05 or less. The greatest increase was seen with the MAC387-positive monocyte-macrophages, which exhibited an overall increase of 9.6-fold compared to the controls. CD20-positive B-lymphocytes and plasma cells had an overall 4.5-fold increase compared to the control samples, while the MUM-1-positive plasma cells (and, to a lesser extent, mature B-lymphocytes) had an overall 2.2-fold increase compared to the controls. CD3-positive T-lymphocytes had an overall 2.1-fold increase compared to the control samples. CD204-positive monocyte-macrophages had an overall 1.9-fold increase compared to the controls, while Iba-1-positive macrophages and dendritic cells exhibited an overall increase of 1.4-fold compared to the controls.

Perls' Prussian blue-positive haemosiderin granules were typically identified in macrophages in the control and infected liver samples. Thus, the increased number of haemosiderin-containing cells in the infected cases correlates strongly with the increase in MAC387-, CD204- and Iba-1-positive monocyte-macrophages in these cases compared to the controls.

Only CD20-positive B-lymphocytes and plasma cells, CD204- and Iba-1-positive monocyte-macrophages and MAC387-positive leucocytes had median numbers that were higher than the normal range of cells present as established by the control samples in the livers as a whole.

5. DISCUSSION

5.1 HISTOPATHOLOGY

In summary, the histological sections of the infected dogs' livers displayed diffuse lesions affecting all three hepatic zones, with some lesions that had a multifocal-coalescing distribution pattern. Diffuse lesions included dilation of the spaces of Disse, cholestasis, hypertrophic Kupffer cells containing bile and haemosiderin pigments, central venous and sinusoidal congestion, inflammatory cell infiltrates consisting mostly of monocyte-macrophages (as determined by MAC387, Iba-1 and CD204 immunohistochemistry), and evidence of significant extramedullary haematopoiesis. Necrosis of centrilobular hepatocytes occurred in a multifocal to coalescing pattern. Generally, a clear demarcation between the zones of the liver was still apparent, although the presence of centrilobular necrosis did slightly complicate the distinction.

5.1.1 Sinusoids, spaces of Disse and lymphatics

One of the most striking changes noted in the infected cases was severe oedema that widened the space of Disse in all hepatic zones. Similar changes have been noted in bovine babesiosis (Pupin et al., 2019, Esmaeilnejad et al., 2021), gerbil babesiosis (Dkhil et al., 2010, Dkhil et al., 2013), equine babesiosis (Mahoney et al., 1977, Roberts, 1962, De Waal, 1992, Allen et al., 1975), murine babesiosis (Okta et al., 2014b), human malaria (Kochar et al., 2003b, Walters and McGregor, 1960), and human and animal sepsis patients (Hirata et al., 2001, Iwasashi et al., 2003).

Hepatic lymph is formed from the filtration of blood plasma through the sinusoids into the space of Disse (Aspestrand et al., 1991). The main mechanisms responsible for oedema are thought to be an increase in capillary leakage and/or a blockage in the draining lymphatic ducts (Hill et al., 1953). 90% of the infected cases demonstrated distended lymphatic vessels with lymph stasis in both the periportal and centrilobular lymphatics. The subcapsular lymphatic ducts were not examined due to most of the tissues used not including the liver capsule. Blockages in the lymphatic ducts were not observed in our study, however the lymphatic distension seen could be attributed to the increased need to drain the oedematous spaces of Disse. The combination of both capillary leakage and increased drainage of the spaces of Disse could be the cause of the oedema and lymphatic distension observed.

Babesiosis has been likened to bacterial sepsis, because it is also associated with an inflammatory cytokine storm, resulting in many of the same outcomes, clinicopathological findings and histological changes in various organs (Leisewitz et al., 2019a). Lymphatic distension and lymph stasis in the liver has also been demonstrated in patients with endotoxaemia and sepsis. It is thought to be due to endotoxins inhibiting the pumping mechanism of the lymphatic vessels, as well as the increasing lymph production associated with the massive inflammatory response (Goto et al., 1981, Elias et al., 1987). The lymph stasis and oedema in the space of Disse in the infected samples could therefore also be attributed to the endotoxaemia-like state of babesiosis. The dilated lymphatic vessels are also possibly an extension of the stasis observed in the extra- and intrahepatic lymph vessels during endotoxaemia (Shibayama et al., 1992). No correlation was found between the development of hepatocyte injury and the intrahepatic lymph stasis observed in endotoxaemia (Shibayama et al., 1992), however this contrasts what was observed in this study. Increased capillary permeability is seen in endotoxaemia and sepsis caused by the massive inflammatory state present, leading to interstitial fluid accumulation and protein loss (Groeneveld et al., 1986). Albumin is a negative acute phase protein that decreases during infection or inflammation, therefore hypoalbuminaemia may exacerbate capillary leakage as it results in decreased intravascular oncotic pressure within already compromised blood vessels (Sibbald and Vincent, 2012, Marx, 2003). This was supported by serum

hypoalbuminaemia (reference range 28-41g/L) that was demonstrated in 9/10 of our infected samples.

Another possible cause of distension of the space of Disse and the lymphatic vasculature in the liver could be hypoperfusion of the sinusoids inducing distension of the space of Disse (Hirata et al., 2001). Carbon monoxide (CO) is thought to contribute to sinusoidal dilatation during sepsis as it enhances hepatic sinusoidal perfusion (Gräser et al., 1990, Morita et al., 1995, Vedernikov et al., 1989). Carbon monoxide is endogenously generated during heme breakdown to biliverdin and iron, and its affinity for iron reduces oxygen offloading at the tissue level (Siggaard-Andersen and Siggaard-Andersen, 1990, Iwasashi et al., 2003). Increased carboxyhaemoglobin from severe haemolysis in dogs with babesiosis further compromises oxygen status by about 20% compared to anaemia alone (Taylor et al., 1991). Excessive vasodilation and increased sinusoidal space may exacerbate liver dysfunction and cause further hypoxic damage (Iwasashi et al., 2003).

In this study, mild-moderate endothelial hypertrophy was observed in 7/10 of the infected samples, predominantly of the central veins. Endothelial cell activation has also been demonstrated in the lung endothelium in *Babesia rossi*-infected dogs (Martin, 2020), *B. microti*-infected murine lungs (Hemmer et al., 1999), and human sepsis patients (Hirata et al., 2001). Since direct injury by *B. rossi* parasites is unlikely as they have no direct effect on the vascular endothelium, the damage is most likely caused by pro-inflammatory cytokines (IL-1, IL-6, TNF- α) released by activated macrophages. An increase in these inflammatory cytokines has already been demonstrated in *B. rossi*-infected dogs (Goddard et al., 2016, Leisewitz et al., 2019a). During inflammation and activation of endothelial cells in response to activated Kupffer cell-produced inflammatory cytokines, they are seen to produce increased amounts of their cell-adhesion molecule, ICAM-1 (Brown, 2017), allowing microthrombi to attach and promoting leucocyte migration through the liver parenchyma (Shetty et al., 2018). Ultrastructural analysis of the activated endothelial cells in the lungs was performed in humans infected with *B. microti* where clear adhesion of the inflammatory leukocytes to the endothelial walls was shown. The hypertrophic endothelial cells had increased numbers of caveolae (50-100nm cell-surface plasma membrane invaginations (Frank et al., 2003)), and showed the development of transcellular channels which are believed to allow fluid to leak out of the cells and into the perivascular space (Hemmer et al., 1999). The same mechanisms are suggested to be affecting the endothelial cells lining the hepatic vasculature, contributing to the oedema observed in the space of Disse. Further ultrastructural evaluation of the liver will be necessary before conclusions can be made.

Marked congestion was present in all the samples, with 8/10 of the diseased samples showing severe congestion (classified as congestion present in >70% of the blood vessel lumens in all available histology sections). The congestion involved the portal veins and arteries, sinusoids, and the occasional central vein. Congestion in the liver sinusoids has been reported in mice infected with *B. hylomyisci*, and human malaria (Rupani and Amarapurkar, 2009). Sinusoidal dilatations with increased cellular content and congestion are findings that are associated with extramedullary haematopoiesis (EMH), a common finding in *Babesia* and malaria (Bruguera et al., 1978, Wozniak et al., 1997). Possible causes for this congestion may not be intrahepatic but could be due to acute right-sided heart failure (causing passive congestion) and pulmonary hypertension in sepsis (Bernal, 2016, Ebert, 2006). Right-sided heart failure results in decreased cardiac output and mean arterial pressure, which in turn stimulates peripheral vasoconstriction via activation of the sympathetic vasomotor response. This further decreases end organ-perfusion as it decreases the number of oxygen-carrying erythrocytes available to the hepatocytes and increasing the hypoxic injury (Ebert, 2006). Microthrombi of aggregated erythrocytes, fibrin or platelets adhered to the blood vessel walls obstructing bloodflow was not observed in this study, although it is possible that they dissolved antemortem before tissue were harvested and fixed.

5.1.2 Hepatocytes

Necrosis, hydropic change, anisokaryosis, mildly increased turnover and vesicular nuclei present within the hepatocytes are indicative of hepatocyte injury and response to that injury. These changes were largely located around the centrilobular area, supporting the theory of hypoxia-driven injury.

Single cell necrosis was observed in 8/10 of the infected samples (defined as single hepatocyte necrosis per HPF at 400x magnification), extending into the midzonal areas in 4/10 cases. These findings are consistent with those mentioned in equine babesiosis (Mahoney et al., 1977, Roberts, 1962, De Waal, 1992, Allen et al., 1975), feline babesiosis (Futter and Van Rijswijk, 1981), *B. canis* in dogs (Mathe et al., 2006) but seems absent in canine *B. gibsoni* (Wozniak et al., 1997), *B. hylomyisci* in mice (Hussein, 1977), *P. falciparum* in humans (Viriyavejakul et al., 2014, Whitten et al., 2011), and sepsis in human patients (Ring and Stremmel, 2000, Bhalla et al., 2006, Asaka et al., 1996). Hepatocellular degeneration, seen as hydropic vacuolation within the hepatocyte cytoplasm indicates reversible cell injury and has been noted in canine babesiosis (Máthé, 2006), murine babesiosis (Okla et al., 2014b, Esmailnejad et al., 2018), and human malaria (Das, 2003).

Hypoxic injury to the liver is observed as a consequence of haemolytic disease, despite the fact that the liver has dual blood supply, and the ability to release adenosine to increase its blood supply by dilating the hepatic arteries but not the portal veins (Lautt, 1977). Because the hepatic blood supply flows from the portal tracts through the sinusoids and out through the central veins, the centrilobular hepatocytes are the most susceptible to hypoxic injury (Ebert, 2006). One potential cause of the centrilobular necrosis is reduced cardiac output with associated hypoxia as is seen in late-stage endotoxaemia (Shibayama et al., 1993). The ischemia observed in human malaria has been shown to be caused by a reduction in splanchnic and hepatic blood flow (Molyneux et al., 1989), as well as aggregates of parasitized erythrocytes, leucocytes and fibrin that form microthrombi and blockages within the sinusoids, further reducing blood flow to those areas (Bhalla et al., 2006, Asaka et al., 1996). These processes would lead to swelling of the already injured hepatocytes, Kupffer cells, and endothelial cells following the initial hypoxic injury. This swelling could narrow the sinusoidal lumens, further impeding blood supply and exacerbating the hypoxia significantly (Lescot et al., 2012, Asaka et al., 1996). Another study, in contrast, presented evidence of hepatic injury despite an increase in blood flow to the splanchnic organs. This finding led to speculations that the splanchnic organs may have heightened oxygen consumption during sepsis (Pastor and Suter, 1999). It is hypothesised that there are increased metabolic demands, decreased ability of the haem molecule to offload oxygen molecules, or inadequate extraction of oxygen by the hepatocytes during *B. rossi* infection, as there is in sepsis patients (Dunn, 1973, Gibson and Dudley, 1984, Rawson and Achord, 1985, Han, 2002, Asaka et al., 1996, Ring and Stremmel, 2000, Dahn et al., 1990). Severe anaemia (present in all ten of our infected dogs) also contributes to the decreased delivery of oxygen to the tissues.

In a normal healthy subject, the mean value of oxygen uptake by the liver is 3.1-fold higher than the intestine (Lutz et al., 1975). During low oxygen supply in healthy subjects, the oxygen extraction ability of the hepatocytes increased to 97%, whereas the intestinal oxygen extraction ability did not exceed 75% (Lutz et al., 1975). This means that the increased oxygen demand is met by increased hepatic oxygen uptake, with no obvious hepatic vasodilation and hepatic artery hyperaemia (Lutz et al., 1975). During conditions such as anaemia, the hepatic arterial blood can be normoxic due to normal oxygen tension (dissolved free oxygen concentration), but hypoxemic due to reduced haemoglobin-bound oxygen (Jungermann and Kietzmann, 2000). During sepsis, blood flow to the liver increases by 72%, with a 60% increase in hepatic oxygen consumption in comparison to normal, healthy livers. The causes of decreased hepatic oxygen availability could be attributed to reduced haemoglobin or 2,3-diphosphoglycerate levels, low oxygen saturation, an altered microcirculation (Dahn et al., 1990), or severe anaemia (Okas et al., 2001). The hepatocytes require increased oxygen supply to meet their

sepsis-induced hypermetabolic aerobic needs, however, the oxygen extraction ability of the hepatocytes becomes increasingly inefficient the more injured the liver becomes. The sinusoidal oxygen tension was found to be significantly decreased in patients with sepsis, and was lowest in the centrilobular regions. As hepatocyte size/swelling and metabolic rate increased, there was a proportional decrease in sinusoidal oxygen tension, suggesting a rise in oxygen utilization during the injury (Dahn et al., 1990). The critical oxygen tension (the oxygen partial pressure below which an animal's normal metabolic rate can no longer be maintained) of the hepatocytes increases significantly during sepsis, and with a decrease in sinusoidal oxygen tension it leaves the hepatocytes increasingly sensitive to hypoxia, despite an increase in oxygen delivery to the liver during sepsis (Dahn et al., 1990).

Hypoxic liver injury is associated with acutely increased levels of serum transaminases (AST and ALT) and LDH (between 12-48 hours after initial injury) (Ebert, 2006). Our study validated this observation, as the samples exhibiting the most pronounced necrosis, hydropic change, and hepatocyte turnover also correlated with the highest transaminase values on serum biochemistry. In one study of sepsis, hepatocellular dysfunction, as indicated by serum biochemistry, was found to actually occur before relative hypoxaemia was noted (Wang and Chaudry, 1996). The elevated liver enzymes observed (ALP, ALT, AST) in this study were likely released by the hypermetabolic dysfunctional hepatocytes during septic injury despite increased perfusion (Wang and Chaudry, 1996). Hepatocyte function modulation and dysregulation results from the effects of pro-inflammatory cytokines (such as tumour necrosis factor- α (TNF- α) and interleukin-6 (IL-6)) that are released during sepsis by activated Kupffer cells (Wang and Chaudry, 1996). In addition to systemic inflammation associated with sepsis, a translocation of endotoxins and pancreatic enzymes flood into the draining portal blood once the gut barrier becomes impaired. This causes further damage to the already compromised hepatocytes and sinusoidal endothelial cells (Meng et al., 1992, Gaynor, 1973, Nayyar et al., 1989). The recruitment of monocytes and neutrophils into the liver by the resident macrophages (Kupffer cells) stimulates the production of reactive oxygen species (ROS), the principal toxic mediators of cell death. These ROS, however, cause cell death not only of invading bacteria/protozoa, but also of hepatocytes and other liver cells. By inflicting intracellular oxidant stress, ROS damage the cell membranes and mitochondrial bodies - promoting mitochondrial dysfunction (Meng et al., 1992), but can also result in enhanced lipid peroxidation and DNA damage (Chaudhuri et al., 2008). This leads to oncotic necrosis (involving mitochondrial permeability transition pore opening, breakdown of the membrane potential, and ATP depletion (Nieminen et al., 1997)) rather than apoptosis (Jaeschke, 2011). During sepsis, when comparing the liver, kidneys, lung, and small intestine, the first notable decrease in adenosine triphosphate (ATP) was observed within the liver. It is also the organ that becomes most susceptible to injury, being the first target of free radical injury. Mitochondrial dysfunction (resulting in a decrease of ATP) leads to a decrease in the oxygen extraction and metabolic capability of the hepatocytes, inciting further damage (Chaudhuri et al., 2008). The hepatic dysfunction noted does not normally lead to failure resulting in mortality, however it does reflect a liver in stress and may well contribute to the icterus often observed in babesiosis.

Mitotic figures and hepatocyte binucleation were considered as indicators of increased hepatocyte turnover. It was found to be mostly mild (turnover present in 1-2 hepatocytes per HPF at 400x magnification) in the periportal and centrilobular areas, but moderate in the midzonal areas. These results were only slightly increased in comparison to the controls. The liver has a high regenerative capacity which is activated during sepsis (Weiss et al., 2001). DNA-labeling studies performed on a normal, healthy human liver have provided evidence that the percentage of hepatocytes involved in DNA synthesis is remarkably low, measuring less than 0.2%. Furthermore, this low rate of DNA synthesis is consistent across different zones of the liver (Michalopoulos, 2007, Fausto et al., 2006, Michalopoulos and Bhushan, 2021, DeFrances and Michalopoulos, 2011, Monga, 2020). Hepatocyte regeneration has been observed solely in cases of mild sepsis, while the absence of regeneration in

severe sepsis is believed to be due to hepatocyte dysfunction (Weiss et al., 2001). Activation of regeneration is stimulated by the presence of pro-inflammatory cytokines (IL-1, IL-6, and TNF- α) released from Kupffer cells and other damaged hepatocytes and endothelial cells during sepsis (Kovalovich et al., 2000, Yamada et al., 1997, Blackwell and Christman, 1996, Michalopoulos and Bhushan, 2021, Wang and Chaudry, 1996). Regeneration is a compensatory mechanism and is only noted after the processes of necrosis and apoptosis have already begun (Weiss et al., 2001), but has also been demonstrated during cholestasis due to inflammatory cytokines released by cholangiocytes themselves (Michalopoulos, 2007). In *B. rossi*-infected dogs, the degree of regeneration noted was fairly similar to the controls despite the severe inflammatory state we know to be present in infected dogs (Goddard et al., 2016). We predict that the disease is of such acute nature that there is inadequate time for regeneration to become evident.

5.1.3 Cholestasis

For the purpose of this study, cholestasis refers to the presence of bile in histologic sections of the liver (Lefkowitz, 2004). Bile stasis was present within the portal tract bile ducts in 8/10 samples, however canalicular bile and bile pigment within the hepatocytes was present in all samples and across all zones. Increased numbers of hypertrophic Kupffer cells containing phagocytosed bile pigment, with larger amounts of intrahepatocellular and canalicular bile were observed in the centrilobular areas. The centrilobular predominance of cholestasis can be explained by hypoxia, which directly impairs the ATP pumps responsible for bile salt excretion (Lefkowitz, 2004). Ductular and canalicular cholestasis is a very common finding in patients with sepsis and is thought to be attributed to circulating endotoxins causing disorders in bile secretion, ductular contraction and ischaemia (Koskinas et al., 2008, Hirata et al., 2001). Sepsis patients also present with intrahepatocellular bile pigmentation (Lefkowitz, 2004), similar to what was observed in our *B. rossi*-infected livers. Intrahepatocellular bile pigment has been noted in porcine babesiosis (Avenant et al., 2021), equine babesiosis (Mahoney et al., 1977), human babesiosis (Fitzpatrick et al., 1969) and malaria (Losert et al., 2000, Chawla et al., 1989).

Measured total bilirubin was above the reference interval for all the *B. rossi*-infected dogs that were studied, while 7/10 of the cases were visibly icteric upon presentation. Elevated levels of total bilirubin result from both increased production and reduced hepatic clearance, and these higher levels have been linked to a poorer prognosis (Leisewitz et al., 2019b). Livers in primary haemolytic or with hepatobiliary disease were found to have a 30-50% reduction in bilirubin clearance (Rothuizen et al., 1992). The icterus observed during *B. rossi* infection undoubtedly has a significant pre-hepatic component due to the haemolysis, but also may very well have a hepatic component considering the extent of the hepatocyte injury described here resulting in the increased unconjugated bilirubin observed during disease (Rothuizen et al., 1992).

Inflammation-induced cholestasis is facilitated by endotoxins (Crawford, 1997), causing Kupffer cells to produce pro-inflammatory cytokines (IL-1, IL-6, IL-8 and TNF- α). These cytokines have cholestatic effects by activating neutrophils, T- and B-lymphocytes, and increasing cellular adhesions (Trauner et al., 1999, Geier et al., 2006, Crawford and Boyer, 1998). They also damage the intracellular architecture and cell junctions of the hepatocytes and cholangiocytes therefore decreasing the uptake of bile salts, decreasing the secretion of bile and causing disturbances in canalicular contraction (Whiting et al., 1995, Green et al., 1994, Lescot et al., 2012, Scheuer and Lefkowitz, 2005, Hirata et al., 2001, Crawford and Boyer, 1998, Lefkowitz, 2004). Looking ultrastructurally at the bile ductules during cholestasis in sepsis, the microvilli within the ductules were seen to actually disappear, reducing the bile flow within the ductules, further exacerbating the cholestasis (Hirata et al., 2001). Similar mechanisms may be at play within the ductules and canaliculi in canine babesiosis.

5.1.4 Extramedullary haematopoiesis (EMH)

In cases of *B. rossi* and falciparum malaria (Krause et al., 2007), an inappropriate response to anaemia is observed. This is shown by a decrease in the absolute reticulocyte count (ARC) after infection in response to a decrease in haematocrit. In one study, this was contrasted to dogs that had non-*Babesia*-related immune-mediated haemolytic anaemia (IMHA), where the ARC increased significantly in response to a similar haematocrit. Canine babesiosis impacts the bone marrow, which serves as the primary organ of haematopoiesis. The reticulocytes that are visualized during babesiosis are hypochromic with a lower haemoglobin concentration compared to reticulocytes of control animals (Seejarim, 2020). It has been reported in *B. rossi*, as well as in human falciparum malaria (Krause et al., 2007), that a non-regenerative anaemia is present as a result of dyserythropoiesis (Bumby, 2022). In dogs with fatal *B. rossi* infection, the bone marrow contains increased numbers of rubriblasts, however decreased numbers of metarubricytes that also display dyserythropoetic changes are present. These findings suggest suppression of erythropoiesis in the bone marrow (Bumby, 2022), and have been associated with increased levels of TNF- α and nitric oxide which are observed during *B. rossi* infection (Goddard et al., 2016, Awandare et al., 2011).

Extramedullary haematopoiesis (EMH) refers to the production of red blood cells outside the medullary cavity of the bone marrow (Johns and Christopher, 2012). EMH was evident in all infected samples, with over five nucleated erythrocytes observed per high-power field (HPF; 400x magnification) in over half of the samples, primarily in the centrilobular and midzonal sinusoids. Megakaryocytes were not visualized, which is similar to what was observed within the bone marrow of *B. rossi*-infected dogs (Bumby, 2022). Similar results have been reported in the liver in canine babesiosis (Wozniak et al., 1997, Irizarry-Rovira et al., 2001), murine babesiosis (Hussein, 1982), human malaria (Abo and Sekikawa, 2002), as well as in cases of severe infection and inflammation (Cenariu et al., 2021).

There are four main causes for the stimulation of EMH: 1) bone marrow failure, 2) bone marrow stimulation (myelostimulation), 3) tissue inflammation or injury and 4) abnormal systemic or local chemokine production (Johns and Christopher, 2012, Valli et al., 2015). Myelostimulation (also called compensatory reactivation or reactive EMH), is probably the main cause for the EMH observed in canine babesiosis (Wozniak et al., 1997). This occurs when there is a need for increased red blood cell production with concurrent hypoxia, occurring in many inflammatory disorders and haemolytic anaemias (Johns and Christopher, 2012, Adamson, 1988). This stimulates reactivation of stem cell niches, increases chemokine production, as well as erythropoiesis from embryonic sites (mainly the spleen and liver) (Johns and Christopher, 2012, Kaushansky, 2016).

Hypoxic EMH, also referred to as stress EMH seen in tissue inflammation/injury, causes expansion and differentiation of erythroid progenitor cells particularly in the spleen, but also in the liver (Johns and Christopher, 2012). Activated macrophages have been thought to stimulate EMH as they are distributed widely throughout the vasculature and tissues, they can induce stromal proliferation, and have an enhanced ability to interact with other cells (Bienzle et al., 1995, Milner et al., 2010, Sadahira and Mori, 1999). Stimulation of granulopoiesis (production of neutrophils, eosinophils and basophils) in inflammatory disease also has the ability to stimulate EMH (Johns and Christopher, 2012). The numerous cytokines and inflammatory mediators in states of inflammation create the correct environment to activate the erythroid niches stimulating EMH in certain tissues including the liver (Wright et al., 2001, Watanabe et al., 1991, Maxie et al., 2007, O'Malley, 2007). Kupffer cells were found to be capable of stimulating EMH in livers of mice that had their bone marrow macrophages depleted (Otsuka et al., 2011). Hepatic EMH is usually seen intrasinusoidally (O'Malley, 2007) as well as perisinusoidally, within portal veins and portal tracts (Maxie et al., 2007, Valli et al., 2015).

Collectively, these liver findings, along with previous observations in dogs with fatal *B. rossi* infection, suggest that EMH is triggered in the liver when the bone marrow's red blood cell production is insufficient to compensate for concurrent anemia and hypoxia.

5.1.5 Kupffer cells

Kupffer cell hypertrophy is a common finding in canine babesiosis (Wozniak et al., 1997, Ayoob et al., 2010), gerbil babesiosis (Dkhil et al., 2013), human malaria (Anand and Puri, 2005, Rupani and Amarapurkar, 2009, Kochar et al., 2003a), and in human sepsis (Banks et al., 1982). Hypertrophic Kupffer cells were observed in all the infected samples. Abundant Perl's Prussian blue-positive haemosiderin pigment (classified as pigment present in more than 20% of Kupffer cells/HPF at 400x magnification) was observed in the centrilobular and midzonal areas in 50% of the samples, while the remaining 50% showed only minimal presence. Haemosiderin was the primary pigment found in Kupffer cells, accompanied by significant phagocytosed bile pigment in centrilobular areas, with lesser extension into the midzonal areas.

Kupffer cells play an important role in the innate immune response in the liver. When activated by toxins, endotoxins and other harmful substances in the bloodstream, they release potent inflammatory cytokines (TNF- α and IL-1), growth factors, reactive oxygen species (ROS), reactive nitrogen species (e.g. nitric oxide/NO), proteases, and lipid metabolites (prostaglandins and thromboxane) (Luster et al., 1994, Su, 2002, Li et al., 2017b, Roberts et al., 2007). While this mechanism aims to safeguard the liver from harm, these metabolites can also inflict liver damage during severe endotoxaemia. They achieve this by directly injuring hepatocytes and endothelial cells (Thurman, 1998). In mild infections, endotoxemia can stimulate Kupffer cells to release cytokines, but in lesser amounts and for shorter durations, offering protection rather than causing injury (Roberts et al., 2007).

Studies have shown that experimentally induced Kupffer cell inhibition during sepsis results in a decrease in the systemic inflammatory response (shown by decreased levels of IL-6). However, in the context of reduced inflammation, there was an observed increase in mortality, underscoring their vital role in immunity. In the presence of decreased inflammation however, was an increase in mortality, highlighting their importance in immunity (Callery et al., 1990). Kupffer cell inflammatory mediators released during sepsis have also been found to play a significant role in immunosuppression and dysfunction in resident splenic lymphocytes (Ayala et al., 1997), indicating their role in the systemic immune response, not just within the liver.

5.1.6 Haemosiderin

Perl's Prussian Blue staining confirmed a large increase in haemosiderin-laden Kupffer cells and hepatocytes in the infected samples. This is a frequently observed phenomenon in haemolytic diseases, occurring after excessive extravascular haemolysis. Increased numbers of haemosiderin-laden macrophages have been visualized within the hepatic sinusoids in *Plasmodium yoelii* in mice (Ono et al., 2021), and avian malaria (Sijbranda et al., 2017).

Haemosiderin, along with ferritin, is classified as one of the storage proteins of non-haem iron. It is visualized as intracellular aggregates of fine granules that stain sky-blue with Perls' Prussian Blue stain (Iancu, 1992) and increases in haemolytic conditions as a result of an overload of iron released from erythrocytes phagocytosed by macrophages (Radicheva, 2011). In our samples, haemosiderin pigment was found mostly within the sinusoids and perivascular interstitium, and within the cytoplasm of mononuclear leucocytes. The Perls' stain demonstrated a 106x increase in the infected samples compared to the controls indicating massive iron accumulation within the liver. This mimics the

findings noted within the bone marrow of *B. rossi*-infected dogs, arguing against the possibility of an iron-restricted erythropoiesis as the cause of the non-regenerative anaemia observed (Bumby, 2022). However, anaemia during infection or chronic disease is associated with massive inflammatory cytokine and free radical release, resulting in release of increased amounts of hepcidin, inappropriate erythropoietin levels or a hyporesponsiveness to erythropoietin, and decreased red blood cell survival time. Hepcidin binds to the iron export protein, ferroportin, located on the cell membranes of macrophages, hepatocytes, and enterocytes, and causes the trapping of iron within their cytoplasm. This results in a dysregulation of iron homeostasis and a functional iron deficiency (Gangat and Wolanskyj, 2013, Weiss and Goodnough, 2005). The stored iron remains inaccessible during haematopoiesis, making it a potential contributor to the non-regenerative anaemia observed during the early stages of *Babesia* infections. Haemosiderin pigment has been demonstrated in macrophages in the spleen, lymph nodes and within the hepatocytes and the Kupffer cells of the liver in ovine babesiosis (Marco et al., 2000, Habela et al., 1991), in the Kupffer cells of the liver in canine babesiosis (Wozniak et al., 1997), murine babesiosis (Hussein, 1977) and bovine babesiosis (Patarroyo et al., 1982), as well as within bone marrow macrophages in *B. rossi*-infected dogs (Bumby, 2022). Intracytoplasmic haemosiderin pigment within hepatocytes has also been observed in human malaria (Kochar et al., 2003b, Vannaphan, 2009). There are no reports of elevated haemosiderin pigment in the liver of sepsis patients. This implies that the observed increase in babesiosis cases is likely attributed to the significant haemolysis that takes place.

5.2 IMMUNOHISTOCHEMISTRY (IHC)

The study revealed a significant increase in mononuclear leucocytes throughout the infected livers, particularly monocyte-macrophages. Immunohistochemical staining using MAC387 demonstrated a 9.6-fold increase in monocyte-macrophages, and CD204 and Iba-1 stains confirmed the increase, showing 1.9-fold and 1.4-fold increases, respectively. Increased monocyte-macrophages have also been identified in the lung, spleen, bone marrow, and brain of *B.rossi*-infected dogs (Martin, 2020, Henning et al., 2020, Bumby, 2022, Lewis et al., 2022). Furthermore, myeloid lineage proliferation was observed in the bone marrow (Bumby, 2022), aligning with the inflammatory nature of the disease. The significant increase in Perl's Prussian blue positive staining correlated strongly with the labelled monocyte-macrophages.

5.2.1 Monocyte-macrophages

A significant increase in monocyte-macrophages was demonstrated in the infected cases compared to the controls. This increase is proposed to be cytokine-driven, as these cells form part of the innate immune system and are the first line of defense against invading parasites. The most significant increase was seen in the centrilobular areas of the CD204 and Iba-1 stains, while MAC387 showed its largest increase within the portal tracts. Among the monocyte-macrophage markers (CD204, Iba-1, and MAC387) used in the study, MAC387 showed the most significant increase and stained both circulating monocytes and Kupffer cells. This suggests that the higher number of circulating monocytes might be responsible for the notable MAC staining compared to the other markers.

MAC387 labels myeloid/histiocyte antigens expressed on circulating and tissue monocytes, reactive tissue macrophages and neutrophils, but not dendritic cells (Villiers et al., 2006b). Contrasting results as to whether or not MAC387 stains Kupffer cells have been reported (Rofina et al., 2003, McGuinness et al., 2000), however it did seem to stain Kupffer cells in this study. This IHC stain showed a 26.5-fold increase in the portal tracts of the infected cases compared to the controls, a 17-fold increase in the centrilobular areas, and an 8.6-fold increase in the midzonal areas. Increased numbers of positive cells were seen largely within the vasculature, with some increase in the perivascular and periductular interstitium. The presence of increased circulating monocytes above the reference interval on

complete blood counts (CBCs) was only a finding in 4/10 cases, arguing that the increase observed in the livers is predominantly due to an increase in hypertrophic Kupffer cells, or that there is some degree of sequestration of monocyte-macrophages within the organs after increased expression of a macrophage ligand on activated endothelium (Brown, 2017). Indeed, what happens at a tissue level may very not be reflected in circulating blood. The scarcity of neutrophils in the *B. rossi*-infected cases indicates that the rise in MAC387-positive (mononuclear) leucocytes in this study is likely caused by two factors. First, the recruitment of circulating monocyte-macrophages, stimulated by inflammatory cytokines, and second, hypertrophic Kupffer cells, found within the sinusoidal lumens (Nguyen-Lefebvre and Horuzsko, 2015). Low numbers of segmented neutrophils were also demonstrated within the bone marrow of *B. rossi*-infected dogs despite an increase in neutrophils in the peripheral blood counts (Bumby, 2022). Decreased amounts of IL-8 (a neutrophil chemoattractant (Bickel, 1993)) were also demonstrated in canine *B. rossi* (Goddard et al., 2016), indicating that neutrophils do not appear to play a dominant role in the solid tissues in *B. rossi* infections. However, neutrophils may very well still play a role in triggering inflammation through their neutrophil extracellular traps (NETs) as is observed in human malaria (Knackstedt et al., 2019).

Ionized calcium-binding adapter molecule 1, or Iba-1, is expressed specifically on resident and tissue macrophages and dendritic cells (Nakagawa et al., 2017), and has been associated with increased levels of TNF- α and IL-10, meaning that the cells that express this molecule are pro-inflammatory (Pisanu et al., 2014). The Iba-1 positive macrophages appeared significantly larger in the infected cases, suggesting an increase in reactivity. This has been demonstrated in cases of haemorrhage, acute ischaemic injury (Neri et al., 2018) and sepsis (Zrzavy et al., 2019).

The CD204 scavenger receptor, also known as scavenger receptor A (SRA) or macrophage scavenger receptor 1 (MSR1), is a cell surface receptor that is expressed predominantly on resident and tissue macrophages as well as dendritic cells (Kato et al., 2013a). It functions as a pattern recognition receptor (PRR) and binds to a large variety of ligands on gram-negative and -positive bacteria (Hampton et al., 1991, Dunne et al., 1994). CD204-positive cells are also implicated in clearing apoptotic bodies, preventing cellular lysis and release of harmful cellular contents, while also being associated with a lack of inflammatory cytokines, suggesting their non-inflammatory nature (Fadok et al., 2001). CD204-positive monocyte-macrophages are otherwise known as alternatively activated macrophages or suppression macrophages (Tomioka et al., 2012).

Macrophage activation can lead to four distinct outcomes: Classical activation through microbial phagocytosis, or alternative activation involving anti-inflammatory processes, wound repair, and fibrosis (Brown, 2017). Microbicidal processes are mediated by reactive oxygen species (ROS), nitric oxide (NO), interferon- α , - β , and - γ (IFN- α , - β and - γ) and lysosomal enzymes, while inflammation is mediated by IL-1, IL-12, IL-23 and chemokines. Transforming growth factor- β (TGF- β) and IL-10 mediate anti-inflammatory processes, whereas wound repair and fibrosis are facilitated by arginase, proline polyaminases, and TGF- β (Brown, 2017). Classical activation uses the monocyte-macrophages' ability to recognize cell surface- and cytosolic receptors on parasites or infected erythrocytes (Liehl and Mota, 2012, Stafford et al., 2002). When merozoites invade erythrocytes, they insert a parasite protein (also known as a pathogen-associated molecular pattern (PAMP)) into the surface of the erythrocyte. Monocyte-macrophages and dendritic cells recognize parasites or parasitized erythrocytes through their PRR or toll-like receptors (TLRs) that are activated directly by the PAMPs (Chua et al., 2013). Pathogen-associated molecular patterns (PAMPs) (such as glycosylphosphatidylinositol (GPI)) induce nitric oxide (NO) synthase expression and upregulate cell adhesion molecules on monocyte-macrophages and vascular endothelial cells (Tachado et al., 1996). Monocyte-macrophage Fc γ receptors are activated when engaged either by C3b fragment (deposition on the infected erythrocyte surface occurs with red cell infection), or by antibody recognition of infected erythrocytes. Phagocytosis of the infected erythrocytes or parasites is mediated either by

these opsonins (complement fragments or antibodies), or by non-opsonic phagocytosis which involves direct binding of the infected erythrocyte to the monocyte-macrophage by CD36 receptors. Non-opsonic phagocytosis is seen more frequently in individuals that lack antibodies against the invading parasite (Chua et al., 2013). Inflammatory cytokine responses differ between immune-naïve and immune individuals in human falciparum malaria, as TNF- α does not seem to be released when erythrocytes bind to monocyte-macrophage CD36 receptors, but it is released during Fc γ receptor phagocytosis (Ludlow et al., 2012). Increases in macrophage-associated cytokines and chemokines such as IL-10, IL-6 and MCP-1 have been demonstrated in *B. rossi* in previous studies (Goddard et al., 2016). These cytokines and expression of immunohistochemical markers highlight both the pro-inflammatory and anti-inflammatory roles that monocyte-macrophages play in *B. rossi*.

The greatest number of monocyte-macrophages occurred predominantly in the centrilobular zone, where they were clearly associated with reversibly and irreversibly injured hepatocytes. This is supportive of the hypoxic injury theory together with the release of inflammatory cytokines from activated Kupffer cells, damaged hepatocytes, and endothelial cells. This contributes to the strong inflammatory response initiating the recruitment of monocyte-macrophages. Macrophage-specific cytokines (such as TNF- α) have already been observed in large amounts in blood samples during the course of *B. rossi* infections and are associated with disease severity and outcome (Leisewitz et al., 2019a). These cytokines prime phagocytes for parasite clearance (Dobbs et al., 2020). Monocytes activated within lesions enter lymphatic vessels that drain into nearby lymph nodes via the afferent lymphatic vessels (Brown, 2017), possibly being a contributing factor to the distension of the spaces of Disse observed. Notably, in protozoal sepsis, monocyte-macrophage immunocytes play a dominant role in inflammation, while bacterial sepsis is characterized by tissue inflammation dominated by neutrophils. This suggests distinct drivers for haemoprotozoal sepsis (Brown et al., 2006).

A lack of correlation between the severity of anaemia and parasitaemia has been established, indicating the involvement of additional mechanisms in the destruction of erythrocytes beyond phagocytosis of parasitized erythrocytes alone (Dondorp et al., 1999, Schofield, 2007, Murase et al., 1996). Infected and uninfected erythrocytes have been shown to show decreased deformability in human malaria, decreased expression of complement regulatory proteins and increased opsonin deposition on the red blood cells. This would stimulate the already hyperactive monocyte-macrophages even further, leading to increased destruction of uninfected erythrocytes too (Kai and Roberts, 2008). *Babesia rossi* infections may potentially involve similar mechanisms of red cell destruction.

Tissue macrophage homeostasis is dependent on the influx of circulating monocytes, proliferation of recruited monocytes within tissue, and physiological apoptosis during cell turnover (Brown, 2017). Most tissue macrophages are formed prior to birth and continue to renew themselves throughout an individual's life (Ginhoux and Guillems, 2016, Perdiguero and Geissmann, 2016, Sheng et al., 2015). However during inflammatory conditions monocyte-macrophages exhibit migratory, chemotactic, pinocytic, and phagocytic behaviour (Brown, 2017). They also possess the capacity to replace depleted resident macrophages in the liver and spleen (Lai et al., 2018). Increases in monocyte-macrophages exhibiting increased erythrophagocytic activity have also been observed in cases of *B. gibsoni* in dogs perivascularly and within the central veins (Wozniak et al., 1997, Murase et al., 1996), as well as in murine babesiosis (Hussein, 1977) and human malaria (Cela et al., 2022). This argues for the presence of a parasite-induced hyperactivation (Wozniak et al., 1997).

5.2.2 Lymphocytes and plasma cells

The infected liver samples displayed increased numbers of lymphocytes compared to the control samples, as evidenced by an increase in cells positively labeled with CD3, CD20, and MUM-1 markers. The greatest increase in CD3-positive T-lymphocytes was seen in the midzonal areas within sinusoidal lumens. The greatest increase in CD20 and MUM-1-positive B-lymphocytes and plasma cells was seen in the centrilobular areas, mostly within the perivascular interstitium. CD20-positive B-lymphocytes and plasma cells were the only ones with median numbers higher than the normal range of cells in the entire liver, as established by the control samples.

A greater increase in CD20-positive cells compared to MUM-1-positive cells suggests that the majority of CD20-positive cells are B-lymphocytes in an earlier stage of differentiation. Similarly increased numbers of CD20-positive B-lymphocytes were observed within the bone marrow and lungs of *B. rossi*-infected dogs (Bumby, 2022, Martin, 2020), while no such changes were observed in the spleen (Henning et al., 2020). Like other protozoa, *Babesia* parasites most likely have the capability to influence the development and response of B-lymphocytes and antibodies during infection (Achtman et al., 2003).

B-lymphocytes are antigen-presenting cells and can also differentiate into immunoglobulin-producing plasma cells that can facilitate phagocytosis (Brown, 2017). T-lymphocytes regulate long-term cell-mediated immunity involving the adaptive immune response and antigen-specific memory T-cells whereas B-lymphocytes regulate humoral or antibody-dependent immunity. B-lymphocytes have been observed to play an important role in the initial phases of bacterial sepsis, being among the first cells to secrete cytokines. A lack of B-lymphocytes has been proven to result in decreased levels of cytokines and IFN-dependent chemokines with decreased host survival rates (Kelly-Scumpia et al., 2011). B-lymphocytes can either be activated by direct presentation of soluble antigens diffusing through lymphoid organs, or through activation by antigen presenting cells, including dendritic cells and macrophages. Macrophages have been proven to play an important role in the initiation of follicular B-lymphocyte responses (Batista and Harwood, 2009). A study investigating *Babesia bovis*, *Trypanosoma cruzi* and *T. brucei* confirmed that protozoal DNA is mitogenic for B-lymphocytes and stimulates macrophages to produce IL-12, TNF- α and NO (Shoda et al., 2001).

Complete blood counts (CBCs) for the infected cases showed lymphopaenia in three out of 10 cases, lymphocytosis in one case, and the remaining six cases had lymphocyte counts within the reference range. A decrease in peripheral/circulating CD3-positive lymphocytes seems to be a more common finding in complicated cases of babesiosis rather than uncomplicated cases (Rautenbach et al., 2017). This leads to the hypothesis that there may be functional immune suppression due to apoptosis, or a redistribution of the T-lymphocytes, or a combination of both (Rautenbach et al., 2017). An increase in CD3-positive lymphocytes was seen within the lungs of *B. rossi*-infected dogs (Martin, 2020), but a decrease was seen within the bone marrow (Bumby, 2022), and no change was noted within the spleen (Henning et al., 2020). Similar findings of increased numbers of T-lymphocytes within the sinusoidal lumens, and lymphocytes and plasma cells within the perivascular interstitium have been reported in the livers of *B. gibsoni* in dogs (Wozniak et al., 1997), *B. divergens* in rats (Dawoud, 2004), *B. microti* in rats (Okła et al., 2014b) and mice (Kuzna-Grygiel and Kolodziejczyk, 2000), *B. bovis* in calves (Everitt et al., 1986), and *Plasmodium berghei yoelii* infection in mice (Moran et al., 1973). It is not a common finding in cases of sepsis. The increase in CD3-positive T-lymphocytes in the lungs (and now the liver) suggests that lymphocyte redistribution might contribute to peripheral lymphopaenia (Martin, 2020). The higher density of sinusoidal T-lymphocytes in *B. gibsoni*-infected dogs' livers suggests hepatic recruitment and sequestration, likely mediated by chemokines and adhesion molecules produced by sinusoidal endothelial cells and Kupffer cells (Wozniak et al., 1997, Garcia-Barcina et al., 1995).

One study hypothesized that in *B. microti* infections in mice, the soluble antigens of the parasite surround the hepatocytes resulting in recruitment of lymphocytes, cytokine release and lysis of the hepatocytes (Kuzna-Grygiel and Kolodziejczyk, 2000). Another study comparing vaccinated and unvaccinated mice with the protozoan *Plasmodium yoelii* was performed. The results showed increased numbers of macrophages, neutrophils, lymphocytes, and plasma cells in unvaccinated mice livers, along with moderate centrilobular necrosis. In contrast, vaccinated mice exhibited even higher numbers of these cells, specifically plasma cells, but only mild centrilobular necrosis was observed (Dockrell et al., 1980). This supports the notion that local immunity in the liver plays a role in the inflammatory response observed. The increase in B-lymphocytes observed in our study, as well as their antigen-presenting ability is further evidence for the possibility of an antibody-related component in the immunity to haemoparasitic diseases.

Our study affirms that the alternative hypothesis is confirmed.

6. CONCLUSION

The liver is a very metabolically active, blood-rich and highly perfused organ that is clearly under stress during *Babesia rossi* infections. This organ plays a critical role in systemic energy metabolism, synthesis, and detoxification. Therefore, it has a high oxygen demand, and during *Babesia* infections it functions in an increasingly oxygen constrained and highly inflammatory environment. The histopathology of the liver in *B. rossi*-infected dogs is similar to that described in severe sepsis, malaria and other *Babesia* spp. infections. Increases in hepatic enzymes (specifically ALP, ALT, GGT) and metabolites of liver origin (urea cycle and conjugated bilirubin), the icteric mucous membrane colour, and hypoglycaemia observed in about a quarter of severely infected dogs all indicate severe hepatic stress. This stress was further confirmed on histology by dilation of the space of Disse due to oedema, ductular and canalicular cholestasis, bile and haemosiderin pigments present within hypertrophic Kupffer cells as well as within hepatocyte cytoplasm, congestion within the central veins and sinusoids, multifocal centrilobular necrosis, and EMH. This stress is likely due to haemolytic anaemia-associated hypoxia and the overwhelming systemic inflammatory response. The main change observed in *B. rossi*-infected dog livers is that of severe organ inflammation dominated by monocyte-macrophages and lymphocytes. This is supported by the increase in macrophage-associated cytokines and chemokines, such as IL-10, IL-6 and MCP-1 that has been shown in previous studies. It is likely that the hepatic inflammation is driven largely by the innate immune response and that this inflammation is responsible for significant collateral damage to the liver.

REFERENCES

- ABDULLAHI, S., MOHAMMED, A., TRIMNELL, A., SANNUSI, A. & ALAFIATAYO, R. 1990. Clinical and haematological findings in 70 naturally occurring cases of canine babesiosis. *Journal of Small Animal Practice*, 31, 145-147.
- ABO, T. & SEKIKAWA, H. 2002. Extrathymic T cells in malaria protection, including evidence for the onset of erythropoiesis in the liver during infection. *Archives of histology and cytology*, 65, 127-132.
- ABRO, A. H., USTADI, A. M., ABRO, H. A., ABDU, A. S., YOUNIS, N. J. & AKAILA, S. I. 2009. Jaundice with hepatic dysfunction in *P. falciparum* malaria. *J Coll Physicians Surg Pak*, 19, 363-6.
- ACHTMAN, A. H., KHAN, M., MACLENNAN, I. & LANGHORNE, J. 2003. *Plasmodium chabaudi chabaudi* infection in mice induces strong B cell responses and striking but temporary changes in splenic cell distribution. *The Journal of Immunology*, 171, 317-324.
- ADAMSON, J. W. 1988. Erythropoietin: in vitro and in vivo studies of the regulation of erythropoiesis. *Soc Gen Physiol Ser*, 43, 57-65.
- AHMED, J. 2002. The role of cytokines in immunity and immunopathogenesis of pirolasmoses. *Parasitology research*, 88, S48-S50.
- AL-SALAHY, M., SHNAWA, B., ABED, G., MANDOUR, A. & AL-EZZI, A. 2016. Parasitaemia and its relation to hematological parameters and liver function among patients malaria in Abs, Hajjah, Northwest Yemen. *Interdisciplinary perspectives on infectious diseases*, 2016.
- ALBERTYŃSKA, M., RUPIK, W., HERMYT, M., OKŁA, H. & JASIK, K. 2017. *Babesia Microti*—Known and Unknown Protists. *Global Journal of Zoology*, 1, 001-007.
- ALLEN, P. C., FRERICHS, W. M. & HOLBROOK, A. 1975. Experimental acute *Babesia caballi* infections: I. Red blood cell dynamics. *Experimental parasitology*, 37, 67-77.
- ANAND, A. C. & PURI, P. 2005. Jaundice in malaria. *Journal of gastroenterology and hepatology*, 20, 1322-1332.
- AREEKUL, S., SRICHAIRAT, S., CHURDCHU, K., YAMARAT, P. & VIRAVAN, C. 1980. Serum cholinesterase activity in patients with malaria infection. *Southeast Asian J Trop Med Public Health*, 11, 498-501.
- ARNAU-BARRÉS, I., GÜERRI-FERNÁNDEZ, R., LUQUE, S., SORLI, L., VÁZQUEZ, O. & MIRALLES, R. 2019. Serum albumin is a strong predictor of sepsis outcome in elderly patients. *European Journal of Clinical Microbiology & Infectious Diseases*, 38, 743-746.
- ARNOLD, B. J., TANGPUKDEE, N., KRUDSOOD, S. & WILAIRATANA, P. 2013. Risk factors of shock in severe falciparum malaria. *Southeast Asian Journal of Tropical Medicine and Public Health*, 44, 541.
- ASAKA, S., SHIBAYAMA, Y. & NAKATA, K. 1996. Pathogenesis of focal and random hepatocellular necrosis in endotoxemia: microscopic observation in vivo. *Liver*, 16, 183-187.
- ASPESTRAND, F., MATHISEN, Ø. & BERGAN, A. 1991. Perivascular low attenuation zone at CT of liver transplants: a follow-up study. *Acta Radiologica*, 32, 244-246.
- AVENANT, A., PARK, J. Y., VORSTER, I., MITCHELL, E. P. & ARENAS-GAMBOA, A. M. 2021. Porcine babesiosis caused by *babesia sp. suis* in a pot-bellied pig in South Africa. *Frontiers in Veterinary Science*, 7, 620462.
- AWANDARE, G. A., KEMPAIAH, P., OCHIEL, D. O., PIAZZA, P., KELLER, C. C. & PERKINS, D. J. 2011. Mechanisms of erythropoiesis inhibition by malarial pigment and malaria-induced proinflammatory mediators in an in vitro model. *American journal of hematology*, 86, 155-162.
- AYALA, A., O'NEILL, P. J., UEBELE, S. A., HERDON, C. D. & CHAUDRY, I. H. 1997. Mechanism of splenic immunosuppression during sepsis: key role of Kupffer cell mediators. *Journal of Trauma and Acute Care Surgery*, 42, 882-888.

- AYOUB, A. L., HACKNER, S. G. & PRITTE, J. 2010. Clinical management of canine babesiosis. *Journal of Veterinary Emergency and Critical Care*, 20, 77-89.
- BANCROFT, J. D. & GAMBLE, M. 2008. *Theory and practice of histological techniques*, Elsevier health sciences.
- BANKS, J., FOULIS, A., LEDINGHAM, I. & MACSWEEN, R. 1982. Liver function in septic shock. *Journal of Clinical Pathology*, 35, 1249-1252.
- BARNES, S., GALLO, G., TRASH, D. & MORRIS, J. 1975. Diagnostic value of serum bile acid estimations in liver disease. *Journal of clinical pathology*, 28, 506-509.
- BATISTA, F. D. & HARWOOD, N. E. 2009. The who, how and where of antigen presentation to B cells. *Nature Reviews Immunology*, 9, 15-27.
- BAUER, M., PRESS, A. T. & TRAUNER, M. 2013. The liver in sepsis: patterns of response and injury. *Current opinion in critical care*, 19, 123-127.
- BELL, P. 2020. *Normal Liver Histology 101* [Online]. Liver Fellow Network. Available: <https://liverfellow.org/post/normal-liver-histology-101> [Accessed 23 September 2022].
- BERNAL, W. 2016. The liver in systemic disease: Sepsis and critical illness. *Clinical Liver Disease*, 7, 88.
- BERRY, W. & REICHEN, J. 1983. Bile acid metabolism: its relation to clinical disease. *Seminars in Liver Disease*, 3, 330-340.
- BETJES, M. & BAJEMA, I. 2006. The pathology of jaundice-related renal insufficiency: cholemic nephrosis revisited. *Journal of nephrology*, 19, 229-233.
- BHALLA, A., SURI, V. & SINGH, V. 2006. Malarial hepatopathy. *Journal of postgraduate medicine*, 52, 315.
- BICKEL, M. 1993. The role of interleukin-8 in inflammation and mechanisms of regulation. *Journal of periodontology*, 64, 456-460.
- BIENZLE, D., KWIECIEN, J. & PARENT, J. 1995. Extramedullary hematopoiesis in the choroid plexus of five dogs. *Veterinary Pathology*, 32, 437-440.
- BILIĆ, P., KULEŠ, J., BARIĆ RAFAJ, R. & MRLJAK, V. 2018. Canine babesiosis: where do we stand. *Acta Vet.(Beograd)*, 68, 127-160.
- BILWAL, A., MANDALI, G. & TANDEL, F. 2018. Liver Enzyme Activity in Dogs Infected with *Babesia canis*. *Intas Polivet*, 19, 313-314.
- BINH, T., DAVIS, T., JOHNSTON, W., THU, L., BOSTON, R., DANH, P. & ANH, T. 1997. Glucose metabolism in severe malaria: minimal model analysis of the intravenous glucose tolerance test incorporating a stable glucose label. *Metabolism*, 46, 1435-1440.
- BLACKWELL, T. & CHRISTMAN, J. 1996. Sepsis and cytokines: current status. *British journal of anaesthesia*, 77, 110-117.
- BOCK, R., JACKSON, L., DE VOS, A. & JORGENSEN, W. 2004. Babesiosis of cattle. *Parasitology*, 129, S247-S269.
- BÖHM, M., LEISEWITZ, A. L., THOMPSON, P. N. & SCHOEMAN, J. P. 2006. Capillary and venous *Babesia canis rossi* parasitaemias and their association with outcome of infection and circulatory compromise. *Veterinary Parasitology*, 141, 18-29.
- BONE, R. C., SIBBALD, W. J. & SPRUNG, C. L. 1992. The ACCP-SCCM consensus conference on sepsis and organ failure. *Chest*, 101, 1481-1483.
- BOSMAN, A.-M., PENZHORN, B. L., BRAYTON, K. A., SCHOEMAN, T. & OOSTHUIZEN, M. C. 2019. A novel *Babesia* sp. associated with clinical signs of babesiosis in domestic cats in South Africa. *Parasites & vectors*, 12, 1-12.
- BOTTA, F., GIANNINI, E., ROMAGNOLI, P., FASOLI, A., MALFATTI, F., CHIARBONELLO, B., TESTA, E., RISSO, D., COLLA, G. & TESTA, R. 2003. MELD scoring system is useful for predicting prognosis in patients with liver cirrhosis and is correlated with residual liver function: a European study. *Gut*, 52, 134-139.
- BOWEN, R. 2020. *Pathophysiology of the Digestive System* [Online]. Available: http://www.vivo.colostate.edu/hbooks/pathphys/digestion/liver/histo_hcytes.html [Accessed 2 May 2022].

- BRAIN, J. D., MOLINA, R. M., DECAMP, M. M. & WARNER, A. E. 1999. Pulmonary intravascular macrophages: their contribution to the mononuclear phagocyte system in 13 species. *American Journal of Physiology-Lung Cellular and Molecular Physiology*, 276, L146-L154.
- BROWN, D. V. W., ARNOUD; CULLEN, M 2017. *Pathologic Basis of Veterinary Disease*, 3251 Riverport Lane, St. Louis, Missouri 63043, Elsevier.
- BROWN, K., BRAIN, S., PEARSON, J., EDGEWORTH, J., LEWIS, S. & TREACHER, D. 2006. Neutrophils in development of multiple organ failure in sepsis. *The Lancet*, 368, 157-169.
- BRUGUERA, M., ARANGUIBEL, F., ROS, E. & RODÉS, J. 1978. Incidence and clinical significance of sinusoidal dilatation in liver biopsies. *Gastroenterology*, 75, 474-478.
- BUMBY, M. M. 2022. *Cytological and histopathological bone marrow findings in dogs with natural Babesia rossi infection*. University of Pretoria.
- CALLERY, M. P., KAMEI, T. & FLYE, M. W. 1990. Kupffer cell blockade increases mortality during intra-abdominal sepsis despite improving systemic immunity. *Archives of Surgery*, 125, 36-41.
- CARVALLO, F. R. & STEVENSON, V. B. 2022. Interstitial pneumonia and diffuse alveolar damage in domestic animals. *Veterinary Pathology*, 59, 586-601.
- CELA, D., KNACKSTEDT, S. L., GROVES, S., RICE, C. M., KWON, J. T. W., MORDMÜLLER, B. & AMULIC, B. 2022. PAD4 controls chemoattractant production and neutrophil trafficking in malaria. *Journal of Leukocyte Biology*, 111, 1235-1242.
- CENARIU, D., ILUTA, S., ZIMTA, A.-A., PETRUSHEV, B., QIAN, L., DIRZU, N., TOMULEASA, C., BUMBEA, H. & ZAHARIE, F. 2021. Extramedullary hematopoiesis of the liver and spleen. *Journal of Clinical Medicine*, 10, 5831.
- CENTER, S., BALDWIN, B., DE LAHUNTA, A., DIETZE, A. & TENNANT, B. 1985. Evaluation of serum bile acid concentrations for the diagnosis of portosystemic venous anomalies in the dog and cat. *Journal of the American Veterinary Medical Association*, 186, 1090-1094.
- CENTER, S., SLATER, M., MANWARREN, T. & PRYMAK, K. 1992. Diagnostic efficacy of serum alkaline phosphatase and gamma-glutamyltransferase in dogs with histologically confirmed hepatobiliary disease: 270 cases (1980-1990). *Journal of the American Veterinary Medical Association*, 201, 1258-1264.
- CENTER, S. A. 2007. Interpretation of liver enzymes. *Veterinary Clinics of North America: Small Animal Practice*, 37, 297-333.
- CHAROENPAN, P., INDRAPRASIT, S., KIATBOONSRI, S., SUVACHITTANONT, O. & TANOMSUP, S. 1990. Pulmonary edema in severe falciparum malaria: hemodynamic study and clinicophysiological correlation. *Chest*, 97, 1190-1197.
- CHAUDHURI, S., VARSHNEY, J. & PATRA, R. 2008. Erythrocytic antioxidant defense, lipid peroxides level and blood iron, zinc and copper concentrations in dogs naturally infected with *Babesia gibsoni*. *Research in Veterinary Science*, 85, 120-124.
- CHAWLA, L., SIDHU, G., SABHARWAL, B., BHATIA, K. & SOOD, A. 1989. Jaundice in *Plasmodium falciparum*. *The Journal of the Association of Physicians of India*, 37, 390-391.
- CHIANG, J. Y. & FERRELL, J. M. 2018. Bile acid metabolism in liver pathobiology. *Gene expression*, 18, 71.
- CHUA, C. L. L., BROWN, G., HAMILTON, J. A., ROGERSON, S. & BOEUF, P. 2013. Monocytes and macrophages in malaria: protection or pathology? *Trends in parasitology*, 29, 26-34.
- CHUGHLAY, M. F., AKAKPO, S., ODEDRA, A., CSERMAK-RENNER, K., DJERIOU, E., WINNIPS, C., LEBoulLEUX, D., GAUR, A. H., SHANKS, G. D. & MCCARTHY, J. 2020. Liver enzyme elevations in *Plasmodium falciparum* volunteer infection studies: findings and recommendations. *The American journal of tropical medicine and hygiene*, 103, 378.
- CLARK, I. & JACOBSON, L. 1998. Do babesiosis and malaria share a common disease process? *Annals of Tropical Medicine & Parasitology*, 92, 483-488.
- COLLETT, M. 2000. Survey of canine babesiosis in South Africa. *Journal of the South African Veterinary Association*, 71, 180-186.
- CORNELIUS, C. E. 1980. Liver function. *Clinical biochemistry of domestic animals*. Elsevier.

- CRAWFORD, J. M. 1997. Cellular and molecular biology of the inflamed liver. *Current opinion in gastroenterology*, 13, 175-185.
- CRAWFORD, J. M. & BOYER, J. L. 1998. Clinicopathology conferences: Inflammation-induced cholestasis. *Hepatology*, 28, 253-260.
- CRAWFORD, P. C., LEVY, J. K. & WERNER, L. L. 2006. Evaluation of surrogate markers for passive transfer of immunity in kittens. *Journal of the American Veterinary Medical Association*, 228, 1038-1041.
- CRAY, C., ZAIAS, J. & ALTMAN, N. H. 2009. Acute phase response in animals: a review. *Comparative medicine*, 59, 517-526.
- CRNOGAJ, M., PETLEVSKI, R., MRLJAK, V., KIS, I., TORTI, M., KUCER, N., MATIJATKO, V., SACER, I. & STOKOVIC, I. 2010. Malondialdehyde levels in serum of dogs infected with *Babesia canis*. *Veterinárni medicína*, 55, 163-171.
- DAHAN, M. S., WILSON, R. F., LANGE, M. P., STONE, A. & JACOBS, L. A. 1990. Hepatic parenchymal oxygen tension following injury and sepsis. *Archives of Surgery*, 125, 441-443.
- DANIEL, S. & MARSHALL, M. 1999. Evaluation of the liver: laboratory tests. Schiff's diseases of the liver. *USA*, 205-239.
- DAS, B. 2003. 1. Changing Clinical Profile of Malaria. *Bioscience Reports*, 23.
- DAS, S., MOHAPATRA, B., MOHANTY, R., DASH, P., KAR, K. & DASH, P. 2007. Malarial hepatitis as a component of multiorgan failure--a bad prognostic sign. *Journal of the Indian Medical Association*, 105, 247-250.
- DASTE, T., LUCAS, M. N. & AUMANN, M. 2013. Cerebral babesiosis and acute respiratory distress syndrome in a dog. *Journal of veterinary emergency and critical care*, 23, 615-623.
- DAVIS, T., LOOAREESUWAN, S., PUKRITTAYAKAMEE, S., LEVY, J., NAGACHINTA, B. & WHITE, N. 1993. Glucose turnover in severe falciparum malaria. *Metabolism*, 42, 334-340.
- DAWOUD, H. 2004. Immunity of *Babesia divergens* in the rat. Histology of the infected liver and its possible role in removing PRBC's. *Journal of the Egyptian Society of Parasitology*, 34, 791-806.
- DAWSON, P. A. 2018. Bile formation and the enterohepatic circulation. *Physiology of the gastrointestinal tract*, 931-956.
- DAY, N. P., PHU, N. H., MAI, N. T. H., CHAU, T. T. H., LOC, P. P., VAN CHUONG, L., SINH, D. X., HOLLOWAY, P., HIEN, T. T. & WHITE, N. J. 2000. The pathophysiologic and prognostic significance of acidosis in severe adult malaria. *Critical care medicine*, 28, 1833-1840.
- DE GOPEGUI, R. R., PEÑALBA, B., GOICOA, A., ESPADA, Y., FIDALGO, L. E. & ESPINO, L. 2007. Clinicopathological findings and coagulation disorders in 45 cases of canine babesiosis in Spain. *The veterinary journal*, 174, 129-132.
- DE LAFORCADE, A. M., FREEMAN, L. M., SHAW, S. P., BROOKS, M. B., ROZANSKI, E. A. & RUSH, J. E. 2003. Hemostatic changes in dogs with naturally occurring sepsis. *Journal of Veterinary Internal Medicine*, 17, 674-679.
- DE VOS, A. A. P., F.T. 1994. *Infectious Diseases of Livestock with Special Reference to Southern Africa*, Cape Town, Oxford University Press.
- DE WAAL, D. 1992. Equine piroplasmiasis: a review. *British Veterinary Journal*, 148, 6-14.
- DEFAUW, P., DAMINET, S., LEISEWITZ, A. L., GODDARD, A., PAEPE, D., DUCHATEAU, L. & SCHOEMAN, J. P. 2018. Renal azotemia and associated clinical and laboratory findings in dogs with *Babesia rossi* infection. *Veterinary parasitology*, 260, 22-29.
- DEFAUW, P., MEYER, E., DUCHATEAU, L., SCHOEMAN, J. P., VAN DE MAELE, I. & DAMINET, S. 2017. Stability of glomerular and tubular renal injury biomarkers in canine urine after 4 years of storage. *Journal of veterinary diagnostic investigation*, 29, 346-350.
- DEFAUW, P., SCHOEMAN, J. P., LEISEWITZ, A. L., GODDARD, A., DUCHATEAU, L., ARESU, L., MEYER, E. & DAMINET, S. 2020. Evaluation of acute kidney injury in dogs with complicated or uncomplicated *Babesia rossi* infection. *Ticks and tick-borne diseases*, 11, 101406.

- DEFAUW, P., SCHOEMAN, J. P., SMETS, P., GODDARD, A., MEYER, E., LIEBENBERG, C. & DAMINET, S. 2012. Assessment of renal dysfunction using urinary markers in canine babesiosis caused by *Babesia rossi*. *Veterinary Parasitology*, 190, 326-332.
- DEFRANCES, M. C. & MICHALOPOULOS, G. K. 2011. Liver regeneration and partial hepatectomy: process and prototype. Walter de Gruyter GmbH & Co. KG, Berlin/Boston.
- DEVARBHAVI, H., ALVARES, J. F. & KUMAR, K. S. 2005. Severe falciparum malaria simulating fulminant hepatic failure. *Mayo Clinic Proceedings*, 80, 355-358.
- DEY, S., BINDU, S., GOYAL, M., PAL, C., ALAM, A., IQBAL, M. S., KUMAR, R., SARKAR, S. & BANDYOPADHYAY, U. 2012. Impact of intravascular hemolysis in Malaria on liver dysfunction involvement of hepatic free heme overload, NF- κ B activation, and neutrophil infiltration. *Journal of Biological Chemistry*, 287, 26630-26646.
- DKHIL, M., ABDEL-BAKI, A., AL-QURAIHY, S. & ABDEL-MONEIM, A. 2013. Hepatic oxidative stress in Mongolian gerbils experimentally infected with *Babesia divergens*. *Ticks and tick-borne diseases*, 4, 346-351.
- DKHIL, M., AL-QURAIHY, S. & ABDEL-BAKI, A. 2010. Hepatic tissue damage induced in *Meriones ungliculatus* due to infection with *Babesia divergens*-infected erythrocytes. *Saudi journal of biological sciences*, 17, 129-132.
- DOBBS, K. R., CRABTREE, J. N. & DENT, A. E. 2020. Innate immunity to malaria—the role of monocytes. *Immunological reviews*, 293, 8-24.
- DOCKRELL, H., DE SOUZA, J. & PLAYFAIR, J. 1980. The role of the liver in immunity to blood-stage murine malaria. *Immunology*, 41, 421.
- DONDORP, A. M., ANGUS, B., CHOTIVANICH, K., SILAMUT, K., RUANGVEERAYUTH, R., HARDEMAN, M. R., KAGER, P. A., VREEKEN, J. & WHITE, N. J. 1999. Red blood cell deformability as a predictor of anemia in severe falciparum malaria. *The American journal of tropical medicine and hygiene*, 60, 733-737.
- DUBOVA, O. & DUBOVIY, A. 2018. Hepathopathy and nephropathy in the dogs' babesiosis: pseudohepatorenal syndrome. *Scientific Messenger of Lviv National University of Veterinary Medicine and Biotechnologies*, 20, 102-107.
- DUFOUR, D. R., LOTT, J. A., NOLTE, F. S., GRETCH, D. R., KOFF, R. S. & SEEFF, L. B. 2000. Diagnosis and monitoring of hepatic injury. I. Performance characteristics of laboratory tests. *Clinical chemistry*, 46, 2027-2049.
- DUMAN, A., AKOZ, A., KAPCI, M., TURE, M., ORUN, S., KARAMAN, K. & TURKDOGAN, K. A. 2016. Prognostic value of neglected biomarker in sepsis patients with the old and new criteria: predictive role of lactate dehydrogenase. *The American journal of emergency medicine*, 34, 2167-2171.
- DUNN, G. 1973. The liver in congestive heart failure: a review. *Am J Med Sci*, 265, 174-189.
- DUNNE, D. W., RESNICK, D., GREENBERG, J., KRIEGER, M. & JOINER, K. A. 1994. The type I macrophage scavenger receptor binds to gram-positive bacteria and recognizes lipoteichoic acid. *Proceedings of the National Academy of Sciences*, 91, 1863-1867.
- DURAIYAN, J., GOVINDARAJAN, R., KALIYAPPAN, K. & PALANISAMY, M. 2012. Applications of immunohistochemistry. *Journal of pharmacy & bioallied sciences*, 4, S307.
- DURILA, M., BRONSKÝ, J., HARUŠTIK, T., PAZDRO, A., PECHOVÁ, M. & CVACHOVEC, K. 2012. Early diagnostic markers of sepsis after oesophagectomy (including thromboelastography). *Bmc Anesthesiology*, 12, 1-7.
- DVIR, E., LOBETTI, R. G., JACOBSON, L. S., PEARSON, J. & BECKER, P. J. 2004. Electrocardiographic changes and cardiac pathology in canine babesiosis. *Journal of Veterinary Cardiology*, 6, 15-23.
- EBERT, E. C. Hypoxic liver injury. *Mayo Clinic Proceedings*, 2006. Elsevier, 1232-1236.
- EGGINTON, S. & GAFFNEY, E. 2010. Experimental Physiology—Review Article: Tissue capillary supply—it's quality not quantity that counts! *Experimental physiology*, 95, 971-979.

- EHIEM, R. C., NANSE, F. A. K., ADU-FRIMPONG, M. & MILLS-ROBERTSON, F. C. 2021. Parasitaemia estimation and prediction of hepatocellular dysfunction among Ghanaian children with acute malaria using haemoglobin levels. *Heliyon*, 7, e07445.
- EICHENBERGER, R. M., RAMAKRISHNAN, C., RUSSO, G., DEPLAZES, P. & HEHL, A. B. 2017. Genome-wide analysis of gene expression and protein secretion of *Babesia canis* during virulent infection identifies potential pathogenicity factors. *Scientific reports*, 7, 1-14.
- EICHENBERGER, R. M., RIOND, B., WILLI, B., HOFMANN-LEHMANN, R. & DEPLAZES, P. 2016. Prognostic markers in acute *Babesia canis* infections. *Journal of Veterinary Internal Medicine*, 30, 174-182.
- ELIAS, R., JOHNSTON, M., HAYASHI, A. & NELSON, W. 1987. Decreased lymphatic pumping after intravenous endotoxin administration in sheep. *American Journal of Physiology-Heart and Circulatory Physiology*, 253, H1349-H1357.
- ESMAEILNEJAD, B., DALIR-NAGHADEH, B., TAVASSOLI, M., ASRI-REZAEI, S., MAHMOUDI, S., RAJABI, S., ALIGOLZADEH, A., AKBARI, H. & MORVARIDI, A. 2021. Assessment of hepatic oxidative damage, paraoxonase-1 activity, and lipid profile in cattle naturally infected with *Babesia bigemina*. *Tropical Animal Health and Production*, 53, 1-8.
- ESMAEILNEJAD, B., TAVASSOLI, M., SAMIEI, A., ABBASI, A., SHAFIPOUR, A. & ESMAEILNEJAD, N. 2018. Histopathological changes and oxidative damage in hepatic tissue of rats experimentally infected with *Babesia bigemina*. *Polish journal of veterinary sciences*, 517-524.
- ESMON, C. T., FUKUDOME, K., MATHER, T., BODE, W., REGAN, L. M., STEARNS-KUROSAWA, D. J. & KUROSAWA, S. 1999. Inflammation, sepsis, and coagulation. *Haematologica*, 84, 254-259.
- EVANS, T. J. 2013. Small Animal Toxicology (Third Edition). In: MICHAEL E. PETERSON, P. A. T. (ed.) *Toxicokinetics and Toxicodynamics*.
- EVERITT, J., SHADDUCK, J., STEINKAMP, C. & CLABAUGH, G. 1986. Experimental *Babesia bovis* infection in Holstein calves. *Veterinary pathology*, 23, 556-562.
- FADOK, V. A., BRATTON, D. L. & HENSON, P. M. 2001. Phagocyte receptors for apoptotic cells: recognition, uptake, and consequences. *The Journal of clinical investigation*, 108, 957-962.
- FAUSTO, N., CAMPBELL, J. S. & RIEHLE, K. J. 2006. Liver regeneration. *Hepatology*, 43, S45-S53.
- FERRER, L., FONDEVILA, D., RABANAL, R., TARRES, J. & RAMIS, A. 1993. Immunohistochemical detection of CD3 antigen (pan T marker) in canine lymphomas. *J Vet Diagn Invest*, 5, 616-20.
- FITZPATRICK, J., KENNEDY, C. C., MCGEOWN, M. G., OREOPOULOS, D., ROBERTSON, J. & SOYANNWO, M. 1969. Further details of third recorded case of redwater (babesiosis) in man. *Br Med J*, 4, 768-772.
- FONTA, C., NÉGYESSY, L., RENAUD, L. & BARONE, P. 2004. Areal and subcellular localization of the ubiquitous alkaline phosphatase in the primate cerebral cortex: evidence for a role in neurotransmission. *Cerebral Cortex*, 14, 595-609.
- FRANK, P. G., WOODMAN, S. E., PARK, D. S. & LISANTI, M. P. 2003. Caveolin, caveolae, and endothelial cell function. *Arteriosclerosis, thrombosis, and vascular biology*, 23, 1161-1168.
- FRIEDMAN, S., MARTIN, P. & MUNOZ, J. 2003. Laboratory evaluation of the patient with liver disease. *Hepatology, a textbook of liver disease. Philadelphia*, 661-709.
- FURLANELLO, T., FIORIO, F., CALDIN, M., LUBAS, G. & SOLANO-GALLEGO, L. 2005. Clinicopathological findings in naturally occurring cases of babesiosis caused by large form *Babesia* from dogs of northeastern Italy. *Veterinary parasitology*, 134, 77-85.
- FURUKAWA, M., KINOSHITA, K., YAMAGUCHI, J., HORI, S. & SAKURAI, A. 2019. Sepsis patients with complication of hypoglycemia and hypoalbuminemia are an early and easy identification of high mortality risk. *Internal and emergency medicine*, 14, 539-548.
- FUTTER, G., BELONJE, PC, VAN DEN BERG, A. & VAN RIJSWIJK, A. 1981. Studies on feline babesiosis. 4 Chemical pathology; macroscopic and microscopic post mortem findings. *Journal of the South African Veterinary Association*, 52, 15-14.

- GANGAT, N. & WOLANSKYJ, A. P. Anemia of chronic disease. *Seminars in hematology*, 2013. Elsevier, 232-238.
- GARCIA-BARCINA, M., LUKOMSKA, B., GAWRON, W., WINNOCK, M., VIDAL-VANACLOCHA, F., BIOULAC-SAGE, P., BALABAUD, C. & OLSZEWSKI, W. 1995. Expression of cell adhesion molecules on liver-associated lymphocytes and their ligands on sinusoidal lining cells in patients with benign or malignant liver disease. *The American journal of pathology*, 146, 1406.
- GATTA, A., VERARDO, A. & BOLOGNESI, M. 2012. Hypoalbuminemia. *Internal and emergency medicine*, 7, 193-199.
- GAYNOR, E. 1973. The role of granulocytes in endotoxin-induced vascular injury. *Blood*, 41, 797-808.
- GEIER, A., FICKERT, P. & TRAUNER, M. 2006. Mechanisms of disease: mechanisms and clinical implications of cholestasis in sepsis. *Nature clinical practice Gastroenterology & hepatology*, 3, 574-585.
- GIANNINI, E. G., TESTA, R. & SAVARINO, V. 2005. Liver enzyme alteration: a guide for clinicians. *Cmaj*, 172, 367-379.
- GIBSON, P. & DUDLEY, F. 1984. Ischemic hepatitis: clinical features, diagnosis and prognosis. *Australian and New Zealand journal of medicine*, 14, 822-825.
- GILLES, H., MAEGRAITH, B. & ANDREWS, W. 1953. The liver in *Babesia canis* infection. *Annals of tropical medicine and parasitology*, 47, 426.
- GINHOUX, F. & GUILLIAMS, M. 2016. Tissue-resident macrophage ontogeny and homeostasis. *Immunity*, 44, 439-449.
- GITLIN, N. & SERIO, K. M. 1992. Ischemic hepatitis: widening horizons. *American Journal of Gastroenterology (Springer Nature)*, 87, 831-836.
- GODDARD, A., LEISEWITZ, A. L., KJELGAARD-HANSEN, M., KRISTENSEN, A. T. & SCHOEMAN, J. P. 2016. Excessive pro-inflammatory serum cytokine concentrations in virulent canine babesiosis. *PLoS one*, 11, e0150113.
- GODDARD, A., WIINBERG, B., SCHOEMAN, J. P., KRISTENSEN, A. T. & KJELGAARD-HANSEN, M. 2013. Mortality in virulent canine babesiosis is associated with a consumptive coagulopathy. *The Veterinary Journal*, 196, 213-217.
- GOLJAN, J., NAHORSKI, W., FELCZAK-KORZYBSKA, I., GORSKI, J. & MYJAK, P. 2000. Liver injury in the course of malaria. *International maritime health*, 51, 30-39.
- GÓMEZ SELGAS, A., BEXFIELD, N., SCASE, T. J., HOLMES, M. A. & WATSON, P. 2014. Total serum bilirubin as a negative prognostic factor in idiopathic canine chronic hepatitis. *Journal of Veterinary Diagnostic Investigation*, 26, 246-251.
- GOTO, Y., BAEZ, S. & ORKIN, L. 1981. The effect of endotoxin on microcirculatory and lymphatic dynamics in the rat (Shwartzman phenomenon). *Circulatory Shock*, 8, 533-542.
- GRÄSER, T., VEDERNIKOV, Y. & LI, D. 1990. Study on the mechanism of carbon monoxide induced endothelium-independent relaxation in porcine coronary artery and vein. *Biomedica biochimica acta*, 49, 293-296.
- GRAY, J., ZINTL, A., HILDEBRANDT, A., HUNFELD, K.-P. & WEISS, L. 2010. Zoonotic babesiosis: overview of the disease and novel aspects of pathogen identity. *Ticks and tick-borne diseases*, 1, 3-10.
- GREEN, R. M., WHITING, J. F., ROSENBLUTH, A. B., BEIER, D. & GOLLAN, J. L. 1994. Interleukin-6 inhibits hepatocyte taurocholate uptake and sodium-potassium-adenosinetriphosphatase activity. *American Journal of Physiology-Gastrointestinal and Liver Physiology*, 267, G1094-G1100.
- GROENEVELD, A. J., BRONSVELD, W. & THIJIS, L. G. 1986. Hemodynamic determinants of mortality in human septic shock. *Surgery*, 99, 140-153.
- GUO, H., SEVINC, F., CEYLAN, O., SEVINC, M., INCE, E., GAO, Y., MOUMOUNI, P. F. A., LIU, M., EFSTRATIOU, A. & WANG, G. 2017. A PCR survey of vector-borne pathogens in different dog populations from Turkey. *Acta parasitologica*, 62, 533-540.

- GUPTA, S., SEYDEL, K., MIRANDA-ROMAN, M. A., FEINTUCH, C. M., SAIDI, A., KIM, R. S., BIRBECK, G. L., TAYLOR, T. & DAILY, J. P. 2017. Extensive alterations of blood metabolites in pediatric cerebral malaria. *PLoS One*, 12, e0175686.
- HABELA, M., REINA, D., NAVARRETE, I., REDONDO, E. & HERNANDEZ, S. 1991. Histopathological changes in sheep experimentally infected with *Babesia ovis*. *Veterinary parasitology*, 38, 1-12.
- HAMID, O. A., RADWAN, M. & ALI, A. F. 2014. Biochemical changes associated with babesiosis infested cattle. *J Appl Chem*, 7, 87-92.
- HAMPTON, R. Y., GOLENBOCK, D. T., PENMAN, M., KRIEGER, M. & RAETZ, C. R. 1991. Recognition and plasma clearance of endotoxin by scavenger receptors. *Nature*, 352, 342-344.
- HAN, D.-W. 2002. Intestinal endotoxemia as a pathogenetic mechanism in liver failure. *World Journal of Gastroenterology*, 8, 961.
- HANK, A., HOFFMANN, W., SANECKI, R., SCHAEFFER, D. & DORNER, J. 1993. Quantitative determination of equine alkaline phosphatase isoenzymes in foal and adult serum. *Journal of Veterinary Internal Medicine*, 7, 20-24.
- HARRIS, H. 1990. The human alkaline phosphatases: what we know and what we don't know. *Clinica chimica acta*, 186, 133-150.
- HEMMER, R. M., FERRICK, D. A. & CONRAD, P. A. 2000. Role of T cells and cytokines in fatal and resolving experimental babesiosis: protection in TNFRp55^{-/-} mice infected with the human *Babesia* WA1 parasite. *Journal of Parasitology*, 86, 736-742.
- HEMMER, R. M., WOZNIAK, E. J., LOWENSTINE, L. J., PLOPPER, C. G., WONG, V. & CONRAD, P. A. 1999. Endothelial cell changes are associated with pulmonary edema and respiratory distress in mice infected with the WA1 human *Babesia* parasite. *The Journal of parasitology*, 479-489.
- HENNING, A., CLIFT, S. J. & LEISEWITZ, A. L. 2020. The pathology of the spleen in lethal canine babesiosis caused by *Babesia rossi*. *Parasite immunology*, 42, e12706.
- HERBECK, R., TEODORESCU BRÎNZEU, D., GIUBELAN, M., LAZĂR, E., DEMA, A. & IONIȚĂ, H. 2011. B-cell transcription factors Pax-5, Oct-2, BOB. 1, Bcl-6, and MUM1 are useful markers for the diagnosis of nodular lymphocyte predominant Hodgkin lymphoma. *Rom J Morphol Embryol*, 52, 69-74.
- HERRMANN, F. R., SAFRAN, C., LEVKOFF, S. E. & MINAKER, K. L. 1992. Serum albumin level on admission as a predictor of death, length of stay, and readmission. *Archives of internal medicine*, 152, 125-130.
- HILL, K. R., RHODES, K., STAFFORD, J. L. & AUB, R. 1953. Serous hepatitis: a pathogenesis of hepatic fibrosis in Jamaican children. *British medical journal*, 1, 117.
- HIRATA, K., IKEDA, S., HONMA, T., MITAKA, T., FURUHATA, T., KATSURAMAKI, T., HATA, F. & MUKAIYA, M. 2001. Sepsis and cholestasis: basic findings in the sinusoid and bile canaliculus. *Journal of hepato-biliary-pancreatic surgery*, 8, 20-26.
- HOEKSTRA, L. T., DE GRAAF, W., NIBOURG, G. A., HEGER, M., BENNINK, R. J., STIEGER, B. & VAN GULIK, T. M. 2013. Physiological and biochemical basis of clinical liver function tests: a review. *Annals of surgery*, 257, 27-36.
- HOMER, M. J., AGUILAR-DELFIN, I., TELFORD III, S. R., KRAUSE, P. J. & PERSING, D. H. 2000. Babesiosis. *Clinical microbiology reviews*, 13, 451-469.
- HORIUCHI, S., KAMIMOTO, Y. & MORINO, Y. 1985. Hepatic clearance of rat liver aspartate aminotransferase isozymes: evidence for endocytotic uptake via different binding sites on sinusoidal liver cells. *Hepatology*, 5, 376-382.
- HUSSEIN, H. 1977. The pathology of *Babesia hylomyisci* infection in mice: I. Clinical signs and liver lesion. *Journal of comparative pathology*, 87, 161-167.
- HUSSEIN, H. S. 1982. The bone marrow response during *Babesia hylomyisci* and *Babesia microti* infections in mice. *Journal of Comparative Pathology*, 92, 613-620.

- IANCU, T. C. 1992. Ferritin and hemosiderin in pathological tissues. *Electron microscopy reviews*, 5, 209-229.
- IGNATIUS, C. M., EMEKA, E. N. & BLESSING, N. E. 2008. Effect of malaria parasitaemia on liver enzyme tests. *Int J Trop Med*, 3, 49-52.
- IRIZARRY-ROVIRA, A. R., STEPHENS, J., CHRISTIAN, J., KJEMTRUP, A., DENICOLA, D. B., WIDMER, W. R. & CONRAD, P. A. 2001. *Babesia gibsoni* infection in a dog from Indiana. *Veterinary Clinical Pathology*, 30, 180-188.
- IRWIN, P. & HUTCHINSON, G. 1991. Clinical and pathological findings of *Babesia* infection in dogs. *Australian Veterinary Journal*, 68, 204-209.
- IWASASHI, H., SUZUKI, M., UNNO, M., UTIYAMA, T., OIKAWA, M., KONDO, N. & MATSUNO, S. 2003. Inhibition of heme oxygenase ameliorates sepsis-induced liver dysfunction in rats. *Surgery today*, 33, 30-38.
- JACOBSON, L. & CLARK, I. 1994. The Pathophysiology of Canine Babesiosis: New Approaches to an Old Puzzle. *Journal of the South African Veterinary Association*, 65, 134-145.
- JACOBSON, L. & LOBETTI, R. 1996. Rhabdomyolysis as a complication of canine babesiosis. *Journal of small animal practice*, 37, 286-291.
- JACOBSON, L. S. 2006. The South African form of severe and complicated canine babesiosis: clinical advances 1994–2004. *Veterinary parasitology*, 138, 126-139.
- JACOBSON, L. S. & LOBETTI, R. G. 2005. Glucose, lactate, and pyruvate concentrations in dogs with babesiosis. *American journal of veterinary research*, 66, 244-250.
- JAESCHKE, H. 2011. Reactive oxygen and mechanisms of inflammatory liver injury: present concepts. *Journal of gastroenterology and hepatology*, 26, 173-179.
- JALOVECKA, M., SOJKA, D., ASCENCIO, M. & SCHNITTGER, L. 2019. *Babesia* life cycle—when phylogeny meets biology. *Trends in parasitology*, 35, 356-368.
- JAYASHANKAR, C., PINNELLI, V. & PRABHU, R. 2016. Alteration of coagulation profile in malaria patients and its correlation with degree of parasitemia: a prospective study. *International Journal of Advances in Medicine*, 3, 388.
- JENNISKENS, M., LANGOUCHE, L., VANWIJNGAERDEN, Y.-M., MESOTTEN, D. & VAN DEN BERGHE, G. 2016. Cholestatic liver (dys) function during sepsis and other critical illnesses. *Intensive care medicine*, 42, 16-27.
- JHA, S., SHRESTHA, S., GOLE, S. G. & DEEP, G. 2014. Assessment of serum bilirubin and hepatic enzymes in malaria patients. *Int J of Biomed & Adv Res*, 5, 160-162.
- JOHNS, J. & CHRISTOPHER, M. M. 2012. Extramedullary hematopoiesis: a new look at the underlying stem cell niche, theories of development, and occurrence in animals. *Veterinary pathology*, 49, 508-523.
- JOHNSTON, D. E. 1999. Special considerations in interpreting liver function tests. *American family physician*, 59, 2223.
- JOVANOVIĆ, P., ŽORIĆ, L., STEFANOVIĆ, I., DŽUNIĆ, B., DJORDJEVIĆ-JOCIĆ, J., RADENKOVIĆ, M. & JOVANOVIĆ, M. 2010. Lactate dehydrogenase and oxidative stress activity in primary open-angle glaucoma aqueous humour. *Bosnian journal of basic medical sciences*, 10, 83.
- JUBALA, C., WOJCIESZYN, J., VALLI, V., GETZY, D., FOSMIRE, S., COFFEY, D., BELLGRAU, D. & MODIANO, J. 2005. CD20 expression in normal canine B cells and in canine non-Hodgkin lymphoma. *Veterinary Pathology Online*, 42, 468-476.
- JUNGERMANN, K. 1988. Metabolic zonation of liver parenchyma. *Seminars in liver disease*, 8, 329-341.
- JUNGERMANN, K. & KIETZMANN, T. 2000. Oxygen: modulator of metabolic zonation and disease of the liver. *Hepatology*, 31, 255-260.
- KAI, O. K. & ROBERTS, D. J. 2008. The pathophysiology of malarial anaemia: where have all the red cells gone? *BMC medicine*, 6, 1-4.

- KAMIMOTO, Y., HORIUCHI, S., TANASE, S. & MORINO, Y. 1985. Plasma clearance of intravenously injected aspartate aminotransferase isozymes: evidence for preferential uptake by sinusoidal liver cells. *Hepatology*, 5, 367-375.
- KATO, Y., MURAKAMI, M., HOSHINO, Y., MORI, T., MARUO, K., HIRATA, A., NAKAGAWA, T., YANAI, T. & SAKAI, H. 2013a. The class A macrophage scavenger receptor CD204 is a useful immunohistochemical marker of canine histiocytic sarcoma. *Journal of comparative pathology*, 148, 188-196.
- KATO, Y., MURAKAMI, M., HOSHINO, Y., MORI, T., MARUO, K., HIRATA, A., NAKAGAWA, T. L., YANAI, T. & SAKAI, H. 2013b. The class A macrophage scavenger receptor CD204 is a useful immunohistochemical marker of canine histiocytic sarcoma. *J Comp Pathol*, 148, 188-96.
- KAUSHANSKY, K. 2016. *Williams hematology*, McGraw-Hill Education.
- KELLER, N., JACOBSON, L. S., NEL, M., DE CLERQ, M., THOMPSON, P. N. & SCHOEMAN, J. P. 2004. Prevalence and risk factors of hypoglycemia in virulent canine babesiosis. *Journal of Veterinary Internal Medicine*, 18, 265-270.
- KELLY-SCUMPIA, K. M., SCUMPIA, P. O., WEINSTEIN, J. S., DELANO, M. J., CUENCA, A. G., NACIONALES, D. C., WYNN, J. L., LEE, P. Y., KUMAGAI, Y. & EFRON, P. A. 2011. B cells enhance early innate immune responses during bacterial sepsis. *Journal of Experimental Medicine*, 208, 1673-1682.
- KETTNER, F., REYERS, F. & MILLER, D. 2003. Thrombocytopaenia in canine babesiosis and its clinical usefulness. *Journal of the South African Veterinary Association*, 74, 63-68.
- KIETZMANN, T. 2017. Metabolic zonation of the liver: The oxygen gradient revisited. *Redox biology*, 11, 622-630.
- KINASEWITZ, G. T., ZEIN, J. G., LEE, G. L., NAZIR, S. A. & TAYLOR JR, F. B. 2005. Prognostic value of a simple evolving disseminated intravascular coagulation score in patients with severe sepsis. *Critical care medicine*, 33, 2214-2221.
- KNACKSTEDT, S. L., GEORGIADOU, A., APEL, F., ABU-ABED, U., MOXON, C. A., CUNNINGTON, A. J., RAUPACH, B., CUNNINGHAM, D., LANGHORNE, J. & KRÜGER, R. 2019. Neutrophil extracellular traps drive inflammatory pathogenesis in malaria. *Science immunology*, 4, eaaw0336.
- KOCHAR, D., AGARWAL, P., KOCHAR, S., JAIN, R., RAWAT, N., POKHARNA, R., KACHHAWA, S. & SRIVASTAVA, T. 2003a. Hepatocyte dysfunction and hepatic encephalopathy in *Plasmodium falciparum* malaria. *Qjm*, 96, 505-512.
- KOCHAR, D., SINGH, P., AGARWAL, P., KOCHAR, S., POKHARNA, R. & SAREEN, P. 2003b. Malarial hepatitis. *JOURNAL-ASSOCIATION OF PHYSICIANS OF INDIA*, 51, 1069-1076.
- KONTO, M., BIU, A., AHMED, M., MBAYA, A. & LUKA, J. 2014. Clinico-biochemical responses of dogs to experimental infection with *Babesia canis*. *Veterinary World*, 7, 113-118.
- KOSKINAS, J., GOMATOS, I. P., TINIAKOS, D. G., MEMOS, N., BOUTSIKOU, M., GARATZIOTI, A., ARCHIMANDRITIS, A. & BETROSIAN, A. 2008. Liver histology in ICU patients dying from sepsis: a clinico-pathological study. *World journal of gastroenterology: WJG*, 14, 1389.
- KÖSTER, L. S., LOBETTI, R. G. & KELLY, P. 2015. Canine babesiosis: a perspective on clinical complications, biomarkers, and treatment. *Veterinary medicine: research and reports*, 6, 119.
- KOSTER, L. S., SCHOEMAN, J. P., STEINER, J. M. & SUCHODOLSKI, J. S. 2015. Serum canine pancreatic-specific lipase concentrations in dogs with naturally occurring *Babesia rossi* infection. *Journal of the South African Veterinary Association*, 86, 1-7.
- KÖSTER, L. S., VAN SCHOOR, M., GODDARD, A., THOMPSON, P. N., MATJILA, P. T. & KJELGAARD-HANSEN, M. 2009. C-reactive protein in canine babesiosis caused by *Babesia rossi* and its association with outcome. *Journal of the South African Veterinary Association*, 80, 87-91.
- KOVALOVICH, K., DEANGELIS, R. A., LI, W., FURTH, E. E., CILIBERTO, G. & TAUB, R. 2000. Increased toxin-induced liver injury and fibrosis in interleukin-6-deficient mice. *Hepatology*, 31, 149-159.

- KOZAT, S. & SEPEHRIZADEH, E. 2017. Methods of diagnosing in liver diseases for dog and cats. *Türk Bilimsel Derlemeler Dergisi*, 10, 36-46.
- KRAJE, A. C. 2001. Canine haemobartonellosis and babesiosis. *COMPENDIUM ON CONTINUING EDUCATION FOR THE PRACTISING VETERINARIAN-NORTH AMERICAN EDITION*, 23, 310-319.
- KRAUSE, P. J., DAILY, J., TELFORD, S. R., VANNIER, E., LANTOS, P. & SPIELMAN, A. 2007. Shared features in the pathobiology of babesiosis and malaria. *Trends in parasitology*, 23, 605-610.
- KRAUSE, P. J., MCKAY, K., GADBAW, J., CHRISTIANSON, D., CLOSTER, L., LEPORÉ, T., TELFORD, S. R., 3RD, SIKAND, V., RYAN, R., PERSING, D., RADOLF, J. D., SPIELMAN, A. & TICK-BORNE INFECTION STUDY, G. 2003. Increasing health burden of human babesiosis in endemic sites. *The American journal of tropical medicine and hygiene*, 68, 431-6.
- KRISHNAN, A. & KARNAD, D. R. 2003. Severe falciparum malaria: an important cause of multiple organ failure in Indian intensive care unit patients. *Critical care medicine*, 31, 2278-2284.
- KUČER, N., MATIJATKO, V., KIŠ, I., GRDEN, D., BRKLAČIĆ, M., FORŠEK, J., ŽVORC, Z. & BARIĆ RAFAJ, R. 2008. White blood cell count and neutrophil to lymphocyte ratio in uncomplicated and complicated canine babesiosis caused by *Babesia canis canis*. *Veterinarski arhiv*, 78, 321-330.
- KULEŠ, J., DE TORRE-MINGUELA, C., RAFAJ, R. B., GOTIĆ, J., NIŽIĆ, P., CERON, J. & MRLJAK, V. 2016. Plasma biomarkers of SIRS and MODS associated with canine babesiosis. *Research in Veterinary Science*, 105, 222-228.
- KULEŠ, J., MRLJAK, V., RAFAJ, R. B., SELANEC, J., BURCHMORE, R. & ECKERSALL, P. D. 2014. Identification of serum biomarkers in dogs naturally infected with *Babesia canis canis* using a proteomic approach. *BMC veterinary research*, 10, 1-10.
- KUTZLER, M. A., SOLTER, P. F., HOFFMAN, W. E. & VOLKMANN, D. H. 2003. Characterization and localization of alkaline phosphatase in canine seminal plasma and gonadal tissues. *Theriogenology*, 60, 299-306.
- KUZNA-GRYGIEL, W. & KOŁODZIEJCZYK, L. 2000. Studies of liver of mice in the course of an experimental infection with *Babesia microti*. I: Histopathological changes and changes in the glycogen content. *The Journal of Protozoology Research*, 10, 14-23.
- LAI, S. M., SHENG, J., GUPTA, P., RENIA, L., DUAN, K., ZOLEZZI, F., KARJALAINEN, K., NEWELL, E. W. & RUEDL, C. 2018. Organ-specific fate, recruitment, and refilling dynamics of tissue-resident macrophages during blood-stage malaria. *Cell reports*, 25, 3099-3109. e3.
- LALA, V., ZUBAIR, M. & MINTER, D. 2022. Liver function tests. *StatPearls*.
- LAUTT, W. W. 1977. Hepatic vasculature: a conceptual review. *Gastroenterology*, 73, 1163-1169.
- LEFKOWITZ, J. H. 2004. Histological assessment of cholestasis. *Clinics in Liver Disease*, 8, 27-40.
- LEIBY, D. A. 2011. Transfusion-transmitted *Babesia* spp.: bull's-eye on *Babesia microti*. *Clinical microbiology reviews*, 24, 14-28.
- LEISEWITZ, A., GODDARD, A., DE GIER, J., VAN ENGELSHOVEN, J., CLIFT, S., THOMPSON, P. & SCHOEMAN, J. P. 2019a. Disease severity and blood cytokine concentrations in dogs with natural *Babesia rossi* infection. *Parasite immunology*, 41, e12630.
- LEISEWITZ, A., GUTHRIE, AJ & BERRY, W. 1996. Evaluation of the effect of whole-blood transfusion on the oxygen status and acid-base balance of *Babesia canis* infected dogs using the oxygen status algorithm. *Journal of the South African Veterinary Association*, 67, 20-26.
- LEISEWITZ, A. L., GODDARD, A., CLIFT, S., THOMPSON, P. N., DE GIER, J., VAN ENGELSHOVEN, J. M. & SCHOEMAN, J. P. 2019b. A clinical and pathological description of 320 cases of naturally acquired *Babesia rossi* infection in dogs. *Veterinary parasitology*, 271, 22-30.
- LEISEWITZ, A. L., JACOBSON, L. S., DE MORAIS, H. S. & REYERS, F. 2001. The mixed acid-base disturbances of severe canine babesiosis. *Journal of Veterinary Internal Medicine*, 15, 445-452.
- LEONARD N, E. K. 2021. *Liver and Intrahepatic Bile Ducts* [Online]. PathologyOutlines.com website. Available: <https://www.pathologyoutlines.com/topic/livernormalhistology.html>. [Accessed 23 September 2022].

- LESCOT, T., KARVELLAS, C., BEAUSSIER, M., MAGDER, S. & RIOU, B. 2012. Acquired liver injury in the intensive care unit. *The Journal of the American Society of Anesthesiologists*, 117, 898-904.
- LEWIS, M., LEISEWITZ, A. L. & CLIFT, S. J. 2022. *Histopathology of cerebral babesiosis in dogs with naturally acquired Babesia rossi infection*. MMedVet (Path), University of Pretoria.
- LI, M., CAI, S.-Y. & BOYER, J. L. 2017a. Mechanisms of bile acid mediated inflammation in the liver. *Molecular aspects of medicine*, 56, 45-53.
- LI, P., HE, K., LI, J., LIU, Z. & GONG, J. 2017b. The role of Kupffer cells in hepatic diseases. *Molecular immunology*, 85, 222-229.
- LIEHL, P. & MOTA, M. M. 2012. Innate recognition of malarial parasites by mammalian hosts. *International journal for parasitology*, 42, 557-566.
- LIMAYE, C. S., LONDHEY, V. A. & NABAR, S. 2012. The study of complications of vivax malaria in comparison with falciparum malaria in Mumbai. *The Journal of the Association of Physicians of India*, 60, 15-18.
- LIMDI, J. & HYDE, G. 2003. Evaluation of abnormal liver function tests. *Postgraduate medical journal*, 79, 307-312.
- LOBETTI, R., DVIR, E. & PEARSON, J. 2002. Cardiac troponins in canine babesiosis. *Journal of Veterinary Internal Medicine*, 16, 63-68.
- LOBETTI, R. & JACOBSON, L. 2001. Renal involvement in dogs with babesiosis. *Journal of the South African Veterinary Association*, 72, 23-28.
- LOBETTI, R., REYERS, F. & NESBIT, J. 1996. The comparative role of haemoglobinaemia and hypoxia in the development of canine babesial nephropathy. *Journal of the South African Veterinary Association*, 67, 188-198.
- LOSERT, H., SCHMID, K., WILFING, A., WINKLER, S., STAUDINGER, T., KLETZMAYR, J. & BURGMANN, H. 2000. Experiences with severe *P. falciparum* malaria in the intensive care unit. *Intensive care medicine*, 26, 195-201.
- LU, J., WEI, Z., JIANG, H., CHENG, L., CHEN, Q., CHEN, M., YAN, J. & SUN, Z. 2018. Lactate dehydrogenase is associated with 28-day mortality in patients with sepsis: a retrospective observational study. *Journal of Surgical Research*, 228, 314-321.
- LUDLOW, L. E., ZHOU, J., TIPPETT, E., CHENG, W.-J., HASANG, W., ROGERSON, S. J. & JAWOROWSKI, A. 2012. HIV-1 inhibits phagocytosis and inflammatory cytokine responses of human monocyte-derived macrophages to *P. falciparum* infected erythrocytes. *PloS one*, 7, e32102.
- LUSTER, M. I., GERMOLEC, D. R., YOSHIDA, T., KAYAMA, F. & THOMPSON, M. 1994. Endotoxin-induced cytokine gene expression and excretion in the liver. *Hepatology*, 19, 480-488.
- LUTZ, J., HENRICH, H. & BAUEREISEN, E. 1975. Oxygen supply and uptake in the liver and the intestine. *Pflügers Archiv*, 360, 7-15.
- MADRID, L., LANASPA, M., MACULUVE, S. A. & BASSAT, Q. 2015. Malaria-associated hypoglycaemia in children. *Expert review of anti-infective therapy*, 13, 267-277.
- MAEGRAITH, B., GILLES, H. & DEVAKUL, K. 1957. Pathological Processes in *Babesia canis* Infections. *Zeitschrift für Tropenmedizin und Parasitologie*, 8, 485-514.
- MAHONEY, D., WRIGHT, I., FRERICHS, W., GROENENDYK, S., O'SULLIVAN, B., ROBERTS, M. & WADDELL, A. 1977. The identification of *Babesia equi* in Australia. *Australian veterinary journal*, 53, 461-464.
- MALHERBE, W. 1965. Clinico-pathological studies of *Babesia canis* infection in dogs, IV. The effect on bilirubin metabolism. *Journal of the South African Veterinary Association*, 36, 569-572.
- MANTHORPE, E. M., JERRETT, I. V., RAWLIN, G. T. & WOOLFORD, L. 2020. Plant and fungal hepatotoxicities of cattle in australia, with a focus on minimally understood toxins. *Toxins*, 12, 707.
- MARCO, I., VELARDE, R., CASTELLÀ, J., FERRER, D. & LAVÍN, S. 2000. Presumptive *Babesia ovis* infection in a spanish ibex (*Capra pyrenaica*). *Veterinary parasitology*, 87, 217-221.
- MARIK, P. E. & RAGHAVAN, M. 2004. Stress-hyperglycemia, insulin and immunomodulation in sepsis. *Intensive care medicine*, 30, 748-756.

- MARTIN, C. A. 2020. *Pathology of complicated Babesia rossi-associated acute lung injury and respiratory distress syndrome in dogs*. University of Pretoria.
- MARX, G. 2003. Fluid therapy in sepsis with capillary leakage. *European journal of anaesthesiology*, 20, 429-442.
- MASUDA, M., OTSUKA-YAMASAKI, Y., SHIRANAGA, N., IGUCHI, A., UCHIDA, N., SATO, R. & YAMASAKI, M. 2019. Retrospective study on intercurrent pancreatitis with *Babesia gibsoni* infection in dogs. *Journal of Veterinary Medical Science*, 81, 1558-1563.
- MÁTHÉ, Á. 2006. Clinicopathological alterations in canine babesiosis.
- MATHE, A., VÖRÖS, K., NÉMETH, T., BIKSI, I., HETYEY, C., MANCZUR, F. & TEKES, L. 2006. Clinicopathological changes and effect of imidocarb therapy in dogs experimentally infected with *Babesia canis*. *Acta Veterinaria Hungarica*, 54, 19-33.
- MATHEWS, S. E., BHAGWATI, M. M. & AGNIHOTRI, V. 2019. Clinical spectrum of *Plasmodium vivax* infection, from benign to severe malaria: A tertiary care prospective study in adults from Delhi, India. *Tropical Parasitology*, 9, 88.
- MATIJATKO, V., KIŠ, I., TORTI, M., BRKLIJAČIĆ, M., KUČER, N., RAFAJ, R. B., GRDEN, D., ŽIVIČNJAK, T. & MRLJAK, V. 2009. Septic shock in canine babesiosis. *Veterinary parasitology*, 162, 263-270.
- MATIJATKO, V., MRLJAK, V., KIŠ, I., KUČER, N., FORŠEK, J., ŽIVIČNJAK, T., ROMIĆ, Ž., ŠIMEC, Z. & CERON, J. J. 2007. Evidence of an acute phase response in dogs naturally infected with *Babesia canis*. *Veterinary Parasitology*, 144, 242-250.
- MATIJATKO, V., TORTI, M. & SCHETTERS, T. P. 2012. Canine babesiosis in Europe: how many diseases? *Trends in parasitology*, 28, 99-105.
- MATJILA, P. T., LEISEWITZ, A. L., JONGEJAN, F. & PENZHORN, B. L. 2008. Molecular detection of tick-borne protozoal and ehrlichial infections in domestic dogs in South Africa. *Veterinary parasitology*, 155, 152-157.
- MAVROMMATIS, A. C., THEODORIDIS, T., ORFANIDOU, A., ROUSSOS, C., CHRISTOPOULOU-KOKKINO, V. & ZAKYNTHINOS, S. 2000. Coagulation system and platelets are fully activated in uncomplicated sepsis. *Critical care medicine*, 28, 451-457.
- MAXIE, M. G., JUBB, K., KENNEDY, P. & PALMER, N. 2007. *Judd, Kennedy, and Palmer's pathology of domestic animals*, Elsevier Saunders.
- MCCOWEN, K. C., MALHOTRA, A. & BISTRAN, B. R. 2001. Stress-induced hyperglycemia. *Critical care clinics*, 17, 107-124.
- MCGUINNESS, P., PAINTER, D., DAVIES, S. & MCCAUGHAN, G. 2000. Increases in intrahepatic CD68 positive cells, MAC387 positive cells, and proinflammatory cytokines (particularly interleukin 18) in chronic hepatitis C infection. *Gut*, 46, 260-269.
- MCINTYRE, N. 2008. *Textbook of hepatology: from basic science to clinical practice*, John Wiley & Sons.
- MCINTYRE, N. & ROSALKI, S. 1992. Biochemical investigations in the management of liver disease. In: PRIETO, J., RODÉS, J., SHAFRITZ, D.A. (ed.) *Hepatobiliary diseases*. Berlin, Heidelberg: Springer.
- MENG, X.-J., QIU, B.-A., LI, X.-J. & SONG, X.-H. 1992. The role of Kupffer cells in the development of hepatic dysfunction during sepsis. *Chinese Medical Journal*, 105, 34-38.
- MICHALOPOULOS, G. K. 2007. Liver regeneration. *Journal of cellular physiology*, 213, 286-300.
- MICHALOPOULOS, G. K. & BHUSHAN, B. 2021. Liver regeneration: biological and pathological mechanisms and implications. *Nature reviews Gastroenterology & hepatology*, 18, 40-55.
- MILNE, E. M. 1985. The diagnostic value of alkaline phosphatase in canine medicine: a review. *Journal of Small Animal Practice*, 26, 267-278.
- MILNER, J. D., OREKOV, T., WARD, J. M., CHENG, L., TORRES-VELEZ, F., JUNTILA, I., SUN, G., BULLER, M., MORRIS, S. C. & FINKELMAN, F. D. 2010. Sustained IL-4 exposure leads to a novel pathway for hemophagocytosis, inflammation, and tissue macrophage accumulation. *Blood, The Journal of the American Society of Hematology*, 116, 2476-2483.

- MIZOCK, B. A. 1995. Alterations in carbohydrate metabolism during stress: a review of the literature. *The American journal of medicine*, 98, 75-84.
- MOHAPATRA, M. K., BEHERA, A. K., KARUA, P. C., BARIHA, P. K., RATH, A., AGRAWAL, K. C., NAHAK, S. R. & GUDAGANATTI, S. S. 2016. Urinary bile casts in bile cast nephropathy secondary to severe falciparum malaria. *Clinical Kidney Journal*, 9, 644-648.
- MOHR, A., LOBETTI, R. & VAN DER LUGT, J. 2000. Acute pancreatitis: a newly recognised potential complication of canine babesiosis. *Journal of the South African Veterinary Association*, 71, 232-239.
- MOLYNEUX, M. E., LOOAREESUWAN, S., MENZIES, I. S., GRAINGER, S. L., PHILLIPS, R. E., WATTANAGOON, Y., THOMPSON, R. & WARRELL, D. A. 1989. Reduced hepatic blood flow and intestinal malabsorption in severe falciparum malaria. *The American journal of tropical medicine and hygiene*, 40, 470-476.
- MONGA, S. P. 2020. No zones left behind: democratic hepatocytes contribute to liver homeostasis and repair. *Cell Stem Cell*, 26, 2-3.
- MOORE, P. F., ROSSITTO, P. & DANILENKO, D. 1990. Canine leukocyte integrins: characterization of a CD 18 homologue. *Tissue antigens*, 36, 211-220.
- MORAN, C., DE RIVERA, V. S. & TURK, J. 1973. The immunological significance of histological changes in the spleen and liver in mouse malaria. *Clinical and Experimental Immunology*, 13, 467.
- MORITA, T., PERRELLA, M. A., LEE, M.-E. & KOUREMBANAS, S. 1995. Smooth muscle cell-derived carbon monoxide is a regulator of vascular cGMP. *Proceedings of the National Academy of Sciences*, 92, 1475-1479.
- MORTERS, M. K., ARCHER, J., MA, D., MATTHEE, O., GODDARD, A., LEISEWITZ, A. L., MATJILA, P. T., WOOD, J. L. & SCHOEMAN, J. P. 2020. Long-term follow-up of owned, free-roaming dogs in South Africa naturally exposed to *Babesia rossi*. *International journal for parasitology*, 50, 103-110.
- MUFTUOGLU, M., AKTEKIN, A., OZDEMIR, N. C. & SAGLAM, A. 2006. Liver injury in sepsis and abdominal compartment syndrome in rats. *Surgery today*, 36, 519-524.
- MURASE, T., UEDA, T., YAMATO, O., TAJIMA, M. & MAEDE, Y. 1996. Oxidative damage and enhanced erythrophagocytosis in canine erythrocytes infected with *Babesia gibsoni*. *Journal of Veterinary Medical Science*, 58, 259-261.
- NAKAGAWA, T., OHNISHI, K., KOSAKI, Y., SAITO, Y., HORLAD, H., FUJIWARA, Y., TAKEYA, M. & KOMOHARA, Y. 2017. Optimum immunohistochemical procedures for analysis of macrophages in human and mouse formalin fixed paraffin-embedded tissue samples. *Journal of clinical and experimental hematopathology*, 57, 31-36.
- NALPAS, B., VASSAULT, A., CHARPIN, S., LACOUR, B. & BERTHELOT, P. 1986. Serum mitochondrial aspartate aminotransferase as a marker of chronic alcoholism: diagnostic value and interpretation in a liver unit. *Hepatology*, 6, 608-614.
- NAYYAR, R., HURLEY, R., GOTO, M. & ZELLER, W. 1989. Microvascular endothelium: a major target site of endotoxin induced injury in 10 day old rat. *Journal of experimental pathology*, 4, 57-67.
- NEL, M., LOBETTI, R. G., KELLER, N. & THOMPSON, P. N. 2004. Prognostic value of blood lactate, blood glucose, and hematocrit in canine babesiosis. *Journal of Veterinary Internal Medicine*, 18, 471-476.
- NERI, M., FRATI, A., TURILLAZZI, E., CANTATORE, S., CIPOLLONI, L., DI PAOLO, M., FRATI, P., LA RUSSA, R., MAIESE, A. & SCOPETTI, M. 2018. Immunohistochemical evaluation of aquaporin-4 and its correlation with CD68, IBA-1, HIF-1 α , GFAP, and CD15 expressions in fatal traumatic brain injury. *International journal of molecular sciences*, 19, 3544.
- NGUYEN-LEFEBVRE, A. T. & HORUZSKO, A. 2015. Kupffer cell metabolism and function. *Journal of enzymology and metabolism*, 1.
- NICHOLSON, J., WOLMARANS, M. & PARK, G. 2000. The role of albumin in critical illness. *British journal of anaesthesia*, 85, 599-610.

- NIEMINEN, A. L., BYRNE, A. M., HERMAN, B. & LEMASTERS, J. J. 1997. Mitochondrial permeability transition in hepatocytes induced by t-BuOOH: NAD (P) H and reactive oxygen species. *American Journal of Physiology-Cell Physiology*, 272, C1286-C1294.
- O'MALLEY, D. P. 2007. Benign extramedullary myeloid proliferations. *Modern Pathology*, 20, 405-415.
- OKAS, A., KOWALCZYK, J., STEIN, R., LEE, D. & BERKELHAMMER, C. 2001. Hypoxic hepatitis related to profound anemia: how low can you go? *The American journal of gastroenterology*, 96, 3445.
- OKŁA, H., JASIK, K. P., SŁODKI, J., ROZWADOWSKA, B., SŁODKI, A., JURZAK, M. & PIERZCHAA, E. 2014a. Hepatic tissue changes in rats due to chronic invasion of *Babesia microti*. *Folia Biologica (Kraków)*, 62, 353-359.
- OKŁA, H., JASIK, K. P., SŁODKI, J., ROZWADOWSKA, B., SŁODKI, A., JURZAK, M. & PIERZCHAA, E. 2014b. Hepatic tissue changes in rats due to chronic invasion of *Babesia microti*. *Folia Biologica*, 62, 353-359.
- ONG, J. P., AGGARWAL, A., KRIEGER, D., EASLEY, K. A., KARAFI, M. T., VAN LENTE, F., ARROLIGA, A. C. & MULLEN, K. D. 2003. Correlation between ammonia levels and the severity of hepatic encephalopathy. *The American journal of medicine*, 114, 188-193.
- ONO, T., YAMAGUCHI, Y., NAKASHIMA, H., NAKASHIMA, M., ISHIKIRIYAMA, T., SEKI, S. & KINOSHITA, M. 2021. Lipopolysaccharide preconditioning augments phagocytosis of malaria-parasitized red blood cells by bone marrow-derived macrophages in the liver, thereby increasing the murine survival after *Plasmodium yoelii* infection. *Infection and Immunity*, 89, e00249-21.
- ONYESOM, I. & ONYEMAKONOR, N. 2011. Levels of parasitaemia and changes in some liver enzymes among malarial infected patients in Edo-Delta Region of Nigeria. *Curr Res J Biol Sci*, 3, 78-81.
- OSWARI, H., WIDJAJA, R. K., ROHSISWATMO, R. & CLEGHORN, G. 2013. Prognostic value of biochemical liver parameters in neonatal sepsis-associated cholestasis. *Journal of paediatrics and child health*, 49, E6-E11.
- OTSUKA, H., YAGI, H., ENDO, Y., NONAKA, N. & NAKAMURA, M. 2011. Kupffer cells support extramedullary erythropoiesis induced by nitrogen-containing bisphosphonate in splenectomized mice. *Cellular Immunology*, 271, 197-204.
- OYEWOLE, I., SENUSIE, S. & MANSARAY, M. 2010. *Plasmodium falciparum*-induced kidney and liver dysfunction in malaria patients in Freetown, Sierra Leone. *Sierra Leone Journal of Biomedical Research*, 2, 70-74.
- OZ, H. S. & WESTLUND, K. H. 2012. "Human babesiosis": an emerging transfusion dilemma. *International journal of hepatology*, 2012.
- PARDINI, A. D. 2010. *The pathology and pathogenesis of canine cerebral babesiosis*. University of Pretoria.
- PASTOR, C. M. & SUTER, P. M. 1999. Hepatic hemodynamics and cell functions in human and experimental sepsis. *Anesthesia & Analgesia*, 89, 344-352.
- PATARROYO, J., VARGAS, M. & BICUDO, P. 1982. Description of lesions in cattle in a natural outbreak of *Babesia bovis* infection in Brazil. *Veterinary parasitology*, 11, 301-308.
- PATEL, J. J., TANEJA, A., NICCUM, D., KUMAR, G., JACOBS, E. & NANCHAL, R. 2015. The association of serum bilirubin levels on the outcomes of severe sepsis. *Journal of intensive care medicine*, 30, 23-29.
- PENZHORN, B. L. 2011. Why is Southern African canine babesiosis so virulent? An evolutionary perspective. *Parasites & vectors*, 4, 1-6.
- PERDIGUERO, E. G. & GEISSMANN, F. 2016. The development and maintenance of resident macrophages. *Nature immunology*, 17, 2-8.
- PISANU, A., LECCA, D., MULAS, G., WARDAS, J., SIMBULA, G., SPIGA, S. & CARTA, A. R. 2014. Dynamic changes in pro-and anti-inflammatory cytokines in microglia after PPAR- γ agonist neuroprotective treatment in the MPTP mouse model of progressive Parkinson's disease. *Neurobiology of disease*, 71, 280-291.

- PLESSIER, A., DENNINGER, M. H., CONSIGNY, Y., PESSIONE, F., FRANCOZ, C., DURAND, F., FRANQUE, S., BEZEAUD, A., CHAUVELOT-MOACHON, L. & LEBREC, D. 2003. Coagulation disorders in patients with cirrhosis and severe sepsis. *Liver international*, 23, 440-448.
- PLUMMER, M. P. & DEANE, A. M. 2016. Dysglycemia and glucose control during sepsis. *Clinics in chest medicine*, 37, 309-319.
- POSTIC, C., DENTIN, R. & GIRARD, J. 2004. Role of the liver in the control of carbohydrate and lipid homeostasis. *Diabetes & metabolism*, 30, 398-408.
- POTGIETER, F. & ELS, H. 1979. An electron microscopic study of intra-erythrocytic stages of *Babesia bovis* in the brain capillaries of infected splenectomized calves. *Onderstepoort Journal of Veterinary Research*, 46.
- PRATT, D. S. & KAPLAN, M. M. 2000. Evaluation of abnormal liver-enzyme results in asymptomatic patients. *New England Journal of Medicine*, 342, 1266-1271.
- PRINS, M., SCHELLENS, C., VAN LEEUWEN, M., ROTHUIZEN, J. & TESKE, E. 2010. Coagulation disorders in dogs with hepatic disease. *The Veterinary Journal*, 185, 163-168.
- PUPIN, R. C., DE CASTRO GUIZELINI, C., DE LEMOS, R. A. A., MARTINS, T. B., DE ALMEIDA BORGES, F., BORGES, D. G. L. & GOMES, D. C. 2019. Retrospective study of epidemiological, clinical and pathological findings of bovine babesiosis in Mato Grosso do Sul, Brazil (1995–2017). *Ticks and tick-borne diseases*, 10, 36-42.
- RADICHEVA, M. 2011. Comparative evaluation of iron overload in patients with chronic liver disease. *Trakia Journal of Sciences*, 9, 10-16.
- RAFAJ, R., MATIJATKO, V., KIŠ, I., KUČER, N., ŽIVIČNJAK, T., LEMO, N., ŽVORC, Z., BRKLAČIĆ, M. & MRLJAK, V. 2009. Alterations in some blood coagulation parameters in naturally occurring cases of canine babesiosis. *Acta Veterinaria Hungarica*, 57, 295-304.
- RAMOS-VARA, J. & MILLER, M. 2014. When tissue antigens and antibodies get along: revisiting the technical aspects of immunohistochemistry—the red, brown, and blue technique. *Veterinary pathology*, 51, 42-87.
- RASKIN, R. & VALENCIANO, A. 2000. Cytochemistry of normal leukocytes. *Schalm's veterinary hematology*, 337-346.
- RAUTENBACH, Y., GODDARD, A., THOMPSON, P. N., MELLANBY, R. J. & LEISEWITZ, A. L. 2017. A flow cytometric assessment of the lymphocyte immunophenotypes in dogs naturally infected with *Babesia rossi*. *Veterinary parasitology*, 241, 26-34.
- RAUTENBACH, Y., SCHOEMAN, J. & GODDARD, A. 2018. Prevalence of canine *Babesia* and *Ehrlichia* co-infection and the predictive value of haematology. *Onderstepoort Journal of Veterinary Research*, 85, 1-5.
- RAWSON, J. & ACHORD, J. 1985. Shock liver. *Southern medical journal*, 78, 1421-1425.
- REDDY, B. S., SIVAJOTHI, S., REDDY, L. V. & RAJU, K. S. 2016. Clinical and laboratory findings of *Babesia* infection in dogs. *Journal of Parasitic Diseases*, 40, 268-272.
- REES, P. & SCHOEMAN, J. P. 2008. Plasma insulin concentrations in hypoglycaemic dogs with *Babesia canis rossi* infection. *Veterinary parasitology*, 152, 60-66.
- REJ, R. 1989. Aminotransferases in disease. *Clinics in laboratory medicine*, 9, 667-687.
- REYERS, F., LEISEWITZ, A., LOBETTI, R., MILNER, R., JACOBSON, L. & VAN ZYL, M. 1998. Canine babesiosis in South Africa: more than one disease. Does this serve as a model for falciparum malaria? *Annals of Tropical Medicine & Parasitology*, 92, 503-511.
- RING, A. & STREMMEL, W. The hepatic microvascular responses to sepsis. *Seminars in thrombosis and hemostasis*, 2000. Copyright© 2000 by Thieme Medical Publishers, Inc., 333 Seventh Avenue, New York, NY 10017, 589-594.
- ROBERT J. WASHBAU, M. J. D. 2013. Liver. In: ROBERT J. WASHBAU, M. J. D. (ed.) *Canine and Feline Gastroenterology*. St. Louis, Missouri 63043: Elsevier Saunders.
- ROBERTS, E. 1962. Equine piroplasmiasis. *J. Am. Vet. Med. Assoc.*, 141, 1323-1329.
- ROBERTS, H. R. & CEDERBAUM, A. I. 1972. The liver and blood coagulation: physiology and pathology. *Gastroenterology*, 63, 297-320.

- ROBERTS, R. A., GANEY, P. E., JU, C., KAMENDULIS, L. M., RUSYN, I. & KLAUNIG, J. E. 2007. Role of the Kupffer cell in mediating hepatic toxicity and carcinogenesis. *Toxicological Sciences*, 96, 2-15.
- ROFINA, J., ANDEL, I. V., VAN EDEREN, A., PAPAIOANNOU, N., YAMAGUCHI, H. & GRUYS, E. 2003. Canine counterpart of senile dementia of the Alzheimer type: amyloid plaques near capillaries but lack of spatial relationship with activated microglia and macrophages. *Amyloid*, 10, 86-96.
- ROTH JR, E. 1990. *Plasmodium falciparum* carbohydrate metabolism: a connection between host cell and parasite. *Blood cells*, 16, 453-60; discussion 461.
- ROTHUIZEN, J., VAN DEN BROM, W. E. & FEVERY, J. 1992. The origins and kinetics of bilirubin in dogs with hepatobiliary and haemolytic diseases. *Journal of hepatology*, 15, 17-24.
- ROTHUIZEN, J. & VAN DEN INGH, T. 1988. Covalently protein-bound bilirubin conjugates in cholestatic disease of dogs. *American Journal of Veterinary Research*, 49, 702-704.
- RUPANI, A. & AMARAPURKAR, A. 2009. Hepatic changes in fatal malaria: an emerging problem. *Annals of Tropical Medicine & Parasitology*, 103, 119-127.
- SAARI, S., NÄREAHO, A. & NIKANDER, S. 2018. *Canine Parasites and Parasitic Diseases*, San Diego, United States, Academic Press.
- SADAHIRA, Y. & MORI, M. 1999. Role of the macrophage in erythropoiesis. *Pathology international*, 49, 841-848.
- SAINI, P., PEAVY, G., HAUSER, D. & SAINI, S. 1978. Diagnostic evaluation of canine serum alkaline phosphatase by immunochemical means and interpretation of results. *American Journal of Veterinary Research*, 39, 1514-1518.
- SAINI, P. & SAINI, S. 1978. Origin of serum alkaline phosphatase in the dog. *American Journal of Veterinary Research*, 39, 1510-1513.
- SARDINHA, L. R., MOSCA, T., ELIAS, R. M., DO NASCIMENTO, R. S., GONÇALVES, L. A., BUCCI, D. Z., MARINHO, C. R. F., PENHA-GONÇALVES, C., LIMA, M. R. D. I. & ÁLVAREZ, J. M. 2010. The liver plays a major role in clearance and destruction of blood trypomastigotes in *Trypanosoma cruzi* chronically infected mice. *PLoS Negl Trop Dis*, 4, e578.
- SCHERF, A., LOPEZ-RUBIO, J. J. & RIVIERE, L. 2008. Antigenic variation in *Plasmodium falciparum*. *Annual review of microbiology*, 62, 445-470.
- SCHETTERS, T. P. & ELING, W. 1999. Can *Babesia* infections be used as a model for cerebral malaria? *Parasitology today*, 15, 492-497.
- SCHETTERS, T. P., KLEUSKENS, J., VAN DE CROMMERT, J., DE LEEUW, P., FINIZIO, A.-L. & GORENFLOT, A. 2009. Systemic inflammatory responses in dogs experimentally infected with *Babesia canis*; a haematological study. *Veterinary parasitology*, 162, 7-15.
- SCHEUER, P. J. & LEFKOWITZ, J. H. 2005. *Liver biopsy interpretation*, Saunders Limited.
- SCHLAEGER, R., HAUX, P. & KATTERMANN, R. 1982. Studies on the mechanism of the increase in serum alkaline phosphatase activity in cholestasis: significance of the hepatic bile acid concentration for the leakage of alkaline phosphatase from rat liver. *Enzyme*, 28, 3-13.
- SCHLEICHER, J., TOKARSKI, C., MARBACH, E., MATZ-SOJA, M., ZELLMER, S., GEBHARDT, R. & SCHUSTER, S. 2015. Zonation of hepatic fatty acid metabolism—the diversity of its regulation and the benefit of modeling. *Biochimica et Biophysica Acta (BBA)-Molecular and Cell Biology of Lipids*, 1851, 641-656.
- SCHNITTGER, L., RODRIGUEZ, A. E., FLORIN-CHRISTENSEN, M. & MORRISON, D. A. 2012. *Babesia*: a world emerging. *Infection, Genetics and Evolution*, 12, 1788-1809.
- SCHOEMAN, J. P. 2009. Canine babesiosis. *Onderstepoort Journal of Veterinary Research*, 76, 59-66.
- SCHOEMAN, J. P., REES, P. & HERRTAGE, M. E. 2007. Endocrine predictors of mortality in canine babesiosis caused by *Babesia canis rossii*. *Veterinary Parasitology*, 148, 75-82.
- SCHOFIELD, L. 2007. Intravascular infiltrates and organ-specific inflammation in malaria pathogenesis. *Immunology and cell biology*, 85, 130-137.
- SEEJARIM, C. 2020. *Reticulocyte count and indices in dogs naturally and experimentally infected with Babesia rossii*. University of Pretoria.

- SEETO, R. K., FENN, B. & ROCKEY, D. C. 2000. Ischemic hepatitis: clinical presentation and pathogenesis. *The American journal of medicine*, 109, 109-113.
- SERGEANT, E. D., A. ; PARROT, L. ; LESTOQUARD, F. 1945. *Etudes sur les piroplasmoses bovines*, Institut Pasteur d'Algérie.
- SHABANI, B., ESMAEILNEJAD, B., TAVASSOLI, M. & IMANI, M. 2020. Assessment of cholinesterase activity and hepatic biofunction in dogs naturally infected with *Babesia gibsoni*. *Comparative Clinical Pathology*, 29, 1265-1269.
- SHAH, S. A., SOOD, N. K. & TUMATI, S. R. 2011. Haemato-biochemical changes in natural cases of canine babesiosis. *Asian Journal of Animal Sciences* 5, 387-392.
- SHAKESPEARE, A. 1995. The incidence of canine babesiosis amongst sick dogs presented to the Onderstepoort Veterinary Academic Hospital. *Journal of the South African Veterinary Association*, 66, 247-250.
- SHENG, J., RUEDL, C. & KARJALAINEN, K. 2015. Most tissue-resident macrophages except microglia are derived from fetal hematopoietic stem cells. *Immunity*, 43, 382-393.
- SHETTY, S., LALOR, P. F. & ADAMS, D. H. 2018. Liver sinusoidal endothelial cells—gatekeepers of hepatic immunity. *Nature reviews Gastroenterology & hepatology*, 15, 555-567.
- SHIBAYAMA, Y., URANO, T., ASAKA, S., HASHIMOTO, K. & NAKATA, K. 1993. Pathogenesis of centrilobular necrosis following congestion of the liver. *Journal of gastroenterology and hepatology*, 8, 530-534.
- SHIBAYAMA, Y., URANO, T. & NAKATA, K. 1992. Changes in hepatic lymph vessels in endotoxaemia. *The Journal of Pathology*, 168, 325-330.
- SHODA, L. K., KEGERREIS, K. A., SUAREZ, C. E., RODITI, I., CORRAL, R. S., BERTOT, G. M., NORIMINE, J. & BROWN, W. C. 2001. DNA from protozoan parasites *Babesia bovis*, *Trypanosoma cruzi*, and *T. brucei* is mitogenic for B lymphocytes and stimulates macrophage expression of interleukin-12, tumor necrosis factor alpha, and nitric oxide. *Infection and immunity*, 69, 2162-2171.
- SHORTT, H. 1973. *Babesia canis*: the life cycle and laboratory maintenance in its arthropod and mammalian hosts. *International Journal for Parasitology*, 3, 119-148.
- SIBBALD, W. J. & VINCENT, J.-L. 2012. Clinical trials for the treatment of sepsis.
- SIEGEL, J. H., CERRA, F. B., COLEMAN, B., GIOVANNINI, I., SHETYE, M., BORDER, J. R. & MCMENAMY, R. H. 1979. Physiological and metabolic correlations in human sepsis: invited commentary. *Surgery*, 86, 163-193.
- SIGGAARD-ANDERSEN, O. & SIGGAARD-ANDERSEN, M. 1990. The oxygen status algorithm: a computer program for calculating and displaying pH and blood gas data. *Scandinavian Journal of Clinical and Laboratory Investigation*, 50, 29-45.
- SIJBRANDA, D., HUNTER, S., HOWE, L., LENTING, B., ARGILLA, L. & GARTRELL, B. 2017. Cases of mortality in little penguins (*Eudyptula minor*) in New Zealand associated with avian malaria. *New Zealand veterinary journal*, 65, 332-337.
- SINGH, R., KAUR, M. & ARORA, D. 2010. Prospective study of hepatic involvement in *Plasmodium falciparum* malaria. *Journal of Clinical and Diagnostic Research*, 4, 2190-2197.
- SLEIGHT, D. R. & THOMFORD, N. R. 1970. Gross anatomy of the blood supply and biliary drainage of the canine liver. *The Anatomical Record*, 166, 153-160.
- SOLANO-GALLEGO, L. & BANETH, G. 2011. Babesiosis in dogs and cats—expanding parasitological and clinical spectra. *Veterinary parasitology*, 181, 48-60.
- SRICHAIKUL, T. 1959. A study of pigmentation and other changes in the liver in malaria. *American Journal of Tropical Medicine and Hygiene*, 8, 110-18.
- STAFFORD, J. L., NEUMANN, N. F. & BELOSEVIC, M. 2002. Macrophage-mediated innate host defense against protozoan parasites. *Critical reviews in microbiology*, 28, 187-248.
- SU, G. L. 2002. Lipopolysaccharides in liver injury: molecular mechanisms of Kupffer cell activation. *American Journal of Physiology-Gastrointestinal and Liver Physiology*, 283, G256-G265.

- TACHADO, S. D., GEROLD, P., MCCONVILLE, M. J., BALDWIN, T., QUILICI, D., SCHWARZ, R. T. & SCHOFIELD, L. 1996. Glycosylphosphatidylinositol toxin of *Plasmodium* induces nitric oxide synthase expression in macrophages and vascular endothelial cells by a protein tyrosine kinase-dependent and protein kinase C-dependent signaling pathway. *Journal of immunology (Baltimore, Md.: 1950)*, 156, 1897-1907.
- TAMION, F. 2010. Albumin in sepsis. *Annales francaises d'anesthesie et de reanimation*, 29, 629-634.
- TAYLOR, J., GUTHERIE, A. & LEISEWITZ, A. 1991. The effect of endogenously produced carbon monoxide on the oxygen status of dogs infected with *Babesia canis*. *Journal of the South African Veterinary Association*, 62, 153-155.
- TAYLOR JR, F. B., TOH, C.-H., HOOTS, K. W., WADA, H. & LEVI, M. 2001. Towards definition, clinical and laboratory criteria, and a scoring system for disseminated intravascular coagulation. *Thrombosis and haemostasis*, 86, 1327-1330.
- THANKACHAN, A., VINODKUMAR, K., SHYMA, V., ASHA, R. & VIJAYAKUMAR, K. 2020. Haemato-biochemical alterations and ultrasonographical changes in canines affected with *Babesia gibsoni*. *The Pharma Innovation Journal*, 9, 480-483.
- THAPA, B. & WALIA, A. 2007. Liver function tests and their interpretation. *The Indian Journal of Pediatrics*, 74, 663-671.
- THOMAS, H. 2017. Bile acids promote inflammation in cholestasis-associated sepsis. *Nature Reviews Gastroenterology & Hepatology*, 14, 324-325.
- THURMAN, R. 1998. Mechanisms of hepatic toxicity II. *Am J Physiol*, 275, G605-G611.
- TOMIOKA, H., TATANO, Y., MAW, W. W., SANO, C., KANEHIRO, Y. & SHIMIZU, T. 2012. Characteristics of suppressor macrophages induced by mycobacterial and protozoal infections in relation to alternatively activated M2 macrophages. *Journal of Immunology Research*, 2012.
- TORTI, M., KULEŠ, J., MATIJATKO, V., BRKLIJAČIĆ, M., KIŠ, I., GOTIĆ, J., MRLJAK, V. & ŠMIT, I. 2020. Acid-base status in canine babesiosis caused by *Babesia canis*. *Veterinarski arhiv*, 90, 603-610.
- TRAUNER, M., FICKERT, P. & STAUBER, R. E. 1999. Inflammation-induced cholestasis. *Journal of gastroenterology and hepatology*, 14, 946-959.
- TROSKIE, M., DE VILLIERS, L., LEISEWITZ, A., OOSTHUIZEN, M. C. & QUAN, M. 2019. Development and validation of a multiplex, real-time PCR assay for *Babesia rossi* and *Babesia vogeli*. *Ticks and tick-borne diseases*, 10, 421-432.
- TURNER, R. & MCDONNELL, S. 2003. Alkaline phosphatase in stallion semen: characterization and clinical applications. *Theriogenology*, 60, 1-10.
- TUTTLE, A. D., BIRKENHEUER, A. J., JUOPPERI, T., LEVY, M. G. & BREITSCHWERDT, E. B. 2003. Concurrent bartonellosis and babesiosis in a dog with persistent thrombocytopenia. *JOURNAL-AMERICAN VETERINARY MEDICAL ASSOCIATION*, 223, 1306-1310.
- UBAH, A. S., ABALAKA, S. E., IDOKO, I. S., OBETA, S. S., EJIORFOR, C. E., MSHELBWALA, P. P., OMEJE, J. N. & AJAYI, I. E. 2019. Canine babesiosis in a male Boerboel: Hematobiochemical and anatomic pathological changes in the cardiorespiratory and reproductive organs. *Veterinary and animal science*, 7, 100049.
- UILENBERG, G. 1981. Theilerial species of domestic livestock. In: IRVIN, A. C. M. Y. A. (ed.) *Advances in the Control of Theileriosis*. Martinus Nijhoff Publishers.
- UILENBERG, G. 2006. *Babesia*—a historical overview. *Veterinary parasitology*, 138, 3-10.
- ULLAL, T., BIRKENHEUER, A. & VADEN, S. 2018. Azotemia and proteinuria in dogs infected with *Babesia gibsoni*. *Journal of the American Animal Hospital Association*, 54, 156-160.
- UNDERWOOD, W. & ANTHONY, R. 2020. AVMA guidelines for the euthanasia of animals: 2020 edition. *AVMA*, 2013, 2020-1.
- VÁLI, L., TABA, G., SZENTMIHÁLYI, K., FÉBEL, H., KURUCZ, T., PALLAI, Z., KUPCSULIK, P. & BLÁZOVICS, A. 2006. Reduced antioxidant level and increased oxidative damage in intact liver lobes during ischaemia-reperfusion. *World Journal of Gastroenterology: WJG*, 12, 1086.

- VALLI, V., KIUPEL, M., BIENZLE, D. & WOOD, R. D. 2015. Hematopoietic system. *Jubb, Kennedy, and Palmer's pathology of domestic animals*, 3, 102-268.
- VANNAPHAN, S. 2009. *Pocket Guidelines for the Care of Malaria Patients*, WHO Collaborating Center for Clinical Management of Malaria.
- VANNAPHAN, S., WALTERS, N., SAENGNEDSAWANG, T., TANGPUKDEE, N., KHAM-IN, P., KLUBPRASIT, M., WILAIRATANA, P. & LOOAREESUWAN, S. 2010. Factors associated with acute renal failure in severe falciparum malaria patients. *Southeast Asian journal of tropical medicine and public health*, 41, 1042.
- VEDERNIKOV, Y., GRÄSER, T. & VANIN, A. 1989. Similar endothelium-independent arterial relaxation by carbon monoxide and nitric oxide. *Biomedica biochimica acta*, 48, 601-603.
- VERCAMMEN, F., DEKEN, R. D. & MAES, L. 1997. Haematological and biochemical profile in experimental canine babesiosis (*Babesia canis*). *Vlaams Diergeneeskundig Tijdschrift (Belgium)*, 66, 174-178.
- VILLIERS, E., BAINES, S., LAW, A. M. & MALLOWS, V. 2006a. Identification of acute myeloid leukemia in dogs using flow cytometry with myeloperoxidase, MAC387, and a canine neutrophil-specific antibody. *Vet Clin Pathol*, 35, 55-71.
- VILLIERS, E., BAINES, S., LAW, A. M. & MALLOWS, V. 2006b. Identification of acute myeloid leukemia in dogs using flow cytometry with myeloperoxidase, MAC387, and a canine neutrophil-specific antibody. *Veterinary clinical pathology*, 35, 55-71.
- VIRIYAVEJAKUL, P., KHACHONSAKSUMET, V. & PUNSAWAD, C. 2014. Liver changes in severe *Plasmodium falciparum* malaria: histopathology, apoptosis and nuclear factor kappa B expression. *Malaria journal*, 13, 1-10.
- WALTERS, J. & MCGREGOR, I. A. 1960. The mechanism of malarial hepatomegaly and its relationship to hepatic fibrosis. *Transactions of the Royal Society of Tropical Medicine and Hygiene*, 54, 135-145.
- WANG, J., GUO, G., LI, A., CAI, W.-Q. & WANG, X. 2021. Challenges of phototherapy for neonatal hyperbilirubinemia. *Experimental and therapeutic medicine*, 21, 1-1.
- WANG, J., WANG, Z., WANG, X., ZHU, Q. & ZHENG, S. 2008. The prognostic value of serum gamma glutamyltransferase activity in Chinese infants with previously diagnosed idiopathic neonatal hepatitis. *HK J Paediatr (new series)*, 13, 39-45.
- WANG, J. S., TAN, N. & DHAWAN, A. 2006. Significance of low or normal serum gamma glutamyl transferase level in infants with idiopathic neonatal hepatitis. *European journal of pediatrics*, 165, 795-801.
- WANG, P. & CHAUDRY, I. H. 1996. Mechanism of hepatocellular dysfunction during hyperdynamic sepsis. *American Journal of Physiology-Regulatory, Integrative and Comparative Physiology*, 270, R927-R938.
- WATANABE, S., NAKAYAMA, N., YOKOTA, T., ARAI, K.-I. & MIYAJIMA, A. 1991. Colony-stimulating factors and cytokine receptor network. *Current Opinion in Biotechnology*, 2, 227-237.
- WEBSTER, C. & COOPER, J. 2014. Diagnostic approach to hepatobiliary disease. In: BONAGURA, J., TWEDT, D. (ed.) *Kirk's Current Veterinary Therapy*. 15th ed. St Louis, MO: Saunders Elsevier.
- WEESE, J. S. & EVASON, M. 2020. Infectious diseases of the dog and cat. In: WEESE, J. S. & EVASON, M. (eds.). Boca Raton: CRC Press.
- WEISS, G. & GOODNOUGH, L. T. 2005. Anemia of chronic disease. *New England Journal of Medicine*, 352, 1011-1023.
- WEISS, Y. G., BELLIN, L., KIM, P. K., ANDREJKO, K. M., HAAXMA, C. A., RAJ, N., FURTH, E. E. & DEUTSCHMAN, C. S. 2001. Compensatory hepatic regeneration after mild, but not fulminant, intraperitoneal sepsis in rats. *American Journal of Physiology-Gastrointestinal and Liver Physiology*, 280, G968-G973.
- WELZL, C., LEISEWITZ, A., JACOBSON, L., VAUGHAN-SCOTT, T. & MYBURGH, E. 2001. Systemic inflammatory response syndrome and multiple-organ damage/dysfunction in complicated canine babesiosis. *Journal of the South African Veterinary Association*, 72, 158-162.

- WHITE, N. J., COOK, C. & ZUMLA, A. 2003. Malaria. In: WHITE, N. J., COOK, C. & ZUMLA, A. (eds.) *Manson's Tropical Diseases*. 22nd ed. Philadelphia: Saunders Elsevier.
- WHITFIELD, J. 2001. Gamma glutamyl transferase. *Critical reviews in clinical laboratory sciences*, 38, 263-355.
- WHITING, J. F., GREEN, R. M., ROSENBLUTH, A. B. & GOLLAN, J. L. 1995. Tumor necrosis factor–alpha decreases hepatocyte bile salt uptake and mediates endotoxin-induced cholestasis. *Hepatology*, 22, 1273-1278.
- WHITTEN, R., MILNER JR, D. A., YEH, M. M., KAMIZA, S., MOLYNEUX, M. E. & TAYLOR, T. E. 2011. Liver pathology in Malawian children with fatal encephalopathy. *Human pathology*, 42, 1230-1239.
- WHO 2000. Severe Falciparum Malaria, World Health Organization Communicable Diseases Cluster. *Trans R Soc Trop Med Hyg*, 94, S1-S9.
- WILKINS, P. A., OTTO, C. M., BAUMGARDNER, J. E., DUNKEL, B., BEDENICE, D., PARADIS, M. R., STAFFIERI, F., SYRING, R. S., SLACK, J. & GRASSO, S. 2007. Acute lung injury and acute respiratory distress syndromes in veterinary medicine: consensus definitions: The Dorothy Russell Havemeyer Working Group on ALI and ARDS in Veterinary Medicine. *Journal of Veterinary Emergency and Critical Care*, 17, 333-339.
- WOZNIAK, E. J., BARR, B. C., THOMFORD, J. W., YAMANE, I., MCDONOUGH, S. P., MOORE, P. F., NAYDAN, D., ROBINSON, T. W. & CONRAD, P. A. 1997. Clinical, anatomic, and immunopathologic characterization of *Babesia gibsoni* infection in the domestic dog (*Canis familiaris*). *The Journal of Parasitology*, 83, 692-699.
- WRIGHT, D. E., WAGERS, A. J., GULATI, A. P., JOHNSON, F. L. & WEISSMAN, I. L. 2001. Physiological migration of hematopoietic stem and progenitor cells. *Science*, 294, 1933-1936.
- WRIGHT, I., GOODGER, B., BUFFINGTON, G., CLARK, I., PARRODI, F. & WALTISBUHL, D. 1989. Immunopathophysiology of babesial infections. *Transactions of the Royal Society of Tropical Medicine and Hygiene*, 83, 11-13.
- WRIGHT, I., GOODGER, B. & MAHONEY, D. 1981. Virulent and avirulent strains of *Babesia bovis*: the relationship between parasite protease content and pathophysiological effect of the strain. *The Journal of protozoology*, 28, 118-120.
- WSAVA 2006. WSAVA standards for clinical and histological diagnosis of canine and feline liver disease. In: WORLD SMALL ANIMAL VETERINARY ASSOCIATION. LIVER STANDARDIZATION, G. (ed.). Edinburgh: Saunders/Elsevier.
- YAMADA, Y., KIRILLOVA, I., PESCHON, J. J. & FAUSTO, N. 1997. Initiation of liver growth by tumor necrosis factor: deficient liver regeneration in mice lacking type I tumor necrosis factor receptor. *Proceedings of the National Academy of Sciences*, 94, 1441-1446.
- YAMANO, S., SHIMIZU, K., OGURA, H., HIROSE, T., HAMASAKI, T., SHIMAZU, T. & TASAKI, O. 2016. Low total cholesterol and high total bilirubin are associated with prognosis in patients with prolonged sepsis. *Journal of critical care*, 31, 36-40.
- YAMASAKI, M., HOSSAIN, M. A., JEONG, J.-R., CHANG, H.-S., SATOH, H., YAMATO, O. & MAEDE, Y. 2003. *Babesia gibsoni*–specific isoenzymes related to energy metabolism of the parasite in infected erythrocytes. *Journal of Parasitology*, 89, 1142-1146.
- YAMASHITA, K., FUJINAGA, T., MIYAMOTO, T., HAGIO, M., IZUMISAWA, Y. & KOTANI, T. 1994. Canine acute phase response: relationship between serum cytokine activity and acute phase protein in dogs. *Journal of veterinary medical science*, 56, 487-492.
- YERUHAM, I., HADANI, A., GALKER, F., AVIDAR, Y. & BOGIN, E. 1998. Clinical, Clinico-Pathological and Serological Studies of *Babesia ovis* in Experimentally Infected Sheep. *Journal of Veterinary Medicine, Series B*, 45, 385-394.
- ZAIDI, S. A. & SINGER, C. 2002. Gastrointestinal and hepatic manifestations of tickborne diseases in the United States. *Clinical infectious diseases*, 34, 1206-1212.

- ZEIN, J. G., LEE, G. L., TAWK, M., DABAJA, M. & KINASEWITZ, G. T. 2004. Prognostic significance of elevated serum lactate dehydrogenase (LDH) in patients with severe sepsis. *Chest*, 126, 873S.
- ZHANG, X., YANG, S., CHEN, J. & SU, Z. 2019. Unraveling the regulation of hepatic gluconeogenesis. *Frontiers in endocrinology*, 9, 802.
- ZIJLMANS, W., VAN KEMPEN, A., ACKERMANS, M., DE METZ, J., KAGER, P. & SAUERWEIN, H. 2008. Glucose kinetics during fasting in young children with severe and non-severe malaria in Suriname. *The American journal of tropical medicine and hygiene*, 79, 605-612.
- ZINTL, A., MULCAHY, G., SKERRETT, H. E., TAYLOR, S. M. & GRAY, J. S. 2003. *Babesia divergens*, a bovine blood parasite of veterinary and zoonotic importance. *Clinical microbiology reviews*, 16, 622-636.
- ZRZAVY, T., HÖFTBERGER, R., BERGER, T., RAUSCHKA, H., BUTOVSKY, O., WEINER, H. & LASSMANN, H. 2019. Pro-inflammatory activation of microglia in the brain of patients with sepsis. *Neuropathology and applied neurobiology*, 45, 278-290.
- ZYGNER, W., GOJSKA-ZYGNER, O., DŁUGOSZ, E. & WĘDRYCHOWICZ, H. 2011. Liver enzyme activity in dogs infected with *Babesia canis*. *Bull Vet Inst Pulawy*, 55, 423-427.
- ZYGNER, W., RAPACKA, G., GÓJSKA-ZYGNER, O., DŁUGOSZ, E. & WĘDRYCHOWICZ, H. 2007. Biochemical abnormalities observed in serum of dogs infected with large *Babesia* in Warsaw (Poland). *Polish Journal of Veterinary Sciences*, 10, 245-253.
- ZYGNER, W. & WĘDRYCHOWICZ, H. 2009. Influence of anaemia on azotaemia in dogs infected with *Babesia canis* in Poland. *Bull Vet Inst Pulawy*, 53, 663-668.

APPENDICES

Appendix A: Full blood results

Haematology:

Control cases

Table 14: Liver-specific haematology values from control dogs

Control no.	Red cell count (RCC) ($\times 10^{12}/L$)	Haematocrit (Hct) (L/L)	Platelet concentration ($\times 10^9/L$)	White cell count (WCC) ($\times 10^9/L$)	Neutrophils (mature) ($\times 10^9/L$)	Neutrophils (band) ($\times 10^9/L$)	Lymphocytes ($\times 10^9/L$)	Monocytes ($\times 10^9/L$)
2	7,04	0,44	391	6,01	3,61	0	1,92	0,48
4	5,73	0,37	289	8,18	6,05	0	1,55	0,41
9	6,66	0,41	327	5,17	2,22	0	1,6	0,36
11	7,49	0,47	477	8,95	5,73	0,09	2,33	0,45

Infected cases

Table 15: Liver-specific haematology values from *B. rossi*-infected dogs

<i>B. rossi</i> -infected case no.	Red cell count (RCC) ($\times 10^{12}/L$)	Haematocrit (Hct) (L/L)	Platelet concentration ($\times 10^9/L$)	White cell count (WCC) ($\times 10^9/L$)	Neutrophils (mature) ($\times 10^9/L$)	Neutrophils (band) ($\times 10^9/L$)	Lymphocytes ($\times 10^9/L$)	Monocytes ($\times 10^9/L$)
50	5,25	0,34	91	103,55	67,31	21,75	1,04	13,46
20	1,02	0,09	74	5,5	4,13	0,99	0,39	0
117	1,48	0,12	102	19,12	9,94	2,49	3,82	2,87
110	1,48	0,11	62	12,17	9,01	0,97	1,22	0,97
54	0,97	0,07	25	21,6	15,12	0,86	4,97	0,65
59	2,77	0,2	11	14,36	9,19	2,87	0,86	1,44
91	3,96	0,28	23	3,35	0,9	1,04	0,77	0,64
61	3,19	0,22	24	10,25	6,36	0,51	1,64	1,64
88	5	0,35	15	16,74	10,88	2,18	3,18	0,5
106	1,48	0,13	56	12,5	7,75	1,5	2,75	0,25

Serum Biochemistry:

Control cases

Table 16: Liver-specific serum biochemistry values from control dogs

Control no.	ALP (U/L)	ALT (U/L)	Bile acids ($\mu\text{mol/L}$)	Urea (mmol/L)	Albumin (g/L)	TSP (g/L)	Bilirubin ($\mu\text{mol/L}$)	Glucose (mmol/L)
2	126	25	3	4,3	34,8	48,5	Not measured	Not measured
4	102	17,8	4	3,3	31,7	47,3	Not measured	Not measured
9	27	10,3	<1	2,6	19,2	54,1	Not measured	Not measured
11	59	25,7	2	2,9	37	60,2	Not measured	Not measured

Infected cases

Table 17: Liver-specific serum biochemistry values from *B. rossi*-infected dogs

<i>B. rossi</i> -infected case no.	ALP (U/L)	ALT (U/L)	Bile acids ($\mu\text{mol/L}$)	Urea (mmol/L)	Albumin (g/L)	TSP (g/L)	Bilirubin ($\mu\text{mol/L}$)	Glucose (mmol/L)
50	1428	216	690	104,3	24,3	46,9	465,4	9,2
20	203	930	27	18,7	16	71,7	103,4	0,4
117	229	719	Not measured	Not measured	19,4	70,3	172,2	3,4
110	225	34	Not measured	Not measured	13,1	68,4	175,4	5
54	80	88	6	28,3	19,7	57,1	98,9	9,9
59	93	89	22	22	14,9	38,2	67,7	3,7
91	106	85	11	63,9	22,7	50,3	15,4	2,4
61	125	38	27	31,5	22,3	58,9	42,5	2,6
88	113	63	2	19,4	28,5	50	7,2	1,8
106	82	45	Not measured	Not measured	17,7	46,1	9,4	15,3

Appendix B: Histopathology score sheet

Criteria	S-number:					Comments:
Signalment						
Hx of icteric mucous membranes (absent/present)						
RT-qPCR results						
Liver histopathology						
Autolysis	<input type="checkbox"/> Absent	<input type="checkbox"/> Mild	<input type="checkbox"/> Moderate	<input type="checkbox"/> Severe		
Microscopic lesions	<input type="checkbox"/> Absent	<input type="checkbox"/> Present				
Lesion distribution	<input type="checkbox"/> Absent	<input type="checkbox"/> Focal	<input type="checkbox"/> Multifocal	<input type="checkbox"/> Coalescing	<input type="checkbox"/> Diffuse	
		<input type="checkbox"/> Centrilobular	<input type="checkbox"/> Midzonal	<input type="checkbox"/> Periportal		
Congestion	Centrilobular	<input type="checkbox"/> Absent	<input type="checkbox"/> Mild	<input type="checkbox"/> Moderate	<input type="checkbox"/> Severe	
	Midzonal	<input type="checkbox"/> Absent	<input type="checkbox"/> Mild	<input type="checkbox"/> Moderate	<input type="checkbox"/> Severe	
	Periportal	<input type="checkbox"/> Absent	<input type="checkbox"/> Mild	<input type="checkbox"/> Moderate	<input type="checkbox"/> Severe	
Average:						
Haemorrhage	<input type="checkbox"/> Absent	<input type="checkbox"/> Present				
Gross differentiation between zones	<input type="checkbox"/> Absent	<input type="checkbox"/> Present				

							Score
Periportal	Bile ducts	Bile stasis	<input type="checkbox"/> Absent (0)	<input type="checkbox"/> Present (1)			
		Proliferation	<input type="checkbox"/> Absent (0)	<input type="checkbox"/> Present (1)			
	Hepatocytes (limiting plate)	Necrosis	<input type="checkbox"/> Absent (0)	<input type="checkbox"/> Mild (1)	<input type="checkbox"/> Moderate (2)	<input type="checkbox"/> Severe (3)	
		Hydropic change	<input type="checkbox"/> Absent (0)	<input type="checkbox"/> Mild (1)	<input type="checkbox"/> Moderate (2)	<input type="checkbox"/> Severe (3)	
		Fatty change	<input type="checkbox"/> Absent (0)	<input type="checkbox"/> Mild (1)	<input type="checkbox"/> Moderate (2)	<input type="checkbox"/> Severe (3)	
		Vesicular nuclei	<input type="checkbox"/> Absent (0)	<input type="checkbox"/> Present (1)			
		Turnover	<input type="checkbox"/> Absent (0)	<input type="checkbox"/> Mild (1)	<input type="checkbox"/> Moderate (2)	<input type="checkbox"/> Severe (3)	
		Anisokaryosis	<input type="checkbox"/> Absent (0)	<input type="checkbox"/> Present (1)			
		Pigments:	Lipofuscin/ceroid	<input type="checkbox"/> Absent (0)	<input type="checkbox"/> Present (1)		
	Haemosiderin		<input type="checkbox"/> Absent (0)	<input type="checkbox"/> Present (1)			
	Bile		<input type="checkbox"/> Absent (0)	<input type="checkbox"/> Present (1)			
	Portal vein	Leukostasis	<input type="checkbox"/> Absent (0)	<input type="checkbox"/> Mild (1)	<input type="checkbox"/> Moderate (2)	<input type="checkbox"/> Severe (3)	
		Endothelial cell integrity	<input type="checkbox"/> Absent (0)	<input type="checkbox"/> Mild (1)	<input type="checkbox"/> Severe (2)		
	Hepatic artery	Endothelial cell integrity	<input type="checkbox"/> Absent (0)	<input type="checkbox"/> Mild (1)	<input type="checkbox"/> Severe (2)		
	Lymphatics	Distension	<input type="checkbox"/> Absent (0)	<input type="checkbox"/> Present (1)			
		Proteinaceous fluid-filled	<input type="checkbox"/> Absent (0)	<input type="checkbox"/> Present (1)			

	Extra-medullary haematopoiesis	<input type="checkbox"/> Absent (0)	<input type="checkbox"/> Mild (1)	<input type="checkbox"/> Prominent (2)			
	Sinusoids/Space of Disse	Oedema	<input type="checkbox"/> Absent (0)	<input type="checkbox"/> Present (1)			
	Cellular infiltrate	Monocyte-macrophages	<input type="checkbox"/> Absent (0)	<input type="checkbox"/> Few (1)	<input type="checkbox"/> Many (2)		
		Lymphocytes	<input type="checkbox"/> Absent (0)	<input type="checkbox"/> Few (1)	<input type="checkbox"/> Many (2)		
		Plasma cells	<input type="checkbox"/> Absent (0)	<input type="checkbox"/> Few (1)	<input type="checkbox"/> Many (2)		
		Neutrophils	<input type="checkbox"/> Absent (0)	<input type="checkbox"/> Few (1)	<input type="checkbox"/> Many (2)		
		Eosinophils	<input type="checkbox"/> Absent (0)	<input type="checkbox"/> Few (1)	<input type="checkbox"/> Many (2)		
		Erythrocytes	Intracellular parasites	<input type="checkbox"/> Absent (0)	<input type="checkbox"/> Few (1)	<input type="checkbox"/> Many (2)	
Midzonal	Hepatocytes	Necrosis	<input type="checkbox"/> Absent (0)	<input type="checkbox"/> Mild (1)	<input type="checkbox"/> Moderate (2)	<input type="checkbox"/> Severe (3)	
		Hydropic change	<input type="checkbox"/> Absent (0)	<input type="checkbox"/> Mild (1)	<input type="checkbox"/> Moderate (2)	<input type="checkbox"/> Severe (3)	
		Fatty change	<input type="checkbox"/> Absent (0)	<input type="checkbox"/> Mild (1)	<input type="checkbox"/> Moderate (2)	<input type="checkbox"/> Severe (3)	
		Vesicular nuclei	<input type="checkbox"/> Absent (0)	<input type="checkbox"/> Present (1)			
		Turnover	<input type="checkbox"/> Absent (0)	<input type="checkbox"/> Mild (1)	<input type="checkbox"/> Moderate (2)	<input type="checkbox"/> Severe (3)	
		Anisokaryosis	<input type="checkbox"/> Absent (0)	<input type="checkbox"/> Present (1)			
		Pigments:	Lipofuscin/ceoid	<input type="checkbox"/> Absent (0)	<input type="checkbox"/> Present (1)		
			Haemosiderin	<input type="checkbox"/> Absent (0)	<input type="checkbox"/> Present (1)		
			Bile	<input type="checkbox"/> Absent (0)	<input type="checkbox"/> Present (1)		
		Fibrin	<input type="checkbox"/> Absent (0)	<input type="checkbox"/> Mild (1)	<input type="checkbox"/> Moderate (2)	<input type="checkbox"/> Severe (3)	
		Extra-medullary haematopoiesis	<input type="checkbox"/> Absent (0)	<input type="checkbox"/> Mild (1)	<input type="checkbox"/> Prominent (2)		
		Sinusoids/Space of Disse	Oedema	<input type="checkbox"/> Absent (0)	<input type="checkbox"/> Present (1)		
		Kupffer cells	Hypertrophy/Activation	<input type="checkbox"/> Absent (0)	<input type="checkbox"/> Few (1)	<input type="checkbox"/> Many (2)	
			Intracellular haemosiderin pigment	<input type="checkbox"/> Absent (0)	<input type="checkbox"/> Few (1)	<input type="checkbox"/> Many (2)	
		Bile	<input type="checkbox"/> Absent (0)	<input type="checkbox"/> Few (1)	<input type="checkbox"/> Many (2)		
		Cell injury	<input type="checkbox"/> Absent (0)	<input type="checkbox"/> Few (1)	<input type="checkbox"/> Many (2)		
	Erythrocytes	Intracellular parasites	<input type="checkbox"/> Absent (0)	<input type="checkbox"/> Few (1)	<input type="checkbox"/> Many (2)		
	Hepatocytes	Necrosis	<input type="checkbox"/> Absent (0)	<input type="checkbox"/> Mild (1)	<input type="checkbox"/> Moderate (2)	<input type="checkbox"/> Severe (3)	
		Hydropic change	<input type="checkbox"/> Absent (0)	<input type="checkbox"/> Mild (1)	<input type="checkbox"/> Moderate (2)	<input type="checkbox"/> Severe (3)	

Centrilobular		Fatty change	<input type="checkbox"/> Absent (0)	<input type="checkbox"/> Mild (1)	<input type="checkbox"/> Moderate (2)	<input type="checkbox"/> Severe (3)			
		Vesicular nuclei	<input type="checkbox"/> Absent (0)	<input type="checkbox"/> Present (1)					
		Turnover	<input type="checkbox"/> Absent (0)	<input type="checkbox"/> Mild (1)	<input type="checkbox"/> Moderate (2)	<input type="checkbox"/> Severe (3)			
		Anisokaryosis	<input type="checkbox"/> Absent (0)	<input type="checkbox"/> Present (1)					
		Pigments:	Lipofuscin/ceroid	<input type="checkbox"/> Absent (0)	<input type="checkbox"/> Present (1)				
			Haemosiderin	<input type="checkbox"/> Absent (0)	<input type="checkbox"/> Present (1)				
			Bile	<input type="checkbox"/> Absent (0)	<input type="checkbox"/> Present (1)				
	Central veins	Perivascular leukostasis	<input type="checkbox"/> Absent (0)	<input type="checkbox"/> Present (1)					
		Endothelial cell integrity/hypertrophy	<input type="checkbox"/> Absent (0)	<input type="checkbox"/> Mild (1)	<input type="checkbox"/> Moderate (2)	<input type="checkbox"/> Severe (3)			
	Lymphatics	Distension	<input type="checkbox"/> Absent (0)	<input type="checkbox"/> Present (1)					
		Proteinaceous fluid-filled	<input type="checkbox"/> Absent (0)	<input type="checkbox"/> Present (1)					
	Terminal hepatic vein								
	Sublobular hepatic vein								
	Fibrin	<input type="checkbox"/> Absent (0)	<input type="checkbox"/> Mild (1)	<input type="checkbox"/> Moderate (2)	<input type="checkbox"/> Severe (3)				
	Extra-medullary haematopoiesis	<input type="checkbox"/> Absent (0)	<input type="checkbox"/> Mild (1)	<input type="checkbox"/> Prominent (2)					
	Sinusoids/Space of Disse	Oedema	<input type="checkbox"/> Absent (0)	<input type="checkbox"/> Present (1)					
	Cellular infiltrate	Monocyte-macrophages	<input type="checkbox"/> Absent (0)	<input type="checkbox"/> Few (1)	<input type="checkbox"/> Many (2)				
		Lymphocytes	<input type="checkbox"/> Absent (0)	<input type="checkbox"/> Few (1)	<input type="checkbox"/> Many (2)				
		Plasma cells	<input type="checkbox"/> Absent (0)	<input type="checkbox"/> Few (1)	<input type="checkbox"/> Many (2)				
		Neutrophils	<input type="checkbox"/> Absent (0)	<input type="checkbox"/> Few (1)	<input type="checkbox"/> Many (2)				
		Eosinophils	<input type="checkbox"/> Absent (0)	<input type="checkbox"/> Few (1)	<input type="checkbox"/> Many (2)				
	Kupffer cells	Hypertrophy/Activation	<input type="checkbox"/> Absent (0)	<input type="checkbox"/> Few (1)	<input type="checkbox"/> Many (2)				
		Intracellular haemosiderin pigment	<input type="checkbox"/> Absent (0)	<input type="checkbox"/> Few (1)	<input type="checkbox"/> Many (2)				
		Bile	<input type="checkbox"/> Absent (0)	<input type="checkbox"/> Few (1)	<input type="checkbox"/> Many (2)				
		Cell injury	<input type="checkbox"/> Absent (0)	<input type="checkbox"/> Few (1)	<input type="checkbox"/> Many (2)				
	Erythrocytes	Intracellular parasites	<input type="checkbox"/> Absent (0)	<input type="checkbox"/> Few (1)	<input type="checkbox"/> Many (2)				
								Total /126	

Appendix C: Histopathology detailed scoring scheme

PARAMETER	GRADING/ SCORE	CRITERIA	
AUTOLYSIS			
Severity	Mild	Anatomical architecture easily distinguishable, cellular morphology well-defined.	
	Moderate	Anatomical architecture still easily distinguishable, cellular morphology not well-defined, red blood cells still preserved, small numbers of putrefactive (Clostridial) bacteria may be present in some fields.	
	Severe	Cellular morphology cannot be defined, anatomical architecture barely distinguishable, red blood cells lysed and difficult to identify, numerous putrefactive (Clostridial) bacteria present.	
HISTOPATHOLOGY	(All changes in comparison with normal control liver).		
Microscopic lesions	Absent	No evidence of microscopic lesions when scanning on 40x and 100x magnification.	
	Present	Evidence of microscopic lesions, regardless of severity or distribution.	
Lesion distribution (histologic) <i>Will have lesion distribution too - periportal, centrilobular, midzonal</i>	Absent	No evidence of microscopic lesions.	
	Focal	Single well circumscribed area affected.	
	Multifocal	Multiple non-overlapping areas affected.	
	Coalescing	Multiple overlapping areas affected.	
	Diffuse	Entire section of tissue OR all specific anatomical sites affected	
Congestion <i>Will have lesion distribution here too - periportal, centrilobular, midzonal (Intravascular accumulation of rbc's)</i>	Absent	No evidence of congestion/hyperaemia	
	Mild	Congestion present in <35% of blood vessels in all available histology sections	
	Moderate	Congestion present in <70% of blood vessels in all available histology sections	
	Severe	Congestion is present in most blood vessels (>70%) in all available histology sections. Note: check venules, arterioles and capillaries. If present in arterioles make a note (= hyperaemia). Check sinusoids as well. If packed look at controls. Need to look at density inside lumens	
Haemorrhage = extravasated erythrocytes	Absent	No evidence of haemorrhage	
	Present	Evidence of erythrocytes present outside of the blood vessels	
Gross differentiation between the zones	Absent	Periportal, midzonal and centrilobular zones are not easily differentiable at first glance	
	Present	Periportal, midzonal and centrilobular zones are easily differentiable and are noticeably different colours.	
Periportal			
Bile ducts	Bile stasis	Absent (0)	No evidence of bilirubin in the bile ducts

		Present (1)	Evidence of bilirubin in the bile ducts	
	Proliferation	Absent (0)	No evidence of an increase in thickness of the bile duct walls	
		Present (1)	Evidence of an increase in the thickness of the bile duct walls or increase in number	
Hepatocytes (limiting plate) <i>(40x magnification in 3 FOV)</i>	Necrosis <i>(Eosinophilic, surrounding necrosis)</i>	Absent (0)	No necrotic hepatocytes visualized	
		Mild (1)	Single cell necrosis	
		Moderate (2)	Necrosis of small clusters/groups of hepatocytes – 2-5 cells	
		Severe (Krause et al.)	Necrosis of 6 or more cells	
	Hydropic change <i>(Feathery changes)</i>	Absent (0)	No evidence of hydropic change present	
		Mild (1)	Hydropic changes present in 1 hepatocyte	
		Moderate (2)	Hydropic changes in small clusters/groups of hepatocytes – 2-5 cells	
		Severe (Krause et al.)	Hydropic changes in and more than 6 hepatocytes	
	Fatty change <i>(Punched out holes)</i>	Absent (0)	No evidence of fatty change present in any cells	
		Mild (1)	Fatty changes present in 1 hepatocyte	
		Moderate (2)	Fatty changes in small clusters/groups of hepatocytes – 2-5 cells	
		Severe (Krause et al.)	Fatty changes in and more than 6 hepatocytes	
	Vesicular nuclei <i>(Euchromatic. 1.5x size of average of hepatocyte nucleus)</i>	Absent (0)	No evidence of vesicular nuclei present (< and including 1 per FOV).	
		Present (1)	Evidence of vesicular nuclei present (>1 per FOV).	
	Turnover <i>(Mitotic bodies, binucleates)</i>	Absent (0)	No evidence of any turnover present	
		Mild (1)	Evidence of turnover present in 1-2 hepatocytes per field	
		Moderate (2)	Evidence of turnover present in 2-5 hepatocytes per field	
		Severe (Krause et al.)	Evidence of turnover present in more than 5 hepatocytes per field	
	Anisokaryosis	Absent (0)	No evidence of anisokaryosis present	
		Present (1)	Evidence of anisokaryosis	
	Pigments:			
	Lipofuscin/ceroid	Absent (0)	No evidence of pigment present	
		Present (1)	Evidence of pigment present	
Haemosiderin	Absent (0)	No evidence of pigment present		
	Present (1)	Evidence of pigment present		
Bile canalicular	Absent (0)	No evidence of bile present		
	Present (1)	Evidence of bile present		

Portal vein	Leukostasis <i>Use similar sized vessels</i>	Absent (0)	No evidence of leukostasis present. (Look out for normoblasts).	
		Mild (1)	Less than one quarter of the blood vessel's lumen displays leukostasis at 40x magnification, when checking at least 3 FOV.	
		Moderate (2)	Half of the blood vessel's lumen displays leukostasis at 40x magnification, when checking at least 3 FOV.	
		Severe (Krause et al.)	More than and including three quarters of the blood vessel's lumen displays leukostasis at 40x magnification, when checking at least 3 FOV.	
		Cellular infiltrate	Identify and describe predominant cellular component (mononuclear or PMN) in leukostatic blood vessels, based on HE (IMP will confirm later).	
	Endothelial cell integrity/hypertrophy <i>(Endothelial hypertrophy = nucleus width is double or more than the normal thickness)</i>	Absent (0)	No evidence of endothelial cell hypertrophy. Endothelial cell diameter is less than RBC.	
		Mild (1)	Less than one third of endothelial cells display nuclear activation/hypertrophy. Endothelial cell diameter is the same as a RBC.	
		Severe (2)	More than two thirds of endothelial cells display nuclear activation/hypertrophy. Endothelial cell diameter is bigger than one RBC. Note: Comparing to control samples diameter of endothelial cells at central veins. Should be flat and the same diameter as a flat rbc. Diameter <1 rbc = mild Diameter >1 rbc = severe	
	Hepatic artery	Endothelial cell integrity/hypertrophy <i>(Endothelial hypertrophy = nucleus width is double or more than the normal thickness)</i>	Absent (0)	No evidence of endothelial cell hypertrophy.
			Mild (1)	Less than one third of endothelial cells display nuclear activation/hypertrophy.
Moderate (2)			One to two thirds of endothelial cells display nuclear activation/hypertrophy.	
Severe (Krause et al.)			More than two thirds of endothelial cells display nuclear activation/hypertrophy.	
Lymphatics <i>(Subcapsular, portal and central venous areas. Will have endothelial cells)</i>	Distended	Absent (0)	No evidence of lymphatic distension	
		Present (1)	Evidence of lymphatic distension	
	Proteinaceous fluid-filled	Absent (0)	No evidence of proteinaceous fluid present	
		Present (1)	Evidence of proteinaceous fluid present	
Fibrin <i>(Confirmed on MSB histochemical stain)</i> <i>Take note of where the fibrin is deposited</i>	Absent (0)	No evidence of fibrinous exudate		
	Mild (1)	Affecting less than a third of the blood vessels (under 40x magnification, estimated over 3 x FOV).		
	Moderate (2)	Affecting more than a third to two thirds of the blood vessels (under 40x magnification, estimated over 3 x FOV).		

	Severe (Krause et al.)	Affecting more than two thirds of the blood vessels (under 40x magnification, estimated over 3 x FOV).		
Extra-medullary haematopoiesis <i>(Megakaryocytes and metarubricytes/normoblasts)</i>	Absent (0)	No evidence of extra-medullary haematopoiesis present intravascularly.		
	Mild (1)	Less than 5 megakaryocytes/metarubricytes/normoblasts seen in 3x FOV under 40x magnification		
	Prominent (2)	More than 5 megakaryocytes/metarubricytes/normoblasts seen in 3 x FOV under 40x magnification		
Sinusoids/Spaces of Disse	Oedema <i>(= amorphous clear to eosinophilic extravascular fluid)</i>	Absent (0)	No evidence of oedema	
		Present (1)	Expansion of the perivascular areas by oedema fluid	
Cellular infiltrate <i>(Confirmed with IHC)</i> 40x magnification	Monocyte-macrophages	Absent (0)	No monocytes/macrophages seen	
		Few (1)	Less than 20 monocytes/macrophages seen per FOV	
		Many (2)	More than and including 20 monocytes/macrophages seen per FOV	
	Lymphocytes	Absent (0)	No lymphocytes seen	
		Few (1)	Less than 20 lymphocytes seen per FOV	
		Many (2)	More than and including 20 lymphocytes seen per FOV	
	Plasma cells	Absent (0)	No plasma cells seen	
		Few (1)	Less than 20 plasma cells seen per FOV	
		Many (2)	More than and including 20 plasma cells seen per FOV	
	Neutrophils	Absent (0)	No neutrophils seen	
		Few (1)	Less than 20 neutrophils seen per FOV	
		Many (2)	More than and including 20 neutrophils seen per FOV	
	Eosinophils	Absent (0)	No eosinophils seen	
		Few (1)	1-2 eosinophils seen per FOV	
		Many (2)	More than 2 eosinophils seen per FOV	
	Erythrocytes <i>(Confirmed with LFB histochemical stain)</i> 60x magnification	Intraerythrocytic parasites	Absent (0)	No evidence of parasitized erythrocytes.
			Few (1)	Less than 10 parasitized erythrocytes seen per FOV.
			Many (2)	More than and including 10 parasitized erythrocytes seen per FOV.
Midzonal				
Hepatocytes 40x magnification in 3x FOV	Necrosis <i>(Eosinophilic, surrounding necrosis)</i>	Absent (0)	No necrotic hepatocytes visualized	
		Mild (1)	Single cell necrosis	
		Moderate (2)	Necrosis of small clusters/groups of hepatocytes – 2-5 cells	
		Severe (Krause et al.)	Necrosis of 6 or more cells	
	Hydropic change	Absent (0)	No evidence of hydropic change present	

	<i>(Feathery changes)</i>	Mild (1)	Hydropic changes present in 1 hepatocyte
		Moderate (2)	Hydropic changes in small clusters/groups of hepatocytes – 2-5 cells
		Severe (Krause et al.)	Hydropic changes in and more than 6 hepatocytes
	Fatty change <i>(Punched out holes)</i>	Absent (0)	No evidence of fatty change present in any cells
		Mild (1)	Fatty changes present in 1 hepatocyte
		Moderate (2)	Fatty changes in small clusters/groups of hepatocytes – 2-5 cells
		Severe (Krause et al.)	Fatty changes in and more than 6 hepatocytes
	Vesicular nuclei <i>(Euchromatic. 1.5x size of average of hepatocyte nucleus)</i>	Absent (0)	No evidence of vesicular nuclei present (< and including 1 per FOV).
		Present (1)	Evidence of vesicular nuclei present (>1 per FOV).
	Turnover <i>(Mitotic bodies, binucleates)</i>	Absent (0)	No evidence of any turnover present
		Mild (1)	Evidence of turnover present in 1-2 hepatocytes per field
		Moderate (2)	Evidence of turnover present in 2-5 hepatocytes per field
		Severe (Krause et al.)	Evidence of turnover present in more than 5 hepatocytes per field
	Anisokaryosis	Absent (0)	No evidence of anisokaryosis present
		Present (1)	Evidence of anisokaryosis
	Pigments:		
	Lipofuscin/ceroid	Absent (0)	No evidence of pigment present
		Present (1)	Evidence of pigment present
	Haemosiderin	Absent (0)	No evidence of pigment present
		Present (1)	Evidence of pigment present
Bile	Absent (0)	No evidence of bile present	
	Present (1)	Evidence of bile present	
Fibrin <i>(Confirmed on MSB histochemical stain)</i> <i>Take note of where the fibrin is deposited</i>	Absent (0)	No evidence of fibrinous exudate	
	Mild (1)	Affecting less than a third of the blood vessels (under 40x magnification, estimated over 3 x FOV).	
	Moderate (2)	Affecting more than a third to two thirds of the blood vessels (under 40x magnification, estimated over 3 x FOV).	
	Severe (Krause et al.)	Affecting more than two thirds of the blood vessels (under 40x magnification, estimated over 3 x FOV).	
Extra-medullary haematopoiesis <i>(Megakaryocytes and metarubricytes/normoblasts)</i>	Absent (0)	No evidence of extra-medullary haematopoiesis present intravascularly.	
	Mild (1)	Less than 5 megakaryocytes/metarubricytes/normoblasts seen in 3x FOV under 40x magnification	

	Prominent (2)	More than 5 megakaryocytes/metarubricytes/normoblasts seen in 3 x FOV under 40x magnification	
Sinusoids/Spaces of Disse	Oedema (= amorphous clear to eosinophilic extravascular fluid)	Absent (0)	No evidence of oedema
		Present (1)	Expansion of the perivascular areas by oedema fluid
Kupffer cells	Hypertrophy/Activation (Look for pigment)	Absent (0)	Less than one third of Kupffer cells display nuclear activation/hypertrophy.
		Few (1)	One to two thirds of Kupffer cells display nuclear activation/hypertrophy.
		Many (2)	More than two thirds of Kupffer cells display nuclear activation/hypertrophy.
	Intracellular haemosiderin pigment	Absent (0)	No intracellular haemosiderin pigment visible
		Few (1)	Intracellular haemosiderin pigment visible in less than 20% of cells
		Many (2)	Intracellular haemosiderin pigment visible in more than 20% of cells
	Bile	Absent (0)	No evidence of intracellular bile pigment
		Few (1)	Intracellular bile pigment visible in less than 20% of cells
		Many (2)	Intracellular bile pigment visible in more than 20% of cells
	Cell injury (necrosis/apoptosis) Centrilobular bridging necrosis extending into midzonal	Absent (0)	All cells intact and no evidence of injury
		Few (1)	Evidence of cell injury in less than 20% of cells
		Many (2)	Evidence of cell injury in more than 20% of cells
Erythrocytes (Confirmed with LFB histochemical stain) 60x magnification in 3x FOV	Intraerythrocytic parasites	Absent (0)	No evidence of parasitized erythrocytes.
		Few (1)	Less than 10 parasitized erythrocytes seen per FOV.
		Many (2)	More than and including 10 parasitized erythrocytes seen per FOV.
Centrilobular			
Hepatocytes 40x magnification in 3x FOV	Necrosis (Eosinophilic, surrounding necrosis)	Absent (0)	No necrotic hepatocytes visualized
		Mild (1)	Single cell necrosis
		Moderate (2)	Necrosis of small clusters/groups of hepatocytes – 2-5 cells
		Severe (Krause et al.)	Necrosis of 6 or more cells
	Hydropic change (Feathery changes)	Absent (0)	No evidence of hydropic change present
		Mild (1)	Hydropic changes present in 1 hepatocyte
		Moderate (2)	Hydropic changes in small clusters/groups of hepatocytes – 2-5 cells

		Severe (Krause et al.)	Hydropic changes in and more than 6 hepatocytes	
Fatty change (Punched out holes)		Absent (0)	No evidence of fatty change present in any cells	
		Mild (1)	Fatty changes present in 1 hepatocyte	
		Moderate (2)	Fatty changes in small clusters/groups of hepatocytes – 2-5 cells	
		Severe (Krause et al.)	Fatty changes in and more than 6 hepatocytes	
Vesicular nuclei (Euchromatic. 1.5x size of average of hepatocyte nucleus)		Absent (0)	No evidence of vesicular nuclei present (< and including 1 per FOV).	
		Present (1)	Evidence of vesicular nuclei present (>1 per FOV).	
Turnover (Mitotic bodies, binucleates)		Absent (0)	No evidence of any turnover present	
		Mild (1)	Evidence of turnover present in 1-2 hepatocytes per field	
		Moderate (2)	Evidence of turnover present in 2-5 hepatocytes per field	
		Severe (Krause et al.)	Evidence of turnover present in more than 5 hepatocytes per field	
Anisokaryosis		Absent (0)	No evidence of anisokaryosis present	
		Present (1)	Evidence of anisokaryosis	
Pigments:				
Lipofuscin/ceroid		Absent (0)	No evidence of pigment present	
		Present (1)	Evidence of pigment present	
Haemosiderin		Absent (0)	No evidence of pigment present	
		Present (1)	Evidence of pigment present	
Bile		Absent (0)	No evidence of bile present	
		Present (1)	Evidence of bile present	
Central vein	Endothelial cell integrity/ hypertrophy <i>Endothelial hypertrophy = nucleus width is double or more than the normal thickness.</i>	Absent (0)	No evidence of endothelial cell hypertrophy.	
		Mild (1)	Less than one third of endothelial cells display nuclear activation/hypertrophy.	
		Moderate (2)	One to two thirds of endothelial cells display nuclear activation/hypertrophy.	
		Severe (Krause et al.)	More than two thirds of endothelial cells display nuclear activation/hypertrophy.	
	Leukostasis <i>Use similar sized vessels</i>		Absent (0)	No evidence of leukostasis present. (Look out for normoblasts).
			Mild (1)	Less than one quarter of the blood vessel's lumen displays leukostasis at 40x magnification, when checking at least 3 FOV.

		Moderate (2)	Half of the blood vessel's lumen displays leukostasis at 40x magnification, when checking at least 3 FOV.
		Severe (Krause et al.)	More than and including three quarters of the blood vessel's lumen displays leukostasis at 40x magnification, when checking at least 3 FOV.
		Cellular infiltrate	Identify and describe predominant cellular component (mononuclear or PMN) in leukostatic blood vessels, based on HE (IMP will confirm later).
Lymphatics <i>(Subcapsular, portal and central venous areas. Will have endothelial cells)</i>	Distended	Absent (0)	No evidence of lymphatic distension
		Present (1)	Evidence of lymphatic distension
	Proteinaceous fluid-filled	Absent (0)	No evidence of proteinaceous fluid present
		Present (1)	Evidence of proteinaceous fluid present
Terminal hepatic vein			
Sublobular hepatic vein			
Fibrin <i>(Confirmed on MSB histochemical stain)</i> <i>Take note of where the fibrin is deposited</i>	Absent (0)	No evidence of fibrinous exudate	
	Mild (1)	Affecting less than a third of the blood vessels (under 40x magnification, estimated over 3 x FOV).	
	Moderate (2)	Affecting more than a third to two thirds of the blood vessels (under 40x magnification, estimated over 3 x FOV).	
	Severe (Krause et al.)	Affecting more than two thirds of the blood vessels (under 40x magnification, estimated over 3 x FOV).	
Extra-medullary haematopoiesis <i>(Megakaryocytes and metarubricytes/normoblasts)</i>	Absent (0)	No evidence of extra-medullary haematopoiesis present intravascularly.	
	Mild (1)	Less than 5 megakaryocytes/metarubricytes/normoblasts seen in 3x FOV under 40x magnification	
	Prominent (2)	More than 5 megakaryocytes/metarubricytes/normoblasts seen in 3 x FOV under 40x magnification	
Sinusoids/Spaces of Disse	Oedema <i>(= amorphous clear to eosinophilic extravascular fluid)</i>	Absent (0)	No evidence of oedema
		Present (1)	Expansion of the perivascular areas by oedema fluid
Cellular infiltrate <i>(Confirmed with IHC)</i> <i>40x magnification</i>	Monocyte-macrophages	Absent (0)	No monocytes/macrophages seen
		Few (1)	Less than 20 monocytes/macrophages seen per FOV
		Many (2)	More than and including 20 monocytes/macrophages seen per FOV
	Lymphocytes	Absent (0)	No lymphocytes seen
		Few (1)	Less than 20 lymphocytes seen per FOV
		Many (2)	More than and including 20 lymphocytes seen per FOV
	Plasma cells	Absent (0)	No plasma cells seen
		Few (1)	Less than 20 plasma cells seen per FOV
		Many (2)	More than and including 20 plasma cells seen per FOV
	Neutrophils	Absent (0)	No neutrophils seen
Few (1)		Less than 20 neutrophils seen per FOV	

		Many (2)	More than and including 20 neutrophils seen per FOV
	Eosinophils	Absent (0)	No eosinophils seen
		Few (1)	1-2 eosinophils seen per FOV
		Many (2)	More than 2 eosinophils seen per FOV
Kupffer cells	Hypertrophy/Activation (Look for pigment)	Absent (0)	Less than one third of Kupffer cells display nuclear activation/hypertrophy.
		Few (1)	One to two thirds of Kupffer cells display nuclear activation/hypertrophy.
		Many (2)	More than two thirds of Kupffer cells display nuclear activation/hypertrophy.
	Intracellular haemosiderin pigment	Absent (0)	No intracellular haemosiderin pigment visible
		Few (1)	Intracellular haemosiderin pigment visible in less than 20% of cells
		Many (2)	Intracellular haemosiderin pigment visible in more than 20% of cells
	Bile	Absent (0)	No evidence of intracellular bile pigment
		Few (1)	Intracellular bile pigment visible in less than 20% of cells
		Many (2)	Intracellular bile pigment visible in more than 20% of cells
	Cell injury (necrosis/apoptosis) <i>Centrilobular bridging necrosis extending into midzonal</i>	Absent (0)	All cells intact and no evidence of injury
		Few (1)	Evidence of cell injury in less than 20% of cells
		Many (2)	Evidence of cell injury in more than 20% of cells
Erythrocytes (Confirmed with LFB histochemical stain) <i>60x magnification in 3x FOV</i>	Intraerythrocytic parasites	Absent (0)	No evidence of parasitized erythrocytes.
		Few (1)	Less than 10 parasitized erythrocytes seen per FOV.
		Many (2)	More than and including 10 parasitized erythrocytes seen per FOV.



Faculty of Veterinary Science
Animal Ethics Committee

22 September 2021

**Approval Certificate
New Application**

AEC Reference No.: REC040-21
Title: The Histopathology of the Liver in naturally infected Canine Babesiosis that died
Researcher: Miss HD Horrell
Student's Supervisor: Prof AL Leisewitz

Dear Miss HD Horrell,

The **New Application** as supported by documents received between 2021-05-24 and 2021-09-03 for your research, was approved by the Animal Ethics Committee on its quorate meeting of 2021-09-03.

Please note the following about your ethics approval:

1. The use of species is approved:

Species	Number
Dogs	10 carcasses (Tshwane SPCA)
Samples Liver samples	10
Liver samples	10 (Stored- Historic/Retrospective) (V034-14)

2. Ethics Approval is valid for 1 year and needs to be renewed annually by 2022-09-22.
3. Please remember to use your protocol number (REC040-21) on any documents or correspondence with the AEC regarding your research.
4. Please note that the AEC may ask further questions, seek additional information, require further modification, monitor the conduct of your research, or suspend or withdraw ethics approval.
5. All incidents must be reported by the PI by email to Ms Marleze Rheeder (AEC Coordinator) within 3 days, and must be subsequently submitted electronically on the application system within 14 days.
6. The committee also requests that you record major procedures undertaken during your study for own-archiving, using any available digital recording system that captures in adequate quality, as it may be required if the committee needs to evaluate a complaint. However, if the committee has monitored the procedure previously or if it is generally can be considered routine, such recording will not be required.

Ethics approval is subject to the following:

- The ethics approval is conditional on the research being conducted as stipulated by the details of all documents submitted to the Committee. In the event that a further need arises to change who the investigators are, the methods or any other aspect, such changes must be submitted as an Amendment for approval by the Committee.

We wish you the best with your research.

Yours sincerely

Dr Heike Lutermann
DEPUTY CHAIRMAN: UP-Animal Ethics Committee